Bifunctional immunostimulatory fusion proteins for therapeutic applications

Von der Fakultät Energie-, Verfahrens- und Biotechnik der Universität Stuttgart zur Erlangung der Würde eines Doktors der Naturwissenschaften (Dr. rer. nat.) genehmigte Abhandlung

Vorgelegt von

Sina Fellermeier

aus Schorndorf

Hauptberichter: Prof. Dr. Roland Kontermann
Mitberichter: apl. Prof. Dr. Wolfgang Hauber

Tag der mündlichen Prüfung: 25.11.2016

Institut für Zellbiologie und Immunologie
Universität Stuttgart

2016

Für meine Eltern

Table of Contents

Table of Contents **5**

Abbreviations **9**

Zusammenfassung **11**

Abstract **13**

1 Introduction **15**

1.1 Cancer Immunotherapy 15

1.2 Costimulation of T cells via TNF superfamily members 18

1.2.1 4-1BB and 4-1BBL 20

1.2.2 OX40 and OX40L 21

1.2.3 CD27 and CD27L 22

1.2.4 CD40 and CD40L 23

1.2.5 Spatiotemporal regulation of TNFSF-mediated costimulation 24

1.3 Therapeutic strategies incorporating natural TNFSF ligands 26

1.4 Targets of anti-cancer antibodies 28

1.4.1 Epithelial cell adhesion molecule (EpCAM, CD326) 29

1.4.2 Claudins 30

1.5 Purpose of this study 31

2 Materials and Methods **33**

2.1 Materials 33

2.1.1 General declaration 33

2.1.2 Antibodies 33

2.1.3 Bacteria strains 34

2.1.4 Buffers and solutions 34

2.1.5 Cell lines 35

2.1.6 Enzymes 36

2.1.7 Instruments 36

2.1.8 Kits and markers 37

2.1.9 Media and reagents for bacterial culture 37

2.1.10 Media and reagents for cell culture 38

2.1.11 Mice 38

2.1.12 Plasmids 38

2.1.13 Primer 39

2.1.14 Proteins 41

2.1.15 Software and online tools 41

2.1.16 Special implements 41

2.2 Cloning procedures 42

2.2.1 Polymerase chain reaction (PCR) 42

2.2.2 Restriction digestion 42

2.2.3 DNA electrophoresis and gel extraction 43

2.2.4 Ligation and heat shock transformation 43
2.2.5 Screening of clones 43
2.2.6 Plasmid DNA isolation 44
2.2.7 Sequence analysis 44
2.3 Cloning strategies 44
2.3.1 Cloning of ECD-Fc fusion proteins 44
2.3.2 Cloning of single-chain fragment variable (scFv) 45
2.3.3 Cloning of (single-chain) TNFSF ligands 46
2.3.4 Cloning of scFv-ligand fusion proteins 47
2.3.5 Cloning of Duokines 47
2.3.6 Cloning of single-chain Duokines 48
2.3.7 Cloning of murine homologs of Duokines and scDuokines 48
2.3.8 Cloning of EHD2 single-chain Duokines 49
2.4 Humanization of antibody fragments 49
2.5 Cell culture 50
2.5.1 General cell culture techniques 50
2.5.2 Transfection and selection of transfectants 50
2.5.3 Isolation and handling of peripheral blood mononuclear cells (PBMC) 51
2.6 Expression and purification of recombinant protein 52
2.6.1 Periplasmic protein expression in *E. coli* TG1 52
2.6.2 Eukaryotic protein expression in adherent HEK293T 52
2.6.3 Immobilized metal ion affinity chromatography (IMAC) 52
2.6.4 Protein A affinity chromatography 53
2.6.5 FLAG affinity chromatography 53
2.7 Biochemical protein characterization 53
2.7.1 Protein concentration 53
2.7.2 SDS polyacrylamide gel electrophoresis 54
2.7.3 Size exclusion chromatography (SEC) 54
2.7.4 Thermal stability 55
2.8 General experimental practices for functional experiments 55
2.9 Enzyme-linked immunosorbent assay (ELISA) 55
2.10 Flow cytometry 56
2.10.1 Cell surface marker expression 56
2.10.2 Determination of half-maximal binding 56
2.11 Protein Stability 57
2.11.1 *In vitro* serum stability 57
2.11.2 *In vivo* pharmacokinetics 57
2.12 Functional characterization 58
2.12.1 Interleukin-8 release assay 58
2.12.2 Interferon-γ release assay 58
2.12.3 Proliferation 59
2.13 *In vivo* lung tumor model 60
2.14 Statistics 61

3 Results 62
3.1 Development of tumor-targeting single-chain fragment variable (scFv) 62
3.1.1 Humanization of anti-CLDN4/6 scFv4H6E9 62
3.1.2 Humanization of anti-EpCAM scFv323A3 67
3.2 Tumor-targeted immunostimulatory antibody-cytokine fusion proteins 70
3.2.1 Characterization of scFv-ligand fusion proteins 70
3.2.2 Binding of scFv-ligand fusion proteins to antigens and cytokine receptors 72
3.2.3 *In vitro* stability and *in vivo* pharmacokinetics of scFv-ligand fusion proteins 76
3.2.4 T cell costimulatory potential of scFv-ligand fusion proteins 77
3.3 Dual-acting immunostimulatory cytokine fusion proteins (Duokines) 80
3.3.1 Biochemical characterization of Duokines and scDuokines 82
3.3.2 Binding and activation of cytokine receptors by Duokines and scDuokines 84
3.3.3 *In vitro* stability of Duokines and scDuokines 90
3.3.4 Duokines and scDuokines enhance proliferation of prestimulated T cells 91
3.3.5 Single-chain Duokines target various leukocyte populations 94
3.3.6 Trans-acting scDuokines in solution activate B cells 96
3.3.7 Trans-acting scDuokines in solution activate unstimulated T cells 97
3.3.8 *In vivo* pharmacokinetics and pharmacodynamics of scDuokines 99
3.4 Homodimerized single-chain Duokines (EHD2-scDuokines) 103
3.4.1 Characterization of EHD2-scDuokines 103
3.4.2 Binding and activation of cytokine receptors by EHD2-scDuokines 105
3.4.3 *In vitro* plasma stability of EHD2-scDuokines 107
3.4.4 Costimulatory activity of EHD2-scDuokines 108

4 Discussion 109
4.1 Extending the target spectrum for antibody-cytokine fusion proteins 109
4.2 Advancing bifunctional antibody-cytokine fusion proteins by introducing TNFSF ligands in a single-chain format 111
4.3 Duokines and scDuokines are a novel format of bifunctional immuno-stimulatory cytokine fusion proteins 116
4.4 EHD2-scDuokines as initial approach towards directed oligomerization of bifunctional cytokine fusion proteins 123
4.5 Conclusion and Outlook 125

5 Bibliography 128

6 Sequences 146
6.1 Single-chain fragment variable 146
6.2 TNFSF ligands 152
6.3 Single-chain TNFSF ligands 153
6.4 scFv-ligand fusion proteins 156
6.5 Dual-acting Cytokines 157
6.6 Murine dual-acting Cytokines 158
6.7 TNFRSF receptor-Fc fusion proteins 161

List of Figures 163

List of Tables **165**

Erklärung **166**

Declaration **166**

Danksagung **167**

Short Curriculum Vitae **168**

Abbreviations

aa	amino acid
Ab	antibody
ACT	adoptive T cell therapy
ADCC	antibody-dependent cellular cytotoxicity
Amp	ampicillin
AP-1	activator protein 1
APC	antigen-presenting cell
APS	ammonium persulfate
AUC	area under the curve
ATROSAB	antagonistic tumor necrosis factor receptor one-specific antibody
Bcl-x_L	B cell lymphoma-extra large
BiTE	bispecific T cell engager
BLAST	basic local alignment search tool
BSA	bovine serum albumin
CAR	chimeric antigen receptor
CD	cluster of differentiation
CDC	complement-dependent cytotoxicity
CDR	complementarity-determining region
CFSE	carboxyfluorescein succinimidyl ester
CLDN	claudin
CPE	*Clostridium perfringens* enterotoxin
CRD	cysteine-rich domain
CTL	cytotoxic T lymphocyte
CTLA-4	cytotoxic T lymphocyte-associated protein 4
DC	dendritic cell
Db	diabody
dd	double distilled
DMSO	dimethyl sulfoxide
DNA	deoxyribonucleic acid
dNTP	deoxynucleotide
DR	death receptor
EC_{50}	half-maximal effective concentration
ECD	extracellular domain
EDTA	ethylenediaminetetraacetic acid
EGFR	epidermal growth factor receptor
EHD2	IgE heavy chain domain 2
ELISA	enzyme-linked immunosorbent assay
EpCAM	epithelial cell adhesion molecule
FAP	fibroblast activation protein
FasL	Fas ligand
FBS	fetal bovine serum
FC	flow cytometry
Fc	fragment crystallizable
FITC	fluorescein isothiocyanate
FLAG	DYKDDDDK polypeptide-tag
FR	framework region
GIFT	GM-CSF interleukin fusion transgene
GITR	glucocorticoid-induced TNFR-related protein
GITRL	ligand of glucocorticoid-induced TNFR-related protein
GM-CSF	granulocyte-macrophage colony-stimulating factor
HAMA	human anti-mouse antibodies
HEK	human embryonic kidney
HER2/3	human epidermal growth factor receptor 2 or 3
His	hexa histidine-tag
HPLC	high-pressure liquid chromatography
HRP	horseradish peroxidase
hu	human
HVEM	herpes virus entry mediator
IFN	interferon
Ig	Immunoglobulin
IL	interleukin
ICOS	inducible T cell costimulator
ICOSL	inducible T cell costimulatory ligand
ILZ	isoleucine zipper
IMAC	immobilized metal ion affinity chromatography
IPTG	isopropyl β-D-1-thiogalactopyranoside
JNK	c-Jun N-terminal kinase
kcps	kilo counts per second
LAG-3	lymphocyte activation gene 3
LB	lysogeny broth
LIGHT	homologous to **L**ymphotoxin, exhibits **I**nducible expression and competes with HSV **G**lycoprotein D for binding to **H**erpesvirus entry mediator, a receptor expressed on **T** lymphocytes
m/mo	murin/mouse
mAb	monoclonal antibody
MFI	mean fluorescence intensity
MHC	major histocompatibility complex
mRNA	messenger ribonucleic acid
NFκB	nuclear factor kappa-light-chain-enhancer of activated B cells
NK	natural killer
NSCLC	non-small cell lung cancer
NTA	nitrilotriacetic acid
OD	optical density
PAA	polyacrylamide
PAGE	polyacrylamide gel electrophoresis

PBA	phosphate-buffered saline containing sodium azide
PBMC	peripheral blood mononuclear cell
PBS	phosphate-buffered saline
PCR	polymerase chain reaction
PD-1	programmed cell death protein 1
PD-L1/2	programmed death ligand 1/2
PE	phycoerythrin
Pen/Strep	penicillin/streptomycin
PLAD	pre-ligand assembly domain
RPMI	Roswell Park Memorial Institute
sc	single-chain
scDb	single-chain diabody
scFv	single-chain fragment variable
SDS	sodium dodecyl sulfate
SEC	size exclusion chromatography
$t_{1/2}$	half-life
TAA	tumor-associated antigen
TAE	tris-acetate-EDTA
taFv	tandem scFv
TCR	T cell receptor
TEMED	tetramethylethylenediamine
THD	TNF homology domain
TIM-3	T cell immunoglobulin and mucin domain-containing 3
TLR	toll-like receptor
TMB	3,3’-5,5’-tetramethylbenzidine
TNC	tenascin-C
TNF	tumor necrosis factor
TNFSF	tumor necrosis factor superfamily
TNFRSF	tumor necrosis factor receptor superfamily
TRAF	TNF receptor associated factor
TRAIL	TNF related apoptosis inducing ligand
Treg	regulatory T cell
v/v	volume per volume
VH	variable domain of the heavy chain
VL	variable domain of the light chain
wt	wildtype
w/v	weight per volume

Zusammenfassung

Im Bereich der Krebsimmuntherapie hat sich die Kostimulation mittels der Rezeptoren der Tumornekrosefaktor-Rezeptor-Superfamilie (TNFRSF) zu einer vielversprechenden Strategie entwickelt. Adressiert man diese Rezeptoren über ihre natürlichen Liganden, wird eine bestehende Immunantwort verstärkt, ohne dass dabei super-agonistische Aktivität ausgelöst wird, wie es für agonistische Antikörper beobachtet wurde. Eine für diesen Ansatz besonders geeignete Variante sind tumor-gerichtete bifunktionelle Antikörper-Ligand Fusionsproteine, wodurch die kostimulatorische Aktivität auf den Tumor begrenzt wird. Die natürliche homotrimere Struktur der TNFSF Liganden bedingt allerdings die Ausbildung komplexer Fusionsproteine, so dass das etablierte Format homotrimerer scFv-TNFSF Fusionsproteine zu einer einfacheren und stabileren Konfiguration weiterentwickelt wurde. Durch die lineare Verknüpfung dreier extrazellulärer Domänen zu einem einzelkettigen (genannt: single-chain) Format der TNFSF Liganden und die Fusion eines solchen einzelkettigen kostimulatorischen Liganden (sc4-1BBL oder scOX40L) an ein gegen die Tumorantigene EpCAM oder CLDN4/6 gerichtetes scFv-Fragment entstand ein Set an neuartigen monomeren scFv-scTNFSF Fusionsproteinen. Hinsichtlich der Stabilität und den pharmakokinetischen Eigenschaften zeigten die monomeren scFv-scTNFSF Fusionsproteine eine deutliche Verbesserung gegenüber ihren homotrimeren Pendants, wobei scFv-sc4-1BBL stärker vom neuen Format profitierte als scFv-scOX40L. Zusätzlich zeigte monomeres scFv-scTNFSF bessere Aktivierung der Rezeptoren, was trotz geringerer Avidität bei der Antigenbindung in gleicher oder verstärkter kostimulatorischer Aktivität resultierte. Interessanterweise war die Steigerung der T-Zell-Kostimulation abhängig vom verwendeten Antikörperfragment, was darauf hindeutet, dass die Targeting-Einheit sorgfältig ausgewählt werden sollte um verbesserte zielgerichtete Kostimulation durch scFv-scTNFSF Fusionsproteine zu erreichen.

Der zweite Teil dieser Arbeit beschäftigte sich mit der Entwicklung eines neuartigen Formates für nicht-zielgerichtete bifunktionelle kostimulatorische Zytokin-Fusionsproteine. Durch Verknüpfung zweier verschiedener TNFSF Liganden entstanden dual-wirkende Zytokine, genannt Duokines, in sowohl einer homotrimeren Form (Fusion von zwei einzelnen extrazellulären Domänen der TNFSF Liganden) als auch einer einzelkettigen Form (Fusion von zwei einzelkettigen scTNFSF Liganden). Die Verbindung von 4-1BBL, OX40L und CD27L in allen möglichen Kombinationen resultierte in sogenannten cis-wirkenden Duokines, die auf dieselbe oder benachbarte T-Zellen wirken, während die Kombination von CD40L mit

4-1BBL, CD27L und OX40L sogenannte trans-wirkende Duokines erzielte, die gleichzeitig auf Antigen-präsentierende Zellen und T-Zellen wirken. Alle Duokines bildeten die korrekte Proteinkonfiguration stabil aus und aktivierten ihre jeweiligen Rezeptoren. Kostimulation von T-Zellen wurde für alle Proteine in einem löslichen sowie einem trans-präsentierenden Setting beobachtet, wobei sich die einzelkettigen scDuokines etwas aktiver zeigten. Die darauffolgende Untersuchung der Immunzell-Zielpopulationen ausgewählter scDuokines ergab, dass cis-wirkende scDuokines bevorzugt an T-Zellen und trans-wirkende scDuokines bevorzugt an B-Zellen binden. Die kostimulatorische Aktivität von sowohl cis- als auch trans-wirkenden scDuokines konnte anhand der Verstärkung von CD3-vermittelter T-Zell-Proliferation nachgewiesen werden. Zusätzlich induzierten trans-wirkende scDuokines in gewissem Umfang auch die *de novo* Aktivierung von $CD8^+$ T-Zellen, was auf eine Kommunikation zwischen Antigen-präsentierenden Zellen und T-Zellen hindeutet. Tatsächlich aktivierten trans-wirkende scDuokines B-Zellen, die als Antigen-präsentierende Zellen agieren können. Abschließend wurde die antitumorale Wirkung von scDuokines *in vivo* evaluiert, wobei scDuokines als kostimulatorischer Wirkstoff gemeinsam mit einem primären T-Zell-Stimulus die Ausbildung von Tumoren in der Lunge reduzierten. Zusammenfassend wurden mit den Duokines neue bifunktionelle Zytokin-Fusionsproteine etabliert, die auf verschiedene Immunzellen eine immunmodulierende Wirkung haben und deren kostimulatorische Effekte die antitumorale Wirkung von anderen immun-therapeutischen Strategien verstärken. Dadurch ergibt sich ein breites Spektrum an Möglichkeiten zur Weiterentwicklung, was das enorme Potential dieser vielversprechenden Moleküle verdeutlicht.

Abstract

Costimulation via the receptors of the tumor necrosis factor receptor super family (TNFRSF) emerged as promising strategy in cancer immunotherapy. By targeting the receptors with their natural ligands, consisting T cell responses are supported without any supra-agonistic activity that has been observed for agonistic antibodies. Bifunctional tumor-targeted antibody-ligand fusion proteins present a suitable option for this approach, as the costimulatory activity is restricted to the tumor site. However, the natural homotrimeric assembly of the TNFSF ligands results in rather complex proteins. Aiming at a more simple and stable protein configuration, the established format of homotrimeric scFv-TNFSF fusion proteins was advanced by introducing the TNFSF ligand in a single-chain version with three extracellular domains connected in a row. By fusing costimulatory single-chain ligands (sc4-1BBL or scOX40L) to scFv fragments against EpCAM or CLDN4/6, a set of novel monomeric scFv-scTNFSF fusion proteins was generated. Regarding protein stability and *in vivo* pharmacokinetics, the performance of the monomeric scFv-scTNFSF was clearly improved compared to their homotrimeric counterparts, with scFv-sc4-1BBL benefitting even more than scFv-scOX40L. Furthermore, the monomeric scFv-scTNFSF showed superior receptor activation properties, resulting in equal or enhanced costimulatory activity, both despite reduced avidity in antigen binding. Interestingly, an increase in T cell costimulation was depending on the incorporated antibody fragment, indicating that the targeting moiety has to be selected carefully in order to achieve improved target-dependent costimulation by scFv-scTNFSF fusion proteins.

In the second part of this study, a novel type of non-tumor-targeted bifunctional costimulatory cytokine fusion proteins was established. Connecting two different TNFSF ligands resulted in dual-acting cytokines (“Duokines”) that were generated in both a homotrimeric, i.e. fusion of two single TNFSF ligand extracellular domains, and a monomeric protein configuration, i.e. fusion of two scTNFSF ligands. By connecting 4-1BBL, OX40L and CD27L in all possible combinations, cis-acting Duokines that act on the same or adjacent T cells were generated, while combining CD40L with 4-1BBL, OX40L and CD27L resulted in trans-acting Duokines simultaneously acting on APCs and T cells. All Duokines stably assembled in the correct protein configuration and activated their receptors. Costimulation of T cells was seen for all proteins in a soluble as well as a trans-presented setting, but the scDuokines proved to be slightly more active. Therefore, selected scDuokines were analyzed

for their target immune cell populations, revealing that cis-acting scDuokines preferably bind to T cells, while trans-acting scDuokines bind to B cells. Both cis- and trans-acting scDuokines proved their costimulatory nature by enhancing CD3-mediated T cell activation. However, trans-acting scDuokines also induced some *de novo* activation of $CD8^+$ T cells, indicating crosstalk between APCs and T cells. In fact, trans-acting scDuokines activated B cells, which can act as APCs. Finally, the anti-tumoral potential of scDuokines was evaluated *in vivo*, where scDuokines as costimulatory agent in combination with a primary T cell stimulus successfully reduced the formation of lung tumors. In conclusion, Duokines have been established as novel bifunctional cytokine fusion proteins that address their immunomodulatory activity to several immune cells. The costimulatory effects of Duokines enhance the anti-tumoral activity of other immunotherapeutic approaches, thus creating a wide array of opportunities for further developments, which proves the enormous potential of these promising molecules.

1 Introduction

The history of cancer immunotherapy begins as early as in the mid-nineteenth century when the immunologist pioneer Rudolf Virchow discovered that the body's own immune system can act against cancer (Balkwill & Mantovani 2001) and a first immunotherapeutic approach was pursued by William Coley. In 1891, he injected bacterial cultures into unresectable sarcomas, which at least partly resulted in inflammatory immune reactions and disappearance of the tumors (Coley 1891). Interestingly, the effects mediated by "Coley's toxins" were later identified as being induced by the release of tumor necrosis factor (TNF), the eponymous member of the TNF superfamily (Carswell et al. 1975). However, severe side effects and insufficient knowledge about the underlying mechanisms within our complex immune system thwarted the progress in immunotherapies for years. Not until the 1970s cancer immunotherapy regained particular research interest, as initial success was achieved by vaccination or high-dose recombinant cytokines and tremendous efforts have been undertaken in the field during the following decades (Atkins & Sznol 2015).

1.1 Cancer Immunotherapy

Ever since the approval of ipilimumab for the treatment of metastatic melanoma in 2011, cancer immunotherapy has evolved into a rapidly growing field with a plethora of different strategies being evaluated in preclinical and clinical studies. Ipilimumab is a monoclonal antibody blocking cytotoxic T lymphocyte antigen 4 (CTLA-4), the most important immune checkpoint that down-regulates T cell activation (Hodi et al. 2010). Besides ipilimumab, two other immune checkpoint inhibitors, nivolumab and pembrolizumab, have been approved for the treatment of metastatic melanoma and non-small cell lung cancer (NSCLC) in 2014 and 2015. Both antibodies block programmed cell death protein 1 (PD-1), the main regulator of T cell exhaustion and tolerance (Robert et al. 2015, Larkin et al. 2015). Ideally, cancer immunotherapy (alternatively: immuno-oncology) aims at the mobilization of the immune system independent of individual tumor histology or specific mutations. To date, best therapeutic results, i.e. substantially enhanced overall patient survival, have been achieved with the aforementioned, antibody-based immune checkpoint inhibitors (Schadendorf et al. 2015), in some cases even replacing chemotherapy as the standard of care. However, as both positive and negative regulators drive the balance of the immune response,

immunomodulatory antibodies targeting various immune-activating pathways, like the costimulatory receptors 4-1BB and OX40, are likewise investigated. By now, more than 20 immunomodulatory antibodies are being tested in clinical phases I to III (Table 1).

Table 1: Immunomodulatory antibodies for cancer treatment approved or in ongoing clinical trials. Extended from Mahoney et al. 2015, Smyth et al. 2015 with *http://www.clinicaltrials.gov*, status from May 2016.

Target	Generic name	Indication	Status
Co-inhibitory pathways			
CTLA-4	Ipilimumab	Metastatic melanoma	Approved (2011)
		Melanoma, multiple cancers	Phase I-III
	Tremelimumab	NSCLC, head and neck cancer, solid tumors	Phase I-III
PD-1	Nivolumab	Metastatic melanoma	Approved (2014)
		Metastatic NSCLC	Approved (2015)
		NSCLC, melanoma, solid tumors	Phase I-III
	Pembrolizumab	Metastatic melanoma	Approved (2014)
		NSCLC, melanoma, solid tumors	Phase I-III
	BMS-936558	(Metastatic) solid tumors, leukemia, melanoma	Phase I-III
	Pidilizumab	Lymphoma	Phase II
	MEDI0680 (AMP-514)	Advanced cancers, B cell lymphoma	Phase I/II
	PDR001	Advanced solid tumors	Phase I/II
	AMP-224	Colorectal carcinoma	Phase I
PD-L1	Atezolizumab	Solid tumors, multiple myeloma, melanoma	Phase I-III
	Avelumab	Solid tumors, Hodgkin's lymphoma	Phase I-III
	Durvalumab (MEDI4736)	Advanced solid tumors	Phase I-III
Costimulatory pathways			
4-1BB	Urelumab	B cell lymphoma, advanced solid tumors, multiple myeloma, leukemia, melanoma	Phase I/II
	PF-05082566	Advanced/metastatic solid tumors, lymphoma	Phase I
OX40	MEDI6469	Advanced solid tumors, B cell lymphoma	Phase I/II
	MEDI0562	Solid tumors	Phase I
	PF-04518600	Advanced solid tumors	Phase I
CD27	Varlilumab	Stage III/IV melanoma, B cell malignancies, advanced solid tumors	Phase I/II
CD40	CP-870,893	Metastatic melanoma, advanced solid tumors	Phase I
GITR	TRX518	Stage III/IV melanoma, advanced solid tumors	Phase I
	MK-4166	Advanced solid tumors	Phase I
ICOS	MEDI-570	T cell lymphoma	Phase I

Cancer immunotherapy does not only focus on immunomodulating antibodies, but a broad range of cytokines (Lee & Margolin 2011), cancer vaccines (Melero et al. 2014), cellular therapies (Klebanoff et al. 2016), oncolytic viruses (Lichty et al. 2014), small molecules (Adams et al. 2015), bispecific T cell engagers (BiTEs, Newman & Benani 2016) and antibody-

cytokine fusion proteins (Kontermann 2012) are evaluated or approved for clinical use as well. Cancer vaccines that are intended to induce T cell responses against tumor cells have been investigated for years without showing the desired results, but regained broad attention just recently, when mRNA vaccines designed against patient-individual mutation-derived tumor antigens proved to be effective and clinically applicable (Kranz et al. 2016). Also, adoptive T cell therapies (ACT) employing either chimeric antigen receptor-expressing T cells (CAR-Ts, Maude et al. 2014) or specific T cell receptor-transduced T cells (Rapoport et al. 2015) evolved as very promising strategies with up to 90% response rates in B cell malignancies. Despite the vast effectiveness of some immunotherapeutic concepts as monotherapies, the future of immuno-oncology clearly points to combinatorial strategies rationally combining different approaches in order to create synergistic effects (Figure 1).

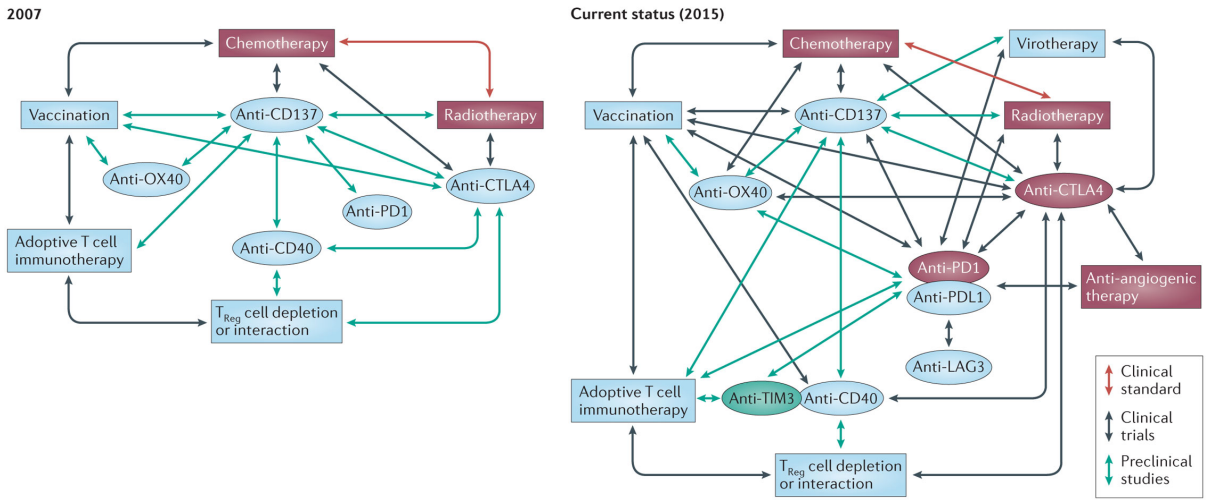

Figure 1: The evolution of combinatorial cancer immunotherapy. The schemes show the rapid development in the field of cancer immunotherapy over the last 8 years. Immune checkpoint inhibitors entered the clinic as single treatments and a plethora of immunomodulatory antibodies are combined with various other therapeutic strategies in clinical or preclinical studies. Red boxes: approved treatments; Blue boxes: treatments in clinical trials; Green boxes: treatments in preclinical evaluation. Combinatorial approaches are depicted as color-coded arrows. Picture from Melero et al. 2015.

Nowadays, renowned scientists in the field believe that the immune checkpoint blockade will constitute the backbone of combination cancer immunotherapy, because only after breaking immunoinhibition other immunostimulating therapies can unfold their full potential (Mahoney et al. 2015, Melero et al. 2015). Extensive research has been conducted in the field of combining the immune checkpoint blockade with conventional therapies (e.g. chemotherapy, Lynch et al. 2012), cellular therapies (e.g. CAR-Ts, Morales-Kastresana et al. 2013a) or other immunotherapies (e.g. anti-4-1BB/-OX40, Melero et al. 2015 or combined

CTLA-4/PD-1 blockade, Postow et al. 2015). Based on rational design, a plethora of combinations of numerous other immunotherapeutic strategies are being evaluated (Figure 1), where even previously inconceivable combinations of three or four different therapies can act synergistically, as it has been shown for combinations of antibodies against PD-L1, 4-1BB and OX40 together with ACT (Morales-Kastresana et al. 2013b). Since the targeting of costimulatory pathways gains increasing interest especially in combination cancer immunotherapy, crucial players and interactions in T cell costimulation are illustrated.

1.2 Costimulation of T cells via TNF superfamily members

Naïve T cells circulating in the periphery are in a resting state and necessarily require multiple signals for complete activation resulting in clonal expansion and acquisition of pro-inflammatory or cytotoxic functions (Sanmamed et al. 2015). The first signal in the process of T cell activation is mediated by the recognition of a peptide presented on the major histocompatibility complex (MHC) class I/II of antigen-presenting cells (APCs) via the T cell receptor (TCR), which leads to the formation of the immunological synapse (Chen & Flies 2013). Here, peptide-MHC class II is only recognized by $CD4^+$ T cells and peptide-MHC class I by $CD8^+$ T cells (König et al. 1992). If a T cell encounters its specific MHC-presented antigen in a non-inflammatory environment, i.e. second stimuli are missing, the T cell will undergo apoptosis or enter an anergic state in which it is not able to elicit any immune responses (Sanmamed et al. 2015). Therefore, accessory immunomodulatory signals delivered by various membrane-attached receptor/ligand pairs at the immune synapse are crucial for shaping the outcome of the TCR signaling in terms of balanced T cell activation and tolerance. Besides activating costimulatory molecules, co-inhibitory immune checkpoint ligands and receptors that temper the immune response are also involved in this regulatory process (Figure 2, Mahoney et al. 2015). From the wide range of known costimulatory and co-inhibitory molecules most can be assigned to either the tumor necrosis factor (TNF) superfamily or the immunoglobulin (Ig) superfamily (Chen & Flies 2013). CD28, the most prominent costimulatory receptor is a member of the Ig superfamily and has two known ligands, B7-1 (CD80) and B7-2 (CD86). Notably, these ligands are also able to interact with the co-inhibitory receptors PD-1 (B7-1 and B7-2) or CTLA-4 (only B7-1), both belonging to the Ig superfamily as well (Mahoney et al. 2015).

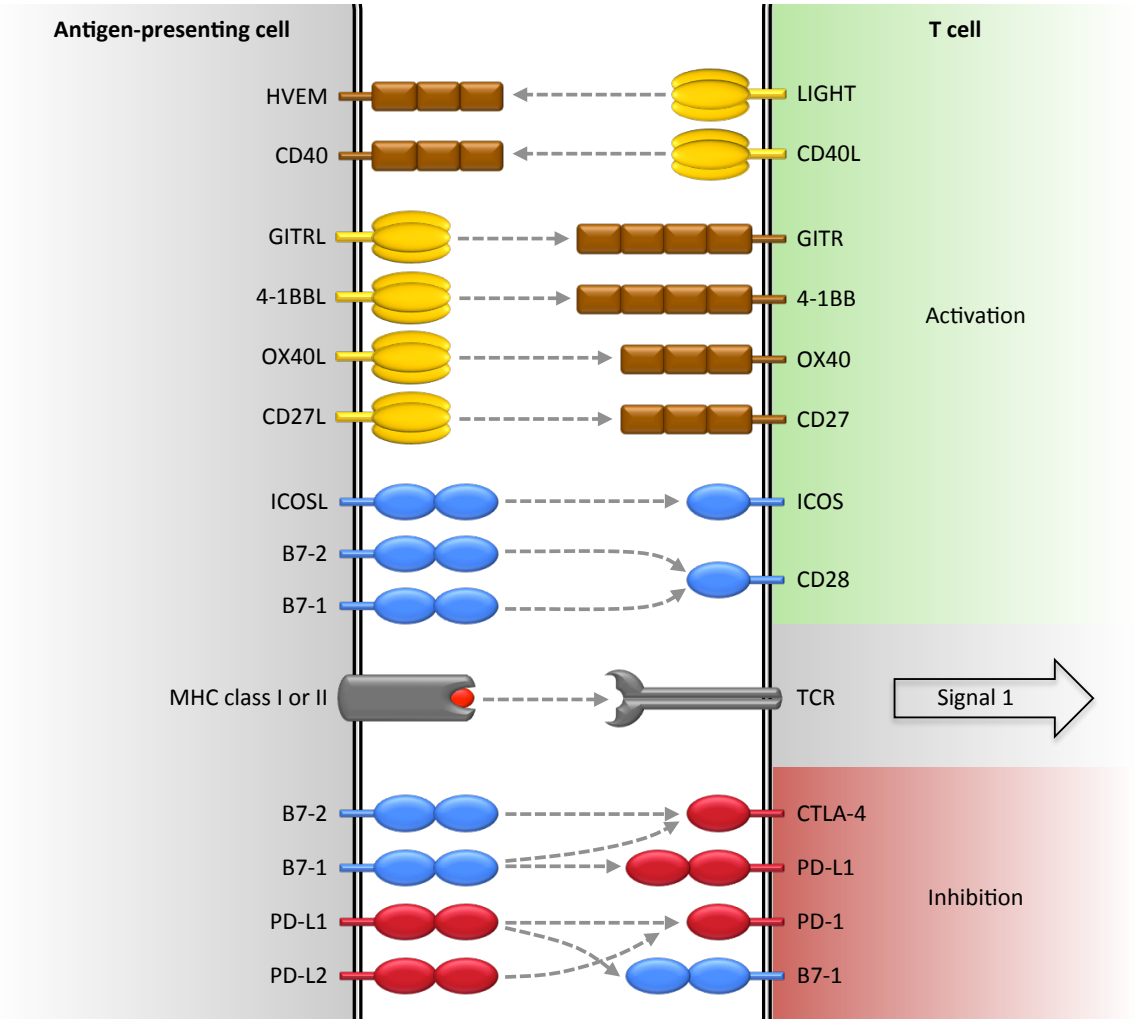

Figure 2: Costimulatory and co-inhibitory signaling at the immune synapse. The first signal is mediated via the interaction of MHC-presented peptide antigen with the T cell receptor. Activation or inhibition of T cells is regulated by various costimulatory or co-inhibitory receptors. Due to the complexity of the system, only the most common ligand/receptor pairs including members of the TNFRSF (brown), their ligands (yellow), costimulatory Ig superfamily members (blue) and immune checkpoint blockers of the Ig superfamily (red) are depicted. Picture adapted from Mahoney et al. 2015.

According to current knowledge, the TNF superfamily comprises 19 ligands and 29 corresponding receptors (denoted as TNFR superfamily), holding various important functions in the immune system (Bodmer et al. 2002). The TNFRSF can be divided into three simplified groups. The first group includes the death receptors (DRs) comprising an intracellular death domain that induce cell death in cells expressing those receptors. Apoptotic signaling is initiated upon ligation with the death-inducing TNFSF ligands TNF, FasL and TRAIL (TNF related apoptosis inducing ligand). Secondly, the so-called decoy receptors constitute a group of receptors lacking own signaling capabilities (Wajant 2015), while the aforementioned costimulatory receptors with T cell-activating effects during an immune response are part of the third group of TRAF-interacting receptors (Bremer 2013). Like all

members of the TNFRSF, the receptors engaged in this function are type I transmembrane proteins (i.e. extracellular N-terminus and intracellular C-terminus) with one to four extracellular cysteine-rich domains (CRDs) forming elongated ladder-like structures stabilized by disulfide bridges that exist on the cell surface either as monomers or self-assembled oligomers (Bodmer et al. 2002, Locksley et al. 2001). Costimulatory receptors initiate signaling upon oligomerization via ligation of their trimerized ligands, followed by the recruitment of TNF receptor-associated factors (TRAFs) as adaptor proteins. Downstream signaling varies between the various receptors, but finally leads to the activation of several pathways like NFκB, JNK/AP1 and anti-apoptotic proteins like Bcl-x_L resulting in pro-inflammatory and pro-survival functions (Watts 2005). All TNFSF ligands are expressed as type II transmembrane proteins (i.e. intracellular N-terminus and extracellular C-terminus), but following proteolytic cleavage or alternative splicing most TNFSF ligands can be processed into soluble ligands. The key feature of TNFSF ligands is their extracellular TNF homology domain (THD), a beta-sandwich structure that is responsible for the characteristic formation of non-covalent homotrimers and mediates binding to the CRDs of their respective receptor (Bodmer et al. 2002). Generally, in the course of an immune response the formation of fully competent effector cells relies on several costimulatory TNF superfamily members. The main focus of this study will be on 4-1BBL, OX40L and CD27L, which are important for T lymphocytes as well as CD40L, which is crucial for B lymphocytes and dendritic cells.

1.2.1 4-1BB and 4-1BBL

One of the most studied members of the TNFRSF is the inducible 4-1BB (CD137, Kwon & Weissman 1989), which is mainly expressed transiently on both activated T cells and NK cells, but also constitutively on regulatory T cells (T_{regs}). Its cognate ligand 4-1BBL (CD137L, Goodwin et al. 1993a) is expressed on activated APCs, i.e. dendritic cells, B cells and macrophages (Melero et al. 2013), where its expression is regulated by CD40 signaling (Croft 2003b). Triggering 4-1BB leads to proliferation, cytokine secretion and enhanced effector functions (Cannons et al. 2001, Wen et al. 2002) as well as increased survival by preventing activation-induced cell death. Although these stimulatory effects of 4-1BB address both $CD8^+$ and $CD4^+$ T cell populations, the $CD8^+$ T cells are primarily activated (Shuford et al. 1997, Lee et al. 2002). Due to its important costimulatory functions, 4-1BB evolved as a prime target for therapeutic manipulations. After first pioneering work with

agonistic anti-4-1BB monoclonal antibodies (Melero et al. 1997), various approaches targeting 4-1BB have been pursued, including vaccination strategies with oligomerized 4-1BBL (Srivastava et al. 2012, Schabowsky et al. 2009) and third generation CAR-T cells comprising the intracellular signaling domain of 4-1BB (Maude et al. 2014). The anti-tumor effects triggered upon stimulation of 4-1BB are mainly mediated by strong $CD8^+$ cytotoxic T lymphocyte (CTL) responses and are often associated with the activation of NK cell functions (Sanmamed et al. 2015). Additionally, the suppression of T_{regs} (Madireddi et al. 2012) and increased migration of activated T cells to the tumor site (Palazón et al. 2011) have been observed. Currently, two full-length 4-1BB-specific agonistic monoclonal antibodies are under clinical investigation. Safety and tolerability of PF-05082566 alone or in combination with rituximab (Segal et al. 2014; NCT01307267) as well as combinations with other immunomodulatory mAbs (NCT02179918, NCT02315066) are being evaluated in clinical phase I trials. Also, several phase I and II studies combining reduced doses of urelumab (BMS-663513) with various other mAbs (rituximab, NCT02420938; cetuximab, NCT02110082; elotuzumab, NCT02252263; nivolumab, NCT02253992) are ongoing, although in 2009 a phase II study of urelumab was terminated due to severe liver toxicity causing two fatalities (Ascierto et al. 2010). Since ubiquitous activation of 4-1BB after systemic delivery of agonistic mAbs partially resulted in severe side effects, strategies that are activating 4-1BB in a more (tumor-) selective way ought to be investigated. Here, the targeted delivery of recombinant trimeric 4-1BBL becomes of increasing interest.

1.2.2 OX40 and OX40L

OX40 (CD134, Paterson et al. 1987) is expressed on activated T cells of various types including also $Foxp3^+$ $CD4^+$ T_{regs}, but not on naïve or memory T cells. Depending on the environment, the expression of OX40 is more pronounced on $CD4^+$ T cells than $CD8^+$ T cells and can also be upregulated on NK cells, NKT cells and neutrophils. Its unique ligand OX40L (CD134L, Godfrey et al. 1994) exists on professional APCs like activated B cells, mature dendritic cells and macrophages, where its expression is stimulated by CD40 signaling, the B cell receptor and inflammatory cytokines (Croft 2010). Signaling through OX40/OX40L interactions and accompanying modulation of the cytokine environment support and control the expansion and survival of activated, especially $CD4^+$, T cell subsets (Gramaglia et al. 1998, Rogers et al. 2001). Furthermore, OX40 has key functions in establishing and reactivating the $CD4^+$ T cell memory (Soroosh et al. 2007, Croft 2010) and it can antagonize regulatory T cells

(So & Croft 2007, Ito et al. 2006). Targeting of OX40 has been extensively studied for cancer immunotherapy, revealing effective tumor eradication in preclinical studies (Weinberg et al. 2011). However, in accordance with the costimulatory nature of OX40 the anti-tumor effects were mostly seen in highly immunogenic mouse tumor models (Kjærgaard et al. 2000), suggesting that anti-OX40 therapies might be more effective in combinatorial approaches. In fact, several strategies combining agonistic OX40 treatment with chemotherapy, radiation, cytokines or vaccination have been evaluated successfully (Sanmamed et al. 2015). Special interest exists for combining OX40 agonists with other immunomodulatory antibodies targeting 4-1BB (Lee et al. 2004), CTLA-4 (Redmond et al. 2014) or PD-1 (Guo et al. 2014), leading to synergistic anti-tumor immune responses, mainly mediated by stimulation of $CD4^+$ and $CD8^+$ T cells and inhibition of T_{regs}. First clinical trials have been pursued with a murine anti-OX40 mAb (MEDI6469) showing good tolerability, but limited clinical responses owing to the emergence of human anti-mouse antibodies (HAMA; Curti et al. 2013). Nevertheless, further clinical trials employ MEDI6469 in combination with chemotherapy and radiation (NCT01303705) or other immunomodulatory antibodies (Powderly et al. 2015; NCT02205333). In order to circumvent immunogenicity, a humanized (MEDI0562, Leidner et al. 2015) and a fully human (PF-04518600, Hamid et al. 2016) agonistic anti-OX40 antibody entered clinical investigation after showing high anti-tumor efficacy in preclinical models.

1.2.3 CD27 and CD27L

Unlike the inducible 4-1BB and OX40 receptors, CD27 (van Lier et al. 1987) is constitutively expressed on naïve, mature and memory T cells as well as memory B cells and the expression is further upregulated upon activation (de Jong et al. 1991, Borst et al. 2005). Its ligand CD27L (CD70, Goodwin et al. 1993b) is transiently induced on mature dendritic cells, NK cells and activated T and B cells in healthy tissue, where the expression of CD27L is tightly regulated, as this constitutes the main control mechanism for the costimulatory CD27 activity in immune regulation (Borst et al. 2005). Importantly, the CD27/CD27L interactions induce *de novo* immune responses by priming the expansion of naïve $CD4^+$ and $CD8^+$ T cells. Triggering CD27 also enhances survival of cytotoxic $CD8^+$ T cells and promotes differentiation of memory $CD8^+$ T cells by inducing T_H1-type $CD4^+$ T helper cells (Nolte et al. 2009). In B cell biology, CD27 expands the population of activated B cells and supports their differentiation to plasma cells (Borst et al. 2005). Due to the aforementioned tight regulation of CD27L-expression, normal non-hematopoietic tissue is lacking CD27L and $CD27L^+$ cells are barely

found in lymphoid tissues. On the contrary, CD27L is commonly expressed on various T and B cell lymphomas as well as solid tumors like renal cell carcinoma, pancreatic cancer, ovarian cancer and melanoma (Wajant 2016). Currently, most studies suggest that tumor-associated CD27L induces continuous engagement of CD27, creating an immunosuppressive and thus pro-tumoral environment characterized by T cell exhaustion (Yang et al. 2014), apoptosis induction in T lymphocytes (Diegmann et al. 2006) and increased survival of natural T_{regs} (Coquet et al. 2013, Claus et al. 2012). Consequently, therapeutic antibodies eliciting their antitumoral potential regardless of their costimulatory activity by the induction of antibody-dependent cellular cytotoxicity (ADCC) and complement-dependent cytotoxicity (CDC) have been developed against CD27L-expressing tumor cells. Currently, three such anti-CD27L antibodies or antibody-drug conjugates are under clinical investigation (Wajant 2016). Additionally, CD27 is a potent target in cancer immunotherapy with soluble CD27L, CD27L-electroporated dendritic cells and agonistic anti-CD27 antibodies being evaluated both preclinically and clinically (Wajant 2016). First encouraging clinical results have been achieved with TriMix vaccination, a strategy where peptide-loaded dendritic cells are transfected with mRNA mixtures encoding TLR4, CD40L and CD27L (Bonehill et al. 2008, Wilgenhof et al. 2015). Furthermore, a first fully human agonistic CD27-specific antibody (varlilumab) has entered clinical trials after proving its anti-tumoral effects (He et al. 2013) and is evaluated as a potential candidate for combinatorial approaches with immune checkpoint inhibitors (Buchan et al. 2015; NCT02413827, NCT02335918, NCT02543645).

1.2.4 CD40 and CD40L

In contrast to the three previously described TNFRSF members predominantly expressed on T cells, CD40 (Paulie et al. 1985) is constitutively expressed on APCs like B cells, dendritic cells, monocytes and macrophages. Its ligand CD40L (CD154, Armitage et al. 1992) is mainly found on $CD4^+$ and $CD8^+$ T cells after activation, but also on other non-immune cell types (van Kooten & Banchereau 2000). CD40 is a critical player in both cellular and humoral immune responses. During the latter, CD40 essentially contributes to the crosstalk between B cells and T helper cells resulting in the expansion of B cells, antibody production and the development of memory B cells (Elgueta et al. 2009). In cell-mediated immunity, CD40 is important for shaping the communication between T lymphocytes and antigen-presenting cells, thus enabling APCs to prime $CD8^+$ T cells for differentiation into cytotoxic T lymphocytes. During this “licensing” of particularly dendritic cells, CD40L expressed on

$CD4^+$ T helper cells interacts with CD40 on DCs, leading to increased DC survival that is accompanied by improved antigen-presentation, the upregulation of costimulatory molecules on T cells and the secretion of immunostimulatory cytokines (Cella et al. 1996, Ridge et al. 1998, Bremer 2013). Consequently, therapeutic anti-cancer approaches on triggering CD40 aim at the effective induction of cytotoxic T cell immune responses via APC maturation that is achieved by CD40 agonists without T cell help (French et al. 1999). Pursuing this strategy, both solid tumors (Todryk et al. 2001) and hematological malignancies (Rüter et al. 2010) were treated successfully with agonistic anti-CD40 antibodies, but also recombinant soluble CD40L (Vonderheide et al. 2001). Interestingly, in combination with chemotherapy the very strong CD40 agonist CP-870,839 exhibited its antitumoral activity on pancreatic cancer independently from DCs and T cells, but directly through CD40-positive macrophages (Beatty et al. 2013). As CD40 is also expressed on various malignancies (Eliopoulos & Young 2004), triggering of CD40 can directly act against CD40-expressing tumors via apoptosis induction and growth inhibition (Zhou et al. 2012, Vonderheide & Glennie 2013). However, in some $CD40^+$ low-grade B-cell malignancies activation of CD40 resulted in growth signals, providing a rationale for the development of an antagonistic anti-CD40 mAb (lucatumumab, Fanale et al. 2014). In summary, therapeutic anti-CD40 treatment can act either on tumor cells or various immune cells, with DCs, B cells and macorphages addressed directly, while T cells and NK cells are activated indirectly via the aforementioned immune cells (Khong 2012).

1.2.5 Spatiotemporal regulation of TNFSF-mediated costimulation

All introduced costimulatory receptors are crucially contributing to the complex regulation network that controls the development of a functional immunity, including not only T cell activation, but also survival and formation of effector and memory phenotypes. During a primary T cell response, various signals are required at distinct stages, which is why the expression of TNFSF receptors and ligands is up- or downregulated depending on the dynamics of the inflammatory environment, cell subtypes and timing. This multifaceted spatiotemporal expression of costimulatory modulators influences the progress of immune activation both quantitatively and qualitatively. TNFSF ligand and receptor interactions initially occur between APCs and T cells or B cells and T cells, but with ongoing activation ligands can get upregulated on T cells and signaling between T cells arises (Croft 2003a, Chen & Flies 2013). The most important implications of 4-1BB, OX40, CD27 and CD40

costimulation on T cell immunity that have been outlined previously are summarized in Figure 3 and will be put into temporal relation in the following. Due to the complexity of the immune network the presentation focuses only on the most relevant aspects.

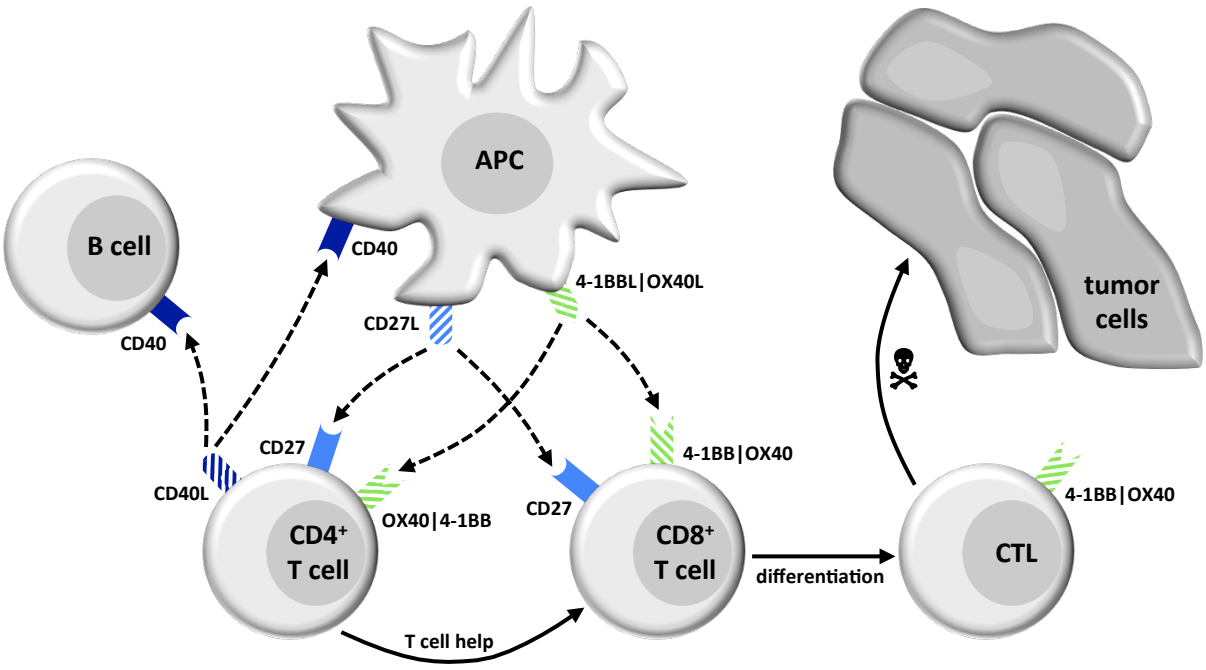

Figure 3: Antitumoral immune activation through TNFSF members. In response to primary TCR activation both naïve $CD4^+$ and $CD8^+$ T cells are primed upon CD27 engagement. Primed $CD4^+$ T cells then contribute to B cell activation and APC licensing via CD40 signals. Delayed upregulation of 4-1BB/OX40 and their ligands further activates both T cell types and promotes differentiation into effector phenotypes like tumor-reactive cytotoxic $CD8^+$ T lymphocytes (CTLs). Dashed arrows indicate interactions between TNFSF ligands and TNFRSF receptors. Normal arrows indicate other interactions. Constitutively expressed receptors are depicted as filled symbols and inducible receptors/ligands as patterned symbols. Picture based on Bremer 2013.

Following early signaling through the TCR, CD28 and the TNFRSF receptor HVEM, the constitutively expressed CD27 contributes to the process of $CD4^+$ and $CD8^+$ T cell priming, but it reaches its full expression levels not until approximately 24 hours after initial T cell activation. Consequently, CD27 appears to be critical during the clonal expansion phase (Croft 2003a). Within minutes after T cell activation, $CD4^+$ T cells transiently express CD40L and these primed $CD4^+$ T cells contribute to B cell activation and APC maturation via constitutively expressed CD40 (Schoenbeck & Libby 2001). Mature APCs are crucially involved in further progression of the immune response, where the expression of the receptors 4-1BB and OX40 is induced on T cells, accompanied by their inducible ligands on the mature APCs. From a temporal perspective, OX40 occurs within 12 to 24 hours and peaks after 2 to 3 days following antigen recognition, while 4-1BB exhibits a slightly delayed kinetic with first induction after 24 hours. Both receptors are important regulators that

sustain the ongoing immune response by promoting expansion and survival of $CD4^+$ and $CD8^+$ effector phenotypes during the survival phase (Croft 2003b). As the TNFRSF receptors are essentially involved in various spatiotemporal and functional stages of the immune response, modulation via their natural ligands evolved as a promising therapeutic approach.

1.3 Therapeutic strategies incorporating natural TNFSF ligands

As outlined previously, agonistic antibodies targeting costimulatory receptors show promising antitumoral potential, but due to potential supra-agonistic activity this artificial immunostimulation bears the risk for severe side effects like cytokine release syndrome (Suntharalingam et al. 2006) and hepatotoxicity (Ascierto et al. 2010). Consequently, the therapeutic use of the natural TNFSF ligands possibly presents an advantageous alternative. For example, the recombinant Fc:OX40L fusion protein MEDI6383 (Morris et al. 2007) exhibits strictly TCR-mediated activation of $CD4^+$ T cells and potent anti-tumor activity in xenograft mouse tumor models (Hammond et al. 2015), leading to the initiation of a phase I study in metastatic solid tumors (Bauer et al. 2015). Furthermore, oligomerized forms of CD40L and 4-1BBL have been successfully employed in various vaccination strategies, where they promote strong $CD8^+$ T cell responses (Gupta et al. 2014, Sharma et al. 2010) and a CD40L-armed oncolytic virus has entered clinical studies (Pesonen et al. 2012). However, employing costimulatory ligands in their natural homotrimeric form is associated with particular challenges. It has been observed that the soluble TNFSF ligands OX40L, 4-1BBL, CD27L and CD40L are active only in an oligomerized state, which can be realized artificially by introducing e.g. a crosslinkable FLAG-tag, a multimerization domain (N Müller et al. 2008, Wyzgol et al. 2009) or an Fc-part (Morris et al. 2007). In the physiological environment, cross-linking of costimulatory ligands is achieved by cell surface expression that can be mimicked by genetically fusing the ligand to an antibody fragment against a tumor-associated antigen, thus generating antibody-cytokine fusion proteins. This antibody-mediated presentation also confines the costimulatory activity to the tumor site (Figure 4 A), drastically reducing systemic side effects otherwise induced by ubiquitious TNFRSF-signaling (Müller 2015). Here, the smallest and most commonly used antigen-binding fragment is the monovalent single chain fragment variable (scFv), in which an antibody's variable domains of the heavy (VH) and the light (VL) chain are connected by a 15 aa linker that allows correct folding into one antigen binding site. Reducing the linker length by 5 to 10 amino acids

forces the VH and VL domain to pair with the complementary domains on a second chain, creating a bivalent diabody (Db) that can be either mono- or bispecific. Other bivalent antibody fragments like the single-chain diabody (scDb) or the tandem scFv (taFv) are characterized by further modifications of the connecting linkers (Kontermann 2005).

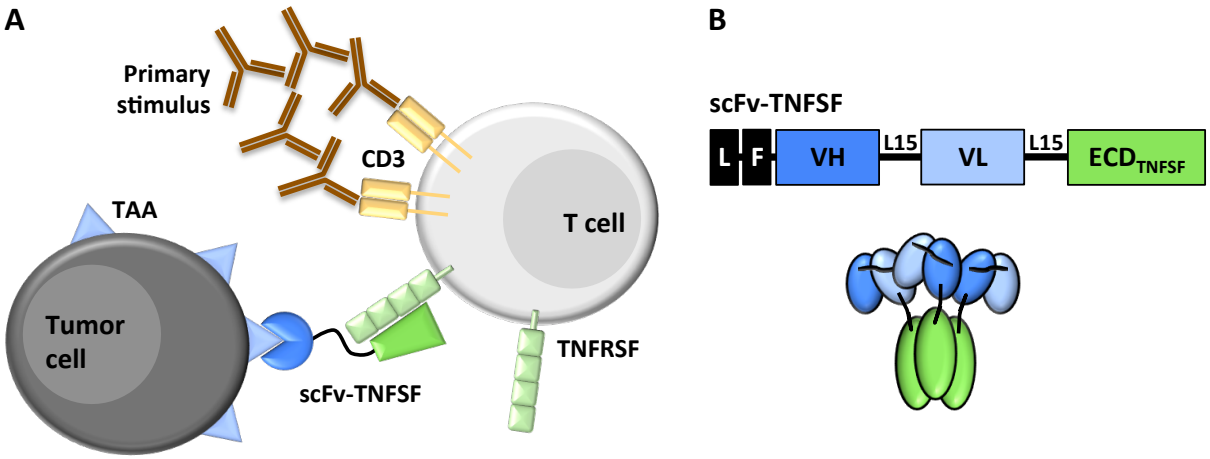

Figure 4: T cell activation via tumor-targeted costimulatory antibody-cytokine fusion proteins. A) The primary signal is mediated via the T cell coreceptor CD3 by either addressing it with crosslinked anti-CD3 mAbs (as depicted) or bispecific antibodies (Hornig et al. 2012). As a second signal, the antibody-cytokine fusion proteins bind antigens on the tumor cell, thus presenting their effector moiety to receptors on the T cell, which is subsequently activated directly at the tumor site. **B)** Genetic arrangement and structural assembly of an antibody-cytokine fusion protein in the classical scFv-TNFSF arrangement. L, leader peptide; F, FLAG-tag; V, variable domain of the heavy (H) and the light (L) chain; ECD, extracellular domain.

Furthermore, in order to preserve the biological activity of both the antibody fragment and the linked effector moiety, structural features have to be carefully considered. With immunomodulating cytokines being either monomeric (e.g. IL-2, IL-6, IL-15), homodimeric (e.g. IL-10, IFN-γ) or homotrimeric (e.g. CD40L, TNF, TRAIL), not only the selected antibody format, but also the immune-activating component influences valency and size of the fusion protein (Kontermann 2012). In fact, numerous studies evaluated the activity of various antibody-IL-2 fusion proteins, like IgG-IL-2, scFv-IL-2, scFv-Fc-IL-2 or diabody-IL-2, of which several entered clinical investigation, but other interleukins and interferons were used as effector moieties as well (Müller 2015). Antibody-cytokine fusion proteins incorporating homotrimeric TNFSF ligands like 4-1BBL, OX40L, CD27L and OX40L are mostly generated by connecting one monovalent scFv to one extracellular domain of the ligand, thus resulting in large molecules comprising one functional homotrimeric ligand and three antibody moieties (scFv-TNFSF, Figure 4 B). The costimulatory activity and the antitumoral potential of such homotrimeric scFv-TNFSF fusion proteins have been extensively demonstrated using a

FAP-directed scFv-4-1BBL fusion protein in both single and combinatorial settings (D Müller et al. 2008, Hornig et al. 2012, Hornig et al. 2013). According to the concept of tumor-targeted immune modulation, the costimulatory fusion protein itself is not able to induce T cell activation, but its effects depend on a first T cell signal. Primary stimuli for T cells can be mediated artificially either via cross-linked anti-CD3 monoclonal antibodies (Dixon et al. 1989) or bispecific antibodies that retarget cytotoxic T lymphocytes to tumor cells. In both cases, activation occurs in a MHC-independent manner by triggering the non-variable T cell coreceptor CD3 (Baeuerle et al. 2003).

1.4 Targets of anti-cancer antibodies

Direct targeting of tumor cells with immunotherapeutic approaches requires precise distinction between healthy and cancerous cells. Although cancer has developed various strategies to escape immunosurveillance, tumor cells can be recognized via a plethora of specific antigens. The majority of the known tumor antigens are the so-called tumor-associated antigens (TAAs) with shared expression between normal and tumor cells. TAAs can be classified into cancer-testis antigens, oncofetal antigens, differentiation antigens and overexpressed antigens. Cancer-testis antigens are normally found only in immune privileged organs but become aberrantly expressed in tumors, a fact rendering them highly immunogenic. The less immunogenic oncofetal antigens are present on healthy tissue only during embryonic development but can be reactivated in cancer. Differentiation antigens are associated with the differentiation stages of specific tissues and overexpressed on tumors originating from these differentiated cells. Overexpressed antigens are comprehensively found in low quantities on healthy cells but are highly overexpressed on malignant cells (Wurz et al. 2016, Seledtsov et al. 2015). The antigens targeted by the antibody-cytokine fusion proteins characterized in this study belong to the group of differentiation antigens (EpCAM) and oncofetal antigens (CLDN4/6). Besides the various TAAs, the class of tumor-specific antigens recently attracted growing attention in cancer immunotherapy. Tumor-specific antigens (mutation-derived antigens, neoantigens) are unique antigenic structures on tumor cells that develop via somatic mutations exclusive for individual tumors, therefore constituting ideal T cell targets (Lu & Robbins 2016). In fact, patient-individual sets of tumor-specific mutations (“the mutanome”) have been characterized as immunogenic and successfully employed in personalized vaccination strategies (Kreiter et al. 2014).

1.4.1 Epithelial cell adhesion molecule (EpCAM, CD326)

The epithelial cell adhesion molecule (EpCAM) was discovered in 1979 on human colon carcinoma as one of the first identified tumor-associated antigens (Herlyn et al. 1979). EpCAM is a 39 – 42 kDa type I transmembrane glycoprotein with a large extracellular domain and a short cytoplasmic tail. The first motif of the ECD resembles no clear homology to other known folds, the second is a thyroglobulin type I repeat and the third a cysteine-free domain (Patriarca et al. 2012, Schnell et al. 2013). The single transmembrane domain of EpCAM was identified to associate with the tight junction protein claudin-7 leading to a co-localization of EpCAM and claudin-7 at tight junctions (Ladwein et al. 2005, Lei et al. 2012). Though present during embryonic development promoting differentiation processes, EpCAM expression in normal adult tissue is limited to intercellular areas of simple epithelia. Here, EpCAM supports cell-cell-adhesions by promoting junctional complex formation, but it has also been identified to act as a negative regulator of adhesion by antagonizing E-cadherin. Furthermore, EpCAM is also involved in various other cellular processes like signaling, migration, proliferation and differentiation (Trzpis et al. 2007, Schnell et al. 2013). EpCAM is abundantly expressed on a plethora of mostly epithelia-derived malignancies, including nearly all carcinomas of the gastrointestinal tract as well as breast, ovarian, prostatic, bladder, lung and thyroid carcinomas (Went et al. 2004). Enhanced EpCAM expression levels are often associated with high tumorigenicity, metastasis formation and therefore poor prognosis. These findings are supported by the fact that EpCAM is expressed on circulating tumor cells (Allard et al. 2004) as well as cancer stem cells, a self-renewing cell type promoting tumor expansion and resistant to most current therapies (Patriarca et al. 2012). Due to the reduced accessibility of anyhow lower EpCAM levels in healthy tissue and its extensive overexpression on malignant cells, EpCAM targeting is of particular therapeutic interest. Already in 1995 the murine anti-EpCAM antibody edrecolomab was approved in Germany as an adjuvant therapy in patients with colon cancer, but due to lacking efficacy its approval was withdrawn shortly after (Schmoll & Arnold 2009). Since 2009, the full-length bispecific trifunctional anti-EpCAM/anti-CD3 antibody catumaxomab is approved for intraperitoneal treatment of malignant ascites in patients with $EpCAM^+$ carcinomas. The tumoricidal effects of catumaxomab are not only exerted by T cell-mediated lysis but also ADCC and phagocytosis via Fcγ receptor-engaged accessory cells (Seimetz 2011). Solitomab (AMG110, MT110), an anti-EpCAM/anti-CD3 bispecific T cell engager (BiTE) has recently

completed a clinical phase I study with patients suffering from advanced solid tumors (Fiedler et al. 2012; NCT00635596). Several other antibody-based approaches directed against $EpCAM^+$ tumors are in preclinical or early clinical investigation (Andersson et al. 2015, Liao et al. 2015), highlighting the great potential of such therapeutic concepts. The anti-EpCAM antibody fragment employed in this study is derived from 323/A3, an antibody originally generated in 1986 by immunization of mice with MCF-7 breast cancer cells (Edwards et al. 1986) that is widely used as a commercial EpCAM-detecting antibody.

1.4.2 Claudins

Claudins (CLDN, from the latin word “claudere” meaning “to close”) are a family of tetraspan membrane proteins located in the tight junctions between epithelial and endothelial cellular sheets that have first been identified in 1998 (Furuse et al. 1998). Over the following years, the claudin gene family has expanded to 27 members known today (Mineta et al. 2011). Based on sequence similarities these closely related proteins are divided into two subgroups of classic (1-10, 14, 15, 17, 19) and non-classic claudins (11-13, 16, 18, 20-24; Krause et al. 2008). Structurally, the 20 – 34 kDa proteins feature four transmembrane helices and two extracellular loops and both N- and C-terminal tail reach into the cytoplasm (Lal-Nag & Morin 2009). Claudins are essential structural components of tight junctions forming the backbone of tight junction strands and thus key functional components regulating both paracellular permeability (barrier function) and cell polarity (fence function). Furthermore, claudins are associated with the recruitment of signaling proteins and therefore involved in cellular processes like proliferation and differentiation (Schneeberger & Lynch 2004, Tsukita et al. 2001). Due to their crucial function in cellular organization, integrity and tissue homeostasis, claudins also play an important role in cancer where they show abnormal expression levels. While certain claudins (e.g. CLDN1 and CLDN7) are known to be downregulated, thereby promoting the disruption of tight junctions during tumorigenesis, many other claudins (e.g. CLDN3 and CLDN4) are highly upregulated in various cancer types like breast, prostate, pancreatic or ovarian malignancies, probably contributing to invasion and survival (Morin 2005). The expression patterns of claudins like CLDN4 can even be distinct within particular cancer subtypes, like it has been reported for different kinds of breast and gastric carcinomas (Tökes et al. 2005, Kulka et al. 2009, Resnick et al. 2005) or within the different surfaces of one tumor sample (Ueda et al. 2007). Generally, CLDN4 is one of the most thoroughly investigated claudins with overexpression observed on many

epithelial tumors including colon, esophageal, bladder, renal and endometrial cancer amongst others (Neesse et al. 2012). The widespread presence of CLDN4 on malignancies and the fact that CLDN4 is a receptor of the *Clostridium perfringens* enterotoxin (CPE) makes it an interesting therapeutic target with strategies exploiting either the direct cytotoxic effects of CPE on $CLDN4^+$ tumor cells (Michl et al. 2001, Kominsky et al. 2004) or the selective delivery of drugs coupled to non-toxic fragments of CPE (Yuan et al. 2009, Yao et al. 2010). Furthermore, chimeric antibodies targeting the extracellular loops of CLDN4 inhibited tumor growth in ovarian, pancreatic or gastric xenograft tumor models *in vivo* (Suzuki et al. 2009, Li et al. 2014). However, the expression of CLDN4 in normal healthy tissues like intestines, kidney, adrenal gland, placenta, prostate and skin (Hewitt et al. 2006) potentially complicates the use of CLDN4 as a target for systemic treatments. Targeting CLDN6, an oncofetal member of the claudin family that is expressed on healthy tissue only during early embryonic development (Abuazza et al. 2006, Hewitt et al. 2006), can circumvent this issue. Like CLDN4, CLDN6 is aberrantly activated on various cancer types including ovarian, testis, bladder (Ushiku et al. 2012), gastric (Zavala-Zedejas et al. 2011) and non-small cell lung cancer (Micke et al. 2014). Recently, the anti-CLDN6/anti-CD3 bispecific T cell engager 6PHU3 was reported to elicit almost complete tumor eradication and prolonged survival in mice (Stadler et al. 2016). The high potential of anti-CLDN6 therapy is further reinforced by the fact that the immune-activating antibody IMAB027 has recently entered clinical phase I/II (NCT02054351) showing first promising results in patients with advanced ovarian cancer (Sahin et al. 2015). While IMAB027 and its derivative 6PHU3 are highly selective for CLDN6, the antibody fragment used in this study (4H6E9) was identified as cross-reactive for CLDN4 and CLDN6. 4H6E9 was generated using hybridoma technology and verified VH and VL sequences were provided by Ganymed Pharmaceuticals AG (Mainz, Germany).

1.5 Purpose of this study

With immunotherapy rapidly evolving as a future prime strategy for cancer treatment, considerable attention shifts to the implementation of immunoactivating approaches. This study focuses on costimulatory ligands of the TNF superfamily that have been previously incorporated in bifunctional tumor-targeted antibody-cytokine fusion proteins. Based on the already very encouraging costimulatory and antitumoral effects observed for homotrimeric fusion proteins comprising one functional TNFSF ligand and three antibody units

(scFv-TNFSF), one intention was to advance this protein format into a simpler configuration by introducing the TNFSF ligands in a single-chain format. Following the concept of scFv-scTRAIL fusion proteins (Schneider et al. 2010), monomeric costimulatory fusion proteins (scFv-scTNFSF) with single-chain versions of 4-1BBL and OX40L were created against two different tumor-associated antigens (EpCAM and CLDN4/6). In direct comparison to the homotrimeric antibody-cytokine fusion proteins, the novel monomeric proteins were evaluated for receptor binding and activation, costimulatory activity, stability and pharamacokinetic properties. Secondly, a novel format of bifunctional (dual-acting) cytokine fusion proteins was established, where the two functionalities are mediated by the combination of two distinct costimulatory ligands. All possible combinations of the TNFSF ligands CD40L, CD27L, 4-1BBL and OX40L were realized in the novel “Duokines”, thus exploiting the spatiotemporal expression of their respective receptors during an immune response. Duokines were generated in two different variants, either a homotrimeric format based on intermolecular ligand trimerization or a linker-stabilized single-chain format (scDuokines). Duokines and scDuokines were evaluated in terms of protein assembly and stability, receptor binding and activation as well as immunostimulatory activity on various immune cell subsets. After determining the pharmacokinetic profile, a first proof-of-concept study for the scDuokines was implemented *in vivo* using a syngeneic tumor model with immunocompetent mice. Corresponding to the functional characteristics of TNFRSF receptor activation, fusion proteins bearing homotrimeric TNFSF ligands benefit from secondary oligomerization. Therefore, the homodimerization domain EHD2 successfully used in scFv-EHD2-scTRAIL fusion proteins (Seifert et al. 2014) was incorporated into scDuokines and the resulting EHD2-scDuokines were analyzed for potential improvements.

2 Materials and Methods

2.1 Materials

2.1.1 General declaration

All plastic material was purchased from Greiner Bio-One (Frickenhausen, Germany). All p.a. quality chemicals were purchased from Carl Roth (Karlsruhe, Germany), Merck (Darmstadt, Germany), Sigma-Aldrich (St. Louis, USA), Roche (Basel, Switzerland) or Thermo Fisher Scientific (Waltham, USA). Any different sources are clearly stated.

2.1.2 Antibodies

All antibodies were obtained from Biolegend (San Diego, USA), Ganymed Pharmaceuticals (Mainz, Germany), Immunotools (Friesoythe, Germany), KPL (Gaithersburg, USA), Miltenyi Biotec (Bergisch-Gladbach, Germany), R&D Systems (Minneapolis, USA), Santa Cruz Biotechnology (Dallas, USA) and Sigma Aldrich (St. Louis, USA).

Table 2: Antibodies used in this study.

Antibody	Isotype	Application	Source
Anti-FLAG M2-HRP	Mouse IgG1	ELISA (1:15000)	Sigma Aldrich
His-probe (H-3) HRP	Mouse IgG1	ELISA (1:1000)	SCBT
Anti-Human IgM HRP	Goat polyclonal	Assay (1:1000)	Sigma Aldrich
Human CD3ε Antibody (clone UCHT1)	Mouse IgG1	Assay-dependent	R&D Systems
Anti-mouse IgG (H+L)	Goat polyclonal	Assay-dependent	KPL
Anti-FLAG PE	Monoclonal	FC (1:200)	Miltenyi Biotec
Anti His PE	Mouse IgG1	FC (1:200)	Miltenyi Biotec
Anti-human IgG (γ-chain specific) PE	Goat polyclonal	FC (1:500)	Sigma Aldrich
Anti-mouse IgG (whole molecule) PE	Goat polyclonal	FC (1:500)	Sigma Aldrich
IMAB027-AlexaFluor647 (anti-Claudin6)	Unknown	FC (1:400)	Ganymed
PE anti human CD326 (EpCAM)	Mouse IgG2b, κ	FC (1:100)	Biolegend
FITC anti-human CD40 (5C3)	Mouse IgG1, κ	FC (1:50)	Biolegend
PE anti-human CD40 (5C3)	Mouse IgG1, κ	FC (1:200)	Biolegend
PE anti-human CD27 (O323)	Mouse IgG1, κ	FC (1:200)	Biolegend
PE anti-human CD137 (4B4-1)	Mouse IgG1, κ	FC (1:200)	Biolegend
PE anti-human OX40 (Ber-ACT35)	Mouse IgG1, κ	FC (1:200)	Biolegend
APC anti-human OX40 (Ber-ACT35)	Mouse IgG1, κ	FC (1:200)	Biolegend
FITC anti-human CD40L (24-31)	Mouse IgG1, κ	FC (1:100)	Biolegend
Anti-human CD70 (2F2)	Mouse IgG1	FC (1:100)	Immunotools
PE anti-human 4-1BBL (5F4)	Mouse IgG1, κ	FC (1:100)	Biolegend
PE anti-human OX40L (11C3.1)	Mouse IgG1, κ	FC (1:100)	Biolegend

Antibody	Isotype	Application	Source
Anti-CD3 FITC (BW264/56)	Mouse IgG2a	FC (1:200)	Miltenyi Biotec
PE anti-human CD3 (OKT3)	Mouse IgG2a, κ	FC (1:200)	Biolegend
Anti-CD4 VioBlue® (M-T466)	Mouse IgG1	FC (1:200)	Miltenyi Biotec
Anti-CD8 PE-Vio770™ (BW135/80)	Mouse IgG2a	FC (1:200)	Miltenyi Biotec
APC anti-human CD14 (M5E2)	Mouse IgG2a, κ	FC (1:200)	Biolegend
APC anti-human CD20 (2H7)	Mouse IgG2b, κ	FC (1:200)	Biolegend
Anti-CD56 PE-Vio770™ (AF12-7H3)	Mouse IgG1	FC (1:200)	Miltenyi Biotec
PE anti-human CD69 (FN50)	Mouse IgG1, κ	FC (1:200)	Biolegend
APC mouse IgG1 κ Isotype Ctrl	Mouse IgG1, κ	FC (1:100)	Biolegend
Mouse IgG1 control FITC	Mouse IgG1	FC (1:50)	Immunotools
Mouse IgG1 control PE	Mouse IgG1	FC (1:50)	Immunotools
Mouse IgG1 PE-Vio770™	Mouse IgG1	FC (1:100)	Miltenyi Biotec
Mouse IgG1 VioBlue®	Mouse IgG1	FC (1:100)	Miltenyi Biotec
Mouse IgG2a FITC	Mouse IgG2a	FC (1:50)	Immunotools
Mouse IgG2a PE-Vio770™	Mouse IgG2a	FC (1:100)	Miltenyi Biotec
APC Mouse IgG2a, κ (MOPC-173)	Mouse IgG2a	FC (1:100)	Biolegend
Mouse IgG2b APC	Mouse IgG2b	FC (1:100)	Miltenyi Biotec
PE mouse IgG2b κ Isotype Ctrl	Mouse IgG2b, κ	FC (1:100)	Biolegend

2.1.3 Bacteria strains

Escherichia coli TG1	supE thi-1 Δ(lac-proAB) Δ(mcrB-hsdSM)5 (rK-mK-) [F' traD36 proAB lacI^{q}ZΔM15] (Stratagene, La Jolla, USA)

2.1.4 Buffers and solutions

Unless stated otherwise, all solutions contained water as solvent.

Bradford Reagent	BioRad Protein Assay (BioRad, Munich, Germany)
Buffers for cloning	used as provided by the respective manufacturer
Coomassie staining solution	0.008% (w/v) Coomassie Brilliant Blue G-250, 35 mM HCl
DNA loading buffer (5x)	250 µg/ml xylenecyanol blue, 250 µg/ml bromphenol blue, 50 mM EDTA, 80% glycerol
DPBS (1x)	Dulbecco's phosphate-buffered saline (GIBCO®, Invitrogen, Carlsbad, USA)
ELISA blocking buffer (MPBS)	2% (w/v) non-fat dry milk powder in 1x PBS
ELISA blocking buffer (BSA)	1% (w/v) BSA in 1% PBS
ELISA developing solution	100 mM sodium acetate pH 6.0, 0.1 mg/ml 3,3',5,5'-tetramethylbenzidine (TMB), 0.006% (v/v) H_2O_2

ELISA wash buffer	0.005% (v/v) Tween 20 in 1x PBS
Fekete's solution	63.4% (v/v) ethanol absolute, 8.7% (v/v) formaldehyd (37%), 4.3% glacial acetic acid
HPLC buffer	0.1 M Na_2HPO_4, 0.1 M NaH_2PO_4, 0.1 M Na_2SO_4, pH 6.7
IMAC elution buffer	250 mM imidazole in sodium phosphate buffer
IMAC wash buffer	25 mM imidazole in sodium phosphate buffer
Laemmli loading buffer (5x)	25% (v/v) glycerol, 10% (w/v) SDS, 0.05% (w/v) bromphenol blue in 312.5 mM Tris-HCl pH 6.8; reducing conditions: + 12.5% (v/v) β-mercaptoethanol
PBA	2% (v/v) FBS, 0.02% (v/v) NaN_3 in 1x PBS
PBS (10x)	80.6 mM Na_2HPO_4, 14.7 mM KH_2PO_4, 1.37 M NaCl, 26.7 mM KCl; pH 7.5
Periplasmic preparation buffer	30 mM Tris-HCl pH 8.0, 20% (w/v) sucrose, 1 mM EDTA
Protein A elution buffer	100 mM glycine-HCl, pH 3.0
Protein A wash buffer	100 mM Tris-HCl, pH 7.5
Reagent diluent	0.1% (w/v) BSA, 0.05% (v/v) Tween20, 20 mM Tris, 150 mM NaCl, pH 7.2
SDS-PAGE running buffer	192 mM glycine, 25 mM Tris, 1% (w/v) SDS, pH 8.3
Sodium phosphate buffer (5x)	210 mM Na_2HPO_4, 40 mM NaH_2PO_4, 1.25 M NaCl
TAE buffer (50x)	2 M Tris, 0.95 M glacial acetic acid, 50 mM EDTA, pH 8.0

2.1.5 Cell lines

Table 3: Cell lines used in this study.

Cell line	Origin	Stably transfected	Required medium
B16-FAP	Mouse melanoma	Human FAP	RPMI 1640, 5% FBS, 0.2 mg/ml Zeocin
Bewo	Human choriocarcinoma	–	Ham's F-12 Nutrient Mix, 10% FBS
Colo-205	Human colon adenocarcinoma	–	RPMI 1640, 10% FBS
HEK293T	Human embryonic kidney	–	RPMI 1640, 5% FBS
HT1080 wt	Human fibrosarcoma	–	RPMI 1640, 10% FBS
HT1080-CD40	Human fibrosarcoma	Human CD40	RPMI 1640, 10% FBS
HT1080-CD27	Human fibrosarcoma	Human CD27	RPMI 1640, 10% FBS
HT1080-4-1BB	Human fibrosarcoma	Human 4-1BB	RPMI 1640, 10% FBS
HT1080-OX40	Human fibrosarcoma	Human OX40	RPMI 1640, 10% FBS
PBMC	Human buffy coats	–	RPMI 1640, 10% FBS

2.1.6 Enzymes

FastAP Alkaline Phosphatase	1 U/µl (Thermo Fisher Scientific, Waltham, USA)
Lysozyme	Muramidase from hen egg white (Roche Diagnostics, Mannheim, Germany)
Pfu DNA Polymerase (native)	2.5 U/µl (Thermo Fisher Scientific, Waltham, USA)
Restriction Enzymes	AgeI, ApaI, BamHI, BspEI, EcoRI, EcoRV, HindIII, KpnI, NcoI, NheI, NotI, StuI, XbaI, XhoI: 10 U/µl (Thermo Fisher Scientific, Waltham, USA)
T4 DNA Ligase	5 U/µl (Thermo Fisher Scientific, Waltham, USA)

2.1.7 Instruments

Balances	Feinwaage Basic (Sartorius, Goettingen, Germany), 440-49N, (Kern, Balingen-Frommern, Germany); Adventurer AR5120 (OHAUS, Pine Brook, USA)
Centrifuges	Centrifuge S415D, Centrifuge 5810R (Eppendorf, Hamburg, Germany); Mini Centrifuge (Nippon Genetics, Dueren, Germany); Rotanta 460 RF (Hettich Zentrifugen, Tuttlingen, Germany); Avanti™ J-30I and J2-MC with rotors JA-10, JA-14, JA-30-50; Avanti™ J-26XP with rotor JLA-8.1 (all Beckman Coulter, Krefeld, Germany)
Electrophoresis system	Mini PROTEAN® TetraCell, Mini-Sub® Cell GT and PowerPac™ Basic (Bio-Rad, Munich, Germany)
Flow cytometer	MACSQuant® Analyzer 10 and MACSQuant® VYB (Miltenyi Biotec, Bergisch-Gladbach, Germany)
Gel documentation	Transiluminator (biostep, Jahnsdorf, Germany)
Heat block	TH21, HBT-1-131 (HLC BioTech, Bovenden, Germany)
HPLC	Waters 2695 Separation Module, Waters 2489 UV/Visible Detector (Waters, Milford, USA)
Incubator for bacteria	Infors HT Multitron 2 (Infors AG, Basel, Switzerland)
CO_2 incubator for cell culture	Varocell 140 (varolab GmbH, Giesen, Germany)
Magnetic stirrer	MR3000, MR Hei-Mix S (Heidolph Instruments, Schwabach, Germany)

Laminar flow cabinet	Variolab Mobilien W90 Sicherheitswerkbank (Waldner Laboreinrichtungen, Wangen, Germany)
Microplate reader	Infinite M200 (Tecan Group, Männedorf, Switzerland)
Microscope	CKX31 (Olympus, Hamburg, Germany)
PCR cycler	RoboCycler 96 (Stratagene, La Jolla, USA)
pH-meter	PH 522 (Schütt Labortechnik, Göttingen, Germany)
Spectrophotometer	NanoDrop ND-1000 (Thermo Fisher Scientific, Waltham, USA); BioPhotometer (Eppendorf, Hamburg, Germany)
Vortex	Sky Line (ELMI, Riga, Latvia)
ZetaSizer	ZetaSizer Nano ZS (Malvern, Herrenberg, Germany)

2.1.8 Kits and markers

CellTrace™ CFSE Proliferation Kit	(Thermo Fisher Scientific, Waltham, USA)
GeneRuler™ DNA Ladder Mix	(Thermo Fisher Scientific, Waltham, USA)
Human IFN-γ DuoSet ELISA	(R&D Systems, Minneapolis, USA)
Human Interleukin-8 ELISA	(ImmunoTools, Friesoythe, Germany)
NucleoBond® Xtra Midi	(Macherey-Nagel, Düren, Germany)
NucleoSpin® Gel & PCR clean-up	(Macherey-Nagel, Düren, Germany)
NucleoSpin® Plasmid	(Macherey-Nagel, Düren, Germany)
Prestained Protein Ladder	PageRuler™ (Thermo Fisher Scientific, Waltham, USA)
REDTaq® ReadyMix™	PCR Reaction Mix (Sigma-Aldrich, St. Louis, USA)

2.1.9 Media and reagents for bacterial culture

All media and reagents were prepared as aqueous solutions.

2xTY medium (w/v)	1.6% peptone, 1% yeast extract, 0.5% NaCl
Ampicillin (1000x)	100 mg/ml
IPTG (1000x)	1 M Isopropyl-β-D-thiogalactopyranosid
LB medium (w/v)	1% peptone, 0.5% yeast extract, 0.5% NaCl
$LB_{Amp,Glc}$ agar plates	LB medium, 2% (w/v) agar after autoclaving addition of 1% (w/v) D-glucose and ampicillin to 100 µg/ml

2.1.10 Media and reagents for cell culture

Buffy Coats	from healthy donors (Blutzentrale, Klinikum Stuttgart)
Bovine Albumin (Fraction V)	7.5% (Thermo Fisher Scientific, Waltham, USA)
Cryopreservation solution	10% (v/v) dimethyl sulfoxide (DMSO) in FBS
Eosin solution	0.4 % (w/v) eosin G, 0.02 % (w/v) NaN_3 in PBS, pH 7.4
F-12 Nut Mix	+ GlutaMAX™-I (Thermo Fisher Scientific, Waltham, USA)
FBS	FBS Premium (PAN Biotech, Aidenbach, Germany)
Human Plasma	from healthy donors (Blutzentrale, Klinikum Stuttgart)
Lymphocyte Separation Medium	(PromoCell, Heidelberg, Germany)
Lipofectamine® 2000	(Thermo Fisher Scientific, Waltham, USA)
Opti-MEM®	(Thermo Fisher Scientific, Waltham, USA)
Pen/Strep (P/S)	100x (Thermo Fisher Scientific, Waltham, USA)
Puromycin	50 mg/ml (Sigma-Aldrich, St. Louis, USA)
RPMI Medium 1640 (1x)	+ L-Glutamine (Thermo Fisher Scientific, Waltham, USA)
Trypsin (10x)	0.5% Trypsin-EDTA, diluted to 1x in sterile PBS (Thermo Fisher Scientific, Waltham, USA)
Zeocin™ Selection Reagent	100 mg/ml (Thermo Fisher Scientific, Waltham, USA)

2.1.11 Mice

CD-1®	Crl:CD1(ICR) (Charles River, Wilmington, USA)
C57BL/6	C57BL/6NCrl (Charles River, Wilmington, USA)

2.1.12 Plasmids

pAB1	Vector for periplasmic protein expression in *E. coli* (Kontermann et al. 1997)
pIRESpuro3	Bicistronic mammalian expression vector (Clontech, Mountain View, USA)
pSecTagAL1	Modified vector for eukaryotic protein expression with an additional AgeI restriction site in the Igκ leader

2.1.13 Primer

All primers were synthesized by Sigma Aldrich (St. Louis, USA) and dissolved in H_2O to a concentration of 50 µM.

Table 4: Primer for sequencing.

Name	Target	Sequence (5' – 3')
pIRESpuro-back	pIRESpuro3 (forward)	ATA CGA CTC ACT ATA GGG AG
pIRESpuro3-for-new	pIRESpuro3 (reverse)	CCA ACA GCT GGC CCT CGC AGA
pET-Seq1	pSecTagA (forward)	TAA TAC GAC TCA CTA TAG GG
pSec-Seq2	pSecTagA (reverse)	TAG AAG GCA CAG TCG AGG
LMB3	pAB1 (forward)	CAG GAA ACA GCT ATG ACC
LMB4	pAB1 (reverse)	GGG GAT GTG CTG CAA GG

Table 5: Primer for cloning.

Name	Sequence (5' – 3')
ECD-Fc	
NotI-HingeIgG1-back	G AAT GCG GCC GCA GAC AAA ACT CAC ACA TGC CCA
IgG1CH3-Stop-XbaI-for	GGG TCT AGA TCA TTT ACC CGG AGA CAG GGA GAG
AgeI-hCD27ec-back	TAT ACC GGT GCC ACA CCA GCC CCT AAG
CH1-for	TGG GGG GAA GAG GAA GAC
scFv	
S1a-ATSLET-KpnI-for	GATC GGG TAC CCC GGT TTC CAG AGA GGT GGC
KpnI-S1a-SRFSGS-back	GATC GGG GTA CCC AGC AGA TTT TCC GGC AGC
S1b-ATSLET-KpnI-for	GATC GGG TAC CCC GGT TTC CAG GCT GGT GGC
TNF ligands	
NheI-huCD40Lshort-back	TGC AAA GCT AGC GGC GAC CAG AAC CCC CAG ATT
4-1BBL-Stop-NotI-for	GATC TGC GGC CGC TCA TCA TTC GCT TCT TGG AGA AGG CAG
NheI-OX40L-back	AAA GCT AGC CAG GTA TCA CAT CGG TAT
OX40L-Stop-NotI-for	AAA TGC GGC CGC TCA TCA AAG GAC ACA GAA TTC ACC AGG ATT
scFv-ligand fusion proteins	
FLAG-G_2-AgeI-NheI-for	GATC GCT AGC ACC GGT TCC GCC CTT GTC GTC GTC GTC CTT
323A3hu3-$(G_4S)_3$-NheI-for	GATC GCT AGC GCC ACC TCC AGA TCC CCC ACC GCC ACT TCC GCC TCC ACC TCT CTT GAT TTC CAG CTT GGT
4H6E9-$(G_4S)_3$-NheI-for	GATC GCT AGC GCC ACC TCC AGA TCC CCC ACC GCC ACT TCC GCC TCC ACC TTT GAT TTC CAG CTT GGT CCC
Duokines	
NheI-4-1BBL-back	AAA GCT AGC GAG GGA CCC GAG CTG AGC CCC GAT
BamHI-G_4S-CD40L-back	AAA GGA TCC GGC GGC GGA GGA AGC GGC GAC CAG AAC CCC CAG
BamHI-G_4S-CD27L-back	AAA GGA TCC GGC GGC GGA GGA AGC AGC CTG GGC TGG GAT GTG
BamHI-G_4S-OX40L-back	AAA GGA TCC GGC GGC GGA GGA AGC CAG GTA TCA CAT CGG TAT CCT CGA
BamHI-$(G_4S)_2$-4-1BBL-back	AAA GGA TCC GGC GGC GGA GGA AGC GGC GGA GGG GGA AGT AGA GAA GGA CCT GAA CTG TCT CCC

Name	Sequence (5’ – 3’)
CD40L-G_4SG_3-BamHI-for	TTT GGA TCC TCC GCC GCC GCT TCC TCC GCC GCC CAG CTT CAG CAG TCC GAA GCT GGT
CD27L-G_4SG_3-BamHI-for	TTT GGA TCC TCC GCC GCC GCT TCC TCC GCC GCC GGG GCG CAC CCA CTG CAC GCC GAA
OX40L-G_4SG_3-BamHI-for	TTT GGA TCC TCC GCC GCC GCT TCC TCC GCC GCC AAG GAC ACA GAA TTC ACC AGG ATT
4-1BBL-$(G_4S)_2G_3$-BamHI-for	TTT GGA TCC TCC GCC GCC AGA TCC CCC TCC GCC GCT TCC TCC GCC GCC TTC GCT TCT TGG AGA AGG CAG GCC
single-chain Duokines	
BspEI-random-AgeI-1288-back	GATC TCC GGA AGT AGG TGT CAT TCT ATT CTG AAT ACC GGT ATT CAG TCC ATC AAA GTG
Linker-BspEI-back	GGC GGC TCC GGA GGC GGA
AgeI-G_3S-CD40L-back	AAA ACC GGT GGA GGC GGC AGC GGC GAC CAG AAC CCT CAG ATT
CD40L-G_4SG_4-AgeI-for	TTT ACC GGT TCC GCC TCC GCC AGA TCC TCC GCC GCC CAG CTT CAG CAG CCC GAA AGA
AgeI-G_3S-CD27L-back	AAA ACC GGT GGA GGC GGC AGC TCT CTG GGA TGG GAT GTG GCC
CD27L-G_4SG_4-AgeI-for	TTT ACC GGT TCC GCC TCC GCC AGA TCC TCC GCC GCC TGG GCG CAC CCA CTG CAC CCC
AgeI-G_3S-4-1BBL-back	AAA ACC GGT GGA GGC GGC AGC AGA GAG GGA CCC GAG CTG AGC
4-1BBL-G_4SG_4-AgeI-for	TTT ACC GGT TCC GCC TCC GCC AGA TCC TCC GCC GCC TTC GCT CCG AGG GCT AGG CAG
AgeI-G_3S-OX40L-back	AAA ACC GGT GGA GGC GGC AGC CAG GTG TCC CAC AGA TAC CCC
OX40L-G_4SG_4-AgeI-for	TTT ACC GGT TCC GCC TCC GCC AGA TCC TCC GCC GCC CAG CAC ACA GAA CTC GCC TGG
murine Duokine	
NheI-m4-1BBL-back	GATC GCT AGC AGA ACC GAG CCC AGA CCC
m4-1BBL-Linker-BamHI	GATC GGA TCC TCC GCC GCC AGA TCC CCC TCC GCC GCT TCC TCC GCC GCC CTC CCA GGG GTT GTC GGG
EHD2-scDuokines	
AgeI-FLAG-XbaI-EcoRI-EHD2-back	AAA ACC GGT GAC TAC AAA GAC GAT GAC GAT AAA GGC GGT GGC GGA TCA TCT AGA GAA TTC GGG GGA AGC GGC GGT GAT TTC ACC CCC CCC ACA GTG AAG ATC CTC
EHD2-HindIII-BamHI-NotI-ApaI-for	TTT GGG CCC GGC GGC CGC GGA TCC AAG CTT ACC GCC GCT TCC CCC GTT GCT GTC
HindIII-hCD40L-back	CCC AAG CTT GGC GAC CAG AAC CCT CAG ATT GCC
hCD40L(w/oHindIII)-BamHI-for	CCC GGA TCC TCC GCC CAG TTT CAG CAG GCC GAA ACT TGT GAA GCC GGT GCC GTG
HindIII-CD27L-back	GATC AAG CTT TCT CTG GGA TGG GAT GTG
Linker-BamHI-for	TCC CCC GGA TCC TCC GCC
Linker-BspEI-back	GGC GGC TCC GGA GGC GGA
EcoRI-4-1BBL-for	GATC GAA TTC GCT CCG AGG GCT AGG CAG
NheI-XbaI-CD40L-back	GATC GCT AGC TCT AGA GGC GAC CAG AAC CCT CAG
BamHI-Linker-back	GGC GGA GGA TCC GGC GGA
EcoRI-CD40L-for	GATC GAA TTC CAG CTT CAG CAG CCC GAA

2.1.14 Proteins

Fusion proteins composed of the ECD of TNFRSF members and human Fcγ1 were cloned, produced in HEK293T cells and purified via protein A affinity chromatography.

4-1BB-Fc	Extracellular domain of human 4-1BB (aa 24-186)
OX40-Fc	Extracellular domain of human OX40 (aa 29-214)
CD27-Fc	Extracellular domain of human CD27 (aa 20-183)
CD40-Fc	Extracellular domain of human CD40 (aa 21-193)

2.1.15 Software and online tools

Antibody humanization	IgBLAST (http://www.ncbi.nlm.nih.gov/igblast/); Z-score (http://www.bioinf.org.uk/abs/shab/); IMGT (http://www.imgt.org/genedb/); Cothia Canonicals (http://www.bioinf.org.uk/abs/chothia.html)
Protein parameters	Expasy Tools (http://expasy.org/tools/)
Data evaluation	GraphPad Prism® 6 (GraphPad Software, La Jolla, USA); Microsoft Excel 2011 14.5.2 (Microsoft, Redmond, USA)
Flow cytometry	MACSQuantify 2.6 (Miltenyi Biotec, Bergisch-Gladbach, Germany); FlowJo 8.8.6 (Tree Star Inc., Ashland, USA)
Glycosylation sites	NetNGlyc (http://www.cbs.dtu.dk/services)
Literature research	Pubmed (http://www.ncbi.nlm.nih.gov/pubmed/)
Protein database	UniProt (http://www.uniprot.org/)
Sequence analysis	Serial Cloner 2.6 (http://serialbasics.free.fr/) BLAST (http://blast.ncbi.nlm.nih.gov/Blast.cgi)

2.1.16 Special implements

Anti-FLAG M2 affinity gel	(Sigma-Aldrich, St. Louis, USA)
Chromatography columns	Poly-Prep® (Bio-Rad, Munich, Germany)
Dialysis membrane	(Sigma-Aldrich, St. Louis, USA)
FLAG peptide	5 mg/ml (peptides&elephants, Potsdam, Germany)
HPLC column	Yarra SEC-3000 (Phenomenex, Torrance, USA)
IMAC affinity matrix	Protino Ni-NTA (Macherey-Nagel, Düren, Germany)
Precast protein gels, 4-15%	Mini-PROTEAN®TGX™ (Bio-Rad, Munich, Germany)

TripleFlask™	500cm², Nunclon™ Delta Surface (Thermo Fisher Scientific, Waltham, USA)
Protein A affinity resin	TOYOPEARL® AF rProtein A-650F (Tosoh Bioscience, Stuttgart, Germany)
VIVASPIN 500 Spin Columns	30000 MWCO PES (Sartorius, Goettingen, Germany)

2.2 Cloning procedures

2.2.1 Polymerase chain reaction (PCR)

PCR was used for amplification of desired DNA fragments and introduction of restriction sites for subsequent cloning. The PCR reaction was prepared as followed:

1 µl	template DNA (10 ng/µl)
5 µl	10x *Pfu* buffer with $MgSO_4$
1 µl each	forward & reverse primer (10 µM)
2.5 µl	dNTPs (5 mM each)
0.5 µl	*Pfu* Polymerase (2.5 U/µl)
39 µl	ddH_2O

DNA was amplified using a standard PCR program with 30 cycles of denaturation, annealing and elongation. Due to the limited synthesis rate of the *Pfu* polymerase of 500 nucleotides per min, the elongation time was adjusted to the expected size of the DNA fragment. The annealing temperature was varied according to the melting temperature of the primers.

Initial denaturation	5 min	94°C
Denaturation	1 min	94°C
Annealing	1 min	dependent
Extension	dependent	72°C
Final Extension	5 min	72°C

The obtained DNA was purified using preparative agarose gel electrophoresis.

2.2.2 Restriction digestion

Depending on the experiment, 10 µg DNA or the complete DNA extraction from a preparative agarose gel was digested in a volume of 50 µl. While 10 U of the restriction enzyme were used for overnight digestion, the amount of restriction enzyme was increased to 20 U when the digestion time was shortened to 3 hours. Temperature and buffer

conditions were chosen according to the manufacturer's instructions. If two restriction enzymes required different conditions, the buffer was exchanged using the NucleoSpin® Gel & PCR Clean-up kit, but whenever possible double digestion was performed. In order to prevent spontaneous religation, vector DNA was dephosphorylated using 1 U of FastAP alkaline phosphatase at 37°C for 1 h.

2.2.3 DNA electrophoresis and gel extraction

After amplification or digestion the DNA was analyzed and purified via horizontal agarose gel electrophoresis using 1% (w/v) agarose in 1x TAE buffer supplemented with 1 µg/ml ethidium bromide. DNA samples were mixed with 5x DNA loading buffer to a final concentration of 1x DNA loading buffer and applied together with GeneRuler™ DNA ladder Mix to the precast gels. Separation was performed at 80 V (1 V/cm) for 50 min. After analysis under UV lighting relevant bands were excised and purified using the NucleoSpin® Gel & PCR Clean-up kit according to the manufacturer's instructions. The concentration of the obtained DNA was determined using a NanoDrop® ND-1000 spectrophotometer.

2.2.4 Ligation and heat shock transformation

Linearized vector and insert DNA were ligated at room temperature for 1 h using 5 U T4 DNA ligase in a total volume of 20 µl. Vector and insert DNA were applied at a molar ratio of 1:3 using fixed amounts of 100 ng vector DNA. Afterwards, 10 µl of the ligation mix were incubated together with freshly thawed, chemically competent *E. coli* TG1 on ice for 15 min. The DNA uptake into the cells was achieved through heat-shocking the cells at 42°C for 45 sec and subsequent cooling on ice for 1 min. After addition of 1 ml LB medium, the cells were incubated at 37°C for 1 h to allow the cells to recover. Finally, the cells were harvested (15000 g, 1 min), plated onto $LB_{Amp,Glc}$ and incubated at 37°C over night.

2.2.5 Screening of clones

Transformed clones were screened by analytical PCR using REDTaq® ReadyMix™ by picking single clones from the transformation plates as templates for the PCR reaction and primers were chosen to flank the DNA sequence of interest. Additionally, the picked clones were streaked onto a $LB_{Amp,Glc}$ master plate and incubated at 37°C. After amplification, correct clones were identified on the basis of their predicted size using gel electrophoresis.

2.2.6 Plasmid DNA isolation

Overnight cultures were inoculated from the master plate of positively screened clones in LB with 1% (v/v) glucose and 100 µg/ml ampicillin (100 ml for midi preparation and 6 ml for mini preparation) and incubated at 37°C. The cells were harvested the following day (3500 g, 15 min, 4°C) and the DNA isolation was performed using the NucleoBond® Xtra Midi kit (midi preparation) or the NucleoSpin® Plasmid kit (mini preparation) according to the manufacturer's instructions. In the case of a midi preparation, the isolated DNA was air-dried and dissolved in 100 µl ddH_2O whereas for a mini preparation the DNA was eluted in 30 µl ddH_2O. Purified DNA was checked via sequence analysis.

2.2.7 Sequence analysis

DNA sequencing was performed using the LIGHTrun system of GATC Biotech (Cologne, Germany) and resulting DNA sequences were analyzed using Serial Cloner 2.6 and the embedded BLAST algorithm.

2.3 Cloning strategies

2.3.1 Cloning of ECD-Fc fusion proteins

At first, a tag-free acceptor vector for generating fusion proteins of the extracellular domain of TNFRSF members and a human Fc part was created. Human Fcγ1 was amplified from the plasmid pSecTagA-Fc+his using the primers NotI-HingeIgG1-back and IgG1CH3-Stop-XbaI-for and integrated into pSecTagAL1 via NotI and XbaI resulting in the acceptor vector pSecTagAge-Fc. DNA sequences encoding for the extracellular domains of CD40 (aa 21-193), CD27 (aa 20-191), 4-1BB (24-186) and OX40 (29-214) were synthesized by GeneArt (part of Thermo Fisher Scientific, Regensburg, Germany) with flanking AgeI and NotI restriction sites and ligated N-terminally to the Fc part in pSecTagAge-Fc. As Goodwin et al. 1993b found that the full-length extracellular domain of CD27 is not producible, the ECD of CD27 was shortened by 8 amino acids to aa 20-183 using the primer AgeI-hCD27ec-back and CH1-for and afterwards religated into pSecAge-Fc using AgeI and NotI.

2.3.2 Cloning of single-chain fragment variable (scFv)

DNA encoding for the murine scFv323A3 targeting EpCAM was synthesized by GeneArt including two additional restriction sites (AgeI and XhoI flanking VH) and transferred into pAB1 using flanking NcoI and NotI restriction sites. Different humanized VH and VL domains were ordered as AgeI-VH-XhoI and XhoI-VL-NotI DNA fragments and exchanged in pAB1_scFv323A3 to create pAB1_scFv323A3hu1 to pAB1_scFv323A3hu6 (Table 6).

Table 6: Combinations of scFv323A3.

Construct	VH	VL	Construct	VH	VL
pAB1_scFv323A3	VHmo	VLmo			
pAB1_scFv323A3hu1	VH1	VL1	pAB1_scFv323A3hu4	VH3	VL2
pAB1_scFv323A3hu2	VH1	VL2	pAB1_scFv323A3hu5	VH2	VL1
pAB1_scFv323A3hu3	VH2	VL2	pAB1_scFv323A3hu6	VH3	VL1

DNA sequences encoding for three different murine scFv targeting CLDN4/6 (22A, 33B, 4H6E9) as well as four humanized variants of scFv4H6E9 (hu4H-2a, hu4H-2b, hu4H-S1a, hu4H-S1b) were purchased from GeneArt and exchanged for scFv323A3 in pAB1 via AgeI and NotI. Switching of the VH domains of scFv4H6E9 and the humanized variants scFvhu4H-S1a and scFvhu4H-S1b via AgeI and XhoI resulted in 4 different chimeric scFv (Table 7).

Table 7: Chimera of scFv4H6E9 and scFvhu4H-S1a / scFvhu4H-S1b.

Chimera	VH	VL	Chimera	VH	VL
scFvhu4H-S1a mohu	4H6E9	S1a	scFvhu4H-S1b mohu	4H6E9	S1b
scFvhu4H-S1a humo	S1a	4H6E9	scFvhu4H-S1b humo	S1b	4H6E9

Furthermore, two variants of scFvhu4H-S1b with a chimeric VL domain were generated by introducing a KpnI restriction site via PCR between CDRL2 and FR3 leading to a division of the VL domain in a front part (FR1-CDRL1-FR2-CDRL2) and a back part (FR3-CDRL3-FR4). VL chimeras were cloned by inserting two different VL parts in pAB1_scFvhu4H-S1b during a one-step three-fragment ligation using XhoI, KpnI and NotI. Composition of VL chimera and used primers are shown in Table 8.

Table 8: Cloning of VL chimera of scFvhu4H-S1b.

VL Chimera	VH	VL front	VL back	Primer VL front	Primer VL back
scFvhu4H-S1b VLhumo	S1b	S1b	4H6E9	LBM3 S1b-ATSLET-KpnI-for	KpnI-S1a-SRFSGS-back LMB4
scFvhu4H-S1b VLmohu	S1b	4H6E9	S1b	LMB3 S1a-ATSLET-KpnI-for	KpnI-S1a-SRFSGS-back LMB4

Finally, four positions in FR1, four positions in FR3 and one position in FR4 of the humanized VL S1b were re-mutated to the parental murine residues. The DNA encoding for the modified VL domain was acquired from GeneArt with flanking XhoI and NotI sites and a StuI site in CDRL1. By selectively using the restriction sites only the mutated FR1 (XhoI/StuI), mutated CDRL1-FR4 (StuI/NotI) or the complete mutated VL domain (XhoI/NotI) was exchanged in pAB1_scFvhu4H-S1b resulting in three optimized humanized scFvs (Table 9).

Table 9: Versions of scFvhu4H-S1b with mutated VL.

scFv	VH	VL	Mutation in	Mutated residues
scFvhu4H-S1b VLx	S1b	mutated S1b	FR1	PL8S, L11F, A13V, V15L
scFvhu4H-S1b VLy	S1b	mutated S1b	FR3, FR4	T69K, F71Y, F73L, P80T, V104L
scFvhu4H-S1b VLxy	S1b	mutated S1b	FR1, FR3, FR4	P8S, L11F, A13V, V15L, T69K, F71Y, F73L, P80T, V104L

2.3.3 Cloning of (single-chain) TNFSF ligands

The DNA sequences encoding for the extracellular domain of CD40L (aa 51-261) and CD27L (aa 52-193) were synthesized by GeneArt with flanking EcoRV and NotI sites for cloning into pIRESpuro3. Additionally, a VH leader directly followed by a FLAG tag and an NheI restriction site as well as a stop codon at the C-terminus were included. A shorter version of CD40L (aa 116-261), containing only the TNF homology domain (THD), was cloned from pIRESpuro3_CD40L(51-261) using the primers NheI-huCD40L-short-back and pIRESpuro3-for-new. OX40L (aa 51-183) was amplified using the primers NheI-OX40L-back and OX40L-Stop-NotI with pSecTagA_scFvA5-OX40L as template, while 4-1BBL (aa 71-254) was derived from pIRESpuro3_sc4-1BBL via PCR with the primers pIRESpuro-back and 4-1BBL-Stop-NotI. CD40L(116-261), 4-1BBL and OX40L were introduced in pIRESpuro3 containing the VH leader and a FLAG tag via the restriction sites NheI and NotI. The single-chain versions were designed with three consecutive units of the TNFSF ligands separated by glycine-serine rich linkers containing BamHI (linker 1) or BspEI (linker 2). In case of scCD40L, scCD27L and

scOX40L a G_3SG_3 linker and in case of sc4-1BBL a $(G_4S)_4$ linker was used. DNA encoding for the single-chain versions was synthesized by GeneArt with flanking NheI and NotI restriction sites for cloning into pIRESpuro3 (+ VH leader & FLAG tag).

2.3.4 Cloning of scFv-ligand fusion proteins

In order to prepare for inserting different scFvs in pIRESpuro3_4-1BBL, pIRESpuro3_OX40L, pIRESpuro3_sc4-1BBL and pIRESpuro3_scOX40L, an additional AgeI restriction site was introduced between the FLAG tag and the NheI restriction site. PCR was performed with the primers pIRESpuro-back and FLAG-G_2-AgeI-NheI-for followed by inserting the DNA fragment via EcoRV and NheI. Afterwards, scFv323A3hu3 and scFv4H6E9 were amplified from pAB1 vectors using the primers LMB3, 323A3hu3-$(G_4S)_3$-NheI-for and 4H6E9-$(G_4S)_3$-NheI-for and transferred into the four previously modified plasmids via the restriction sites AgeI and NheI.

2.3.5 Cloning of Duokines

Two different TNFSF ligands (CD40L, CD27L, OX40L or 4-1BBL) were combined to Duokines (TNFSF1-linker-TNFSF2) using a BamHI site in the connecting glycine-serine rich linker. The four ligands were amplified both as N-terminal component and as C-terminal component with flanking restriction sites. Primers, templates and resulting PCR fragments are listed in Table 10. One N-terminal and one C-terminal ligand were one after another inserted in pIRESpuro3_scCD27L gradually replacing the single-chain TNFSF ligand by either NheI/BamHI or BamHI/NotI ligation, thus realizing 12 combinations of the four ligands.

Table 10: Cloning of Duokines.

Component	Primer 1	Primer 2	Template
CD40L, N-terminal	pIRESpuro-back	CD40L-G_4SG_3-BamHI-for	pIRESpuro3_CD40L
CD27L, N-terminal	pIRESpuro-back	CD27L-G_4SG_3-BamHI-for	pIRESpuro3_CD27L
OX40L, N-terminal	NheI-OX40L-back	OX40L-G_4SG_3-BamHI-for	pSecTagA_scFvA5-OX40L
4-1BBL, N-terminal	NheI-4-1BBL-back	4-1BBL-$(G_4S)_2G_3$-BamHI-for	pIRESpuro3_sc4-1BBL
CD40L, C-terminal	BamHI-G_4S-CD40L-back	pIREspuro3-for-new	pIRESpuro3_CD40L
CD27L, C-terminal	BamHI-G_4S-CD27L-back	pIREspuro3-for-new	pIRESpuro3_CD27L
OX40L, C-terminal	BamHI-G_4S-OX40L-back	OX40L-Stop-NotI-for	pSecTagA_scFvA5-OX40L
4-1BBL, C-terminal	BamHI-$(G_4S)_2$-4-1BBL-back	pIREspuro3-for-new	pIRESpuro3_sc4-1BBL

2.3.6 Cloning of single-chain Duokines

Single-chain Duokines (scDuokines, scTNFSF1-linker-scTNFSF2) were cloned by connecting two scTNFSF ligands via a AgeI-containing 15 aa glycine-serine rich linker. Cloning was performed as multi-step strategy gradually inserting the extracellular domains of the various ligands. At first, by replacing the third OX40L in pIRESpuro3_scOX40L with AgeI the new acceptor vector pIRESpuro3_OX40L$_2$-BspEI-AgeI-NotI was generated via PCR with the primers BspEI-random-AgeI-1288-back and pIRESpuro3-for-new. Afterwards, the two remaining OX40L units in the acceptor vector were exchanged with CD40L$_2$, CD27L$_2$ or 4-1BBL$_2$ previously excised from the pIRESpuro3_scTNFSF plasmids via NheI and BspEI, leading to three additional acceptor vectors (pIRESpuro3_CD40L$_2$-BspEI-AgeI-NotI, pIRESpuro3_CD27L$_2$-BspEI-AgeI-NotI, pIRESpuro3_4-1BBL$_2$-BspEI-AgeI-NotI). The third ECD of the N-terminal TNFSF ligand and the whole C-terminal scTNFSF were amplified according to Table 11 and one after another inserted into the acceptor vectors via BspEI/AgeI or AgeI/NotI. In total, 12 different scDuokines were generated.

Table 11: Cloning of single-chain Duokines.

Component	Primer 1	Primer 2	Template
CD40L, N-terminal	Linker-BspEI-back	CD40L-G$_4$SG$_4$-AgeI-for	pIRESpuro3_scCD40L
CD27L, N-terminal	Linker-BspEI-back	CD27L-G$_4$SG$_4$-AgeI-for	pIRESpuro3_scCD27L
4-1BBL, N-terminal	Linker-BspEI-back	4-1BBL-G$_4$SG$_4$-AgeI-for	pIRESpuro3_sc4-1BBL
OX40L, N-terminal	Linker-BspEI-back	OX40L-G$_4$SG$_4$-AgeI-for	pIRESpuro3_scOX40L
scCD40L, C-terminal	AgeI-G$_3$S-CD40L-back	pIREspuro3-for-new	pIRESpuro3_scCD40L
scCD27L, C-terminal	AgeI-G$_3$S-CD27L-back	pIREspuro3-for-new	pIRESpuro3_scCD27L
sc4-1BBL, C-terminal	AgeI-G$_3$S-4-1BBL-back	pIREspuro3-for-new	pIRESpuro3_sc4-1BBL
scOX40L, C-terminal	AgeI-G$_3$S-OX40L-back	pIREspuro3-for-new	pIRESpuro3_scOX40L

2.3.7 Cloning of murine homologs of Duokines and scDuokines

One exemplary murine Duokine was cloned by exchanging CD40L and 4-1BBL with mCD40L and m4-1BBL in pIRESpuro3_CD40L-4-1BBL in a one-step three-fragment ligation via NheI, BamHI and NotI. Therefore, m4-1BBL was amplified from pSecTagA_scFvmE12-m4-1BBL using the primers NheI-m4-1BBL-back and m4-1BBL-Linker-BamHI, while the DNA for mCD40L with an N-terminal linker, a C-terminal stop codon and flanking BamHI and NotI restriction sites was synthesized by GeneArt. BioNTech AG (Mainz, Germany) provided DNA coding for mscCD40L-mscCD27L, msc4-1BBL-mscCD40L and msc4-1BBL-mscCD27L.

2.3.8 Cloning of EHD2 single-chain Duokines

For generating homodimerized scDuokines (scTNFSF1-EHD2-scTNFSF2), the heavy chain domain 2 of IgE (EHD2) was amplified by PCR from pSecTagFLAG_EHD2-scTRAIL using the primers AgeI-FLAG-XbaI-EcoRI-EHD2-back and EHD2-HindIII-BamHI-NotI-ApaI-for, adding various restriction sites for further cloning at the same time. The DNA fragment was introduced in pSecTagAL1 via AgeI and ApaI, resulting in the acceptor vector pSecTagFLAG-EHD2. In order to eliminate a HindIII restriction site from scCD40L, the first CD40L unit was amplified from pIRESpuro3_scCD40L with the primers HindIII-hCD40L-back and hCD40L(w/oHindIII)-BamHI-for, while the two other CD40L units were excised via BamHI and NotI from pIRESpuro3_scCD40L. Consecutively inserting CD40L (HindIII/BamHI) and $CD40L_2$ (BamHI/NotI) in the acceptor vector created the first intermediate construct pSecTagFLAG_EHD2-scCD40L. Similarly, via PCR with pIRESpuro3_scCD27L as template and primers HindIII-CD27L-back and Linker-BamHI-for, CD27L was provided with flanking HindIII and BamHI sites. The PCR fragment and $CD27L_2$ (excised from pIRESpuro3_scCD27L via BamHI/NotI) were afterwards consecutively inserted into the acceptor vector pSecTagFLAG-EHD2, resulting in the second intermediate construct pSecTagFLAG_EHD2-scCD27L. In order to create the N-terminal sc4-1BBL unit, flanking XbaI and EcoRI restriction sites were introduced by PCR with the primers Linker-BspEI-back and EcoRI-4-1BBL-for to the template pIRESpuro3_sc4-1BBL. The DNA fragment XbaI-sc4-1BBL-EcoRI was then introduced into pSecTagFLAG_EHD2-scCD40L and pSecTagFLAG_EHD2-scCD27L resulting in two EHD2-scDuokines. After amplifying scCD40L with flanking XbaI and EcoRI restriction sites via two PCR steps with pIRESpuro3-scCD40L as template and the primer pairs NheI-XbaI-CD40L-back/Linker-BamHI-for and BamHI-Linker-back/EcoRI-CD40L-for, the fragment XbaI-scCD40L-EcoRI was cloned into pSecTagFLAG_EHD2-scCD27L creating the third EHD2-scDuokine.

2.4 Humanization of antibody fragments

The murine antibody fragments scFv323A3 and scFv4H6E9 were humanized *in silico* under guidance of Dr. Roland Kontermann. Therefore, the amino acid sequences of the variable domains (VH and VL) were individually aligned to mouse and human germline genes using the IgBLAST algorithm. Alignments showing the highest homology were evaluated for their humanness (Z-score, Abhinandan et al. 2007) and the sequences with the most suitable Z-scores were further checked for functionality using the IMGT database. Then, the CDR

regions of the murine VH and VL domain were grafted onto the chosen human framework regions and the resulting humanized domains were checked for their Z-score again. As final step, the canonical structure of the newly designed antibody fragment was evaluated using the Cothia Canonical tool provided by Andrew C.R. Martin. If necessary, inappropriate amino acids in the framework regions were substituted and the final humanized scFvs were cloned as described previously.

2.5 Cell culture

2.5.1 General cell culture techniques

Eukaryotic cells were cultivated at 37°C in a humidified 5% CO_2 atmosphere and appropriate medium (Table 3). Adherent cells were detached using 1x Trypsin-EDTA and passaged every two or three days according to their confluence. To determine the cell count, the cell suspension was mixed 1:1 with eosin red (dead-live staining) and counted using a Neubauer chamber. For long-term storage, cells were harvested and resuspended in FBS + 10% (v/v) DMSO, aliquoted into cryo vials and gradually frozen to -80°C using a cryobox filled with isopropanol. Frozen cell stocks were defrosted by washing the content of one cryo vial with 5 ml culture medium to remove residual DMSO and afterwards transferred to a cell culture flask containing the appropriate culture medium.

2.5.2 Transfection and selection of transfectants

For eukaryotic production of recombinant proteins, HEK293T cells were transfected with circular plasmids (pSecTagA and pIRESpuro3). $1*10^6$ cells were seeded in 2 ml culture medium in a 6-well plate and incubated overnight at 37°C. The next day the medium was replaced by 1.4 ml Opti-MEM® and two transfection solutions were prepared. While solution A consisting of 166 µl Opti-MEM® and 6.66 µl lipofectamine was incubated at room temperature for 5 min, solution B was prepared by mixing 2.66 µg DNA with 166 µl Opti-MEM®. Both solutions were combined and incubated for 20 min at room temperature, before carefully adding the mixture to the cells. DNA lipofection occurred during incubation at 37°C and 5% CO_2 for at least six hours up to overnight. To generate stable transfectants, the transfection mix was removed and the cells were transferred to a 75 cm^2 cell culture flask containing culture medium. After incubating the cells at 37°C, 5% CO_2 for approx. 4 h, the appropriate selection antibiotic (300 µg/ml Zeocin™ or 10 µg/ml puromycin) was applied

to select successfully transfected clones. The selection medium was replaced twice a week until resistant cell colonies grew up (approx. three weeks after transfection). After reaching 80% confluence, the stable transfectants were transferred to a medium sized cell culture flask for further expansion and cryopreserved at -80°C.

2.5.3 Isolation and handling of peripheral blood mononuclear cells (PBMC)

PBMCs were isolated from buffy coats of anonymous, healthy donors provided by the blood donation center (Blutzentrale, Klinikum Stuttgart, Germany). All steps during PBMC isolation were performed at room temperature with room temperature reagents. Buffy coats (approx. 60 ml) were diluted with RPMI 1640 to a total volume of 240 ml. In order to separate erythrocytes and granulocytes from leukocytes, 10 ml Lymphocyte Separation Medium were layered with 30 ml buffy coat and centrifuged at 800 g for 20 min (without brake). PBMCs were then extracted from the resulting interphase, diluted to 40 ml with RPMI 1640 and centrifuged at 650 g for 15 min. To remove residual platelets, the cell pellet was washed twice with 40 ml RPMI 1640. In a last step, the total cell count (usually 3 – 5*10^8 cells) was determined and cells were cryopreserved until usage. Generally, PBMCs were defrosted one day before using them in particular experiments.

In order to analyze the proliferation rate upon stimulation, PBMCs were labeled using the CellTrace™ CFSE Proliferation Kit prior to their use in the respective assay. Therefore, PBMCs were resuspended in PBS + 0.1% BSA at a cell density of 1*10^6 cells/ml and CFSE was added to a final concentration of 625 nM. After 10 min incubation at 37°C, staining was quenched by incubating 5 min on ice and adding double the volume of cold RPMI 1640 + 10% FBS. After two washing steps, the cell density was determined and set to meet the requirements of each assay individually. Each newly isolated PBMC batch was specifically tested for its proliferative response by applying serial dilutions of crosslinked anti-human CD3 mAb (1000 – 0.1 ng/ml). Therefore, anti-human CD3 and anti-mouse IgG (H+L) were incubated at a molar ratio of 1:3 for 30 min and afterwards applied to the PBMCs for 6 days. Depending on the individual results, a suboptimal antibody concentration realizing stimulation resulting in 10 – 40% proliferation was implemented for continuative proliferation assays.

2.6 Expression and purification of recombinant protein

2.6.1 Periplasmic protein expression in *E. coli* TG1

1000 ml 2xTY medium containing 0.1% (v/v) glucose and 100 µg/ml ampicillin were inoculated 1:100 with an overnight culture of TG1 transformed with pAB1 and incubated at 37°C until the culture reached the exponential growth phase (OD_{600} 0.8 – 1.0). Adding IPTG to a final concentration of 1 mM induced periplasmic protein expression and the cultures were shaken at room temperature. After 3 h the cells were harvested (6200 g, 10 min) and the cell pellet was dissolved in 50 ml periplasmic preparation buffer. Cell wall lysis was carried out by incubating with 50 µg/ml lysozyme 20 min on ice and followed by adding 10 mM $MgSO_4$ to stabilize the spheroblasts. Cell debris was removed by centrifuging for 10 min at 9820 g (rotor JA-14) and the protein containing supernatant was dialyzed over night against 5 liter 1x PBS at 4°C. The next day, proteins were purified from the dialyzed supernatant via immobilized metal ion affinity chromatography (IMAC).

2.6.2 Eukaryotic protein expression in adherent HEK293T

After successful selection of stable transfectants, HEK293T cells were expanded stepwise to triple flasks using their respective selection medium (+ 10 µg/ml puromycin for pIRESpuro3 plasmids or + 50 µg/ml Zeocin™ for pSecTag plasmids). After reaching 80% confluence the medium was changed to 100 ml serum-free Opti-MEM® per triple flask and replaced every three to four days for at least three times. Protein-rich supernatants were collected, centrifuged (500 g, 5 min), filtered through a 0.45 µm membrane and stored at 4°C until further processing. Before purification, proteins not containing OX40L were precipitated by adding 390 g/l ammonium sulfate and stirring for at least 30 min. The precipitated protein was harvested (11250 g, 30 min, 4°C) and dissolved in PBS.

2.6.3 Immobilized metal ion affinity chromatography (IMAC)

Antibody fragments (scFv and scDb) were purified via their His-tag using immobilized nitrilotriacetic acid (Ni-NTA) agarose beads charged with Ni^{2+} as matrix. During semi-batch processing the precipitated proteins or dialyzed periplasmic extracts were incubated under rotation with usually 0.5 ml agarose beads overnight at 4°C. For further purification the beads-containing suspension was loaded into a Poly-Prep® chromatography column and unspecifically bound proteins were washed away using IMAC wash buffer containing 25 mM

imidazole. Afterwards, the His-tagged protein was eluted from the affinity matrix in 500 µl fractions with IMAC elution buffer containing 250 mM imidazole. The protein level in wash and elution fractions was determined by means of a qualitative Bradford assay (90 µl Bradford reagent plus 10 µl sample). Protein containing fractions were pooled and dialyzed against 5 liter 1x PBS overnight.

2.6.4 Protein A affinity chromatography

Fusion proteins consisting of the extracellular domain of a TNFSF receptor and the Fc part of human IgG1 were purified via protein A affinity chromatography using 250 µl TOYOPEARL® AF rProtein A-650F as matrix. The procedure was performed as described for IMAC with 100 mM Tris-HCl pH 7.5 as wash buffer and 100 mM glycine-HCl pH 3.0 as elution buffer.

2.6.5 FLAG affinity chromatography

All immunostimulatory fusion proteins containing a FLAG-tag were purified via affinity chromatography using anti-FLAG antibodies covalently attached to agarose beads (ANTI-FLAG® M2 affinity gel). 2 ml agarose beads were loaded to a PolyPrep® chromatography column and equilibrated by washing with three column volumes of 100 mM glycine-HCl pH 3.0 und and subsequent recovering with five column volumes of 1x PBS. Semi-batch purification of proteins from either sterile-filtered or precipitated cell culture supernatants was performed as described for IMAC with DPBS as wash buffer. FLAG-tagged proteins were eluted in one fraction from the matrix using 0.1 mg/ml FLAG peptide and dialyzed against 5 liter 1x PBS overnight at 4°C. After elution, the affinity gel was again equilibrated as described before and stored in PBS + 0.02% NaN_3 at 4°C.

2.7 Biochemical protein characterization

2.7.1 Protein concentration

Mass concentrations $c\ [\frac{mg}{ml}]$ of purified proteins were determined with a NanoDrop 1000 spectrophotometer by correlating the absorbance A of tryptophan and tyrosine residues at 280 nm with the molecular weight of the protein using the following formula based on the Beer-Lambert equation

$$c = \frac{A}{\varepsilon_P * b} * M_P$$

with M_P $[\frac{g}{mol}]$ being the molecular weight of the protein, ε_P $[\frac{l}{mol*cm}]$ the molar extinction coefficient of the protein and b $[cm]$ the path length. Molecular weight and molar extinction coefficient of the purified proteins were calculated using the online tool ProtParam.

2.7.2 SDS polyacrylamide gel electrophoresis

Recombinant proteins were analyzed for molecular mass and purity using SDS polyacrylamide gel electrophoresis (SDS-PAGE). Protein samples (3 µg) were mixed with reducing or non-reducing Laemmli loading buffer (final concentration 1x), denatured at 95°C for 5 min and separated at 40 mA per gel in SDS-PAGE running buffer using precast polyacrylamide gels. Depending on the molecular mass of the protein, different polyacrylamide concentrations were used for the separating gels (Table 12). After separation, residual salt and detergent were removed by boiling the polyacrylamide gel three times in H_2O and proteins were visualized by incubating in Coomassie staining solution for at least 1 h and destaining in H_2O over several hours.

Table 12: Composition of polyacrylamide gels (two each).

	Stacking gel 5%	Separating gel 10%	Separating gel 12%	Separating gel 15%
ddH_2O	4.1 ml	5.9 ml	4.9 ml	3.4 ml
30% PAA	1.0 ml	5.0 ml	6.0 ml	7.5 ml
1.5 M Tris-HCl pH 8.0	–	3.8 ml	3.8 ml	3.8 ml
1 M Tris-HCl pH 6.8	0.75 ml	–	–	–
10% SDS	0.06 ml	0.15 ml	0.15 ml	0.15 ml
10% APS	0.06 ml	0.15 ml	0.15 ml	0.15 ml
TEMED	0.006 ml	0.006 ml	0.006 ml	0.006 ml

2.7.3 Size exclusion chromatography (SEC)

Protein purity and assembly under native conditions were determined by analytical gel filtration using high-pressure liquid chromatography (HPLC) with a Yarra SEC-3000 or SEC-2000 column. 25 µl protein with a concentration of 0.1 to 0.3 mg/ml were analyzed at a flow rate of 0.5 ml/min in a 0.1 M Na_2HPO_4/NaH_2PO_4, 0.1 M Na_2SO_4, pH 6.7 mobile phase. Thyroglobulin (669 kDa, 8.5 nm), apoferritin (443 kDa, 6.1 nm), β-amylase (200 kDa, 5.4 nm), alcohol dehydrogenase (150 kDa), bovine serum albumin (67 kDa, 3.55 nm), carbonic anhydrase (29 kDa, 2.35 nm) and FLAG peptide (1 kDa) served as standard proteins for calculating molecular masses and hydrodynamic radii.

2.7.4 Thermal stability

Thermal stability of antibody fragments was analyzed by dynamic light scattering using a ZetaSizer Nano ZS. 100 µg protein in 1 ml PBS were sterile filtered into a quartz cuvette and mean count rates were measured while temperature was increased in 1°C intervals from 35°C up to 90°C with two minutes equilibration at each temperature step. With the mean count rate indicating the size of denatured protein particles and aggregates, the temperature connected with an increase in the mean count rate was defined as aggregation point (T_m) of the protein.

2.8 General experimental practices for functional experiments

In general, all protein samples and serial dilutions were prepared in duplicates using the appropriate solvent (MPBS for binding-ELISA, RPMI 1640 for cytokine-ELISA, PBA for flow cytometry, RPMI 1640 + 10% FBS for cell assays and DPBS for *in vivo* experiments). During all *in vitro* and *in vivo* experiments, the concentrations were determined using the molecular masses of the trimers, therefore referring to functional homotrimeric TNFSF ligand units. Animal care and all *in vivo* experiments were performed in accordance with federal guidelines and approved by the university and state authorities. Dr. O. Seifert or M. Hutt performed all intravenous injections.

2.9 Enzyme-linked immunosorbent assay (ELISA)

Binding of TNFSF ligands incorporated in different fusion proteins to their receptors was assessed by means of ELISA in order to determine the half-maximal binding or the concentration of fusion protein in a sample. Therefore, 200 ng recombinant receptor (CD40-Fc, CD27-Fc, 4-1BB-Fc, OX40-Fc; developed and produced as part of this study) were immobilized on 96-well ELISA plates overnight at 4°C in 100 µl PBS followed by blocking of residual binding sites with 200 µl 2% MPBS. Meanwhile, protein samples were diluted in duplicates in 2% MPBS and after at least 1 h blocking 100 µl of the diluted samples were added to the plate to incubate for 1 h. Bound proteins were detected via their FLAG-tag using 100 µl HRP-conjugated anti-FLAG® M2 antibody (1:15,000 in 2% MPBS, 1 h incubation). After each incubation step, the ELISA plate was washed three times with 0.005% PBS-Tween and two times with PBS. Finally, the ELISA was developed using 100 µl substrate solution

(100 mM sodium acetate buffer pH 6.0, 0.1 mg/ml TMB, 0.006% H_2O_2) and the HRP-mediated enzymatic reaction was stopped by adding 50 µl 1M H_2SO_4. Absorbance was measured at 450 nm with an Infinite M200 microplate reader.

2.10 Flow cytometry

2.10.1 Cell surface marker expression

In general, the cell surface expression of CD markers (CD3, CD4, CD8, CD14, CD20, CD56, CD69), costimulatory receptors (CD40, CD27, 4-1BB, OX40) or tumor-associated antigens (EpCAM, CLDN6) was determined by flow cytometry. The untreated or pre-treated target cells were seeded in a U-bottom microtiter plate and incubated with 100 µl directly labeled monoclonal antibodies (dilutions see Table 2) at 4°C for 1 h. Afterwards, cells were washed three times with 150 µl PBA and analyzed using a MACSQuant Analyzer 10 or MACSQuant VYB. In case of multi-color staining, spectral overlap was compensated prior to the experiment. Receptor or antigen expression on tumor cells (Bewo, HT1080) was analyzed using $1.5*10^5$ untreated cells. The CD69 expression on B cells was determined after stimulating $1.5*10^5$ PBMCs with coated anti-IgM antibody or scDuokines over 24 h. The distribution of monocytes, T cells, B cells and NK cells in the leukocyte population of bulk PBMC batches as well as the upregulation of costimulatory receptors on those cells was tested using $2.5*10^5$ PBMCs stimulated with scDuokines in presence or absence of crosslinked anti-CD3 mAb for 1 h or 72 h. Antibody combinations for determining leukocyte subpopulations are shown in Table 13.

Table 13: Identification of leukocyte subpopulations.

Leukocyte subpopulation	Fluorochrome-conjugated antibodies
$CD4^+$/ $CD8^+$ T cells	CD3-FITC, CD4-VioBlue, CD8-PE-Vio770
$CD14^+$ monocytes	CD3-FITC, CD14-APC
$CD20^+$ B cells	CD3-FITC, CD20-APC
$CD56^+$ NK cells	CD3-FITC, CD56-PE-Vio770

2.10.2 Determination of half-maximal binding

Binding of antibody fragments to surface antigens or of immunostimulatory ligands to cell surface-expressed receptors was analyzed by flow cytometry. Target cells were detached and $1.5 – 2.5*10^5$ cells per well (HT1080-CD40, HT1080-CD27, HT1080-4-1BB, HT1080-OX40,

Bewo, B16-FAP) were seeded in U-bottom microtiter plates. After removal of the culture medium, the cells were incubated with serial dilutions of the different fusion proteins (scFv, scDb, scFv-ligand fusion proteins, Duokines) in 100 µl PBA for 1 h at 4°C. Cells were centrifuged (500 g, 5 min) and washed twice in 150 µl PBA prior to incubating with detection antibody (anti-His PE, anti-FLAG PE; for dilutions refer to Table 2) in 100 µl PBA. After three washing steps with 150 µl PBA, cells were resuspended in 150 µl PBA and analyzed in a MACSQuant Analyzer 10 or MACSQuant VYB. Relative mean fluorescence intensities MFI were calculated with the formula:

$$relative\ MFI = \frac{(MFI_{sample} - (MFI_{detection} - MFI_{cells})}{MFI_{cells}}$$

Following a method published by Benedict et al. 1997 the concentration corresponding to half-maximal binding (EC_{50}) was calculated from the relative MFI using Graphpad Prism 6.

2.11 Protein Stability

2.11.1 *In vitro* serum stability

To determine the serum stability of all immunostimulatory fusion proteins, samples with a protein concentration of 200 nM were prepared in 50% human plasma in duplicates. Samples were frozen at -20°C immediately after preparation (0 d) or after incubating at 37°C for 1 d, 3 d and 7 d. The level of intact protein was determined in ELISA via binding of the C-terminal homotrimeric ligand to its corresponding immobilized receptor (150 ng/well) and detection of the N-terminal FLAG-tag. ELISA with different dilutions of the samples (1:10, 1:40, 1:160, 1:640) was performed as described in chapter 2.9. Protein concentrations in the diluted samples were interpolated from a standard curve of purified fusion protein and the amount of detected protein at day 0 was set to 100%.

2.11.2 *In vivo* pharmacokinetics

In order to determine the bioavailability of the immunostimulatory fusion proteins, groups of three female CD-1® mice at the age of 12-16 weeks received one intravenous injection of 25 µg protein in 150 µl DPBS. Blood samples (50 µl) were taken from the tail vein at different time points (3, 30, 60, 120 min, 6, 24 and 72 h) and directly incubated on ice. Coagulated blood was centrifuged at 13000 g (30 min, 4°C) to separate serum from cellular components and samples were stored at -20°C. Serum concentration of fusion proteins was determined

via ELISA using immobilized human receptors as described in chapter 2.9. Crossreactivity between human receptors and murine ligands was confirmed before and immobilizing the receptor corresponding to the C-terminal ligand followed by detecting the N-terminal FLAG-tag ensured the identification of only intact fusion protein. Pharmacokinetic parameters (initial half-life, $t_{1/2}\alpha$; terminal half-life, $t_{1/2}\beta$; area under the curve, AUC) were calculated using Excel.

2.12 Functional characterization

2.12.1 Interleukin-8 release assay

Functionality of the TNFSF ligands incorporated in the different immunostimulatory fusion proteins was assessed in a cell-based reporter assay measuring IL-8 released by HT1080 cells upon TNFR-dependent NF-κB activation. Therefore, HT1080 wt, HT1080-CD40, HT1080-CD27, HT1080-4-1BB or HT1080-OX40 ($2*10^4$ cells/well) were seeded in culture medium and incubated overnight at 37°C, 5% CO_2. The next day, supernatants were discarded to remove constitutively produced IL-8 and cells were incubated with serial dilutions of the fusion proteins (100 µl, duplicates) at 37°C, 5% CO_2. After 18 hours cell-free supernatants were analyzed directly by Sandwich ELISA using human Interleukin-8 ELISA kit (Immunotools, Friesoythe, Germany) according to the manufacturer's instructions. Supernatants and IL-8 standard were diluted in RPMI 1640, all antibodies in reagent diluent.

2.12.2 Interferon-γ release assay

Costimulatory potential of the scFv-ligand fusion proteins was evaluated by measuring the amount of IFN-γ secreted by activated PBMCs in a targeted setting. Therefore, $3*10^4$ Bewo cells per well were seeded in 100 µl culture medium and incubated overnight at 37°C, 5% CO_2. Also, PBMCs were thawed and kept in culture medium at 37°C, 5% CO_2 overnight to allow adherence of monocytes. The next day, the culture medium was removed and Bewo cells were incubated with 50 µl of serial dilutions of the scFv-ligand fusion proteins for 1 h at room temperature before adding $2*10^5$ PBMCs in 100 µl RPMI 1640 + 10% FBS per well. Additionally, PBMCs were activated by adding 50 µl anti-human CD3 mAb (concentration PBMC-batch dependent) previously crosslinked for 30 min with an anti-mouse IgG mAb at a molar ratio of 1:3. Fusion proteins and crosslinked anti-CD3 mAb were prepared in RPMI 1640 + 10% FBS. After 48 h incubation at 37°C, 5% CO_2 cell-free supernatants were collected

and stored at -20°C until the IFN-γ concentration was determined using a human IFN-γ DuoSet® ELISA kit according to the manufacturer's instructions. As for IL-8 ELISA, supernatants and standard were diluted in RPMI 1640, all antibodies in reagent diluent.

2.12.3 Proliferation

For analyzing T cell or B cell divisions upon stimulation with the various immunostimulatory fusion proteins, PBMCs defrosted the day before the experiment were labeled with CFSE as described in section 2.5.3. Proliferation experiments were carried out in a total volume of 200 µl RPMI 1640 + 10% FBS containing between 1.5 and $2.5*10^5$ PBMCs per well. The T cells of the PBMC bulk populations were activated with crosslinked anti-human CD3 mAb at a batch-specific concentration (3 – 30 ng/ml) leading to suboptimal stimulation, while no anti-CD3 stimulation was applied for B cell proliferation. In different settings PBMCs were incubated together with the examined fusion proteins and the primary anti-CD3 stimulus for 6 days and proliferation was determined by analyzing the CFSE dilution in flow cytometry. In order to identify T and B cell populations additional antibody staining was performed: PBMCs were harvested from the assay plate (500 g, 5 min), incubated with anti-CD3 PE, anti-CD4 VioBlue and anti-CD8 PE-Vio770 or anti-CD3 PE and anti-CD20 APC for 1 h at 4°C and washed twice with 150 µl PBA directly before flow cytometric analysis.

Soluble (untargeted) setting

In this setting dilutions of the examined fusion proteins (scFv-ligand fusion proteins or Duokines) were prepared in 50 µl in an untreated microtiter plate, the primary stimulus (50 µl) and CFSE-labeled PBMCs ($1.5 – 2.5*10^5$ in 100 µl) were added at once and the assay was kept at 37°C, 5% CO_2 for 6 days.

Targeted setting with antigen-positive tumor cells

For the targeted setting $3*10^4$ Bewo cells per well were seeded and incubated overnight at 37°C, 5% CO_2. The next day, supernatants were removed and cells were incubated with serial dilutions of the scFv-ligand fusion proteins (50 µl) for 1 h at room temperature before adding $1.5*10^5$ PBMCs (100 µl) and the primary stimulus (50 µl) at once. Afterwards, the assay was incubated for 6 days at 37°C, 5% CO_2.

Setting with immobilized recombinant receptor

In order to analyze the proliferative effect of Duokines in case of simultaneous receptor binding, 200 ng recombinant receptor (CD40-Fc, CD27-Fc, 4-1BB-Fc, OX40-Fc) were immobilized on 96-well ELISA plates overnight at 4°C in 100 µl PBS followed by blocking of residual binding sites with 200 µl RPMI 1640 + 10% FBS. After incubating with serial dilutions of the Duokines for 1 h, unbound proteins were washed away. After adding the primary CD3 stimulus and $1.5*10^5$ CFSE-labeled PBMCs (final volume of 200 µl) the assay was incubated at 37°C, 5% CO_2 for 6 days.

Blocking with recombinant receptor

The 4-1BBL- or OX40L-mediated costimulatory effects of the scFv-ligand fusion proteins in the targeted setting were blocked by addition of recombinant receptor in 5-fold molar excess. Therefore, target cells were incubated with 10 nM of the scFv-ligand fusion proteins for 1 h at room temperature, followed by a 1 h incubation with 50 nM 4-1BB-Fc or OX40-Fc. Afterwards, the primary anti-CD3 stimulus and CFSE-labeled PBMCs were added and proliferation was measured after 6 days at 37°C, 5% CO_2.

2.13 *In vivo* lung tumor model

The therapeutic potential of scDuokines was assessed in a combinatorial setting using a syngeneic lung colonization tumor model previously established in the laboratory (Hornig et al. 2013, Kermer et al. 2012, Kermer et al. 2014). Groups of six female C57BL/6N mice at the age of 13 weeks (22 – 25 g body weight) received one intravenous injection of $1*10^6$ B16-FAP mouse melanoma cells in 150 µl DPBS per mouse. After 1, 2, 3 and 8, 9, 10 days mice were treated with intraperitoneal injections (150 µl) of 4 pmol scDb332C11 in combination with 0.2 nmol msc4-1BBL-mscCD40L or 0.2 nmol msc4-1BBL-mscCD27L. As control groups, mice were also treated with the particular proteins alone or DPBS. Mice were sacrificed by CO_2 exposure on day 21. Lungs were removed, fixed in formaldehyde (Fekete's solution) and pulmonary tumors counted.

2.14 Statistics

Unless otherwise stated, all data are represented as mean with the corresponding standard deviation of at least three independent experiments. If necessary to compensate the daily variability of effector and target cells, block shift correction was performed according to

$$X'_n = X_n - (Y_n - \bar{Y})$$

with X'_n being the corrected value of X from the experiment n, $\bar{Y}$ the average of the X values from all experiments performed and Y_n the average of the duplicate values of X from experiment n. Significances were calculated from non-blockshifted data using One-Way ANOVA followed by Tukey's post test (GraphPad Prism 6). *P* values below 0.05 were considered statistically significant (*** $P < 0.001$, ** $P < 0.01$, * $P < 0.05$).

3 Results

3.1 Development of tumor-targeting single-chain fragment variable (scFv)

Hybridoma sequences for three different antibodies targeting claudin 4 and 6 were provided by Ganymed Pharmaceuticals AG. The antibodies 22A, 33B and 4H6E9 were produced as scFv fragments and the protein purity was confirmed in SDS-PAGE analysis, where all scFvs appeared as single bands corresponding to the expected size of 29 kDa (Figure 5 A). Both scFv4H6E9 and scFv33B exhibited binding to CLDN6-positive Bewo cells in flow cytometry, but scFv22A did not (Figure 5 B). Because scFv4H6E9 bound to Bewo cells with an EC_{50} value of 25.95 nM and scFv33B only at very high concentrations above 100 nM, scFv4H6E9 was selected for humanization.

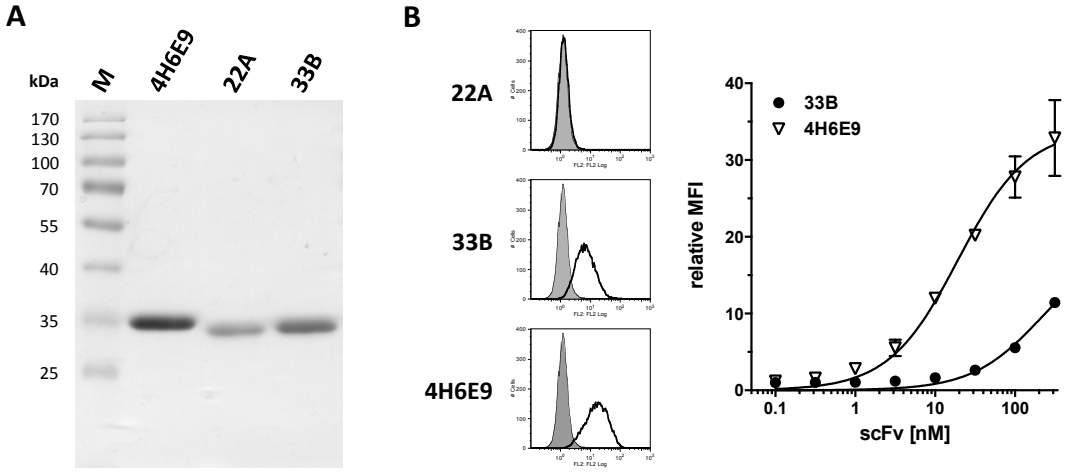

Figure 5: Production and binding analysis of anti-CLDN4/6 scFv antibodies from hybridoma. A) Purified scFv fragments were analyzed in SDS-PAGE under reducing conditions (15% PAA, 3 µg/lane, Coomassie-staining) and **B)** tested for their binding to CLDN6-expressing Bewo cells in flow cytometry. Left panel: grey, cells alone; thin line, detection Ab; bold line, scFv. Right panel: n = 1, duplicates.

3.1.1 Humanization of anti-CLDN4/6 scFv4H6E9

In order to reduce their immunogenicity, the murine VH and VL sequences of CLDN4/6-targeting scFv4H6E9 were humanized using complementarity-determining region (CDR) grafting. Thereby, particular focus was placed on retaining binding affinity in the humanized versions. Template sequences for humanization were identified with the similarity search tool IgBLAST by individually aligning the murine VH and VL domain to human germline genes. The selected human sequences were analyzed for their similarity to scFv4H6E9 and a Z-score (Abhinandan et al. 2007) indicating the humanness of the sequence was assigned (Table 14).

HV3-21 and KV1-39 with high positive Z-scores implying an elevated degree of humanness were chosen to create the humanized variant hu4H-2, while the germline genes HV1-3 and KV1-33 with lower Z-scores were used as a basis for the variant hu4H-S1.

Table 14: Parameters of human germline genes used for humanization of scFv4H6E9.

	Clone	Similarity	Z-score		Clone	Similarity	Z-score
4H6E9moVH	–	–	-1.362	**4H6E9moVL**	–	–	-1.111
HV3-21	DP-77	45.9%	1.892	**KV1-39**	DPK9	73.3%	1.204
HV1-3	DP-25	67.3%	0.119	**KV1-33**	DPK1	73.7%	0.561

Transferring the CDRs of 4H6E9 *in silico* onto the frameworks of the selected human germline genes, generated scFvhu4H-2b and scFvhu4H-S1a. Subsequently, the canonical structures of the new scFvs based on the humanized VH and VL domains were checked to be identical to the parental scFv4H6E9 using an online tool with auto-generated SDR templates (© 1995 Andrew C.R. Martin; Martin & Thornton, 1996). In both humanized versions two atypical residues in the vernier zone (H71, L49) were identified. The residues were changed back to the parental amino acids (R71V, Y49S) resulting in two additional variants scFvhu4H-2a and scFvhu4H-S1b with identical canonical classes as the murine scFv (Figure 6).

A

```
          FR1                              CDRH1 FR2             CDRH2                FR3                                CDRH3       FR4
Kabat     12345678910234567892023456789 3 02345 678940234567 89 502a3456789602345 6789702345678980 2abc3456789902 34 567891abc12 3456789110 3
HV1-26*1  ......................A...... D.YMN ..............  D...N....S.N.....  ..............................
4H6E9-VH  EVQLQQSGPELVKPGASVKISCKTSGYTFT EYTIH WVKQSHGKSLEWIG GINPKNGGTTYKQKFKG KATLTVDKSSSTAYMELRSLTSEDSAVYYCAR DGRSYYYAMDY WGQGTSVTVSS
HV3-21    ....VE..GG.....G.LRL..AA..F..S S.SMN ..R.AP..G...VS S.SSSSSYIY.ADSV.. RF.ISR.NAKNSL.LQMN..RA..T.......
hu-VH2a   ....VE..GG.....G.LRL..AA..F..S EYTIH ..R.AP..G...VS GINPKNGGTTYKQKFKG RF.ISV.NAKNSL.LQMN..RA..T....... DGRSYYYAMDY .....T.....
hu-VH2b   ....VE..GG.....G.LRL..AA..F..S EYTIH ..R.AP..G...VS GINPKNGGTTYKQKFKG RF.ISR.NAKNSL.LQMN..RA..T....... DGRSYYYAMDY .....T.....
HV1.3     Q...V...A.VK.......V...A...... S.AM. ..R.AP.QR...M. W..AG..N.K.S...Q. RV.I.R.T.A.......S..R...T.......
hu-VHS1a  Q...V...A.VK.......V...A...... EYTIH ..R.AP.QR...M. GINPKNGGTTYKQKFKG RV.I.R.T.A.......S..R...T....... DGRSYYYAMDY .....T.....
hu-VHS1b  Q...V...A.VK.......V...A...... EYTIH ..R.AP.QR...M. GINPKNGGTTYKQKFKG RV.I.V.T.A.......S..R...T....... DGRSYYYAMDY .....T.....
```

B

```
          FR1                        CDRL1      FR2             CDRL2   FR3                                CDRL3     FR4
Kabat     12345678910234567892023    456789302 34 56789402345678 9  502345 6  78960234567897023456789802345678 990234567 89100345 67
KV13-84*1 .......................... .......... ..............  ......  .................................. .........
4H6E9-VL  DIQMTQSSSSFSVSLGDRVTITC KASEDIYNRLA WYQQKPGNAPRLLIS GATSLET GVPSRFSGSGSGKDYTLSITSLQTEDVATYYC QQYWSTPRT FGGGTKLEIK
KV1-39    .......P..L.A.V........ R..QS.SSY.N .......K..K...Y A.S..QS ...........T.F..T.S...P..F..... ..SY...
hu-VL2a   .......P..L.A.V........ KASEDIYNRLA .......K..K...S GATSLET ...........T.F..T.S...P..F..... QQYWSTPRT ..Q.......
hu-VL2b   .......P..L.A.V........ KASEDIYNRLA .......K..K...Y GATSLET ...........T.F..T.S...P..F..... QQYWSTPRT ..Q.......
KV1-33    .......P..L.A.V........ Q..Q..S.Y.N .......K..K...Y D.SN... ...........T.F.FT.S...P..I..... ...DNL.
hu-VLS1a  .......P..L.A.V........ KASEDIYNRLA .......K..K...Y GATSLET ...........T.F.FT.S...P..I..... QQYWSTPRT ......V...
hu-VLS1b  .......P..L.A.V........ KASEDIYNRLA .......K..K...S GATSLET ...........T.F.FT.S...P..I..... QQYWSTPRT ......V...
```

Figure 6: Alignment of scFv4H6E9 with germline genes and humanized sequences. Alignment of **A)** heavy and **B)** light chain variable domains of scFv4H6E9 (green) with mouse (top line) and human (bottom lines) germline genes. The humanized domains generated by CDR grafting are aligned below the corresponding human germline sequences. Identical positions are displayed as dots, changed residues are shown as letters. Amino acids in the humanized sequence mutated back to the murine residues are displayed in red.

Afterwards, the humanized VH and VL domains were connected via a 15 aa glycine-serine rich linker, resulting in four humanized antibody fragments scFvhu4H-2a, scFvhu4H-2b, scFvhu4H-S1a and scFvhu4H-S1b (Figure 7 A) that were produced in *E. coli* TG1 and purified

from periplasmic preparations via a C-terminal hexahistidyl-tag. Integer protein expression and purity was confirmed in SDS-PAGE analysis under reducing conditions for the parental scFv4H6E9 and the humanized versions scFvhu4H-S1a and -S1b, while scFvhu4H-2a and -2b appeared to be degraded to varying extent (Figure 7 B).

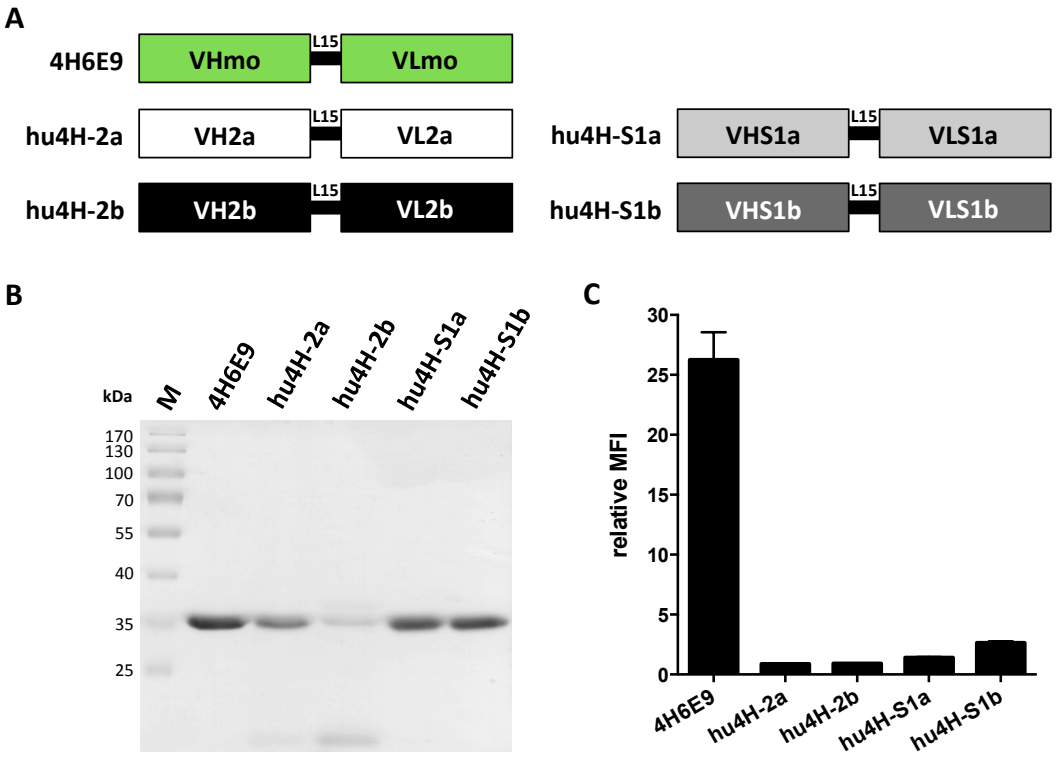

Figure 7: Humanized variants of scFv4H6E9. A) Illustration of the genotype of scFv4H6E9 and four humanized variants. All scFv antibodies were produced in TG1 and **B)** analyzed in SDS-PAGE (15% PAA, 3 µg/lane, reducing conditions, Coomassie-staining). **C)** 30 nM of the purified antibody fragments were tested in flow cytometry for binding to CLDN6-expressing Bewo cells. n = 1, duplicates.

In order to check for preservation of binding properties, binding to CLDN6-expressing Bewo cells was analyzed in flow cytometry. Both scFvhu4H-2a and -2b did not bind the antigen, while scFvhu4H-S1a and -S1b bound only very weakly compared to the parental scFv4H6E9 that was included as control (Figure 7 C). In order to determine if the humanization of VH or VL caused the loss of binding capacity, chimeric versions of scFvhu4H-S1a and -S1b were generated by exchanging either VH or VL for the parental murine domain (Figure 8 A). All chimeras were expressed in *E. coli* TG1 and purified in high purity, as demonstrated in reducing SDS-PAGE analysis (Figure 8 B). Binding of cell surface-expressed CLDN6 was significantly improved for both versions bearing the murine VL domain, though it did still not reach the level of the parental murine scFv4H6E9 (Figure 8 C).

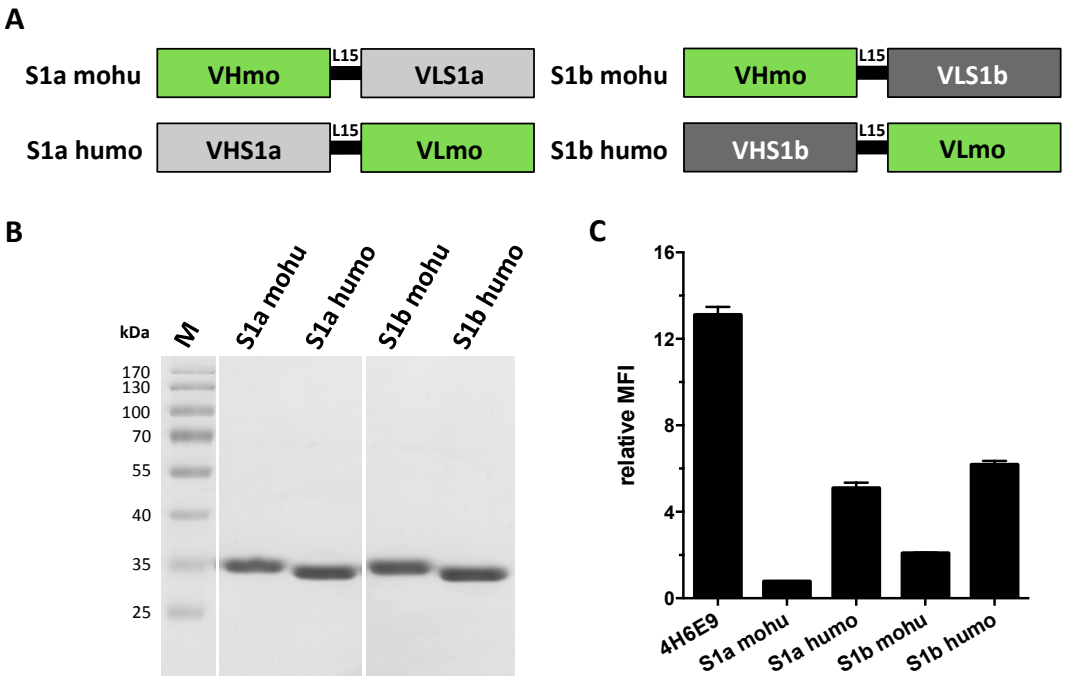

Figure 8: Chimeric versions of scFvhu4H-S1a and scFvhu4H-S1b. A) Arrangement of VH and VL in chimeric antibody fragments. **B)** Purified scFv chimeras were compared in SDS-PAGE (15% PAA, 3 µg/lane, reducing conditions, Coomassie-staining) and **C)** flow cytometry with CLDN6^{+} Bewo cells (5 µg/ml). n = 1, duplicates.

In both its chimeric and its fully humanized form, scFvhu4H-S1b showed slightly better binding than scFvhu4H-S1a, so variant S1b was chosen for further investigations regarding which part of the humanized VL domain was accountable for weakening CLDN6 binding. Therefore, the VL domain was divided into two parts by introducing a restriction site between CDRL2 and FR3, resulting in two VL chimera with either FR1-CDRL1-FR2-CDRL2 or FR3-CDRL3-FR4 exchanged for the corresponding murine parts (Figure 9 A).

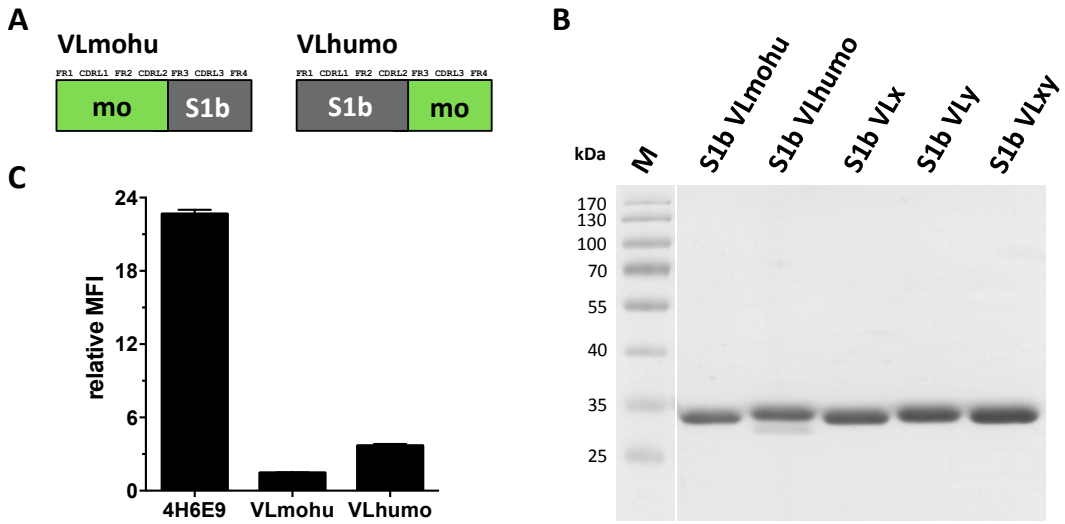

Figure 9: Variants of scFvhu4H-S1b with chimeric VL domains. A) Illustration of two different chimeric VL domains of scFvhu4H-S1b and **B)** SDS-PAGE analysis (15% PAA, 3 µg/lane, reducing conditions, Coomassie-staining) of five versions of scFvhu4H-S1b with various VL domains. **C)** Binding of VL-chimeric scFvs (4 µg/ml) to CLDN6^{+} Bewo cells was determined in flow cytometry. n = 1, duplicates.

Integer protein expression and purity was demonstrated in SDS-PAGE under reducing conditions (Figure 9 B). However, instead of improving, antigen binding was again even reduced for both VL chimeras compared to the parental scFv4H6E9 (Figure 9 C). Taken together, the previous findings indicated that humanizing scFv4H6E9 drastically reduced its capability to bind CLDN6 and that the humanized VL domain was presumably responsible for this loss of binding. Because the problematic area was not reliably localized by further chimerization of the VL domain, nine residues in the VL framework regions 1, 3 and 4 of scFvhu4H-S1b from which two (L69, L71) were located in the Vernier zone, were identified as critical (analysis by Prof. Dr. Roland Kontermann) and thus changed back to the murine amino acids (Figure 10 A). Three final humanized versions of scFvhu4H-S1b (VLx, VLy and VLxy) were expressed in TG1 and obtained in high purity (Figure 9 B). Finally, the parental murine scFv4H6E9, the humanized scFvhu4H-S1b and two chimeras of the latter (scFvhu4H-S1b humo and scFvhu4H-S1b VLhumo) were compared to the new VL versions regarding target cell binding in flow cytometry. None of the humanized variants reached the binding ability of scFv4H6E9 (EC_{50} 5.75 nM). The hu4H-S1b variants VLy and VLhumo ranged between EC_{50} values of 55 and 77 nM, while two other antibody fragments (scFvhu4H-S1b and scFvhu4H-S1b VLx) bound very weakly at concentrations above 100 nM.

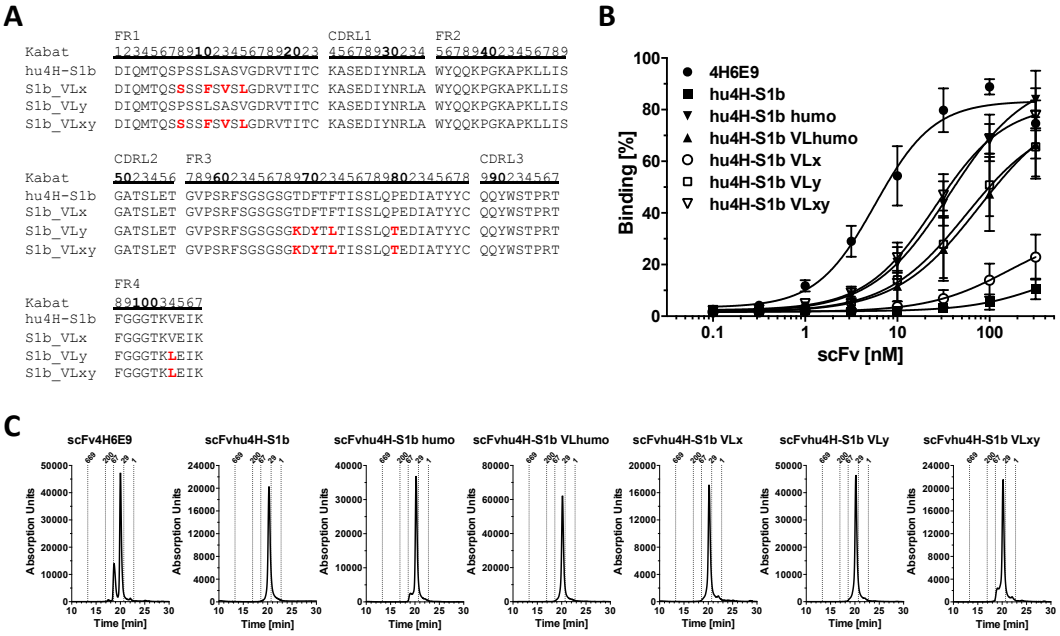

Figure 10: Comparison of scFv4H6E9 with final humanized variants. A) Alignment of the VL domain of scFvhu4H-S1b and VL versions with critical residues in FR1, FR3 and FR4 mutated back to the murine amino acids (shown in red). **B)** Binding of scFv4H6E9 and six humanized variants to CLDN6-expressing Bewo cells was determined in flow cytometry. Mean ± SD, n = 3. **C)** All antibody fragments showing at least weak binding to CLDN6 were analyzed for integrity by size exclusion chromatography (Yarra SEC-3000, flow rate 0.5 ml/min).

The best binding for humanized anti-CLDN4/6 antibody fragments was achieved for scFvhu4H-S1b VLxy (EC_{50} 25.6 nM) and scFvhu4H-S1b humo (EC_{50} 36.7 nM), indicating that the substitutions in VLxy effectively improved the binding properties. Eventually, size exclusion chromatography revealed that all six final humanized versions eluted as a single peak corresponding to the size of a monomeric scFv, while the parental scFv4H6E9 was in part present as a dimeric molecule. Despite this, scFv4H6E9 was chosen for incorporating in immunomodulatory scFv-ligand fusion proteins due to its good CLDN6 binding properties.

3.1.2 Humanization of anti-EpCAM scFv323A3

For targeting the tumor-associated antigen EpCAM, the high-affinity murine antibody fragment scFv323A3 described by Roovers et al. (1998) was chosen and subjected to humanization resulting in six different variants. Like for scFv4H6E9, the IgBLAST similarity search tool was used to identify human VH and VL germline genes as templates for CDR-grafting. In total, three human VH templates (VH7-4.1*2, VH1-3, VH3-30) and two human VL templates (VK2-28, VK3-20) with varying similarity and humanness were chosen (Table 15).

Table 15: Parameters of human germline genes used for humanization of scFv323A3.

	Clone	Similarity	Z-score		Clone	Similarity	Z-score
323moVH	–	–	-1.636	**323moVL**	–	–	-2.248
VH7-4.1*2	DP21	75.5%	-0.042	**VK2-28**	DPK15	78.0%	-1.401
VH1-3	DP25	61.2%	0.119	**VK3-20**	DPK22	55.8%	1.050
VH3-30		n.d.	2.196				

n.d. not determined

By transferring the murine CDRs from 323moVH and 323moVL *in silico* to the selected human germline frameworks, different humanized VH and VL domains were generated (Figure 11). Canonical evaluation with auto-generated SDR templates (© 1995 Andrew C.R. Martin) revealed in case of 323huVH2 or 323huVH3 one atypical amino acid in the vernier zone at position H71. The residue was changed back to the murine amino acid (R71L, Figure 11) resulting in the desired canonical class 2/10A for CDRH2. In summary, humanization of the VH domain resulted in three new domains (Figure 11) showing an increase of the Z-score from initially -1.636 (moVH) to -0.254 (huVH1), -0.329 (huVH2) or even 1.028 (huVH3). Likewise, the VL domain was humanized in two ways (Figure 11) resulting in an improvement of the Z-score from -2.428 (moVL) to -1.499 (huVL1) and -0.303 (huVL2).

A

```
          FR1                             CDRH1 FR2             CDRH2               FR3                                  CDRH3   FR4
Kabat     12345678910234567892023456789 3 02345 6789402345678 9 502a345678960 2345 6789702345678980 2abc345678990 234 5678910 03456789110
VH9.1     ............................. ..... ..K..P.K...... ..........AD.... ............................
323moVH   QIQLVQSGPELKKPGETVKISCKASGYTFT NYGMN WVRQASGEGLKWMG WINTYTGEPTYGEDFKG RFAFSLETSASTAYLQINNLKNEDTATYFCAR FGNYVDY WGQGTTLTVSS
VH7-4.1*2 .V......S......AS..V.......... S.A.. .....P.Q..E... ....N..N...AQG.T. ..V...D..V.......SS..A....V.Y...
323huVH1  .V......S......AS..V.......... NYGMN .....P.Q..E... WINTYTGEPTYGEDFKG ..V...D..V.......SS..A....V.Y... FGNYVDY .....LV....
VH1-3     .V......A.V....AS..V.......... S.A.H .....P.QR.E... ...AGN.NTK.SQK.Q. .VTITRD.......MELSS.RS....V.Y...
323huVH2  .V......A.V....AS..V.......... NYGMN .....P.QR.E... WINTYTGEPTYGEDFKG .VTITLD.......MELSS.RS....V.Y... FGNYVDY .....LV....
VH3-30    .V...E..GGVVQ..RSLRL..A...F..S S.A.H .....P.K..E.VA V.SYDGSNKY.ADSV.. ..TI.RDN.KN.L...M.S.RA....V.Y...
323huVH3  .V...E..GGVVQ..RSLRL..A...F..S NYGMN .....P.K..E.VA WINTYTGEPTYGEDFKG ..TI.LDN.KN.L...M.S.RA....V.Y... FGNYVDY .....LV....
```

B

```
          FR1                        CDRL1           FR2             CDRL2   FR3                                  CDRL3     FR4
Kabat     12345678910234567892023    4567abcde8930234 5678940234567 89 50234 56 7896023456789702345678980234567 8 990234567 89100345678
he24      .......................... ....S........... ..........Q.... ....... ..............................  .....L.
323moVL   DIVMTQAAFSNPVTLGTSASISC RSSKNLLHSNGITYLY WYLQKPGQSPHLLIY QMSNLAS GVPDRFSSSGSGTDFTLRISRVEAEDVGVYYC AQNLEIPRT FGGGTKLEIKR
VK2-28    ......SPL.L...P.EP..... ...QS......YN..D ..........Q.... LG..R.. .......G.........K.............. M.A.QT.
323huVL1  ......SPL.L...P.EP..... RSSKNLLHSNGITYLY ..........Q.... QMSNLAS .......G.........K.............. AQNLEIPRT ..Q........
VK3-20    E..L..SPGTLSLSP.ER.TL.. .A.QSVSS.----..A ..Q.....A.R.... GA.SR.T .I.....G.........T...L.P..FA.... Q.YGSS.
323huVL2  E..L..SPGTLSLSP.ER.TL.. RSSKNLLHSNGITYLY ..Q.....A.R.... QMSNLAS .I.....G.........T...L.P..FA.... AQNLEIPRT ..Q........
```

Figure 11: Alignment of scFv323A3 with germline genes and humanized sequences. Alignment of **A)** heavy and **B)** light chain variable domains of scFv323A3 (green) with mouse (top line) and human (bottom lines) germline genes. The humanized domains generated by CDR grafting are aligned below the corresponding human germline sequences. Identical positions are displayed as dots, changed residues are shown as letters. Amino acids in the humanized sequence mutated back to the murine residues are displayed in red.

The humanized VH and VL domains were connected via a 15 aa glycine-serine rich linker in all possible combinations (Figure 12 A) leading to six humanized variants scFv323A3hu1 to scFv323A3hu6 that were produced in *E. coli* and purified via a C-terminal hexahistidine-tag. Protein integrity and purity were demonstrated in SDS-PAGE analysis under reducing conditions (Figure 12 B), where all proteins appeared as bands corresponding to their calculated molecular mass.

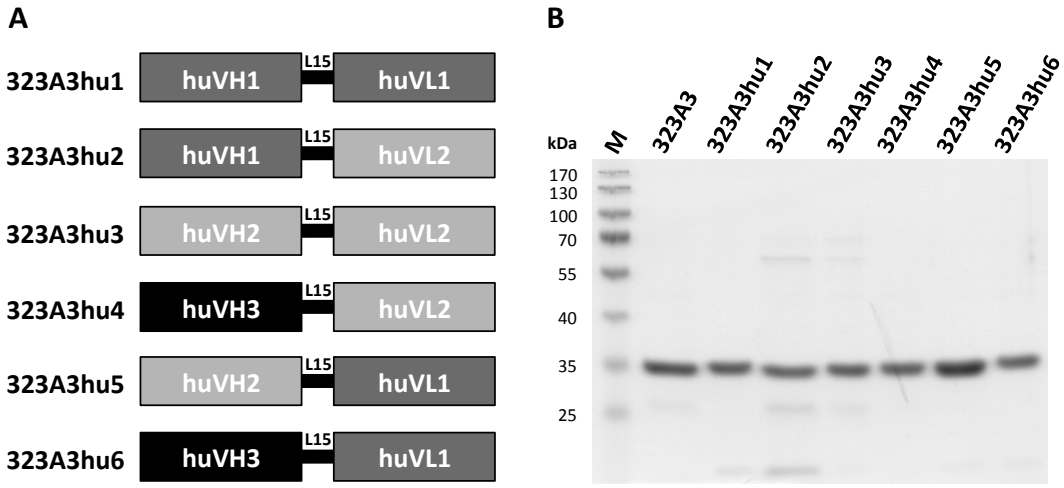

Figure 12: Production of humanized scFv323A3 antibody fragments. A) Schematic illustration of the genotype of the different humanized scFv323A3 variants. L15: $(GGGGS)_3$ linker. **B)** Purified antibody fragments were analyzed in SDS-PAGE under reducing conditions (12% PAA, 2 µg/lane, Coomassie-staining).

Antigen binding was determined by flow cytometry with EpCAM-expressing Colo205 cells (Figure 13 A). While scFv323A3hu4 and scFv323A3hu6 did not bind to EpCAM, all other scFvs bound the antigen in a concentration-dependent manner. Compared to the parental scFv323A3 (EC_{50} 2.45 nM), the variants hu3 and hu5 exhibited similar binding behavior with EC_{50} values of 3.30 nM and 4.45 nM, respectively. Therefore, scFv323A3 and the two best binding humanized scFvs were further analyzed for integrity in SEC and thermal stability in dynamic light scattering. All three scFvs eluted as major peaks corresponding to the calculated molecular mass (Figure 13 B) and did not tend to form higher-order complexes. Humanization drastically increased the aggregation point of the proteins from 40°C (scFv323A3) up to 53°C for scFv323A3hu3 and 55°C for scFv323A3hu5 (Figure 13 C). Based on the nearly unaltered binding properties and the significantly increased thermal stability, the humanized scFv323A3hu3 was selected as the anti-EpCAM targeting moiety employed in immunomodulatory fusion proteins.

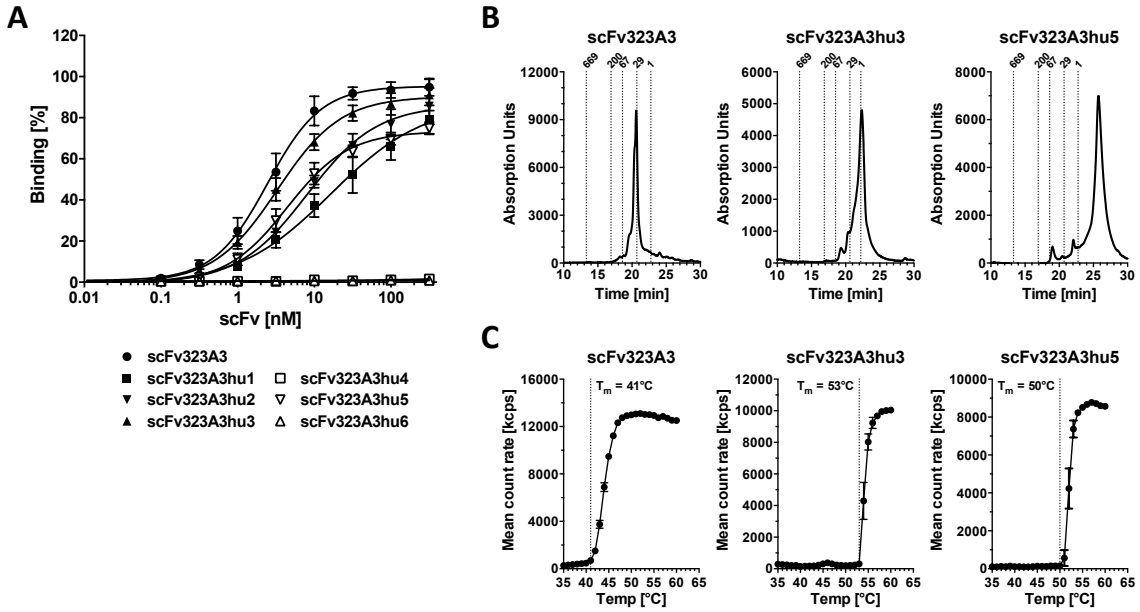

Figure 13: Target cell binding and biochemical properties of scFv323A3 variants. A) Binding of 323A3 antibody fragments to $EpCAM^+$ Colo205 cells was determined in flow cytometry. Mean ± SD, n = 3. The parental and the two best binding scFv molecules were analyzed for **B)** integrity by size exclusion chromatography (Yarra SEC-3000, flow rate 0.5 ml/min) and **C)** thermal stability by dynamic light scattering.

3.2 Tumor-targeted immunostimulatory antibody-cytokine fusion proteins

Several previous studies demonstrated costimulatory activity and anti-tumoral potential of tumor-targeted antibody-cytokine fusion proteins (scFv-TNFSF, D Müller et al. 2008, Hornig et al. 2013) and similar therapeutics incorporating the TNFSF ligand TRAIL have been described (de Bruyn et al. 2013). However, a single-chain format of TRAIL with three covalently linked extracellular domains (scTRAIL) showed clearly extended trimer stability compared to naturally processed TRAIL and was therefore successfully used in scFv-scTRAIL fusion proteins (Schneider et al. 2010). Here, the format of homotrimeric scFv-TNFSF fusion proteins was picked up and advanced by introducing novel single-chain versions of 4-1BBL and OX40L following the scTRAIL approach. Furthermore, the spectrum of targeted tumor-antigens was extended to EpCAM and CLDN4/6 by using the two scFv molecules 323A3hu3 ($scFv_{EpCAM}$) and 4H6E9 ($scFv_{CLDN4/6}$) analyzed in the previous chapter as targeting antibodies.

3.2.1 Characterization of scFv-ligand fusion proteins

Tumor-directed antibody-cytokine fusion proteins were composed of a single-chain fragment variable (scFv) as targeting moiety and the extracellular domain (ECD) of TNF superfamily members (4-1BBL, aa 71 - 254 or OX40L, aa 51 - 183) as effector moiety in two different formats (Figure 14 A). In the classical arrangement, where the scFv was connected to the N-terminus of one single ECD, intermolecular trimerization mediated by the ligand results in a homotrimeric molecule (scFv-TNFSF). In the novel single-chain arrangement, three consecutive ECDs (named sc4-1BBL or scOX40L) were fused to the scFv, leading to a monomeric single-chain molecule with intramolecular ligand-trimerization (scFv-scTNFSF). As a result, fusion proteins with an antibody-to-ligand ratio of either 3:1 (scFv-TNFSF) or 1:1 (scFv-scTNFSF) were established. Independent of the particular format, the glycine-serine linker connecting scFv and TNFSF ligand was 15 amino acids long, while the linkers between the individual ECDs of sc4-1BBL or scOX40L were composed of $(GGGGS)_4$ or GGGSGGG, respectively. In summary, antibody-cytokine fusion proteins presenting two different ligands (4-1BBL, OX40L) to two different tumor-associated antigens (EpCAM, CLDN4/6) were generated in both protein formats (scFv-TNFSF, scFv-scTNFSF), resulting in a total of eight proteins (Table 16, cloning performed by Jan-Erik Meyer).

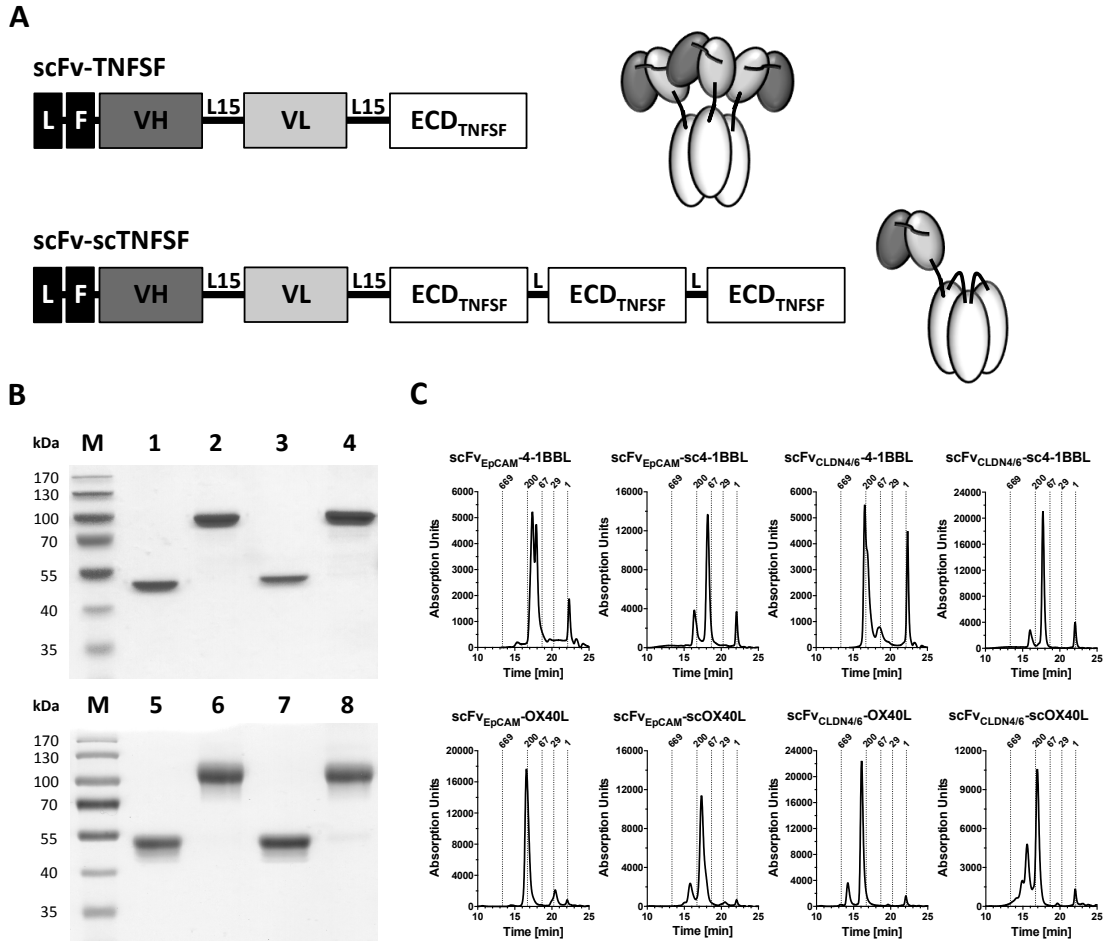

Figure 14: Design and biochemical characterization of scFv-ligand fusion proteins. A) Molecular composition and schematic assembly of scFv-TNFSF and scFv-scTNFSF fusion proteins. L, leader peptide; F, FLAG-tag. **B)** SDS-PAGE analysis (12% PAA, 2 µg/lane) of purified 1: $scFv_{EpCAM}$-4-1BBL, 2: $scFv_{EpCAM}$-sc4-1BBL, 3: $scFv_{CLDN4/6}$-4-1BBL and 4: $scFv_{CLDN4/6}$-sc4-1BBL as well as 5: $scFv_{EpCAM}$-OX40L, 6: $scFv_{EpCAM}$-scOX40L, 7: $scFv_{CLDN4/6}$-OX40L and 8: $scFv_{CLDN4/6}$-scOX40L under non-reducing conditions. SDS-PAGE performed by Jan-Erik Meyer. **C)** Size exclusion chromatography on a Yarra SEC-3000 column (flow rate 0.5 ml/min). Standard proteins and their corresponding molecular masses (kDa) are indicated as dotted lines.

Both formats of scFv-ligand fusion proteins were provided with an N-terminal FLAG-tag and a VH leader sequence for secretion. The proteins were produced in stably transfected HEK293T cells and purified by FLAG tag affinity chromatography with yields ranging from 1 to 4 mg protein per liter cell culture supernatant (Table 16). Protein purity was checked in SDS-PAGE analysis under non-reducing conditions (performed by Jan-Erik Meyer) revealing a single band corresponding to the monomer of each scFv-ligand fusion protein and confirming the absence of disulfide-linked oligomers (Figure 14 B). The determined molecular masses (approx. 50 and 90 kDa) of the 4-1BBL fusion proteins correlated to the calculated ones, while the OX40L fusion proteins, predicted to be highly glycosylated, migrated with 56 and 105 kDa at higher apparent molecular masses than deduced from the sequence (Table 16). Size exclusion chromatography demonstrated largely correct assembly

into trimeric (scFv-TNFSF) or monomeric (scFv-scTNFSF) molecules under native conditions. Only minor fractions of higher-order aggregates were detectable indicating rather homogenous protein compositions. The elution profiles of $scFv_{EpCAM}$-4-1BBL and $scFv_{CLDN4/6}$-4-1BBL, however, presented themselves as both trimers and dimers with the trimeric peak being slightly more dominant (Figure 14 C). In general, all eight antibody-cytokine fusion proteins were purified in high purity and showed mainly correct assembly regardless of format, TNFSF ligand and targeting specificity. All evaluated biochemical characteristics are summarized in Table 16.

Table 16: Biochemical characteristics of scFv-ligand fusion proteins. Calculation of the molecular mass (MW) based on the amino acid sequence. scFv-OX40L and scFv-scOX40L were purified by Jan-Erik Meyer.

Protein	MW_{calc} (kDa, chain)	MW_{PAGE} (kDa, chain)	MW_{SEC} (kDa, native)	N-glycosylation (per chain)	Yield (Ø in mg/L)
$scFv_{EpCAM}$-4-1BBL	48.2	51.6	155.5 / 118.6	0	1.28
$scFv_{CLDN4/6}$-4-1BBL	47.8	53.4	219.2	0	2.29
$scFv_{EpCAM}$-sc4-1BBL	89.6	86.8	105.4	0	4.30
$scFv_{CLDN4/6}$-sc4-1BBL	89.1	89.1	128.2	0	2.64
$scFv_{EpCAM}$-OX40L	44.1	56.2	228.3	4	1.28
$scFv_{CLDN4/6}$-OX40L	43.7	57.2	253.5	4	0.98
$scFv_{EpCAM}$-scOX40L	75.8	103.8	152.9	12	1.37
$scFv_{CLDN4/6}$-scOX40L	75.3	107.5	180.2	12	1.35

3.2.2 Binding of scFv-ligand fusion proteins to antigens and cytokine receptors

The functionality of the antibody moiety of the various scFv-ligand fusion proteins was tested for binding to the cell surface-expressed antigens on tumor cells by flow cytometry. In general, concentration-dependent binding to antigen-positive cells was shown for all fusion proteins. Yet, the initially good binding of $scFv_{EpCAM}$ (EC_{50} 3.9 ± 0.7 nM) was clearly weakened when incorporated in the different scFv-ligand fusion protein formats (Figure 15 A). While the binding of one scFv unit in $scFv_{EpCAM}$-OX40L and $scFv_{EpCAM}$-4-1BBL was decreased to EC_{50} values of 12.7 nM and 44.4 nM, the reduction in binding strength was even more dramatic considering the single-chain versions $scFv_{EpCAM}$-sc4-1BBL and $scFv_{EpCAM}$-scOX40L with EC_{50} values lowered to 92 and 176 nM (Table 17). Similar effects were observed for binding of CLDN6 by $scFv_{CLDN4/6}$ (EC_{50} 14.8 ± 4.0 nM, Figure 15 B). Here, the binding capacity of the antibody moiety was nearly unaltered when incorporated in the homotrimeric variants $scFv_{CLDN4/6}$-4-1BBL and $scFv_{CLDN4/6}$-OX40L (EC_{50} 38.8 ± 6.7 nM and 21.3 ± 3.6 nM), but

again considerably reduced in the scFv-scTNFSF fusion proteins exhibiting EC_{50} values in the high nanomolar range (Table 17). However, when accounting for the fact that the homotrimeric scFv-TNFSF fusion proteins are endowed with three antibody moieties per native molecule, the increased avidity recovers the functional affinity to the antigen within the fusion protein. This effect is more prominent for scFv-OX40L than scFv-4-1BBL fusion proteins, with $scFv_{CLDN4/6}$-OX40L then exceeding the binding capacity of $scFv_{CLDN4/6}$ alone.

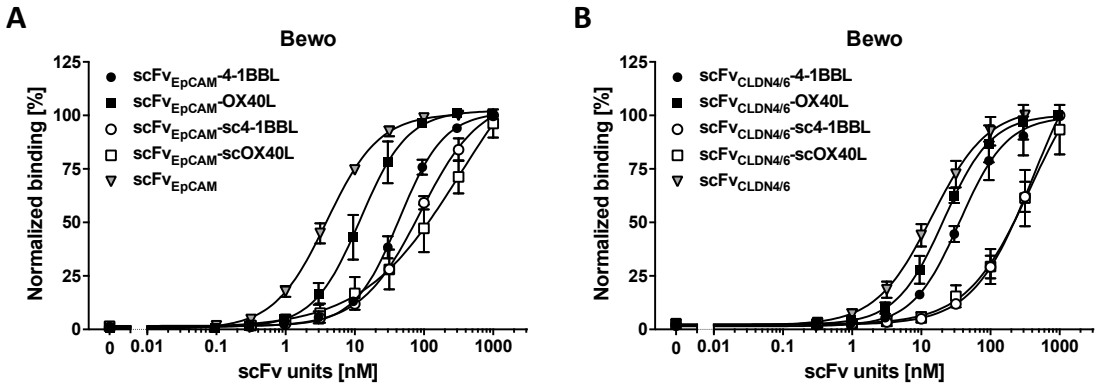

Figure 15: Antigen binding of scFv-ligand fusion proteins. Antigen binding of cell surface-expressed **A)** EpCAM and **B)** CLDN6 was analyzed by flow cytometry with Bewo cells ($EpCAM^+/CLDN6^+$, $1.5*10^5$ cells/well). $scFv_{EpCAM}$ and $scFv_{CLDN4/6}$ were included as controls. Concentrations refer to scFv units. Mean ± SD, n ≥ 3.

Since the correct assembly of the costimulatory ligands within the antibody-cytokine fusion proteins is crucial, effective binding of the ligands to their receptors was analyzed in ELISA. 4-1BBL (EC_{50} 2.2 ± 0.8 nM) and sc4-1BBL (EC_{50} 1.7 ± 0.4 nM) as well as all four different fusion proteins bearing 4-1BBL showed very similar binding capacities to 4-1BB-Fc (Figure 16 A) with EC_{50} values ranging from 1.4 nM to 2.7 nM (Table 17). In the case of OX40L (EC_{50} 1.4 ± 0.4 nM) and scOX40L (EC_{50} 1.3 ± 0.3 nM), transferring the ligand into the single-chain format did not affect receptor-binding strength as well (Figure 16 B). While the addition of an scFv to scOX40L did not alter the binding to OX40-Fc, binding capacities of $scFv_{EpCAM}$-OX40L (EC_{50} 0.2 ± 0.06 nM) and $scFv_{CLDN4/6}$-OX40L (EC_{50} 0.1 ± 0.01 nM) were increased 10-fold compared to the ligand itself (Table 17). In general, converting the costimulatory ligands into the single-chain format and fusing them with an antibody moiety did conserve their receptor binding properties.

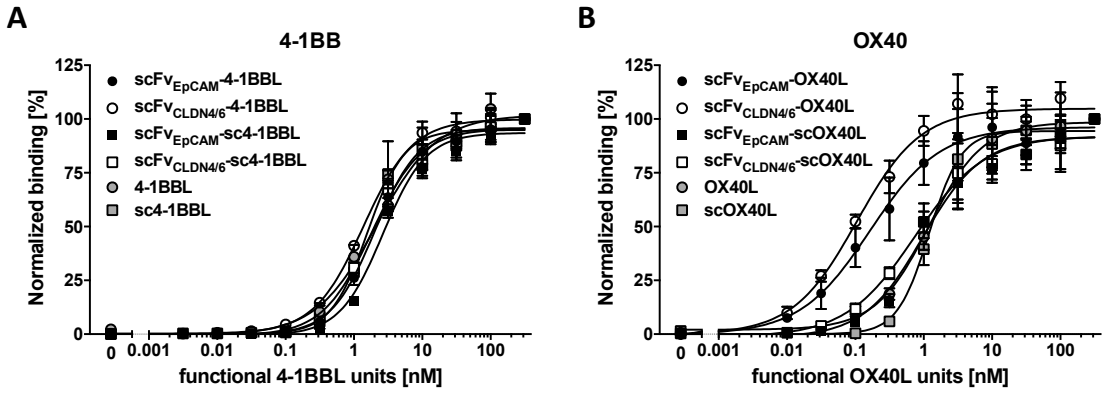

Figure 16: Cytokine receptor binding of scFv-ligand fusion proteins. Binding to 200 ng immobilized **A)** 4-1BB-Fc and **B)** OX40-Fc was analyzed in ELISA. 4-1BBL, sc4-1BBL, OX40L and scOX40L were included as controls. Concentrations refer to functional TNFSF ligand units. Mean ± SD, n = 3.

Measuring the NFκB-induced release of IL-8 from HT1080 cells stably transfected with 4-1BB or OX40 revealed whether ligand-receptor interaction also resulted in receptor activation. In a first step, receptor expression and binding of the scFv-ligand fusion proteins to HT1080 transfectants was confirmed in flow cytometry (Figure 17 A).

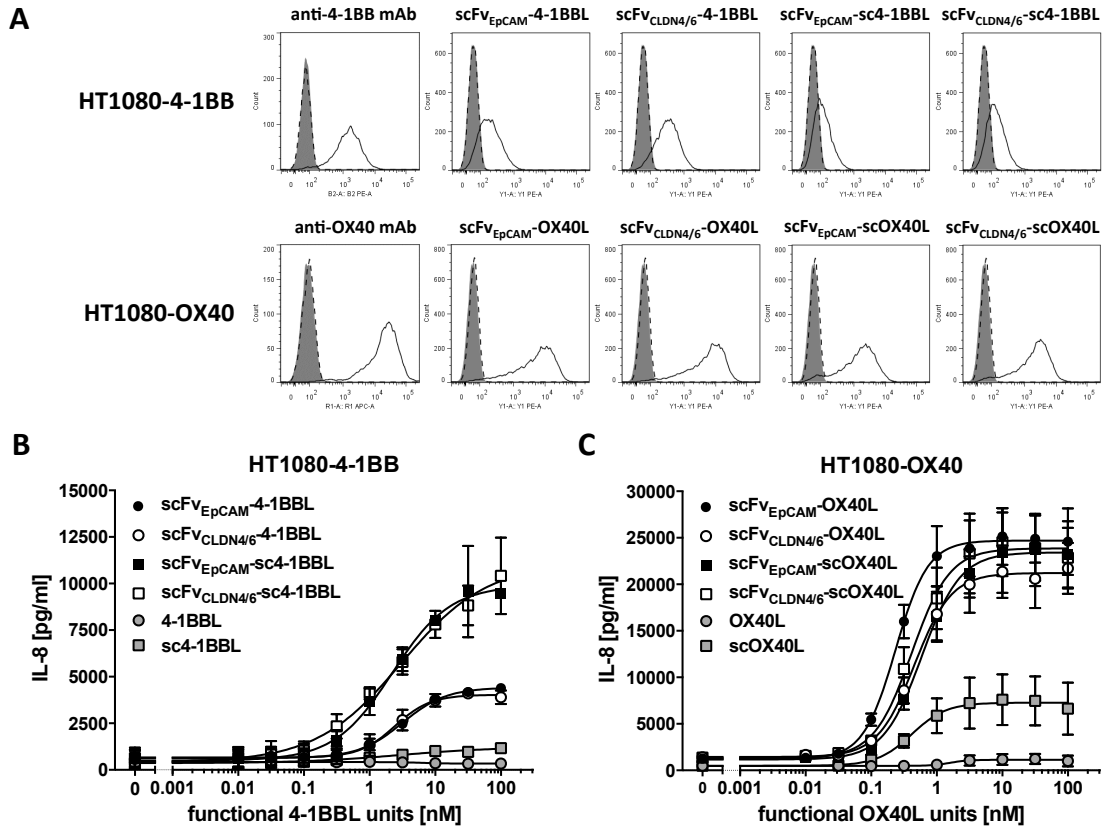

Figure 17: TNFRSF receptor activation measured via IL-8 release upon NFκB activation. A) Receptor expression on and fusion protein binding to HT1080-4-1BB and -OX40 was analyzed by flow cytometry. Solid grey, cells; dashed black line, isotype or detection Ab; normal black line, anti-receptor mAb or fusion protein. **B)** HT1080-4-1BB or **C)** HT1080-OX40 cells ($2*10^4$) were incubated at 37°C, 5% CO_2 with the fusion proteins and amounts of IL-8 released into the supernatant were measured after 18 h by Sandwich-ELISA. Mean ± SD, n = 3.

Though both 4-1BBL and sc4-1BBL were not capable of receptor activation, all scFv-4-1BBL and scFv-sc4-1BBL fusion proteins successfully induced IL-8 release (Figure 17 B). Despite the fact that the measured absolute IL-8 values were higher for scFv-sc4-1BBL, EC_{50} values always ranged between 1.7 nM and 3.9 nM (Table 17). Likewise, scFv-OX40L, scFv-scOX40L and scOX40L induced receptor activation with highly similar EC_{50} values of around 0.4 nM, while OX40L did hardly (Figure 17 C). However, the absolute IL-8 amounts released upon stimulation with scOX40L were lower compared to the fusion proteins. Due to the fact that all proteins were applied in solution, only differences between the various TNFSF ligands and protein formats but not between the target specificities $scFv_{EpCAM}$ and $scFv_{CLDN4/6}$ were identified. In summary, in a soluble setting all antibody-cytokine fusion proteins showed distinct receptor activation properties clearly exceeding the potential of the respective costimulatory ligands alone. Table 17 summarizes the EC_{50} values for antigen binding, receptor binding and receptor activation of all scFv-ligand fusion proteins and their controls.

Table 17: EC_{50} values [nM] for antigen binding and TNFRSF receptor binding and activation. Binding to Bewo cells ($EpCAM^+/CLDN6^+$) was determined by flow cytometry, binding to OX40-Fc and 4-1BB-Fc by ELISA. Receptor activation was measured by NFκB-induced IL-8 release from stable HT1080 transfectants. All EC_{50} values [nM] are represented as mean ± SD, n = 3 (n = 6 for $scFv_{EpCAM}$ and $scFv_{CLDN4/6}$).

	Antigen binding	**Receptor binding**		**Receptor activation**	
	Bewo	**4-1BB**	**OX40**	**HT1080-4-1BB**	**HT1080-OX40**
$scFv_{EpCAM}$-4-1BBL	44.4 ± 6.2	2.1 ± 0.3	–	3.2 ± 0.5	–
$scFv_{CLDN4/6}$-4-1BBL	38.8 ± 6.7	1.4 ± 0.1	–	2.4 ± 0.5	–
$scFv_{EpCAM}$-sc4-1BBL	92.3 ± 15.7	2.7 ± 0.3	–	1.7 ± 0.07	–
$scFv_{CLDN4/6}$-sc4-1BBL	349 ± 106	1.9 ± 0.3	–	3.9 ± 2.3	–
$scFv_{EpCAM}$-OX40L	12.7 ± 5.1	–	0.2 ± 0.06	–	0.2 ± 0.02
$scFv_{CLDN4/6}$-OX40L	21.3 ± 3.6	–	0.1 ± 0.01	–	0.5 ± 0.06
$scFv_{EpCAM}$-scOX40L	176 ± 8.8	–	1.1 ± 0.3	–	0.6 ± 0.05
$scFv_{CLDN4/6}$-scOX40L	403 ± 158	–	0.8 ± 0.2	–	0.4 ± 0.1
4-1BBL	–	2.2 ± 0.8	–	n.d.	–
sc4-1BBL	–	1.7 ± 0.4	–	n.d.	–
OX40L	–	–	1.4 ± 0.4	–	n.d.
scOX40L	–	–	1.3 ± 0.3	–	0.4 ± 0.2
$scFv_{EpCAM}$	3.9 ± 0.7	–	–	–	–
$scFv_{CLDN4/6}$	14.8 ± 4.0	–	–	–	–

– no ligand/receptor interaction n.d. no activation detectable

3.2.3 *In vitro* stability and *in vivo* pharmacokinetics of scFv-ligand fusion proteins

All scFv-ligand fusion proteins were analyzed regarding their stability in human plasma at 37°C. Protein integrity and ligand-receptor binding was preserved over 7 days for both monomeric scFv-sc4-1BBL fusion proteins, but the amount of intact homotrimeric $scFv_{EpCAM}$-4-1BBL and $scFv_{CLDN4/6}$-4-1BBL significantly decreased to approx. 30% and 6% after 7 days (Figure 18 A). While the stability reduction occurred gradually for $scFv_{CLDN4/6}$-4-1BBL, levels of intact $scFv_{EpCAM}$-4-1BBL dropped down to only 30% already within one day. In contrast, differences observed in the *in vitro* stabilities for OX40L-bearing proteins were not as distinct as in the case of 4-1BBL fusion proteins. Here, homotrimeric $scFv_{CLDN4/6}$-OX40L decreased to approx. 40% intact protein after 7 days, while 60 - 80% of the other variants remained intact with the single-chain versions tending to be more stable over the first days (Figure 18 B). Generally, utilizing the ligands in the single-chain format seemed to increase stability of the fusion proteins, an effect particularly prominent for 4-1BBL.

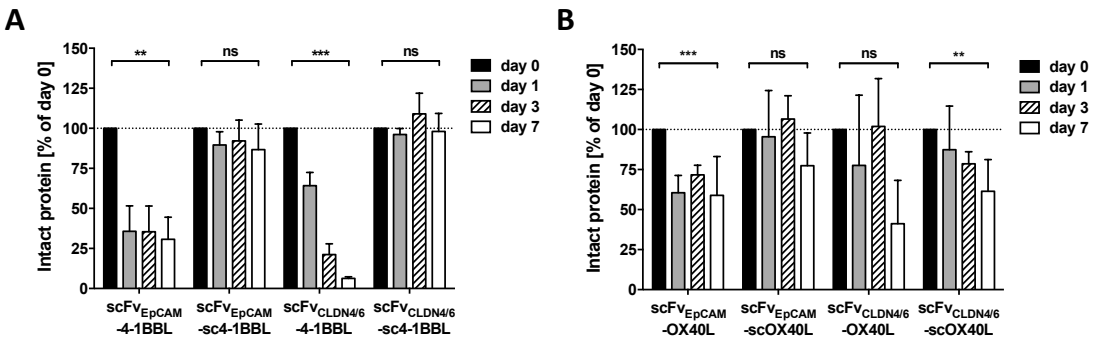

Figure 18: *In vitro* stability of scFv-ligand fusion proteins. Plasma stability of 200 nM protein was assessed over 7 days in 50% human plasma. Levels of intact protein were determined via binding of **A)** 4-1BB-Fc and **B)** OX40-Fc in ELISA. Data was normalized to day 0 and is displayed as mean ± SEM, n = 6, One-Way ANOVA.

Additionally, pharmacokinetic studies were performed in immunocompetent CD-1 mice. As the human antibody fragments are not cross-reactive with the corresponding mouse antigens and no transgenic mice were available, only scFv-ligand fusion proteins targeting EpCAM were analyzed. Serum half-life and bioavailability was determined over 72 hours, with only $scFv_{EpCAM}$-OX40L being no longer detectable already after 24 hours (Figure 19 A). The tested scFv-ligand fusion proteins showed comparable initial (0.5 to 1.3 h) and terminal (12.7 to 16.3 h) half-lives (Table 18). However, the monomeric single-chain $scFv_{EpCAM}$-sc4-1BBL exhibited a clearly prolonged initial half-life of 4.3 h and the homotrimeric $scFv_{EpCAM}$-OX40L a distinct shorter terminal half-life of only 2.3 h.

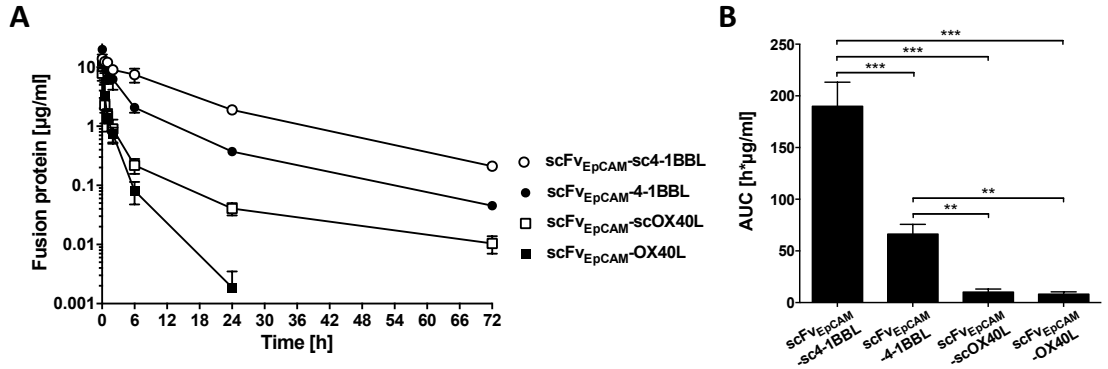

Figure 19: *In vivo* pharmacokinetics of scFv-ligand fusion proteins. A) Female CD1 mice were treated i.v. with the anti-EpCAM fusion proteins (25 µg). Protein concentration in the serum samples was analyzed via ELISA. Mean ± SD, n = 3. **B)** Area under the curve (AUC) was calculated in Excel. Mean ± SD, n = 3, One-Way ANOVA.

In general, the bioavailability of 4-1BBL-containing fusion proteins was significantly higher compared to OX40L-bearing fusion proteins, which exhibited relatively low AUCs between 8 h*µg/ml and 10 h*µg/ml. Also, the AUCs of the OX40L-fusion proteins did not differ significantly between the two formats, while the AUC of the monomeric scFv$_{EpCAM}$-sc4-1BBL (189.98 ± 23.23 h*µg/ml) was increased three-fold compared to the homotrimeric scFv$_{EpCAM}$-4-1BBL (66.27 ± 9.45 h*µg/ml) (Figure 19 B, Table 18).

Table 18: Pharmacokinetic properties of scFv-ligand fusion proteins. Initial and terminal half-lives ($t_{1/2}\alpha$, $t_{1/2}\beta$) and areas under the curve (AUC) were determined over 72 hours in tumor-free CD1 mice. Mean ± SD, n = 3.

	$t_{1/2}\alpha$ [h]	$t_{1/2}\beta$ [h]	AUC [h*µg/ml]
scFv$_{EpCAM}$-4-1BBL	1.28 ± 0.39	12.66 ± 0.44	66.27 ± 9.45
scFv$_{EpCAM}$-sc4-1BBL	4.26 ± 2.58	13.34 ± 0.66	189.98 ± 23.23
scFv$_{EpCAM}$-OX40L	0.52 ± 0.08	2.26 ± 1.45	8.19 ± 2.23
scFv$_{EpCAM}$-scOX40L	0.68 ± 0.06	16.29 ± 0.61	10.20 ± 2.97

3.2.4 T cell costimulatory potential of scFv-ligand fusion proteins

According to the underlying concept of tumor-targeted immunostimulation, it was analyzed whether the different scFv-ligand fusion proteins exhibited their costimulatory activity in a targeted setting. Therefore, tumor cells (Bewo) and PBMCs were co-cultured in the presence of suboptimal concentrations of crosslinked anti-CD3 mAb and the respective scFv-TNFSF or scFv-scTNFSF fusion proteins (the experiments in this chapter were performed by Jan-Erik Meyer). The costimulatory activity of the ligands was measured in respect to IFN-γ release and PBMC proliferation enhanced above the levels of the anti-CD3 stimulation alone (Figure 20). Regardless of antibody specificity, ligand type and protein format, all scFv-ligand fusion proteins proved to be costimulatory active in the presence of target cells and primary

stimulus, but the increase in IFN-γ release and proliferation rate was generally higher for 4-1BBL- than for OX40L-bearing fusion proteins. The costimulatory activity of the homotrimeric scFv-TNFSF and the monomeric scFv-scTNFSF fusion proteins was similar in the proliferation experiments (Figure 20 C, D), but significant differences between the two formats were observed for IFN-γ release. Interestingly, the format-specific differences depended on the antibody fragment incorporated in the fusion proteins. In the case of EpCAM-targeting, single-chain monomeric $scFv_{EpCAM}$-sc4-1BBL and $scFv_{EpCAM}$-scOX40L exhibited higher costimulatory activity at lower concentrations, while in the case of CLDN6-targeting the homotrimeric variants $scFv_{CLDN4/6}$-4-1BBL and $scFv_{CLDN4/6}$-OX40L proved to be advantageous (Figure 20 A, B).

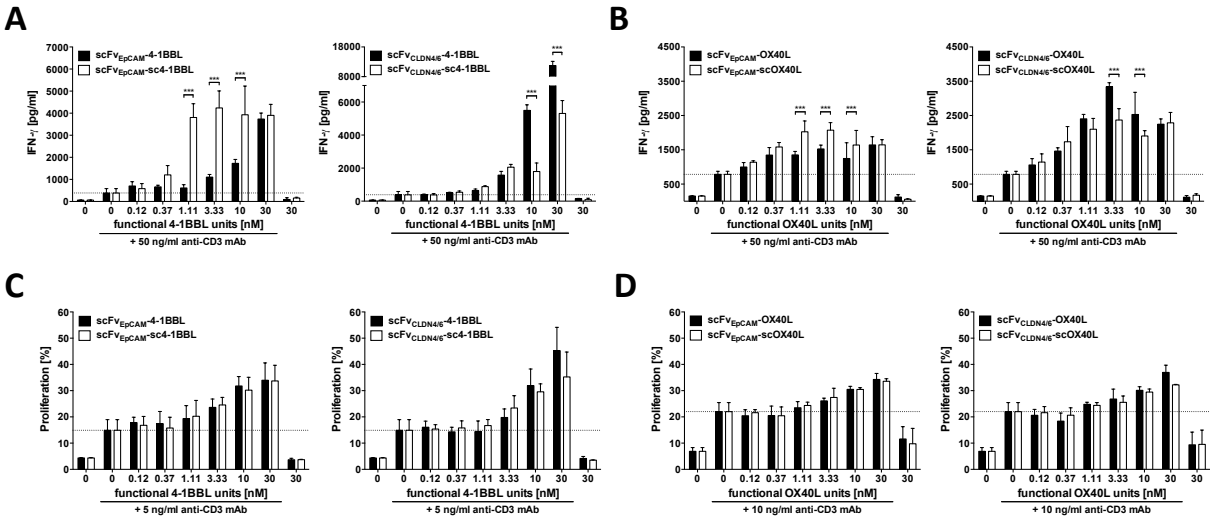

Figure 20: Costimulatory effects of scFv-ligand fusion proteins in a targeted setting. Bewo cells ($3*10^4$) were cocultured with PBMCs in the presence of combinations of anti-CD3 mAb (5 – 50 ng/ml) and scFv-ligand fusion proteins. **A, B)** IFN-γ release (PBMC batch #J03) was measured after 48h via Sandwich-ELISA. **C, D)** The proliferation of CFSE-labeled PBMCs (PBMC batch #J01, #J02) was determined after 6 days via flow cytometry. All data is represented as mean ± SD, n = 3, IFN-γ release with block-shift-correction. Data by Jan-Erik Meyer.

In accordance with the costimulatory nature of 4-1BBL and OX40L, all scFv-ligand fusion proteins did not induce any PBMC activation by themselves, i.e. without CD3-mediated primary stimulation. This effect was present regardless of the overall setting being targeted (Figure 20) or untargeted (Figure 21 A). Furthermore, it was analyzed if the costimulatory activity of the scFv-ligand fusion proteins was target-dependent and ligand-restricted (Figure 21). In an untargeted setting without Bewo cells the costimulatory effect of $scFv_{CLDN4/6}$-4-1BBL, $scFv_{CLDN4/6}$-sc4-1BBL, $scFv_{EpCAM}$-OX40L, $scFv_{EpCAM}$-scOX40L, $scFv_{CLDN4/6}$-OX40L and $scFv_{CLDN4/6}$-scOX40L diminished drastically or was even completely absent.

However, this was not the case for $scFv_{EpCAM}$-4-1BBL and $scFv_{EpCAM}$-sc4-1BBL, where the potential in enhancing PBMC stimulation was unaltered compared to targeted conditions (Figure 21 A). Finally, the costimulatory activity of all scFv-TNFSF and scFv-scTNFSF fusion proteins was blocked by adding the respective recombinant receptor and therefore proven to be strictly ligand-dependent (Figure 21 B). In general, the antibody-mediated presentation of 4-1BBL and OX40L on the cell surface positively affected the costimulatory activity of the scFv-ligand fusion proteins in both formats, although the preferred protein format was in each case still strongly influenced by the particular antibody-cytokine configuration.

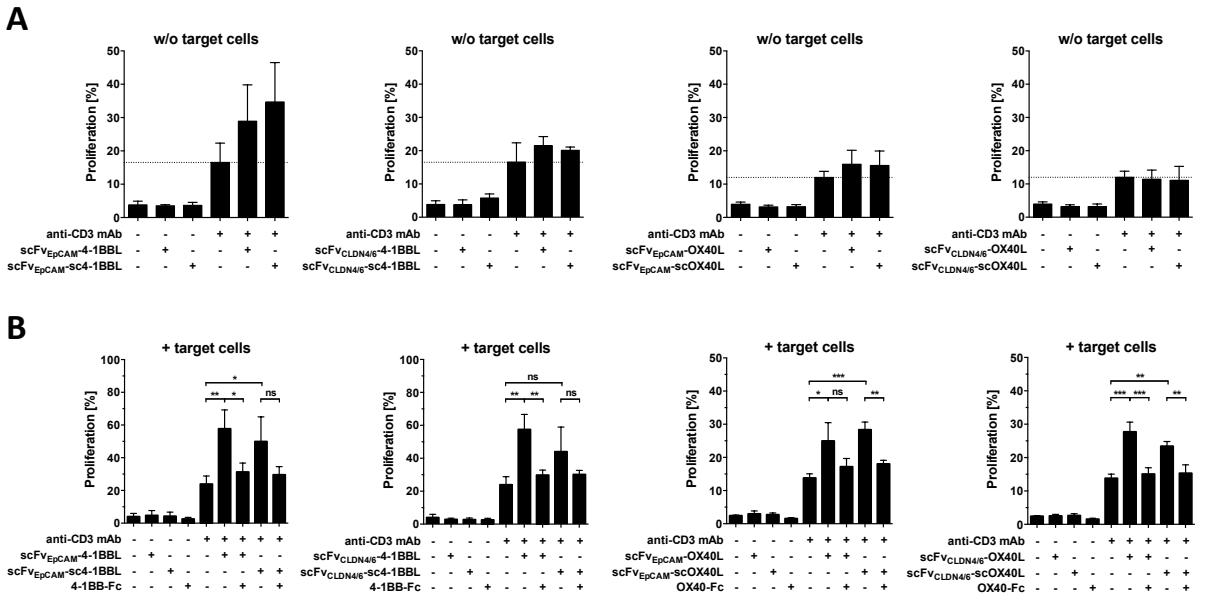

Figure 21: Target- and cytokine-dependence of costimulatory scFv-ligand fusion proteins. A) PBMCs (Batch #J01, #J02) were incubated with combinations of anti-CD3 mAb (5 – 10 ng/ml) and scFv-ligand fusion proteins (30 nM). **B)** Target cells ($3*10^4$ Bewo) were co-cultured with PBMCs (Batch #J04) and combinations of anti-CD3 mAb (10 ng/ml), scFv-ligand fusion proteins (10 nM) and receptors (50 nM). In both settings, proliferation was determined after 6 days via flow cytometry. Mean ± SD, n = 3, One-Way ANOVA. Data by Jan-Erik Meyer.

3.3 Dual-acting immunostimulatory cytokine fusion proteins (Duokines)

Besides refining the previously described approach of tumor site-directed costimulation with antibody-cytokine fusion proteins, the main object of this study was to provide a novel format of bifunctional (dual-acting) cytokine fusion proteins comprising two different costimulatory ligands. With various members of the TNFSF, namely CD40L, CD27L, 4-1BBL and OX40L, key players of T cell costimulation were utilized in this concept, thereby not only exploiting the differential up-regulation of TNFRSF receptors on primed T cells but also the spatial proximity of T cells and antigen-presenting cells (APC) as the latter are targeted by CD40L. This new class of bifunctional immunomodulatory cytokine fusion proteins was named duokines (neologism for "**Du**al-acting Cyt**okines**").

Duokines are composed of the extracellular domain (ECD) of two different TNFSF ligands (CD40L, aa 116 - 261; CD27L, aa 52 - 193; 4-1BBL, aa 71 - 254; OX40L, aa 51 - 183) in two different formats (Figure 22 A). In the classical **Duokine** arrangement a glycine-serine rich linker connects two different single ECDs and intermolecular homotrimerization mediated by the ligands results in a bifunctional homotrimeric hexavalent molecule (Figure 22 B). The length of the connecting linker was chosen with respect to the molecular shape of the incorporated ligands, i.e. $(GGGGS)_4$ if involving 4-1BBL and $(GGGGS)_3$ for the other cytokines. In order to prepare for the alternative single-chain Duokine (**scDuokine**) format, three ECDs of the same ligand were connected in a row (GGGSGGG linkers in case of CD40L, CD27L and OX40L or $(GGGGS)_4$ linkers in case of 4-1BBL), resulting in scCD40L, scCD27L, sc4-1BBL and scOX40L. Afterwards, two of the single-chain ligands were connected via a 15 aa linker, creating a bifunctional monomeric hexavalent single-chain molecule with intramolecular homotrimerization of the ligands (Figure 22 A, B). By incorporating two different cytokines, two modes of action (cis-acting and trans-acting) were realized. Duokines combining two of the ligands CD27L, 4-1BBL and OX40L are targeting CD27, 4-1BB and OX40 expressed on the same T cell and thereby specified to be **cis-acting**. Importantly, in this concept Duokines linking CD27L, 4-1BBL or OX40L are always defined as cis-acting Duokines, although they can also act in trans on two adjacent T cells. Hence, only if CD40L is incorporated in a Duokine, the protein is named **trans-acting** as it is addressing both $CD40^+$ antigen-presenting cells and T cells simultaneously (Figure 22 C).

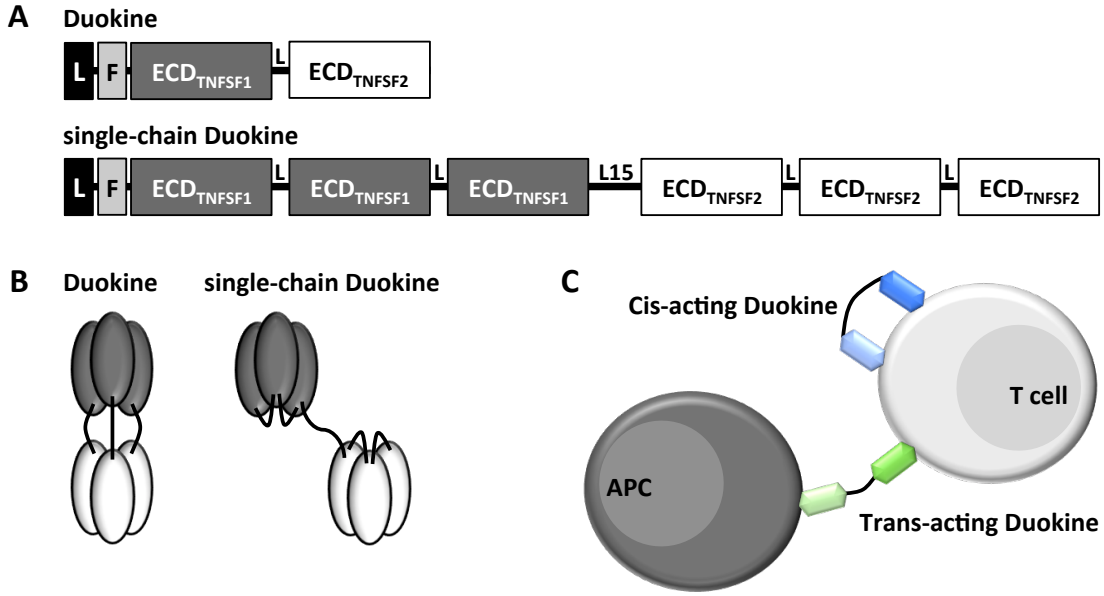

Figure 22: Concept of dual-acting immunostimulatory cytokine fusion proteins. A) Molecular composition of Duokines and scDuokines. **B)** Schematic assembly of homotrimeric hexavalent Duokines (composed of three monomers) and monomeric hexavalent scDuokines (one polypeptide chain). **C)** Illustration of the two different modes of action for Duokines and scDuokines.

In summary, CD40L was combined with each CD27L, 4-1BBL and OX40L in both possible orientations and both protein formats, resulting in six trans-acting Duokines and six trans-acting scDuokines. Likewise, all possible combinations of the costimulatory ligands CD27L, 4-1BBL and OX40L were fused in both orientations and protein arrangements, leading to six cis-acting Duokines and six cis-acting scDuokines (Figure 23). Overall, 24 different Duokines and scDuokines were generated, each provided N-terminally with a FLAG-tag for purification.

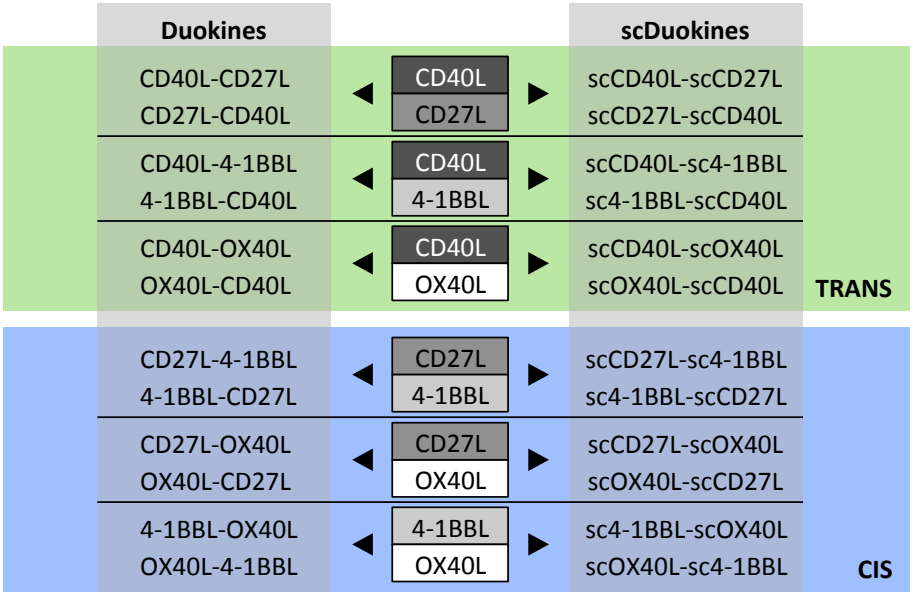

Figure 23: Summary of all Duokines and single-chain Duokines. Graphical illustration of 12 Duokines and 12 scDuokines achieved by combining CD40L, CD27L, 4-1BBL and OX40L in all possible orientations. Trans-acting proteins always contained CD40L.

3.3.1 Biochemical characterization of Duokines and scDuokines

Duokines and scDuokines were produced in stably transfected HEK293T cells and purified from the cell culture supernatant via FLAG affinity chromatography resulting in average yields of 0.9 mg/L (range 0.5 - 1.9 mg/L) for Duokines and 2.4 mg/L (range 1.4 - 4.0 mg/L) for scDuokines (Table 19). Protein purity was checked in SDS-PAGE analysis under reducing and non-reducing conditions, where both Duokines and scDuokines appeared as major bands corresponding to their monomers (Figure 24). Depending on the number of potential N-glycosylation sites (CD40L: 1 site, CD27L: 2 sites, OX40L: 4 sites) the proteins migrated at slightly higher apparent molecular masses than calculated (Duokines 33 - 38 kDa, scDuokines 97 - 111 kDa). Additionally, some Duokines displayed a second minor band around the size of a dimer under non-reducing conditions (Figure 24 A) and all OX40L-bearing scDuokines showed higher molecular mass complexes under reducing conditions (Figure 24 B).

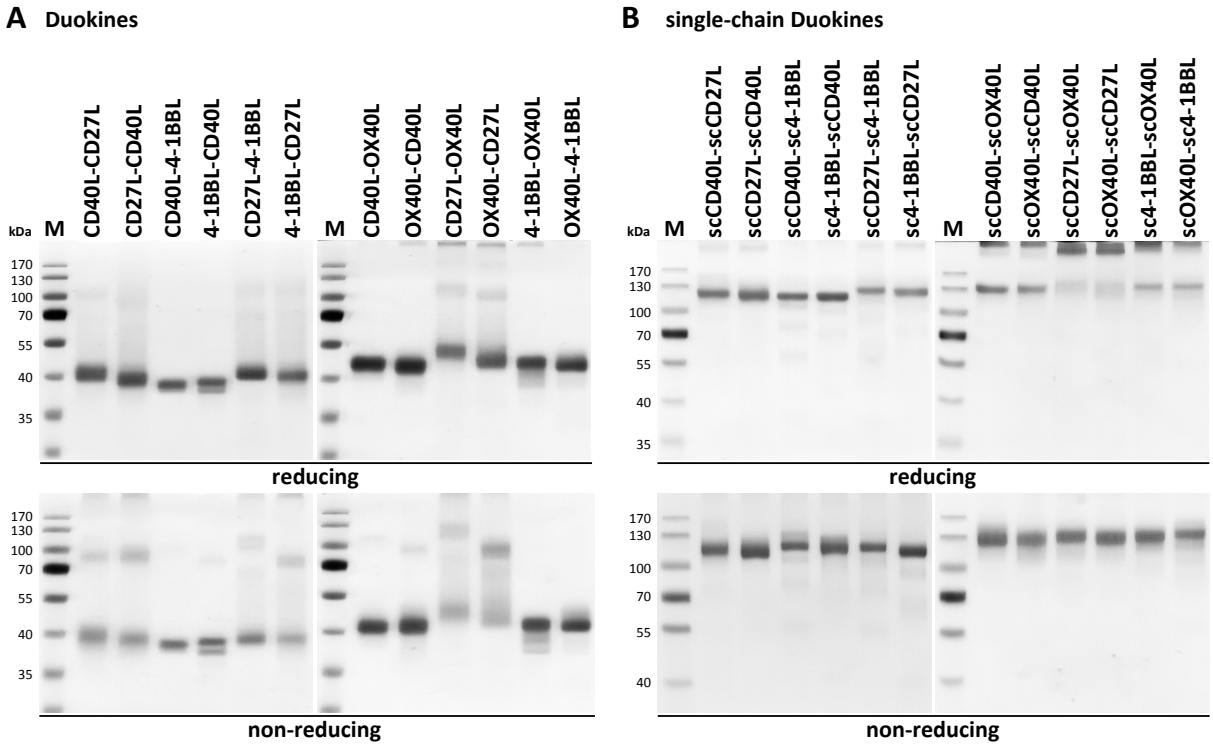

Figure 24: SDS-PAGE analysis of Duokines and scDuokines. 2 µg purified protein of **A)** Duokines (12% PAA) and **B)** scDuokines (10% PAA) were separated under both reducing and non-reducing conditions and visualized by Coomassie-staining.

Size exclusion chromatography confirmed correct assembly into homotrimeric (Duokines) or monomeric (scDuokines) molecules under native conditions and only minor fractions of higher-order complexes were detectable for some of the proteins indicating rather homogenous protein compositions (Figure 25). Table 19 provides an overview of the

molecular masses deduced from the retention times. The less glycosylated Duokines and scDuokines (especially when containing 4-1BBL) exhibited a smaller apparent molecular mass than calculated from the amino acid sequence. This observation was generally in accordance with the number of potential N-glycosylation sites, resulting in the highly-glycosylated OX40L-bearing Duokines and scDuokines showing the highest apparent molecular masses. Regarding the two possible orientations of the particular proteins no clear differences in the apparent molecular masses of all scDuokines and most Duokines were identified. Strikingly though, the Duokines, but not scDuokines, with C-terminal 4-1BBL exhibited a clearly smaller apparent molecular mass than their counterpart with the reversed orientation (Table 19).

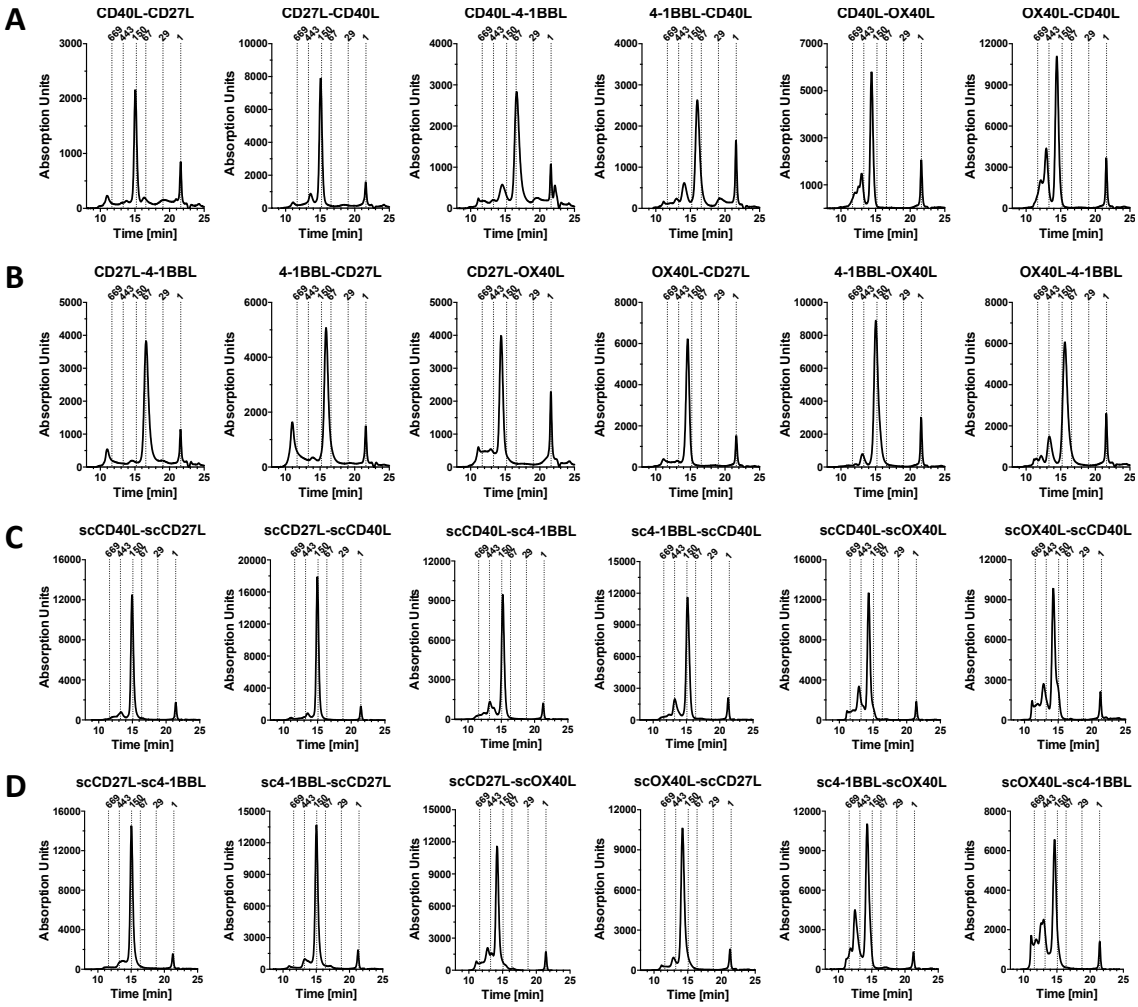

Figure 25: Size exclusion chromatography of Duokines and scDuokines. Native state assembly of **A)** trans-acting and **B)** cis-acting Duokines as well as **C)** trans-acting and **D)** cis-acting scDuokines was analyzed by gel filtration (Yarra SEC-2000, flow rate 0.5 ml/min). Molecular masses (in kDa) of standard proteins are indicated.

In general, the 12 Duokines and 12 scDuokines were produced in adequate purity and showed mostly correct assembly regardless of protein format and ligand combination. All evaluated biochemical characteristics are summarized in Table 19.

Table 19: Biochemical characteristics of Duokines & scDuokines. Molecular mass (MW) calculated from the amino acid sequence. Yields correspond to the amount of protein purified from 1 liter cell culture supernatant.

	Protein	Linker	MW_{calc} (kDa, chain)	MW_{SEC} (kDa, native)	N-glycosylation (per chain)	Yield (Ø in mg/L)
Trans-acting Duokines	**CD40L-CD27L**	$(G_4S)_3$	33.5	162.0	3	0.79
	CD27L-CD40L	$(G_4S)_3$	33.6	162.0	3	0.52
	CD40L-4-1BBL	$(G_4S)_4$	37.8	64.3	1	0.56
	4-1BBL-CD40L	$(G_4S)_4$	37.6	91.5	1	0.58
	CD40L-OX40L	$(G_4S)_3$	33.4	235.1	5	0.79
	OX40L-CD40L	$(G_4S)_3$	33.4	233.0	5	0.67
Cis-acting Duokines	**CD27L-4-1BBL**	$(G_4S)_4$	37.6	65.4	2	0.46
	4-1BBL-CD27L	$(G_4S)_4$	37.4	101.7	2	0.83
	CD27L-OX40L	$(G_4S)_3$	33.2	235.1	6	0.66
	OX40L-CD27L	$(G_4S)_3$	33.2	209.1	6	0.88
	4-1BBL-OX40L	$(G_4S)_4$	37.2	165.2	4	1.80
	OX40L-4-1BBL	$(G_4S)_4$	37.4	118.9	4	1.90
Trans-acting scDuokines	**scCD40L-scCD27L**	$G_4SG_4TG_4S$	98.0	161.1	9	2.96
	scCD27L-scCD40L	$G_4SG_4TG_4S$	98.0	159.5	9	3.52
	scCD40L-sc4-1BBL	$G_4SG_4TG_4S$	111.1	125.7	3	2.19
	sc4-1BBL-scCD40L	$G_4SG_4TG_4S$	111.3	131.1	3	2.11
	scCD40L-scOX40L	$G_4SG_4TG_4S$	97.5	229.7	15	1.97
	scOX40L-scCD40L	$G_4SG_4TG_4S$	97.5	224.1	15	2.14
Cis-acting scDuokines	**scCD27L-sc4-1BBL**	$G_4SG_4TG_4S$	110.6	141.0	6	1.99
	sc4-1BBL-scCD27L	$G_4SG_4TG_4S$	110.7	143.9	6	1.96
	scCD27L-scOX40L	$G_4SG_4TG_4S$	96.9	250.8	18	2.13
	scOX40L-scCD27L	$G_4SG_4TG_4S$	96.9	230.8	18	1.41
	sc4-1BBL-scOX40L	$G_4SG_4TG_4S$	110.2	219.6	12	2.34
	scOX40L-sc4-1BBL	$G_4SG_4TG_4S$	110.1	192.5	12	4.07

3.3.2 Binding and activation of cytokine receptors by Duokines and scDuokines

In order to verify the correct assembly of the costimulatory ligands within the various Duokine protein formats, binding of one TNFRSF receptor at a time was tested in ELISA. Both Duokines (Figure 26 A) and scDuokines (Figure 26 B) showed specific binding to their respective receptors and no crossreactivity with the other TNFRSF receptors was detected. Furthermore, the concentration-dependent interaction of Duokines and scDuokines with their receptors was characterized by EC_{50} values in the low nanomolar range (Table 20).

Compared to the homotrimeric ligand CD40L (EC_{50} 0.8 ± 0.4 nM), the ability to bind CD40 was similar for most trans-acting Duokines, but CD40L-4-1BBL (EC_{50} 8.7 ± 3.6 nM) and CD40L-CD27L (EC_{50} 12.3 ± 3.8 nM) showed 10 to 15-fold lower binding strength. Generally, the CD40-binding of trans-acting Duokines was weaker in the case of N-terminal CD40L than C-terminal CD40L. In contrast, cis-acting Duokines retained the same binding properties as the homotrimeric ligands 4-1BBL (EC_{50} 2.2 ± 0.8 nM) and OX40L (EC_{50} 1.4 ± 0.4 nM) or in the case of CD27L (EC_{50} 14.9 ± 4.0 nM) even improved them up to 10-fold (Table 20). Transferring the homotrimeric ligands into single-chain molecules did not alter their binding capacities (scCD40L: EC_{50} 1.4 ± 0.7 nM, sc4-1BBL: EC_{50} 1.7 ± 0.4 nM, scOX40L: EC_{50} 1.3 ± 0.3 nM). Binding was even improved in the case of scCD27L (EC_{50} 1.8 ± 0.2 nM), similar to the Duokines bearing CD27L. Consequently, both trans-acting and cis-acting scDuokines showed comparable receptor binding properties as the respective single-chain ligands. Only the binding of OX40 by the cis-acting scDuokines scCD27L-scOX40L and scOX40L-scCD27L was clearly reduced with EC_{50} values of 14.3 ± 1.2 nM and 60.2 ± 43.6 nM (Table 20).

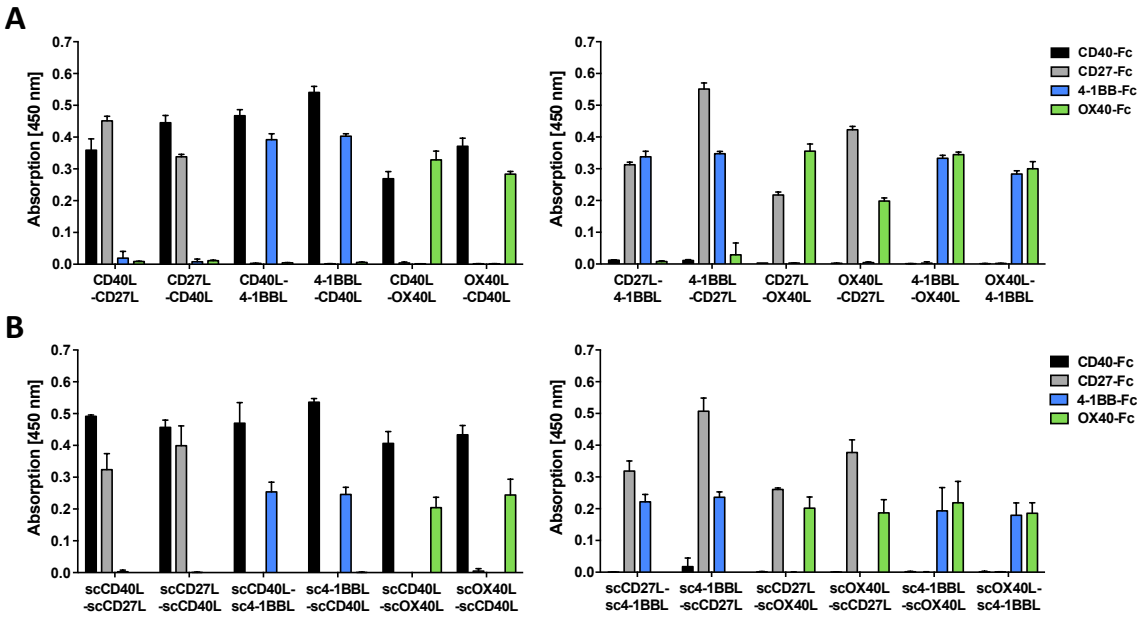

Figure 26: TNFRSF receptor binding of Duokines and scDuokines. Binding of **A)** trans-acting and cis-acting Duokines (100 nM) as well as **B)** trans-acting and cis-acting scDuokines (5 µg/ml) to 200 ng immobilized CD40-, CD27-, 4-1BB- and OX40-Fc was tested in ELISA. Mean ± SD, n = 3. Duokines with block-shift correction.

Table 20: EC_{50} values [nM] for TNFRSF receptor binding by Duokines & scDuokines. Binding of receptors (immobilized as IgG1 Fc fusion proteins) was analyzed in ELISA. EC_{50} values [nM] are shown as mean ± SD, n = 3.

Format	Protein	CD40	CD27	4-1BB	OX40
Ligands	**CD40L**	0.8 ± 0.4	–	–	–
	CD27L	–	14.9 ± 4.0	–	–
	4-1BBL	–	–	2.2 ± 0.8	–
	OX40L	–	–	–	1.4 ± 0.4
Trans-acting Duokines	**CD40L-CD27L**	12.3 ± 3.8	5.0 ± 0.2	–	–
	CD27L-CD40L	3.0 ± 1.4	4.7 ± 0.6	–	–
	CD40L-4-1BBL	8.7 ± 3.6	–	2.2 ± 1.0	–
	4-1BBL-CD40L	1.5 ± 0.4	–	1.4 ± 0.3	–
	CD40L-OX40L	2.5 ± 1.1	–	–	0.6 ± 0.2
	OX40L-CD40L	1.6 ± 0.4	–	–	1.0 ± 0.1
Cis-acting Duokines	**CD27L-4-1BBL**	–	6.9 ± 2.3	1.6 ± 0.2	–
	4-1BBL-CD27L	–	1.9 ± 0.4	2.1 ± 0.5	–
	CD27L-OX40L	–	6.8 ± 0.8	–	7.7 ± 8.9
	OX40L-CD27L	–	1.5 ± 0.5	–	5.6
	4-1BBL-OX40L	–	–	1.1 ± 0.2	0.5 ± 0.2
	OX40L-4-1BBL	–	–	1.3 ± 0.3	2.5 ± 2.5
single-chain Ligands	**scCD40L**	1.4 ± 0.7	–	–	–
	scCD27L	–	1.8 ± 0.2	–	–
	sc4-1BBL	–	–	1.7 ± 0.4	–
	scOX40L	–	–	–	1.3 ± 0.3
Trans-acting scDuokines	**scCD40L-scCD27L**	4.4 ± 0.5	3.6 ± 0.4	–	–
	scCD27L-scCD40L	6.1 ± 2.2	3.3 ± 0.05	–	–
	scCD40L-sc4-1BBL	6.3 ± 1.2	–	2.5 ± 0.6	–
	sc4-1BBL-scCD40L	3.6 ± 1.8	–	2.1 ± 0.3	–
	scCD40L-scOX40L	4.4 ± 0.9	–	–	2.8 ± 1.4
	scOX40L-scCD40L	4.7 ± 1.8	–	–	5.5 ± 3.7
Cis-acting scDuokines	**scCD27L-sc4-1BBL**	–	8.3 ± 0.9	4.2 ± 1.6	–
	sc4-1BBL-scCD27L	–	2.7 ± 0.1	3.6 ± 1.3	–
	scCD27L-scOX40L	–	5.3 ± 1.8	–	14.3 ± 1.2
	scOX40L-scCD27L	–	4.2 ± 1.0	–	60.2 ± 43.6
	sc4-1BBL-scOX40L	–	–	3.0 ± 0.1	4.4 ± 1.4
	scOX40L-sc4-1BBL	–	–	3.8 ± 0.7	4.9 ± 0.8

– no ligand/receptor interaction

Bifunctionality of Duokines and scDuokines was determined by flow cytometry analysis. Here, the binding to receptor-expressing target cells mediated by one ligand was detected via the interaction of the second ligand with its receptor presented as Fc-fusion protein in soluble form. Simultaneous binding of both costimulatory ligands to their receptors was confirmed for all Duokines (Figure 27 A) and scDuokines (Figure 27 B).

In summary, incorporating costimulatory ligands in the novel Duokine and scDuokine format did either conserve or strengthen their receptor binding properties and the bifunctionality of the fusion proteins was assured by simultaneous binding of both targeted receptors.

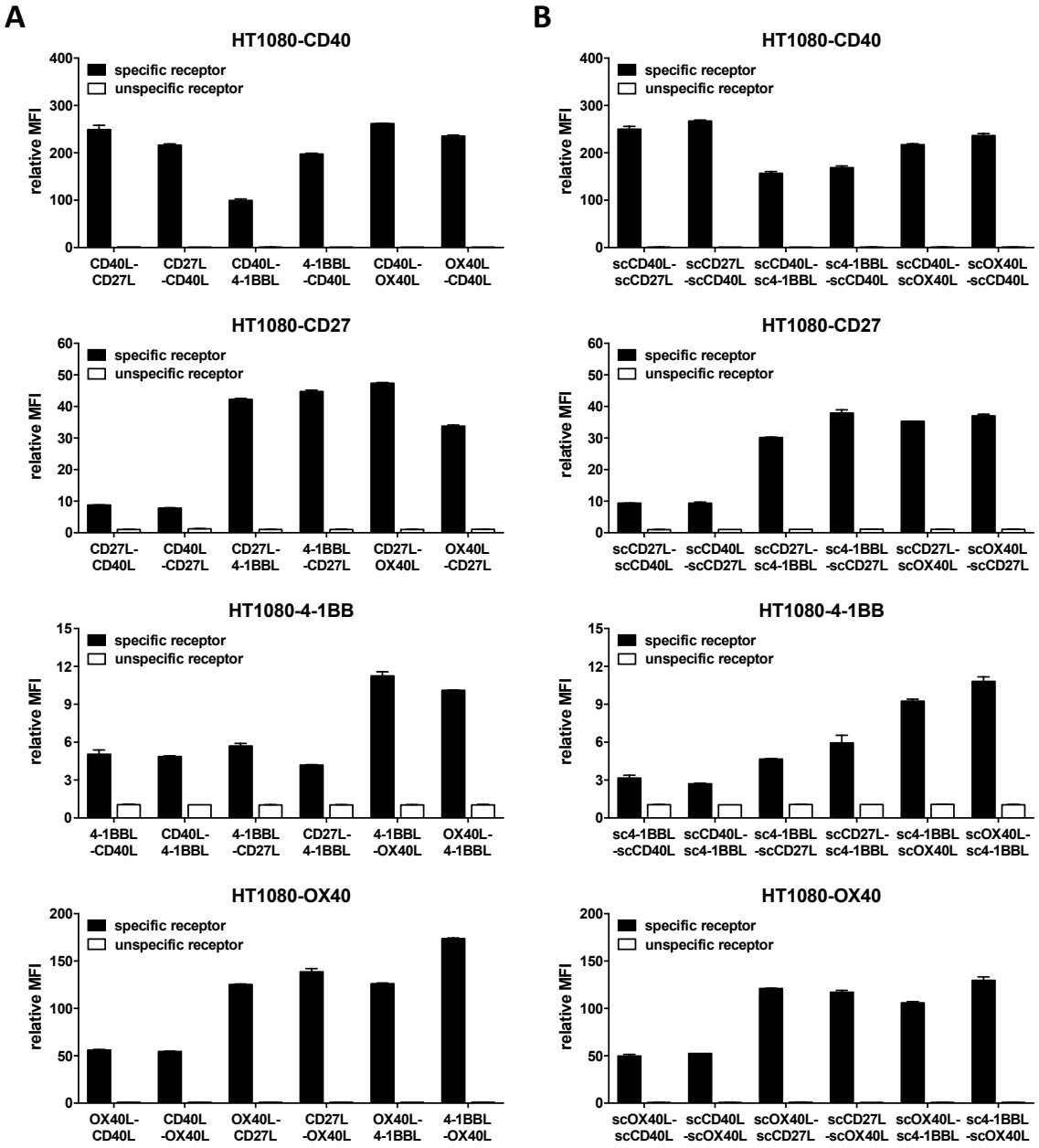

Figure 27: Simultaneous binding of two TNFRSF receptors by Duokines and scDuokines. After binding of **A)** Duokines and **B)** scDuokines (100 nM) to $1.5*10^5$ CD40-, CD27-, 4-1BB- and OX40-expressing HT1080 cells, the bound proteins were detected using the corresponding specific receptor-Fc fusion proteins (10 nM) and a PE-labeled anti-human Fc antibody. TNFR1-Fc was included as unspecific negative control. n = 1, duplicates.

In a next step, the bioactivity of Duokines and scDuokines was assessed by measuring IL-8 release induced upon TNFRSF-dependent NFκB-signaling. First, receptor expression and binding of the fusion proteins to HT1080 cells stably transfected with the TNFRSF receptors was confirmed in flow cytometry (data not shown). In their soluble homotrimeric form

neither CD27L nor 4-1BBL was able to activate its receptor, while CD40L and OX40L only induced minor IL-8 release, preferably at high concentrations. In the case of scCD40L (EC_{50} 2.6 ± 0.06 nM) and scOX40L (EC_{50} 0.4 ± 0.1 nM) converting the ligands into the single-chain format clearly improved their receptor activation properties, while scCD27L and sc4-1BBL exhibited only minor IL-8 release, preferably at higher concentrations (Figure 28).

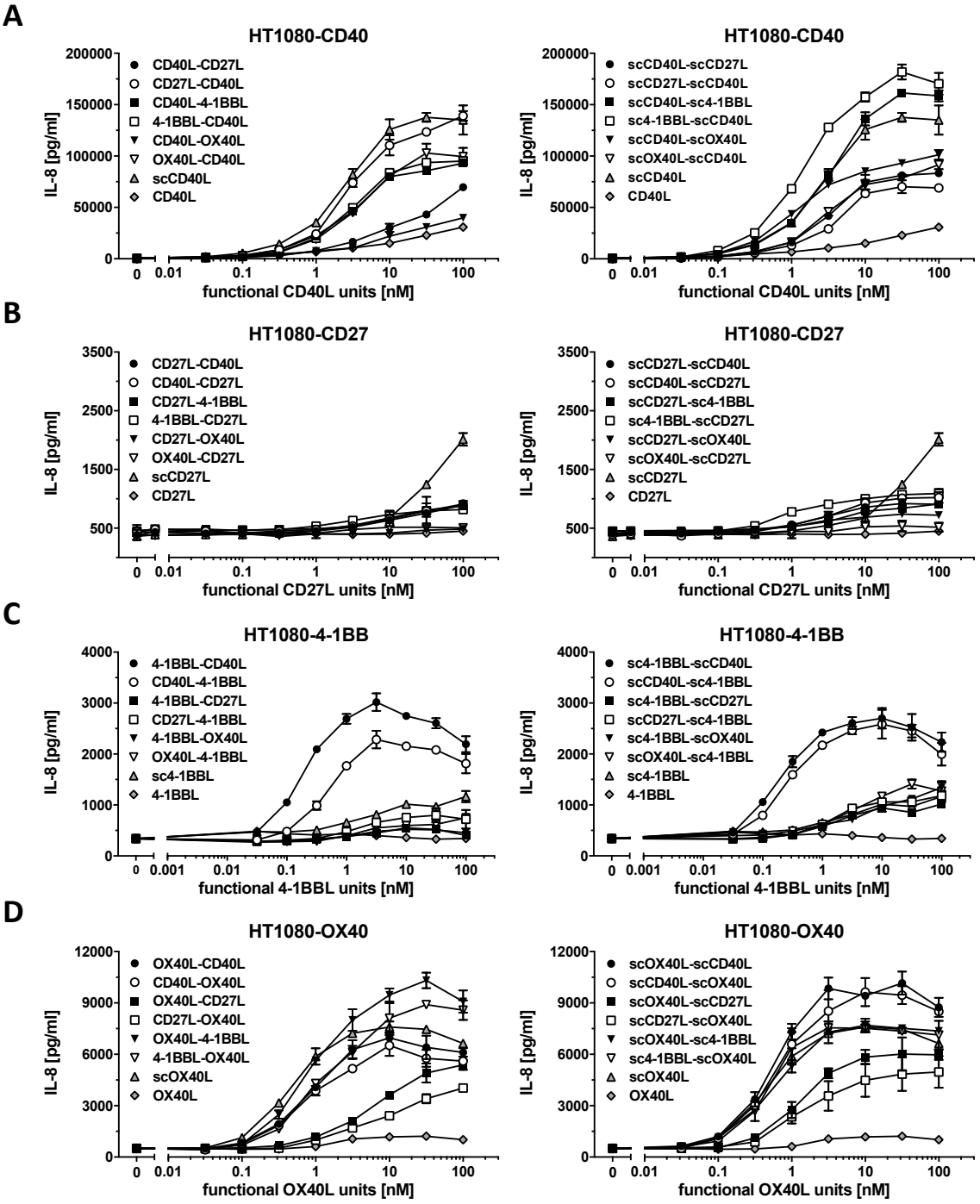

Figure 28: Receptor activation measured via IL-8 release upon TNFRSF-dependent NFκB activation. $2*10^4$ HT1080-CD40, HT1080-CD27, HT1080-4-1BB or HT1080-OX40 cells were incubated with soluble Duokines or scDuokines at 37°C, 5% CO_2 and amounts of released IL-8 were measured after 18 h by Sandwich-ELISA. Mean ± SD, n = 3 (n = 6 for HT1080-CD27), block-shift correction.

Most trans-acting Duokines and scDuokines strongly activated CD40 with low nanomolar EC_{50} values comparable to scCD40L (Table 21). While CD27L-CD40L was the Duokine most potent in stimulating CD40, the reversed ligand orientation (CD40L-CD27L) nearly completely suppressed receptor activation. Generally, scDuokines were more efficient in activating CD40 than Duokines, with scCD40L-sc4-1BBL and sc4-1BBL-scCD40L even exceeding the stimulatory potential of scCD40L (Figure 28 A). In contrast, hardly any IL-8 release was detectable upon stimulating HT1080-CD27 with both Duokines and scDuokines. Compared to the mostly inactive CD27L-Duokines, the scDuokines were more potent in inducing at least some CD27-activation, with sc4-1BBL-scCD27L showing the best EC_{50} value of 1.4 ± 0.6 nM (Figure 28 B). Despite EC_{50} values in the low nanomolar range, sc4-1BBL and most 4-1BBL-containing Duokines and scDuokines induced only limited activation of 4-1BB as shown by the release of small IL-8 amounts. However, addressing 4-1BB with trans-acting Duokines and scDuokines combining 4-1BBL and CD40L (CD40L-4-1BBL, 4-1BBL-CD40L, scCD40L-sc4-1BBL, sc4-1BBL-scCD40L) resulted in strong receptor activation with EC_{50} values enhanced by one order of magnitude (EC_{50} 0.1 - 0.4 nM) and clearly increased IL-8 levels (Figure 28 C). OX40L-mediated activation of the OX40 receptor was generally strong, but slightly more potent when applying scDuokines instead of Duokines (Figure 28 D). For both protein formats, IL-8 secretion induced by proteins combining OX40L with CD40L or 4-1BBL was comparable to scOX40L alone, but especially CD27L-OX40L and OX40L-CD27L showed reduced EC_{50} values (Table 21).

Table 21: EC_{50} values [nM] for TNFRSF receptor activation by Duokines & scDuokines. Receptor activation was measured by NFκB-induced IL-8 release from stable HT1080 transfectants. Mean ± SD, n = 3.

Format	Protein	CD40	CD27	4-1BB	OX40
Ligands	**CD40L**	> 50	–	–	–
	CD27L	–	n.d.	–	–
	4-1BBL	–	–	n.d.	–
	OX40L	–	–	–	n.d.
Trans-acting Duokines	**CD40L-CD27L**	> 50	n.d.	–	–
	CD27L-CD40L	2.8 ± 1.9	n.d.	–	–
	CD40L-4-1BBL	3.8 ± 3.3	–	0.4 ± 0.1	–
	4-1BBL-CD40L	2.9 ± 2.5	–	0.2 ± 0.09	–
	CD40L-OX40L	> 50	–	–	0.9 ± 0.6
	OX40L-CD40L	3.7 ± 2.3	–	–	0.8 ± 0.5
Cis-acting Duokines	**CD27L-4-1BBL**	–	n.d.	1.5 ± 0.4	–
	4-1BBL-CD27L	–	n.d.	1.8 ± 1.6	–
	CD27L-OX40L	–	n.d.	–	18.2 ± 11.8
	OX40L-CD27L	–	n.d.	–	7.7 ± 2.4
	4-1BBL-OX40L	–	–	1.0 ± 0.3	1.5 ± 0.6
	OX40L-4-1BBL	–	–	2.4 ± 1.7	1.0 ± 0.5
single-chain Ligands	**scCD40L**	2.6 ± 0.06	–	–	–
	scCD27L	–	> 50	–	–
	sc4-1BBL	–	–	2.6 ± 1.8	–
	scOX40L	–	–	–	0.4 ± 0.1
Trans-acting scDuokines	**scCD40L-scCD27L**	3.5 ± 0.7	3.2 ± 1.2	–	–
	scCD27L-scCD40L	4.0 ± 0.6	3.0 ± 1.1	–	–
	scCD40L-sc4-1BBL	3.9 ± 2.8	–	0.2 ± 0.08	–
	sc4-1BBL-scCD40L	1.8 ± 0.8	–	0.1 0.05	–
	scCD40L-scOX40L	1.3 ± 0.2	–	–	0.6 ± 0.2
	scOX40L-scCD40L	2.6 ± 1.3	–	–	0.5 ± 0.2
Cis-acting scDuokines	**scCD27L-sc4-1BBL**	–	5.5 ± 2.2	1.6 ± 0.3	–
	sc4-1BBL-scCD27L	–	1.4 ± 0.6	1.6 ± 0.9	–
	scCD27L-scOX40L	–	3.2 ± 2.4	–	1.5 ± 0.3
	scOX40L-scCD27L	–	n.d.	–	1.3 ± 0.2
	sc4-1BBL-scOX40L	–	–	6.1 ± 1.1	0.5 ± 0.03
	scOX40L-sc4-1BBL	–	–	3.2 ± 1.3	0.6 ± 0.2

– no ligand/receptor interaction n.d. no activation detectable

3.3.3 *In vitro* stability of Duokines and scDuokines

All Duokines and scDuokines were analyzed regarding their *in vitro* stability in human plasma at 37°C. Except for CD40L-4-1BBL and OX40L-4-1BBL, which nearly preserved their protein integrity and ligand-receptor binding capacities over the entire analyzed time period, all other proteins showed a time-dependent drop in intact protein level. After 7 days, between

37% and 72% of most Duokines were still detectable, but the amount of intact CD27L-CD40L, CD27L-4-1BBL and 4-1BBL-CD27L significantly decreased to less than 10% (Figure 29 A). In contrast to the Duokines, the stability profiles of all scDuokines were rather similar showing a somewhat reduced stability with 24 - 58% intact protein remaining after 7 days (Figure 29 B). In summary, no major differences in *in vitro* stability were identifiable between the two protein formats. However, the stability of Duokines appeared to be probably influenced by the incorporated costimulatory ligands, while the scDuokines remained more or less unaffected thereof.

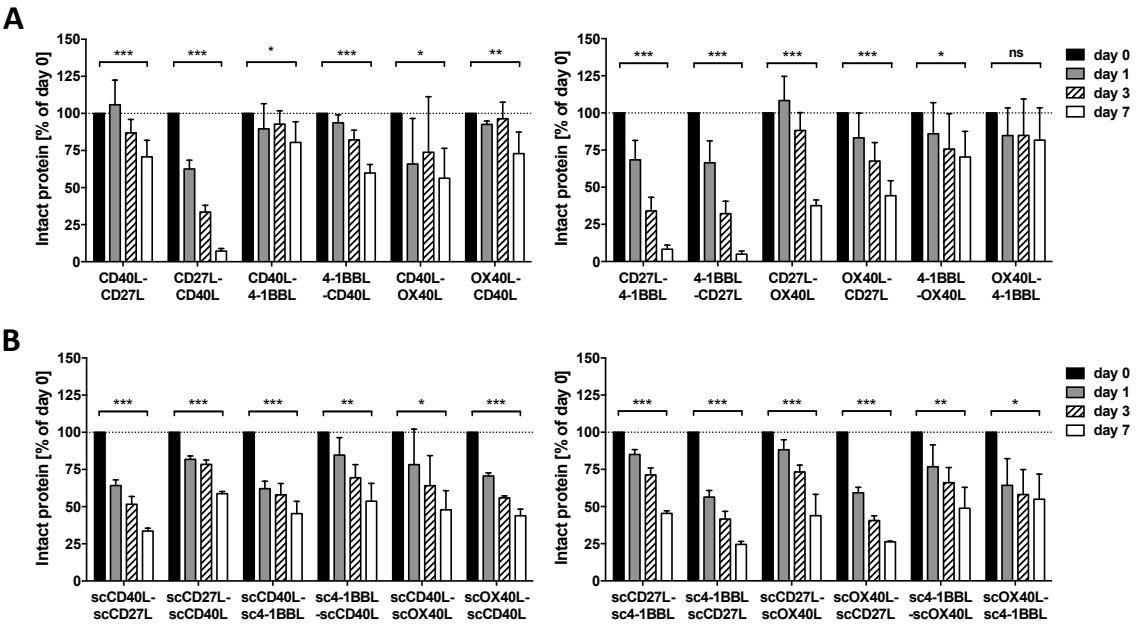

Figure 29: Plasma stability of Duokines and scDuokines. Stability of initially 200 nM **A)** Duokines and **B)** scDuokines was assessed over 7 days in 50% human plasma. Levels of intact protein were determined via binding of CD40-, CD27-, 4-1BB- and OX40-Fc in ELISA. To ensure detection of only full-length proteins the receptor corresponding to the C-terminal ligand was coated and the N-terminal FLAG-tag was detected. Data was normalized to day 0. Mean ± SD, n = 3 (scDuokines) or n = 6 (Duokines), One-Way ANOVA.

3.3.4 Duokines and scDuokines enhance proliferation of prestimulated T cells

The costimulatory activity of Duokines and scDuokines was determined by measuring the enhancement of T cell proliferation above the levels induced by suboptimal anti-CD3 prestimulation. In a first setting, all Duokines and scDuokines in both possible orientations were tested in solution with bulk PBMC populations. Here, most proteins increased the amount of proliferating $CD3^+$ T cells in a dose-dependent manner when applied in combination with crosslinked anti-CD3 mAb (Figure 30) and no differences in proliferative effects were detectable for the different ligand orientations within the fusion proteins. All

Duokines and scDuokines combining 4-1BBL with CD40L or CD27L strongly enhanced T cell proliferation up to three-fold independent of the protein format (Figure 30 B, D), while CD40L-OX40L and OX40L-CD40L showed better proliferative capacities than the respective scDuokines (52% vs. 32% proliferating T cells; Figure 30 C). In contrast, Duokines and scDuokines composed of 4-1BBL and OX40L achieved only minor enhancements in T cell proliferation (Figure 30 F) and all proteins linking CD27L to CD40L or OX40L showed no pro-proliferative effects at all (Figure 30 A, E).

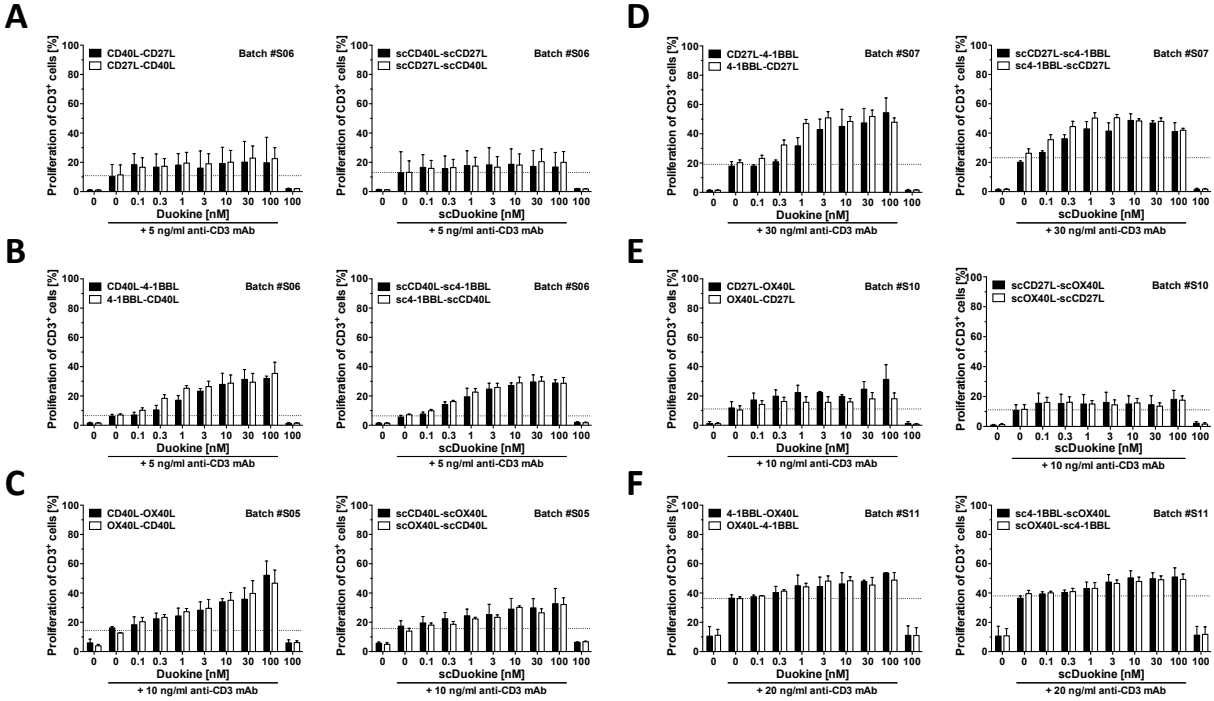

Figure 30: Costimulatory activity of soluble Duokines and scDuokines analyzed by proliferation. $1.5*10^5$ CFSE-stained human PBMCs (bulk population, different batches) were incubated with **A-C)** trans-acting or **D-F)** cis-acting Duokines/scDuokines in presence of cross-linked anti-CD3 mAb (batch-dependent concentration). After 6 days the proliferation of T cells was determined by flow cytometry. Mean ± SEM, n = 3.

So far, Duokines and scDuokines in all possible ligand combinations and orientations, i.e. 24 proteins, were compared in the various experiments. Since no substantial differences were found between the two possible orientations of each Duokine and scDuokine, only one orientation was chosen for further experiments and additionally Duokines and scDuokines combining 4-1BBL and OX40L were excluded from further investigations. As a result, in a second setting the Duokines CD40L-CD27L, 4-1BBL-CD40L and OX40L-CD40L (all trans-acting) as well as 4-1BBL-CD27L and OX40L-CD27L (both cis-acting) were compared to the respective scDuokines in terms of costimulatory activity. Here, it was analyzed whether the selected Duokines and scDuokines were able to enhance T cell proliferation if they are

presented via binding to immobilized TNFRSF receptors with one TNFSF ligand, restricting costimulatory activity to their second TNFSF ligand. In general, simultaneous binding to the immobilized receptor and PBMCs led to proliferation of prestimulated T cells, proving functionality for both binding sites of the fusion proteins (Figure 31).

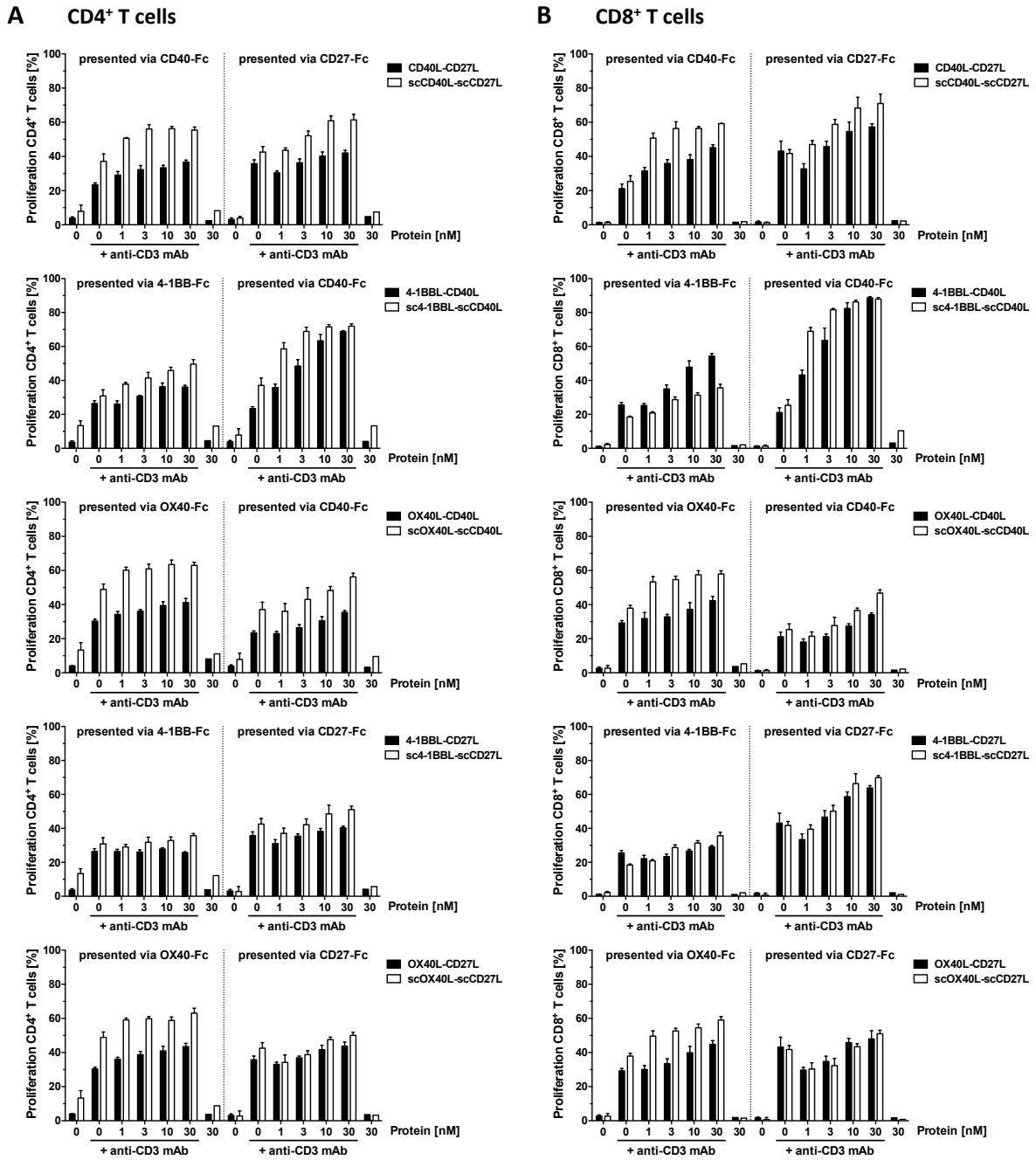

Figure 31: Costimulatory activity of surface-presented Duokines and scDuokines analyzed by proliferation. Selected Duokines and scDuokines were incubated on immobilized TNFRSF-Fc (200 ng/well) for 1 h before washing unbound proteins away. $1.5*10^5$ CFSE-stained human PBMCs (bulk population, batch #S19 for Duokines and #S15 for scDuokines) were added together with crosslinked anti-CD3 mAb (batch #S19: 5 ng/ml and batch #S15: 10 ng/ml). After 6 days the proliferation of $CD4^+$ and $CD8^+$ T cells was determined by flow cytometry. Mean ± SD, n = 3, block-shift correction.

All Duokines and scDuokines increased proliferation of $CD4^+$ and $CD8^+$ T cells above the levels of primary stimulation provided through crosslinked anti-CD3 mAb and no proliferation was observed in the absence of anti-CD3 stimulation supporting the costimulatory nature of surface-presented Duokines and scDuokines (Figure 31). Also, both Duokines and scDuokines equally stimulated $CD4^+$ T cells (Figure 31 A) and $CD8^+$ T cells (Figure 31 B) demonstrating that both T cell subtypes represent target populations. The T cells were activated independently of the ligand that mediated the stimulatory effects, i.e. proliferation was also induced if trans-acting Duokines and scDuokines were presented with CD40L as effector moiety. Thus, no direct interaction between the proteins and T cells was possible, indicating trans-activating mechanisms between different immune cells. Finally, although the actual costimulatory activity of the various fusion proteins was strongly influenced by the kind of surface-presentation and the examined T cell subtype, the scDuokines induced clearly higher proliferation rates than the Duokines, with 4-1BBL-CD40L presented via 4-1BB-Fc (Figure 31 B) as the only exception.

3.3.5 Single-chain Duokines target various leukocyte populations

With scDuokines tending to be more costimulatory active than Duokines, only scCD40L-scCD27L, sc4-1BBL-scCD40L, scOX40L-scCD40L, sc4-1BBL-scCD27L and scOX40L-scCD27L were further investigated. In order to gain a better understanding of the observed effects and the underlying functionality of single-chain Duokines, possible target cell populations within a bulk PBMC population and the actually targeted cell types were identified in flow cytometry. Since the composition of the leukocyte population is naturally subjected to variability between individual donors, three different PBMC batches were analyzed. Without stimulation, $CD8^+$ T cells accounted for 24% to 35% of all leukocytes that have been determined by FSC/SSC-gating. While no changes in the $CD8^+$ T cell population were observed for one donor (#S23), the amount of $CD8^+$ T cells increased after three days of anti-CD3 stimulation for the other two donors (#S21 and #S22). Prestimulation also clearly enhanced the amount of $CD4^+$ T cells from 12 – 38% up to 27 – 45%. This CD3-mediated increase in T cells was accompanied with a decrease in $CD20^+$ B cells, which constituted the third-largest leukocyte subpopulation of around 15 to 30%. Finally, $CD56^+$ NK cells were identified as the smallest population being largely unaffected by CD3-stimulation.

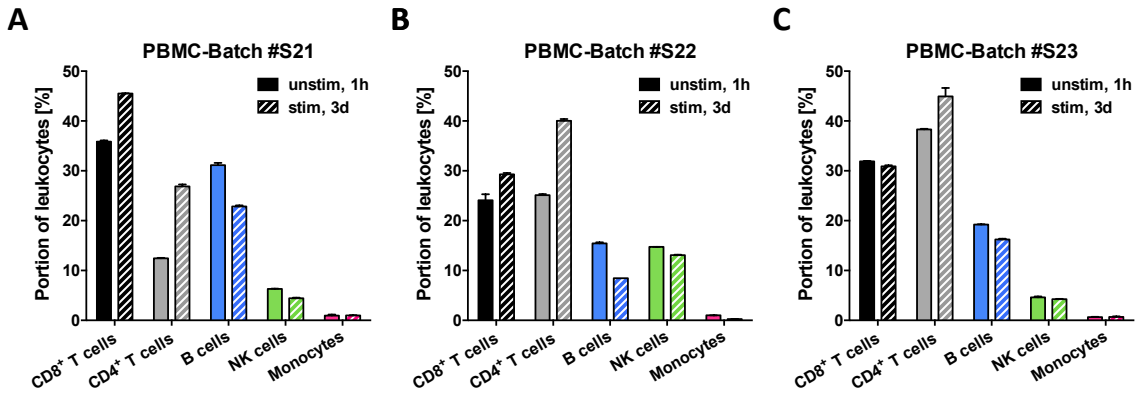

Figure 32: Identification of different immune cell subpopulations. 2.5*10^5 human PBMCs (batches #S21, #S22 and #S23, bulk population) were cultivated at 37°C, 5% CO_2 for 1 h without stimulation or 3 days with anti-CD3 mAb prestimulation (3 – 11 ng/ml, batch-dependent). Subpopulations were identified in flow cytometry by CD marker staining and normalized to the leukocyte gate. T cells: $CD3^+$, $CD4^+$/$CD8^+$. B cells: $CD3^-$, $CD20^+$. NK cells: $CD3^-$, $CD56^+$. Monocytes: $CD3^-$, $CD14^+$. n = 1, duplicates.

In general, due to the treatment of the PBMCs, monocytes adhered to plastic surfaces and were not present in all PBMC experiments (Figure 32). In a next step, the expression pattern of the TNFRSF receptors CD40, CD27, 4-1BB and OX40 was analyzed on the identified cell populations. Regardless of stimulation, CD40 was constitutively expressed on B cells and CD27 on both types of T cells (Figure 33 A, C). Likewise, CD27 was constitutively expressed on approximately 30% of all B cells. While 4-1BB and OX40 were not present on unstimulated PBMCs, both receptors were upregulated on both types of T cells upon CD3-mediated stimulation. Here, 4-1BB was preferably upregulated on $CD8^+$ T cells and OX40 on $CD4^+$ T cells, with a generally more prominent increase in OX40 expression (Figure 33 C). Consistent with the observed receptor expression patterns, the three analyzed trans-acting scDuokines (scCD40L-scCD27L, sc4-1BBL-scCD40L and scOX40L-scCD40L) bound nearly exclusively to B cells in the stimulated and unstimulated setting (Figure 33 B, D). The trans-acting scCD40L-scCD27L targeting both constitutively expressed receptors also bound to a minor share of T cells, although the protein was mainly captured by the B cells. None of the cis-acting scDuokines was detected on B cells, but both bound exclusively to T cells. While sc4-1BBL-scCD27L was detected on both T cell types regardless of the stimulation status, binding of scOX40L-scCD27L was increased after stimulation, which was accompanied by a distinct OX40 upregulation (Figure 33 D). In summary, the results showed that trans-acting scDuokines target B cells independently from stimulation, while cis-acting scDuokines preferably target activated $CD8^+$ and $CD4^+$ T cells.

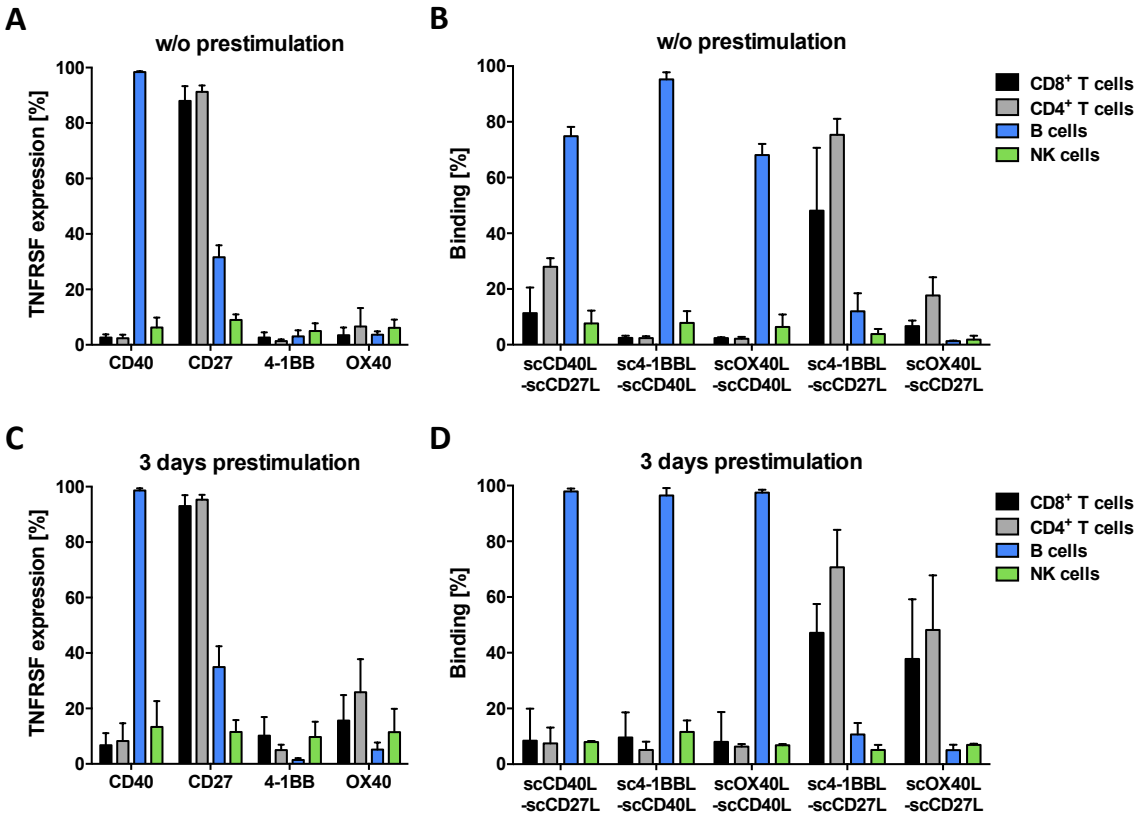

Figure 33: TNFRSF receptor expression on and binding of scDuokines to immune cell subpopulations. $2.5*10^5$ human PBMCs (batches #S21, #S22 and #S23, bulk population) were cultivated at 37°C, 5% CO_2 for **A, B)** 1 hour without stimulation or **C, D)** 3 days with batch-dependent anti-CD3 mAb prestimulation. In flow cytometry, subpopulations were identified and **A, C)** the surface expression of CD40, CD27, 4-1BB and OX40 was determined by antibody staining. **B, D)** The cells were incubated with 10 nM single-chain duokines and binding was detected after 1 hour. Mean ± SD, n = 3 different PBMC batches.

3.3.6 Trans-acting scDuokines in solution activate B cells

As B cells were the major target cells for trans-acting scDuokines, their B cell-activating properties were measured in terms of proliferation and activation marker upregulation. Upon stimulation with the trans-acting scDuokines scCD40L-scCD27L, sc4-1BBL-scCD40L or scOX40L-scCD40L the proliferation rate of $CD20^+$ B cells was increased about 5-fold above the level of mock-treated cells (14% proliferation), while no effects were observed when applying the cis-acting scDuokines. Although all trans-acting scDuokines induced significant proliferation, sc4-1BBL-scCD40L was most effective resulting in 84% proliferating B cells (Figure 34 A). Besides the proliferative effects, upregulation of the B cell activation marker CD69 was also only induced by trans-acting but not cis-acting scDuokines (Figure 34 B). Compared to scCD40L-scCD27L and sc4-1BBL-scCD40L, scOX40L-scCD40L was slightly less activating, but CD69 expression was still significantly increased above the expression level on unstimulated B cells. Additionally, B cell activation mediated by trans-acting scDuokines was

also observed in combination with immobilized anti-IgM antibody, a known activator of B cells (Duddy et al. 2007), resulting in further amplification of the anti-IgM-induced CD69 expression (Figure 34 B). Generally, these observations were in accordance with the previous findings, that trans-acting scDuokines preferably bind to B cells via CD40-CD40L interaction.

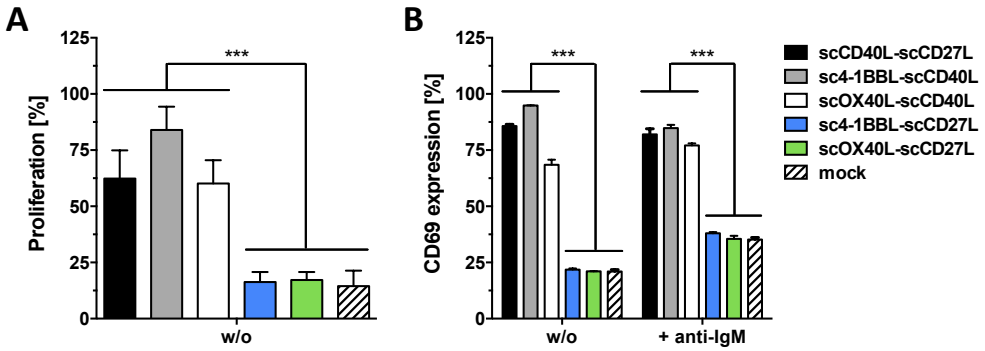

Figure 34: B cell stimulatory activity of selected scDuokines. 1.5*10^5 PBMCs (batch #S23, bulk population) were incubated with 30 nM scDuokines in presence or absence of coated anti-IgM Ab (1:1000). **A)** After 6 days the proliferation of B cells ($CD3^-$, $CD20^+$) was determined by CFSE-dilution in flow cytometry. Mean ± SD, n = 3, One-way ANOVA. **B)** Expression of the activation marker CD69 on B cells ($CD3^-$, $CD20^+$) was assessed after 24 h by flow cytometry. Mean ± SD, n = 3, One-Way ANOVA.

3.3.7 Trans-acting scDuokines in solution activate unstimulated T cells

The proliferation experiments described in chapter 3.3.4 showed that all Duokines and scDuokines were able to enhance CD3-induced T cell activation. With better understanding of the immune cell populations targeted by scDuokines, the connection between the binding to human immune cells and the induction of T cell responses was examined. Therefore, the costimulatory effect on proliferation of $CD4^+$ and $CD8^+$ T cells mediated by scDuokines alone or in combination with an anti-CD3 stimulus was determined using three different PBMC batches. Although immune cell populations varied between the donors (Figure 32), the pattern of scDuokine binding (Figure 33) and the resulting costimulatory effects were comparable. When applied in combination with crosslinked anti-human CD3 mAb as primary stimulus, all analyzed trans-acting and cis-acting scDuokines enhanced the initial CD3-mediated proliferation (43%) of $CD8^+$ T cells up to 2-fold (Figure 35 B). The strongest increase was achieved with the trans-acting sc4-1BBL-scCD40L leading to 89% proliferating $CD8^+$ T cells, while the cis-acting scOX40L-scCD27L resulted in a proliferation rate of only 63%. This proliferation profile triggered by the cis-acting scDuokines was in agreement with the previous findings that sc4-1BBL-scCD27L and scOX40L-scCD27L bind to CD27-, 4-1BB- and OX40-expressing $CD8^+$ T cells in the prestimulated setting. On the contrary, in the case

of the trans-acting scDuokines initial binding to B cells constitutively expressing CD40 presumably enabled trans-presentation of the second costimulatory ligand (CD27L, 4-1BBL or OX40L) incorporated in the scDuokine to primed $CD8^+$ T cells. Without anti-CD3 stimulation the basal proliferation rate of $CD8^+$ T cells was not enhanced by sc4-1BBL-scCD27L and scOX40L-scCD27L. This indicated that cis-acting scDuokines did not exert their costimulatory potential on resting $CD8^+$ T cells, although binding to T cells constitutively expressing CD27 was detected. Strikingly though, trans-acting scCD40L-scCD27L, sc4-1BBL-scCD40L and scOX40L-scCD40L significantly activated resting $CD8^+$ T cells (Figure 35 B). Although this activation resulted only in 11% to 14% proliferating cells, it accounted for a 3-fold increase of proliferation compared to the basal level, suggesting relevant trans-activation of resting $CD8^+$ T cells induced by crosstalk with CD40-expressing B cells.

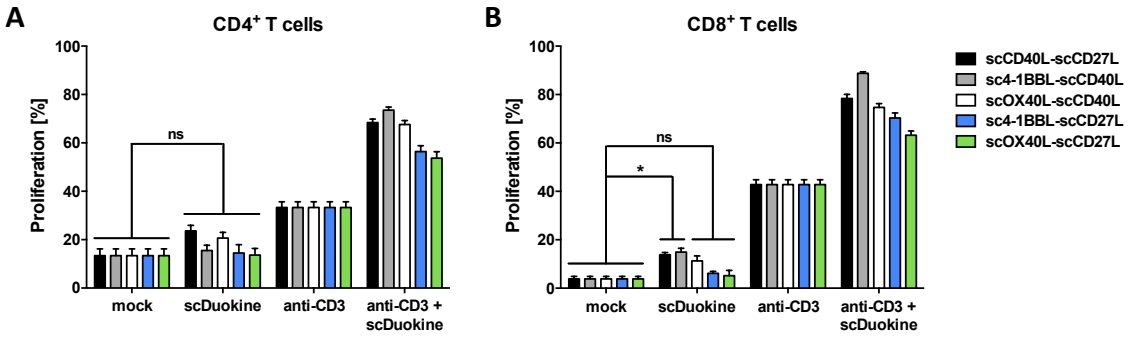

Figure 35: T cell stimulatory activity of selected scDuokines. $1.5*10^5$ PBMCs (batches #S21, #S22 and #S23, bulk population) were incubated with 30 nM scDuokines in presence or absence of anti-CD3 mAb (3 - 11 ng/ml, batch-dependent). After 6 days the proliferation of **A)** $CD4^+$ T cells ($CD3^+$, $CD4^+$) and **B)** $CD8^+$ T cells ($CD3^+$, $CD8^+$) was determined by CFSE-dilution in flow cytometry. Mean ± SD, n = 9 (n = 3 per batch), block-shift correction, One-Way ANOVA.

Although $CD8^+$ T cells reacted slightly more distinctly to scDuokine treatment, all observed scDuokine-mediated costimulatory effects were similarly observed on $CD4^+$ T cells, but generally less $CD4^+$ T cells than $CD8^+$ T cells started to proliferate (Figure 35 A). Interestingly, resting $CD4^+$ T cells were mainly activated by scCD40L-scCD27L, matching the finding that binding of scCD40L-scCD27L to $CD4^+$ T cells was detected in the unstimulated, but not the prestimulated setting, which in turn suggested enhanced crosstalk between B cells and T cells constitutively expressing CD40 and CD27, respectively. In summary, both trans-acting and cis-acting scDuokines successfully exhibited their costimulatory activity on anti-CD3 stimulated $CD4^+$ and $CD8^+$ T cells. Furthermore, *de novo* T cell stimulatory activity was observed for trans-acting scDuokines but not cis-acting scDuokines, which appeared to be linked to the receptor expression profile of the particular T cell subtype.

3.3.8 *In vivo* pharmacokinetics and pharmacodynamics of scDuokines

Pharmacokinetic studies in immunocompetent CD1 mice were performed to assess the *in vivo* bioavailability of Duokines and scDuokines. As inter-species cross-reactivity was not given for all combinations of TNFSF ligands and TNFRSF receptors (Bossen et al. 2006), one mouse-specific Duokine (m4-1BBL-mCD40L) and three mouse-specific scDuokines (msc4-1BBL-mscCD40L, msc4-1BBL-mscCD27L, mscCD40L-mscCD27L) were generated. The murine homologs were produced in HEK293T cells and purified via FLAG affinity chromatography. In SDS-PAGE analysis under reducing conditions, the three mscDuokines showed a single band corresponding to the monomeric molecule. However, due to an uneven number of cysteine in murine 4-1BBL (positions 137, 160, 246) msc4-1BBL-mscCD40L, msc4-1BBL-mscCD27L and m4-1BBL-mCD40L appeared as multimers under non-reducing conditions (Figure 36 A).

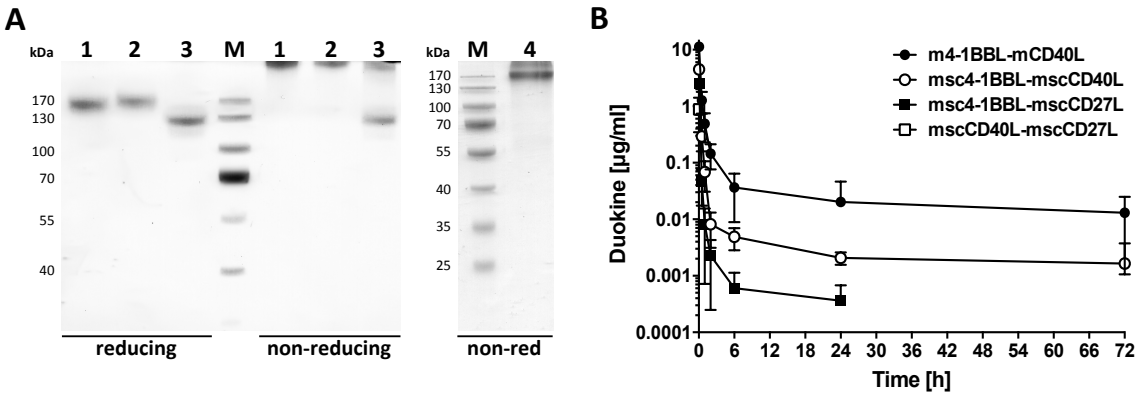

Figure 36: Pharmacokinetics of selected Duokines and scDuokines. A) Murine homologs of Duokines and scDuokines were analyzed in SDS-PAGE (10/12% PAA, 2 µg per lane, Coomassie-staining) under non-reducing or reducing conditions. 1: msc4-1BBL-mscCD40L, 2: msc4-1BBL-mscCD27L, 3: mscCD40L-mscCD27L, 4: m4-1BBL-mCD40L. **B)** Female CD1 mice were treated with 25 µg protein (i.v.) and blood samples were taken over 72 h. Protein concentration in the serum was analyzed via ELISA with human receptors. Mean ± SD, n = 3-6.

All tested immunostimulatory fusion proteins showed pharmacokinetic profiles with particularly short initial half-lives of only 13 to 20 min (Figure 36 B, Table 22). Despite the generally very low bioavailabilities of all Duokines and scDuokines, some differences were observed. Direct comparison of the two protein formats bearing the same costimulatory ligands showed identical terminal half-lives for m4-1BBL-mCD40L and msc4-1BBL-mscCD40L, but the slightly prolonged initial half-life of the mDuokine resulted in a higher bioavailability (AUC 5.25 ± 0.73 h*µg/ml). The two other mscDuokines were even more rapidly cleared from the blood stream with mscCD40L-mscCD27L exhibiting no pharmacokinetic profile at

all, as it was not detectable any more already after 30 min (Figure 36 B). In accordance with the constitutive expression of particular TNFRSF receptors on circulating immune cells analyzed in chapter 3.3.5, which is likely to be similar in the murine system, the general rapid clearance of mDuokines and mscDuokines points to immune cell-specific capturing.

Table 22: Pharmacokinetic properties of murine Duokines and scDuokines. Initial and terminal half-lives ($t_{1/2}\alpha$, $t_{1/2}\beta$) and areas under the curve (AUC) were determined over 72 hours in tumor-free CD1 mice (mean ± SD).

	$t_{1/2}\alpha$ [h]	$t_{1/2}\beta$ [h]	AUC [h*µg/ml]	# of mice
m4-1BBL-mCD40L	0.33 ± 0.05	51.76 ± 3.96	5.25 ± 0.73	5
msc4-1BBL-mscCD40L	0.22 ± 0.03	51.29 ± 27.14	1.31 ± 0.33	6
msc4-1BBL-mscCD27L	0.23 ± 0.00	10.50 ± 0.99	0.62 ± 0.05	3
mscCD40L-mscCD27L	n.d.	n.d.	n.d.	3

n.d. no protein detected

Finally, the therapeutic anti-tumor potential of one trans-acting (msc4-1BBL-mscCD40L) and one cis-acting (msc4-1BBL-mscCD27L) murine scDuokine was investigated *in vivo* using a syngeneic lung tumor model in C57BL/6. Therefore, an experimental setting with B16-FAP mouse melanoma cells previously established in the laboratory (Hornig et al. 2013, Kermer et al. 2012, Kermer et al. 2014) was adapted to the mscDuokines. In this combinatorial approach, a bispecific single-chain diabody targeting human FAP and mouse CD3 (scDb332C11) with known anti-tumor potential was applied as primary MHC-independent T cell stimulatory signal and the murine scDuokines as costimulatory signal enhancer.

The scDb332C11 and both mscDuokines were produced in HEK293T cells and purified via IMAC or FLAG affinity chromatography. SDS-PAGE analysis (Figure 37 A) confirmed sufficient protein purity for the single-chain diabody and multimeric assembly of msc41-BBL-mscCD40L and msc4-1BBL-mscCD27L under non-reducing conditions as already shown in Figure 36 A. Besides some minor impurities, the single-chain diabody eluted as a single peak corresponding to a lower molecular mass than the calculated 55.6 kDa (Figure 37 B). Similar behavior has been identified for various other single-chain diabodies characterized in the laboratory, therefore pointing to normal homogenous assembly of scDb332C11. Both msc4-1BBL-mscCD40L and msc4-1BBL-mscCD27L revealed major peaks indicating apparent molecular masses clearly above their calculated sizes of 124.5 kDa and 123.2 kDa (Figure 37 B). As similar results have been observed in several other in-house studies with scFv36-m4-1BBL, it was presumed that m4-1BBL-bearing fusion proteins form disulfide-linked

oligomers under native conditions (Ranz 2014). Additionally, the predicted high N-glycosylation status of both proteins (12 sites in msc4-1BBL-mscCD40L, 15 sites in msc4-1BBL-mscCD27L) accounted for larger apparent molecular masses. Furthermore, binding of the three proteins to the B16-FAP tumor cells (mouse melanoma stably transfected with human FAP) was tested in flow cytometry. The FAP-specific scDb332C11 bound its target cells in a dose-dependent manner with an EC_{50} value of 4.4 ± 0.9 nM, while both costimulatory mscDuokines did not bind to B16-FAP (Figure 37 C).

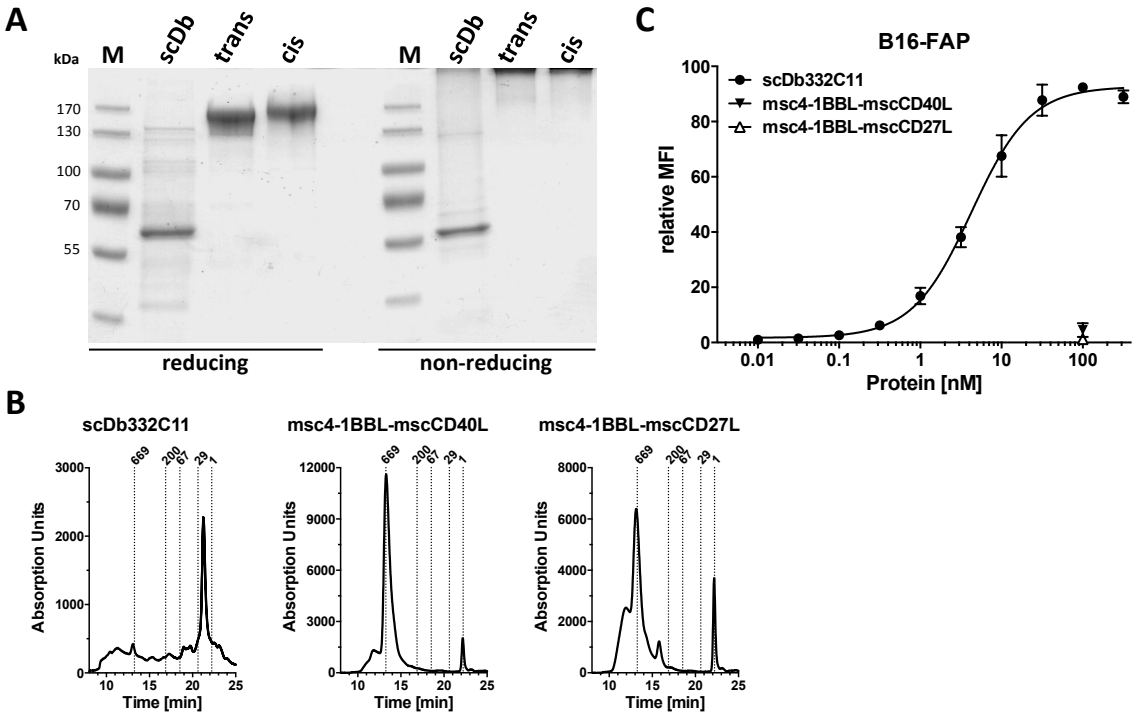

Figure 37: Characterization of proteins used for the *in vivo* lung tumor model. scDb332C11, msc4-1BBL-mscCD40L (trans) and msc4-1BBL-mscCD27L (cis) were analyzed in **A)** SDS-PAGE analysis (10% PAA, 3 µg/lane, Coomassie-staining) and **B)** size exclusion chromatography (Yarra SEC-3000, flow rate 0.5 ml/min). **C)** Binding to B16 mouse melanoma stably transfected with human FAP was tested in flow cytometry. Mean ± SD, n = 3.

Following the combinatorial approach of Hornig et al. 2013, groups of six C57BL/6N mice challenged with B16-FAP (i.v.) were treated with combinations of scDb332C11 (4 pmol) and one mscDuokine each (0.2 nmol) at three early (day 1, 2, 3) and three late (day 8, 9, 10) points in time. After 21 days, mice were sacrificed and tumor burden was evaluated by counting the pulmonary tumor lesions. Lungs with more than 250 tumor lesions, often forming continuous tumor sheets, were considered uncountable and assigned with the fixed value of 250. At the selected dosage of 4 pmol, the mice treated with scDb332C11 showed a very high tumor burden with lungs completely covered by black tumors (Figure 38 A).

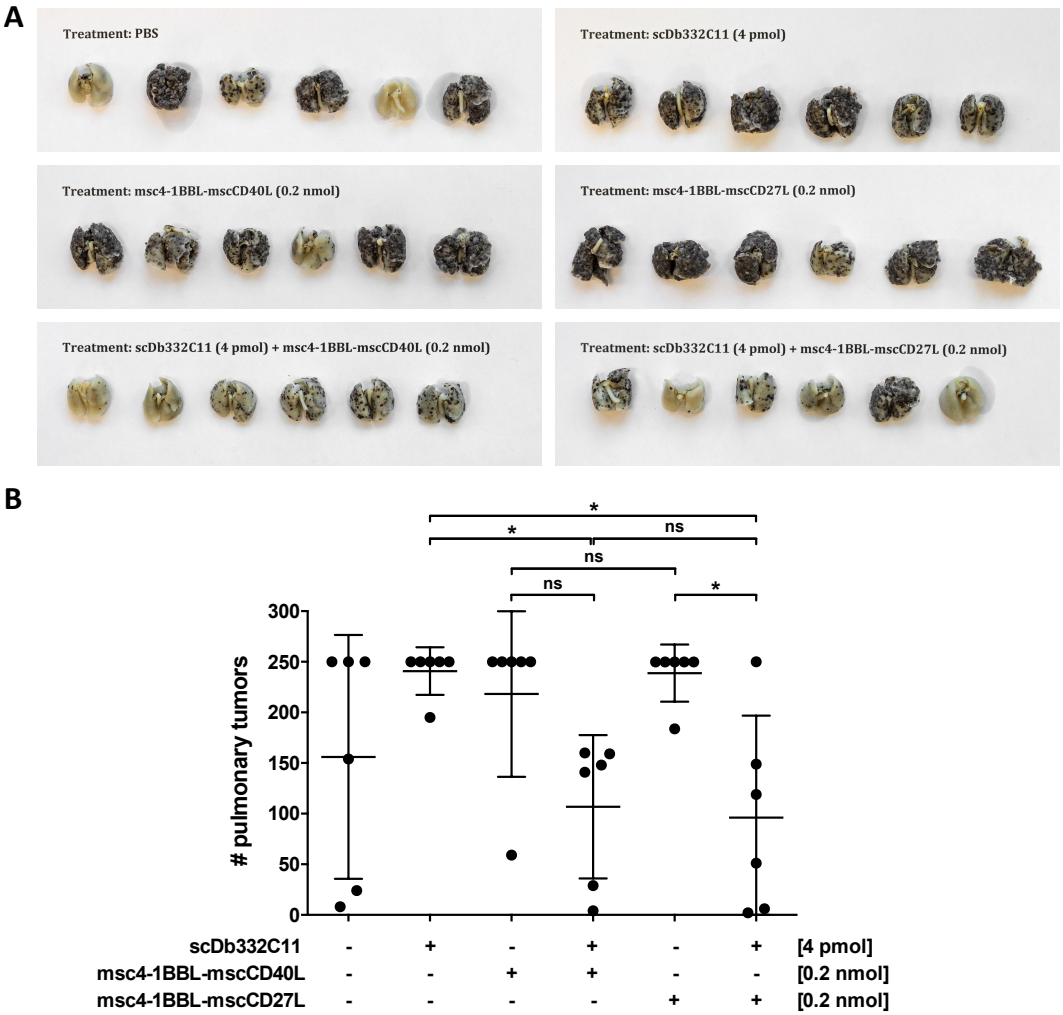

Figure 38: Anti-tumor activity of scDuokines in a combinatorial setting *in vivo*. $1*10^6$ B16-FAP cells were injected i.v. in female C57BL/6 mice. Combined treatment with a mouse-specific scDuokine (0.2 nmol) and an antibody fragment (4 pmol) was performed i.p. on days 1, 2, 3 and days 8, 9, 10 post tumor-cell injection. After sacrificing mice on day 21 **A)** lungs were removed and **B)** pulmonary tumors counted. Mean ± 95% CI, n = 6 mice/group, One-way ANOVA.

When combining one of the costimulatory mscDuokines with scDb332C11, tumor formation was reduced by 55% (msc4-1BBL-mscCD40L) or 60% (msc4-1BBL-mscCD27L). If applied on their own, the mscDuokines resulted in no therapeutic effect indicated by only 10% or even no reduction compared to the single-chain diabody alone. Also, no significant differences between the trans- and cis-acting mscDuokine were observed alone or in combination with the single-chain diabody. Unexpectedly, two out of the six mice treated with PBS showed nearly no colonization with tumors. Most likely, those mice were non-responders to the B16-FAP melanoma cells (Figure 38 B). In summary, this first *in vivo* study indicated high anti-tumor effects exhibited by both trans-acting and cis-acting scDuokines when applied in a combinatorial setting.

3.4 Homodimerized single-chain Duokines (EHD2-scDuokines)

Various studies show that some TNFRSF receptors are not properly activated upon binding of soluble ligand trimers. However, this response has been improved by oligomerization of the trimeric TNFSF ligand molecules. In the case of the TNFSF ligand TRAIL, Seifert et al. (2014) developed a strategy utilizing the heavy chain domain 2 of IgE (EHD2) as homodimerization domain to successfully increase the valency and thus the properties of scTRAIL. Regarding the costimulatory ligands CD40L, CD27L, 4-1BBL and OX40L, it was demonstrated in the previous chapters that the poor receptor activation properties of soluble trimeric ligands were improved slightly by introducing the TNFSF ligands in the single-chain format and clearly by incorporating them in the Duokine or scDuokine format. Pursuing these achievements, it was investigated whether dimerization of scDuokines via EHD2 would result in further improvement of TNFRSF receptor activation.

3.4.1 Characterization of EHD2-scDuokines

Hence, two different single-chain TNFSF ligands (scCD40L, scCD27L or sc4-1BBL) were each fused with GGSGG linkers to both the N-terminus and the C-terminus of the heavy chain domain 2 of IgE (EHD2, Seifert et al. 2014). For purification and detection an N-terminal FLAG-tag was added (Figure 39 A). The formation of two interdomain disulfide bonds between two EHD2 domains resulted in covalently linked homodimeric bifunctional dodecavalent molecules (Figure 39 B). Thus, each EHD2-scDuokine comprised two single-chain units of two different TNFSF ligands (i.e. two times six TNFRSF receptor binding sites). All EHD2-scDuokines were produced in stably transfected HEK293T cells and purified from the cell culture supernatant via FLAG affinity chromatography with high average yields ranging from 4 to 8 mg/L (Table 23). In SDS-PAGE analysis, all EHD2-scDuokines migrated according to the calculated molecular mass of the monomers and all proteins showed EHD2-mediated formation of approx. 50% disulfide-linked dimers under non-reducing conditions (Figure 39 C).

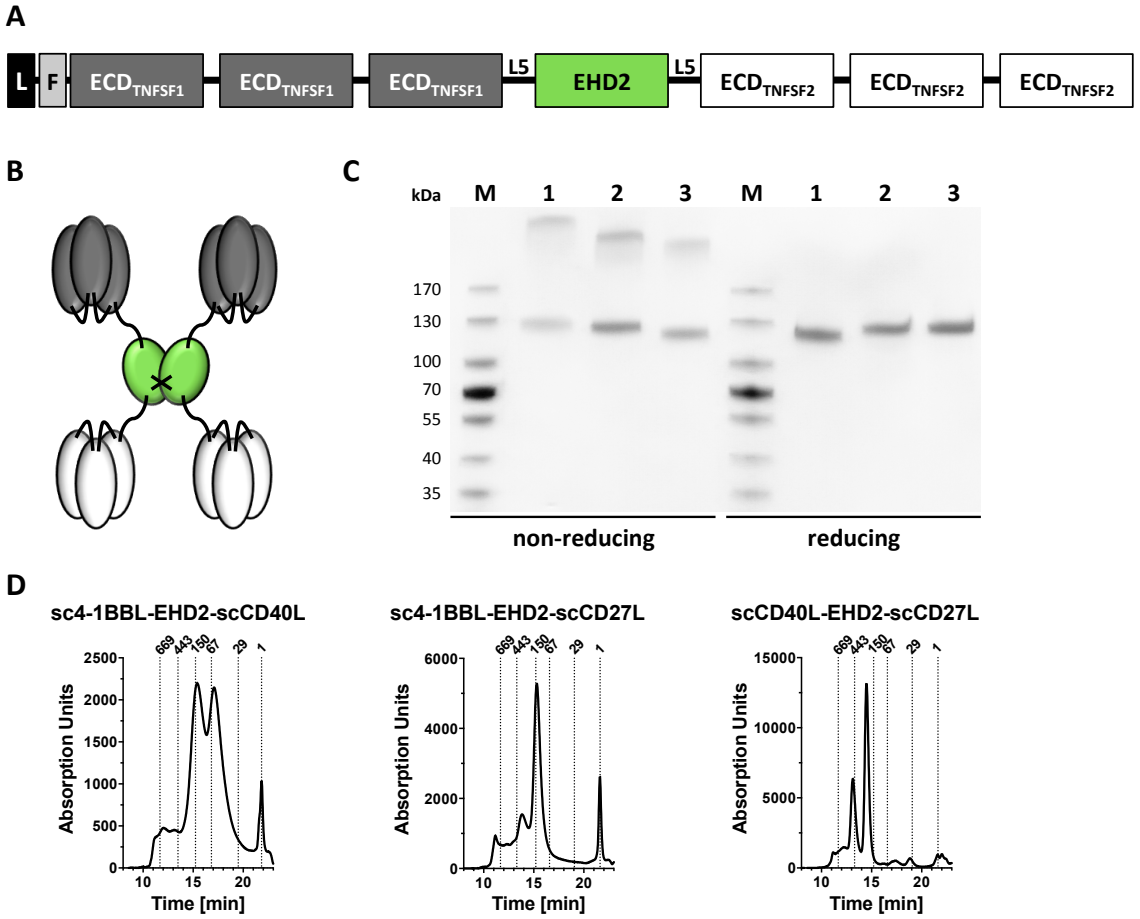

Figure 39: Design and biochemical characterization of EHD2-scDuokines. A) Molecular composition and **B)** schematic assembly of the homodimerized EHD2-scDuokines. The linker between EHD2 and the scDuokines is composed of GGSGG. L, leader peptide; F, FLAG-tag. **C)** SDS-PAGE analysis (4-15% PAA, 2 µg/lane) of purified EHD2-scDuokines under non-reducing and reducing conditions. 1: sc4-1BBL-EHD2-scCD40L, 2: sc4-1BBL-EHD2-scCD27L, 3: scCD40L-EHD2-scCD27L **D)** Size exclusion chromatography (Yarra SEC-3000, flow rate 0.5 ml/min) with standard proteins and their corresponding molecular masses (kDa) indicated as dotted lines.

Size exclusion chromatography did not confirm the assembly of homodimerized molecules under native conditions, but revealed largely inhomogeneous protein compositions with only minor amounts of homodimers (Figure 39 D). All three EHD2-scDuokines eluted as major peaks with apparent molecular masses consistent with the respective monomeric molecule when considering possible N-glycosylation sites (138 kDa for sc4-1BBL-EHD2-scCD40L, 145 kDa for sc4-1BBL-EHD2-scCD27L and 213 kDa for scCD40L-EHD2-scCD27L) (Table 23). Both scCD40L-EHD2-scCD27L and sc4-1BBL-EHD2-scCD27L displayed a second minor peak accounting for the desired homodimer (459 kDa and 355 kDa, respectively), as well as some higher-order complexes. On the contrary, about 50% of sc4-1BBL-EHD2-scCD40L was degraded to the size of a single-chain ligand (61 kDa).

Table 23: Biochemical characteristics of EHD2-scDuokines. Calculation of the molecular mass (MW) based on the amino acid sequence. Yields correspond to the amount of protein purified from 1L cell culture supernatant.

Format	Protein	Linker	MW_{calc} (kDa, chain)	MW_{SEC} (kDa, native)	N-glycosylation (per chain)	Yield (Ø in mg/L)
Trans-acting	**sc4-1BBL-EHD2-scCD40L**	GGSGG-(EHD2)-GGSGG	123.0	138.4 (61.36)	4	8.03
	scCD40L-EHD2-scCD27L	GGSGG-(EHD2)-GGSGG	110.1	213.6 / 458.5	10	3.67
Cis-acting	**sc4-1BBL-EHD2-scCD27L**	GGSGG-(EHD2)-GGSGG	122.4	142.5 / 355.4	7	3.77

3.4.2 Binding and activation of cytokine receptors by EHD2-scDuokines

Specific binding of EHD2-scDuokines to the respective immobilized TNFRSF receptors without any cross-reactivity was confirmed in ELISA (Figure 40 A). The EC_{50} values for receptor binding were in the low nanomolar range of 1 to 3 nM and very similar to those determined for the single-chain costimulatory ligands alone (Table 24).

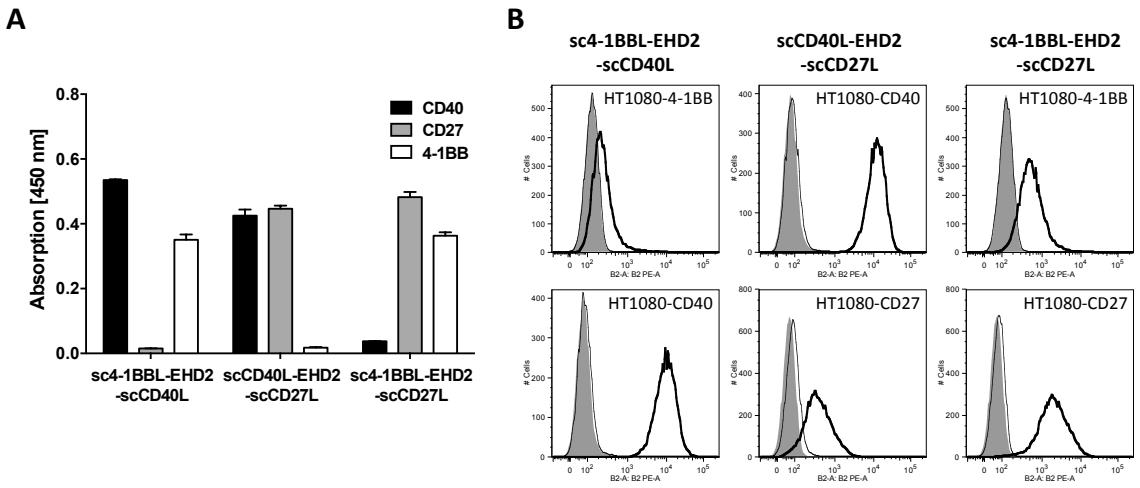

Figure 40: Binding of TNFRSF receptors by EHD2-scDuokines. A) Binding of 100 nM EHD2-scDuokines to immobilized CD40-, CD27- and 4-1BB-Fc (200 ng) was determined in ELISA. Mean ± SD, n = 3, block-shift correction. **B)** Simultaneous binding of EHD2-scDuokines (100 nM) to both receptors was analyzed by detecting the binding to HT1080-CD40, -CD27 or -41BB ($1.5*10^5$ cells) with the corresponding specific receptor-Fc (10 nM) and a PE-labeled anti-human Fc antibody. TNFR1-Fc was included as unspecific negative control. Grey: cells alone, thin black line: unspecific TNFR1-Fc, bold black line: specific receptor-Fc.

As shown previously for Duokines and scDuokines, all EHD2-scDuokines were able to simultaneously bind receptor-expressing HT1080 cells with one costimulatory ligand unit and soluble receptor-Fc fusion proteins with the other, thereby proving their bifunctionality (Figure 40 B). After confirming the ligand-receptor binding properties of the EHD2-scDuokines, it was also investigated whether EHD2-scDuokines activated the TNFRSF

receptors by measuring NFκB-induced IL-8 release from HT1080 transfectants. On HT1080-CD40 both trans-acting EHD2-scDuokines induced strong activation of CD40 (Figure 41 A) with a two-fold improvement in the EC_{50} values of 1.9 ± 0.4 nM for scCD40L-EHD2-scCD27L and 0.8 ± 0.03 nM for sc4-1BBL-EHD2-scCD40L compared to the corresponding scDuokines or scCD40L (Table 24). Although considerably lower amounts of IL-8 were released from HT1080-CD27 than HT1080-CD40, it was clearly demonstrated, that both CD27L-bearing EHD2-scDuokines improved the CD27-activating properties of scCD27L (Figure 41 B) resulting in EC_{50} values in the low nanomolar range (Table 24). While the cis-acting sc4-1BBL-EHD2-scCD27L induced IL-8 release from HT1080-4-1BB only to the same extent as sc4-1BBL, the trans-acting sc4-1BBL-EHD2-scCD40L was considerably more potent in activating 4-1BB as shown by increased IL-8 levels and a nearly 10-fold improved sub-nanomolar EC_{50} value (Table 24, Figure 41 C). This effect observed for sc4-1BBL-EHD2-scCD40L was likewise already shown for sc4-1BBL-scCD40L in chapter 3.3.2.

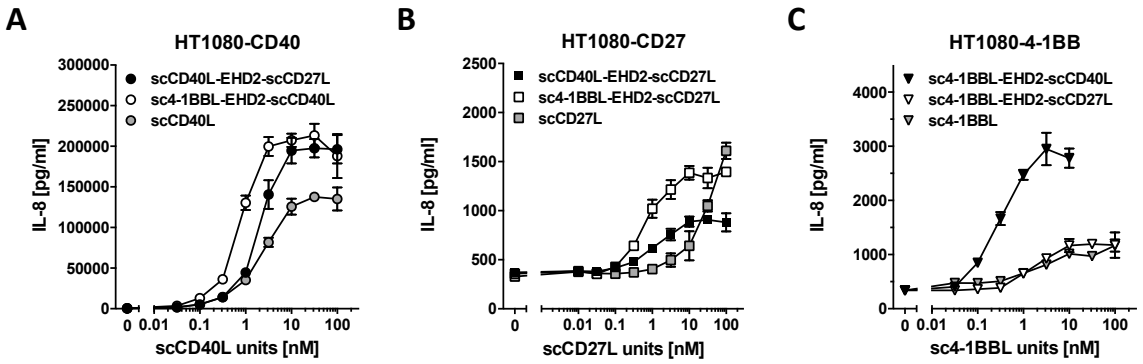

Figure 41: Receptor activation measured via IL-8 release upon NFκB activation. A) HT1080-CD40, **B)** HT1080-CD27 or **C)** HT1080-4-1BB cells ($2*10^4$) were incubated with the EHD2-scDuokines at 37°C, 5% CO_2 and amounts of IL-8 released into the supernatant were measured after 18 h by Sandwich-ELISA. Single-chain TNFSF ligands were included as controls. Mean ± SD, n = 3, block-shift correction.

In summary, all EHD2-scDuokines were able to bind their two TNFRSF receptors and showed distinct receptor activation properties similarly to the respective scDuokines. Table 24 summarizes the EC_{50} values of all EHD2-scDuokines and their controls for receptor binding and activation.

Table 24: EC_{50} values [nM] for TNFRSF receptor binding and activation by EHD2-scDuokines. Binding of EHD2-scDuokines to receptors (immobilized as IgG1 Fc fusion proteins) was analyzed in ELISA. Receptor activation was measured by NFκB-induced IL-8 release from stable HT1080 transfectants. Mean ± SD, n = 3.

Format	Protein	Receptor binding			Receptor activation		
		CD40	CD27	4-1BB	CD40	CD27	4-1BB
single-chain Ligands	scCD40L	1.4 ± 0.7	–	–	2.6 ± 0.06	–	–
	scCD27L	–	1.8 ± 0.2	–	–	> 50	–
	sc4-1BBL	–	–	1.7 ± 0.4	–	–	2.6 ± 1.8
Trans-acting	scCD40L-EHD2-scCD27L	3.0 ± 1.2	1.7 ± 0.7	–	1.9 ± 0.4	1.3 ± 0.5	–
	sc4-1BBL-EHD2-scCD40L	2.6 ± 0.9	–	2.8 ± 0.3	0.8 ± 0.03	–	0.3 ± 0.1
Cis-acting	sc4-1BBL-EHD2-scCD27L	–	1.4 ± 0.6	2.4 ± 1.2	–	0.7 ± 0.4	2.2 ± 0.1

– no ligand/receptor interaction

3.4.3 *In vitro* plasma stability of EHD2-scDuokines

All EHD2-scDuokines were analyzed regarding their *in vitro* stability in human plasma at 37°C. Here, sc4-1BBL-EHD2-scCD40L, which has been identified as a mixture of monomeric and degraded protein under native conditions, nearly completely preserved its initial ligand-receptor binding capacities over the analyzed time period of 7 days. In contrast, both scCD40L-EHD2-scCD27L and sc4-1BBL-EHD2-scCD27L showed a time-dependent drop in intact protein level down to 36 and 43% (Figure 42) in line with the stabilities observed for the corresponding scDuokines. In summary, the observed stability of EHD2-scDuokines was mainly influenced by the initial assembly of the protein and was consequently similar to the scDuokines closely resembling the monomeric form of EHD2-scDuokines.

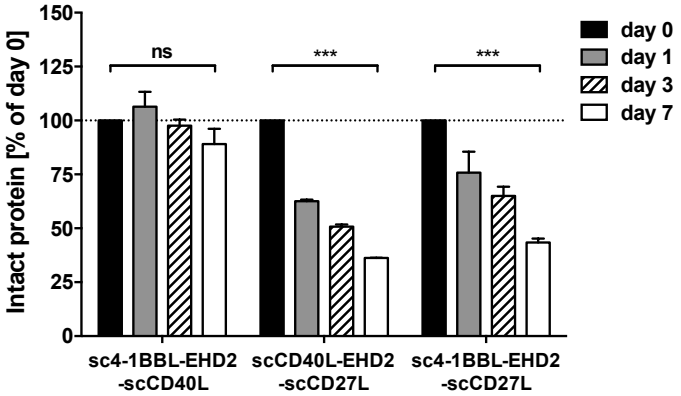

Figure 42: Plasma stability of EHD2-scDuokines. Stability of an initial amount of 200 nM protein was assessed over 7 days in 50% human plasma. Levels of intact EHD2-scDuokines were determined via binding of CD40-, CD27- and 4-1BB-Fc in ELISA. To ensure detection of only full-length proteins the receptor corresponding to the C-terminal ligand was coated and the N-terminal FLAG-tag was detected. Data was normalized to day 0 and is displayed as mean ± SD, n = 3, One-Way ANOVA.

3.4.4 Costimulatory activity of EHD2-scDuokines

Finally, the costimulatory activity of soluble EHD2-scDuokines on prestimulated PBMCs was determined by measuring the enhancement of PBMC proliferation in a single experiment. The basal proliferation rate of around 20% induced by suboptimal stimulation with crosslinked anti-CD3 mAb was clearly improved by all EHD2-scDuokines. Here, a three- or even four-fold increase in proliferating PBMCs was shown for the transacting scCD40L-EHD2-scCD27L (60%) and sc4-1BBL-EHD2-scCD40L (80%), while the cis-acting sc4-1BBL-EHD2-scCD27L only resulted in 40% proliferation. Also, sc4-1BBL-EHD2-scCD40L exhibited its strong costimulatory activity already at low concentrations of 0.1 nM (Figure 43).

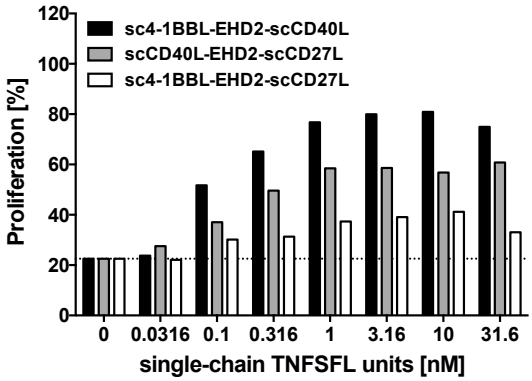

Figure 43: Costimulatory activity of EHD2-scDuokines in solution analyzed by proliferation. $1.8*10^5$ CFSE-labeled human PBMCs (Batch #S02, bulk population) were incubated with EHD2-scDuokines and 10 ng/ml cross-linked anti-CD3 mAb. After 6 days the proliferation of PBMCs was determined by flow cytometry (n = 1).

4 Discussion

Immunomodulation via costimulatory fusion proteins is becoming increasingly attractive for therapeutic applications. In the present study, two types of bifunctional costimulatory cytokine fusion proteins targeting receptors of the tumor necrosis factor receptor superfamily (TNFRSF) have been developed. Firstly, the well-known format of homotrimeric antibody-cytokine fusion proteins comprising a tumor-targeting moiety (antibody fragment) and an effector moiety (costimulatory ligand) was refined by introducing the costimulatory ligand in a single-chain version, which improved stability, pharmacokinetics and – depending on the specific antibody-ligand combination – the costimulatory activity as well. Secondly, two distinct TNFSF ligands were combined in one fusion protein, resulting in novel dual-acting cytokine fusion proteins ("Duokines") targeting two different TNFRSF receptors on T cells (cis-acting) or T cells and APCs (trans-acting). Both homotrimeric and single-chain Duokines were stable and functionally active as proven by the activation of different immune cell subsets and reduced tumor formation *in vivo*.

4.1 Extending the target spectrum for antibody-cytokine fusion proteins

Tumor-targeted antibody-cytokine fusion proteins have been the subjects of various studies (reviewed in Kontermann 2012). Regarding homotrimeric scFv-TNFSF fusion proteins, an extensively targeted tumor-antigen is human fibroblast activation protein (FAP) that is overexpressed on stromal fibroblasts of a wide range of solid tumors. By targeting FAP with scFv36, the costimulatory activity of 4-1BBL, OX40L, LIGHT and GITRL was successfully restricted to the tumor site (D Müller et al. 2008, Hornig et al. 2013, Burkhardt et al. 2010). Furthermore, scFv-ligand fusion proteins that target FAP with other scFv clones like sc40 and OS4 were used to investigate the target-selective receptor activation of CD40L and CD27L (N Müller et al. 2008, Wyzgol et al. 2009) as well as the target-selective apoptosis induction of TNF, FasL and TRAIL (Wüest et al. 2002, Samel et al. 2003, Wajant et al. 2001) In addition to FAP as antigen, other studies report the scFv-mediated targeting of pro-apoptotic TNF and TRAIL towards the tumor antigens EGFR, HER2 and EpCAM (Bremer et al. 2005, Bremer et al. 2004, Rosenblum et al. 2000). Moreover, EpCAM-directed homotrimeric scFv-CD40L effectively induced maturation of dendritic cells in a target antigen-restricted manner (Brunekreeft et al. 2014). As EpCAM is a highly selective tumor marker abundantly

overexpressed on most tumors of epithelial origin, it represents a suitable target antigen for addressing aggressive solid carcinomas with high medical need. According to the underlying concept that the costimulatory activity of antibody-cytokine fusion proteins has to be restricted to the tumor site, a high-affinity anti-EpCAM scFv (323A3, Roovers et al. 1998) was chosen for the scFv-TNFSF and scFv-scTNFSF fusion proteins of this study. Moreover, the antigenic spectrum was further extended by including the protein family of claudins (CLDN) as target structures, as some claudins show limited accessibility on normal cells but frequent expression on tumor cells (e.g. CLDN4, CLDN18.2) or are onco-fetal antigens (e.g. CLDN6). Two antibodies targeting CLDN18.2 (IMAB362, Al-Batran et al. 2016) and CLDN6 (IMAB027, Sahin et al. 2015) are clinically evaluated for the treatment of gastric and ovarian cancer, highlighting their large potential as tumor targets. Consequently, a hybridoma-derived CLDN4/6 antibody (4H6E9) was chosen as second targeting moiety in this study.

However, both scFv antibodies were of murine origin, which is known to be associated with the development of human anti-mouse antibodies (HAMA) and adverse reactions in the therapeutical context. In order to reduce their immunogenicity, both murine scFv fragments were subjected to humanization (Hwang & Foote 2005), a well-established strategy with several representatives in clinical use, like the prominent anti-HER2 antibody trastuzumab. Within the workgroup, humanization has been successfully employed for the anti-EGFR antibody cetuximab (hu225, Kontermann unpublished; used by Seifert et al. 2012) or an antagonistic anti-TNFR1 antibody (IZI-06.1/ATROSAB, Kontermann et al. 2008). Although the same approach for complementarity-determining region (CDR) grafting was applied to scFv323A3 and scFv4H6E9, humanization appeared to be challenging. Out of six humanized variants for scFv323A3 only the variants hu3 and hu5 proved to bind EpCAM with EC_{50} values comparable to the parental antibody, while all others lost their antigen-binding capacities. The difficulties in the humanization process were even more pronounced for scFv4H6E9 where several modifications of the humanized versions did not yield any success. In the literature, it is documented that humanization is accompanied by decreased antigen-binding affinities and that this effect is linked to critical framework residues (Schlapschy et al. 2004, Caldas et al. 2003). Therefore, the homology between the human framework used for humanization and the murine donor sequences should be as high as possible, preventing potential disadvantages in CDR conformation and thus antigen-binding affinity. Key positions

are the residues within the VH/VL-interface and the vernier zone, which influences the structure of the CDR loops and contributes to maintaining the integrity of the antigen-binding site (Gonzales et al. 2005). All humanized variants of scFv4H6E9 exhibited differences in several positions in the vernier zone of VH and the positions L69 and L71 in the vernier zone of VL compared to the murine residues, possibly accounting for impaired or altered folding of the CDRs. Addressing this issue in the early humanization process by remutating two positions (H49, H71) slightly improved the performance of scFvhu4H-S1b. However, although consecutive chimerization revealed that the VL domain was most likely responsible for the loss in antigen binding affinity, a remutation of the vernier zone residues L69 and L71 and other VL framework positions in the variants scFvhu4H-S1b_VLy and VLxy did not rescue, but strengthen the antigen binding of those versions. Similar difficulties emerged in the process of the repeated humanization of the murine antibody H398, which is parental for the TNFR1-antagonist ATROSAB. In this case, *in silico* modeling of the scFv structures revealed a displacement of the CDRH2, which was hypothesized to be responsible for the observed loss of antigen binding in several analyzed humanized variants (Richter 2015). In another case, crystallization studies of an anti-IL-13 antibody with impaired binding affinity after humanization revealed structural disintegrity of the VH/VL interface (Fransson et al. 2010). Consequently, in order to identify the causes for the limitations observed in antigen-binding affinity of the humanized scFv fragments, more detailed structural analyses are likely required in the present case as well.

4.2 Advancing bifunctional antibody-cytokine fusion proteins by introducing TNFSF ligands in a single-chain format

Until now, antibody-cytokine fusion proteins with costimulatory TNFSF ligands have always been described in a homotrimeric protein format (Müller 2014). This particular assembly of scFv-ligand fusion proteins is triggered by the characteristic extracellular TNF homology domain (THD) of TNFSF ligands, which assembles into non-covalently associated trimers. However, a study on scFv-TNFSF fusion proteins with various mouse TNFSF ligands (e.g. CD40L, LIGHT, FasL, TRAIL) reported different biodistribution patterns in mice bearing solid tumors, although all proteins were equipped with the same scFv antibody with proven tumor-targeting properties (Hemmerle et al. 2014). Consequently, this study indicates that the homotrimeric scFv-TNFSF format might not be suitable for all TNFSF members. Based on

their particular structural features, TNFSF ligands can be divided into three sub-families with 4-1BBL and OX40L belonging to the divergent family. This subgroup is characterized by structural divergence compared to e.g. the conventional family, in which the members form tightly packed bell-shaped trimers (Chattopadhyay et al. 2009, Bodmer et al. 2002). Although 4-1BBL bears a THD of typical length, it forms a unique, planar structure resembling a symmetric, three-bladed propeller (Won et al. 2010). In contrast to 4-1BBL, OX40L contains a shortened THD that adapts an expanded organization, where the monomers form an angle of 45° with respect to the trimer axis, resulting in a blooming flower-like structure (Compaan & Hymowitz 2006). So far, only members of the conventional family have been converted into a single-chain format that connects three ligand ectodomains to one polypeptide, with improved stability and performance reported for both TNF (Krippner-Heidenreich et al. 2008) and TRAIL (Schneider et al. 2010). For the first time, this study presents the generation of single-chain versions for the divergent family members 4-1BBL and OX40L. Thereby, the length of the linkers connecting the ECDs (4-1BBL 20 aa, OX40L 7 aa) was chosen with respect to the structural differences of the ligands. Compared to their homotrimeric equivalents, both sc4-1BBL and scOX40L bound equally well to their receptors, indicating adequate linker lengths that enable correct intramolecular homotrimerization. Notably, recent studies revealed that rational linker engineering further increased stability and protein quality of scTRAIL and a Db-scTRAIL fusion protein (Siegemund et al. 2016), thus providing an option for prospective improvements.

Fusion of sc4-1BBL or scOX40L to $scFv_{EpCAM}$ or $scFv_{CLDN4/6}$ did not limit the receptor binding capacities, confirming that scTNFSF ligands are suitable for the generation of monomeric antibody-cytokine fusion proteins. However, due to less avidity of scFv-scTNFSF mediated by a 1:1 instead of 3:1 antibody-to-ligand ratio compared to the homotrimeric fusion proteins, scFv-sc4-1BBL and scFv-scOX40L showed reduced antigen-binding capacities. Unexpectedly, binding of the antigens EpCAM or CLDN4/6 was either reduced (scFv-scTNFSF) or only as good (scFv-TNFSF) compared to the single scFv molecules. Contrary observations were made for similar FAP-directed fusion proteins, with antigen-binding capacities as expected either increased due to avidity effects ($scFv_{FAP}$-4-1BBL) or equal ($scFv_{FAP}$-sc4-1BBL) compared to $scFv_{FAP}$ alone (N. Beha, unpublished data). Here, it has to be considered that the accessibility of the targeted epitope by the individual antibody moiety can be impaired upon

incorporation into the rather large and complex fusion proteins, thus resulting in reduced binding capacities. Antigen binding might, albeit to a lesser extent, also be affected by the localization of the purification tag within the fusion proteins, as the scFv-ligand fusion proteins of this study were provided with a FLAG-tag N-terminally of the scFv, while according to D Müller et al. (2008) the $scFv_{FAP}$ fusion proteins were equipped with a His-tag in the linker separating scFv and 4-1BBL.

Regarding functionality in a targeted setting with tumor cells, all novel monomeric scFv-scTNFSF fusion proteins proved to be costimulatorily active, indicating that one antibody fragment, even with decreased binding capacity, is sufficient for effective cell surface presentation of the costimulatory ligand. Considering the particular TNFSF ligand, 4-1BBL-bearing scFv-ligand fusion proteins exhibited a higher costimulatory activity on PBMCs than OX40L-bearing fusion proteins, regardless of protein format and antibody moiety. In contrast, the direct comparison of endoglin-directed scFv-4-1BBL and scFv-OX40L in a related coculture setting showed comparable effects on T cell proliferation and IFN-γ release (Hornig et al. 2013), but it has to be taken into account that individual costimulatory performance is substantially influenced by various parameters like PBMC donor and experimental setup. Consequently, with both 4-1BBL- and OX40L-fusion proteins generally enhancing T cell costimulation, at this stage of research differences between the protein formats are considered to be more important than between the ligands itself.

Monomeric scFv-scTNFSF and homotrimeric scFv-TNFSF showed significant differences in terms of enhancing IFN-γ release from PBMCs. Here, the monomeric $scFv_{EpCAM}$-sc4-1BBL and $scFv_{EpCAM}$-scOX40L showed superior costimulation in the case of EpCAM-targeted constructs, while the homotrimeric $scFv_{CLDN4/6}$-4-1BBL and $scFv_{CLDN4/6}$-OX40L were advantageous in the case of CLDN4/6-targeted constructs. According to current models of TNFRSF receptor activation, receptors are to a certain amount pre-assembled via the pre-ligand assembly domain (PLAD), creating a high-affinity binding site for trimeric ligands and thereby shifting the dynamic equilibrium towards the formation of $ligand_3$-$receptor_3$ complexes. This initial phase, where ligand-receptor binding occurs in a 3:3 stoichiometry, is followed by secondary clustering of $ligand_3$-$receptor_3$ complexes (Wajant 2015) that is either achieved by cell surface-presentation or oligomerization of the soluble homotrimeric ligands. Examples for

the latter are presented by Fc-mediated dimerization of scTRAIL (Gieffers et al. 2013) as well as Fc-based hexamerization of 4-1BBL and OX40L (Wyzgol et al. 2009, N Müller et al. 2008), which always increased the activity of the fusion protein compared to the soluble trimer. In case of the discussed homotrimeric and monomeric scFv-ligand fusion proteins, antibody-mediated binding to the target antigen mimics membrane-anchored ligands and therefore supports the secondary receptor clustering. Additionally, the results at hand suggest that amongst other influences the antigen expression levels on the tumor target cells determine whether monomeric scFv-scTNFSF or homotrimeric scFv-TNFSF induces stronger costimulatory activity. This hypothesis is supported by the observation that in the targeted setting with Bewo cells ($EpCAM^{high}$ and $CLDN6^{low}$, data not shown) the monomeric fusion proteins were advantageous in combination with EpCAM-targeting, while the homotrimeric $scFv_{CLDN4/6}$-TNFSF variants were favored due to the avidity effects observed for CLDN4/6-binding. Recently, comparative studies with dimeric scFv-Fc-scTRAIL directed against EGFR, HER2, HER3 or EpCAM revealed that binding of the targeting moiety to the cell surface-expressed antigen potentially influences the cytotoxic performance of the fusion proteins. Apoptosis induction observed for scFv-Fc-scTRAIL comprising the HER2-targeting moiety was equal compared to non-targeted Fc-scTRAIL, whereas both EGFR-directed and EpCAM-directed scFv-Fc-scTRAIL showed superior pro-apoptotic activity *in vitro*. Moreover, despite of similar antigen-binding properties compared to the EGFR-targeting construct, the apoptotic effects of anti-HER3 scFv-Fc-scTRAIL were improved only on Colo205 but not on HCT116 cells (M. Hutt, unpublished data), thus supporting the previously discussed antibody-dependent differences in the performance of scFv-sc4-1BBL and scFv-scOX40L.

It has to be considered, that increased costimulatory activity of scFv-scTNFSF might as well result from target-independent oligomerization of the fusion proteins. Soluble TNFSF ligands are functionally inactive, but regain their activity upon artificial crosslinking as described for AviTag-4-1BBL in combination with streptavidin or various FLAG-TNC-TNFSF fusion proteins (including 4-1BBL and OX40L) in combination with an anti-FLAG antibody (Rabu et al. 2005, Lang et al. 2016). In this study, it was accordingly observed that 4-1BBL, sc4-1BBL, OX40L and scOX40L hardly induced activation of TNFRSF receptor-expressing HT1080 cells, while the scFv-ligand fusion proteins and scFv-scTNFSF in particular, exhibited strongly improved receptor activation properties. In fact, both scFv-sc4-1BBL and scFv-scOX40L revealed minor

oligomeric fractions in size exclusion chromatography, potentially due to dimer formation of the scFv, which has been directly observed for scFv4H69 in this study and has been described in the literature for other scFvs (Arndt et al. 1998). The dimerization of scFvs can also be enforced by linker modification creating the diabody format, which has been implemented in the Db-scTRAIL format. These selectively dimerized scTRAIL fusion proteins directed against EGFR showed superior apoptotic activity on target-positive but also target-negative cells *in vitro* (Siegemund et al. 2012), thus clearly supporting the assumption that spontaneous scFv-mediated oligomerization of the TNFSF ligands *per se* causes target-independent receptor activation in the present case. Some off-target effects are described by other studies as well, where activation of receptor-expressing HT1080 cells was induced via $scFv_{FAP}$-OX40L and $scFv_{EpCAM}$-CD40L alone, albeit further enhanced in presence of antigen-positive target cells (N Müller et al. 2008, Brunekreeft et al. 2014). In contrast, there are also reports on $scFv_{FAP}$-4-1BBL fusion proteins mediating receptor activation or costimulation only in coculture settings with target cells (Wyzgol et al. 2009, Hornig et al. 2012). Regarding the costimulatory activity of the fusion proteins in a setting without tumor target cells, only $scFv_{EpCAM}$-4-1BBL and $scFv_{EpCAM}$-sc4-1BBL but not all other scFv-ligand fusion proteins showed target-independent enhancement of PBMC proliferation. Consequently, the observations indicate that the particular combination of costimulatory ligand, fusion protein format and targeting moiety crucially influences the costimulatory performance of antibody-cytokine fusion proteins. Importantly, all scFv-ligand fusion proteins proved to be of a strictly costimulatory nature without supra-agonistic activity, as costimulation was always observed only in presence of primary CD3-mediated stimulation.

In addition to the functional outcomes, converting 4-1BBL and OX40L into the single-chain format clearly stabilized the ligand unit and therefore the entire antibody-cytokine fusion proteins, as demonstrated by enhanced production rates, serum stability and *in vivo* bioavailability for monomeric scFv-scTNFSF compared to homotrimeric scFv-TNFSF. The improvements were generally more pronounced for scFv-sc4-1BBL than scFv-scOX40L, indicating that 4-1BBL with its unique planar structure benefits from linker-mediated stabilization in particular. Previously, increased *in vitro* and *in vivo* stability were likewise reported for scTNF compared to wild-type TNF (Krippner-Heidenreich et al. 2008).

In summary, the single-chain variants of the TNFSF members 4-1BBL and OX40L improved the stability of scFv-ligand fusion proteins and the novel scFv-scTNFSF fusion proteins were costimulatory active, although the individual performance appeared to be influenced by the incorporated antibody fragment. Several reports on monomeric and dimeric scTRAIL-based fusion proteins with improved apoptotic properties (Schneider et al. 2010, Siegemund et al. 2012, Seifert et al. 2014) consolidated the finding that single-chain TNFSF ligands are suitable effector moieties for various antibody-cytokine fusion protein formats and that antibody-mediated tumor targeting assigns a positive effect.

4.3 Duokines and scDuokines are a novel format of bifunctional immunostimulatory cytokine fusion proteins

Bifunctional cytokine fusion proteins are defined as proteins comprising two different cytokines that are either fused directly to each other or implement additional protein domains like antibodies or antibody fragments that can be defined as a third functionality. Various bifunctional cytokine fusion proteins directly combining two monomeric cytokines in one polypeptide have been described, e.g. the GM-CSF interleukin fusion transgenes (GIFTs) linking GM-CSF with various interleukins like IL-2, IL-15, IL-21, IL-4, IL-7 or IL-9. GIFTs induce the clustering of activated GM-CSF and interleukin receptors, leading to unique signals synergistically activating various immune cell subsets (Ng & Galipeau 2015). The connection of single-chain IL-12 with IL-2 presents a slightly more complex protein format that has been engineered with several antibody fragments as well, resulting in fusion proteins like scIL-12_IL-2, Fc_scIL-12_IL-2, scIL-12_IgG_IL-2 (Gillies et al. 2002) or scFv_IL-12_Fc_IL-2. The latter demonstrated tumor-directed activation of resting T cells and NK cells and induced tumor regression in a 9G10 tumor model in Balb/c mice (Jahn et al. 2012). Less work has been done on bifunctional fusion proteins with homotrimeric cytokines of the TNFSF, but two examples for tumor-targeted delivery of a cytokine and a TNFSF ligand in one molecule are reported. While scIL-12_scFv_TNFα failed to show anti-tumor effects (Halin et al. 2003), an RD_IL-15_scFv_4-1BBL fusion protein exhibited superior activity on unstimulated T cells *in vitro* and strongly reduced tumor formation *in vivo* (Kermer et al. 2014). This study is the first to describe bifunctional cytokine fusion proteins composed of two different directly linked homotrimeric (Duokines) or single-chain derivatives (scDuokines) of TNFSF ligands.

In previous studies on recombinant versions of TNFSF ligands, antibody fragments or trimerization domains have always been connected to the N-terminus of the ligand (e.g. Brunekreeft et al. 2014, Wyzogl et al. 2009, D Müller et al. 2008, Morris et al. 2007, Rowley & Al-Shamkhani 2004), an obvious strategy for type II transmembrane proteins. However, due to the architecture of Duokines, the first TNFSF ligand is obligatorily connected by its normally extracellular C-terminus to the N-terminus of the second TNFSF ligand. In order to exclude any structural restrictions for the N-terminal ligand within a Duokine, all Duokines were produced in both orientations, i.e. for each ligand combination the positions of the ligands were interchanged. Size exclusion chromatography revealed homotrimeric assembly and apparent molecular masses within the expected range, indicating that the ligand orientation within the Duokines does not impair structural assembly. The observation that Duokines with C-terminal 4-1BBL appeared to be considerably smaller molecules than their counterparts, however, might be attributed to their unique structure with an atypically long AB loop (Won et al. 2010) possibly folding into a more compact structure when positioned between the two TNFSF ligands close to the connecting linker of the Duokine. These potential differences between the two orientations of the 4-1BBL-bearing Duokines did not manifest in receptor binding studies, since all Duokines independent of orientation and composition effectively bound their two receptors individually as well as simultaneously, proving that both incorporated TNFSF ligands fold correctly.

In the context of single-chain Duokines, the two additional TNFSF ligands CD40L and CD27L were generated as single-chain variants. Regarding their structure, trimeric CD40L adapts the typical compact shape of a truncated pyramid (Karpusas et al. 1995) and therefore belongs to the conventional sub-family. In contrast, CD27L is assigned to the divergent sub-family (Chattopadhyay et al. 2009), although no crystal structure has been resolved yet. Since two conventional TNFSF members (TNF, Krippner-Heidenreich et al. 2008 and TRAIL, Schneider et al. 2010) and two divergent TNFSF members (4-1BBL and OX40L) have been established as single-chain derivatives, the development of both scCD40L and scCD27L in the second part of this study was equally successful as expected. Following the studies of Siegemund et al. (2012), where the linker length in scTRAIL was shortened from 16 to 8 aa, scCD40L, scCD27L and the previously discussed scOX40L were equipped with similarly sized linkers of 7 aa. The receptor binding capacities of all four single-chain ligands (scCD40L,

scCD27L, sc4-1BBL and scOX40L) were equal to those of the soluble ligands or in the case of scCD27L even improved. The half-maximal effective concentrations observed for receptor binding were in the low nanomolar range and thus very similar to the affinities for CD40L:CD40 (K_D 0.8 nM), CD27L:CD27 (K_D 7.1 nM), 4-1BBL:4-1BB (K_D 1.8 nM) and OX40L:OX40 (K_D 1.0 nM) interactions, that have just recently been determined with GpL-Flag-TNC-TNFSF fusion proteins in a comprehensive binding study on intact cells (Lang et al. 2016). Transformation of the TNFSF ligands in the scDuokine as well as the Duokine format conserved their receptor binding. Moreover, all proteins were able to bind both receptors simultaneously, which is an important prerequisite for cis- or trans-active costimulation.

Recombinant soluble TNFSF ligands comprising only the TNF homology domain hardly activate their receptors, probably because the homotrimers are prone to ligand dissociation, but their biological activity is enhanced if they are expressed with their stalk region (the part between the THD and the transmembrane domain) or genetically fused to a trimerization domain like TNC or ILZ (Wyzgol et al. 2009, N Müller et al. 2008, Vonderheide et al. 2001, Morris et al. 1999). In this study, CD27L and CD40L were used without, 4-1BBL with a partial and OX40L with its entire, yet short, stalk region. Accordingly, only soluble OX40L displayed some minor receptor activation *in vitro*. As expected from the experience gained with scTNF and scTRAIL, expressing the ligands in the single-chain format prevented ligand dissociation und therefore stabilized intramolecular homotrimerization, which resulted in increased biological activity. Likewise, the connection of two scTNFSF ligands to a scDuokine resulted in similar receptor activation, which is also explained by the stabilizing effects of the linkers. Interestingly, receptor activation via Duokines was comparable to single-chain ligands and scDuokines as well, indicating that the simultaneous formation of two linked homotrimers clearly supports the individual homotrimer just like additional linkers or special trimerization domains do. With the exception of CD40L-4-1BBL and scCD40L-sc4-1BBL in both orientations, receptor activation via Duokines or scDuokines was mostly comparable to the respective single-chain ligands. In contrast, scFv-TNFSF and scFv-scTNFSF exhibited strongly enhanced biological activity compared to the single-chain ligands, which can be traced back to antibody-mediated oligomerization of the ligands. However, none of the Duokines or scDuokines combining CD40L and 4-1BBL displayed relevant oligomeric fractions in SEC, indicating other mechanisms augmenting the biological activity of these specific fusion proteins that remain to be elucidated.

Regarding stability, scDuokines presented themselves as a relatively robust protein format, not susceptible to ligand dissociation, which is a possible issue for Duokines. Rational molecular evolution of the ligand units and linkers in scTRAIL and scTRAIL-based fusion proteins (Siegemund et al. 2016) illustrates a suitable strategy for improvements of TNFSF members and is due to the highly conserved structure of all TNFSF ligands likely applicable to costimulatory scDuokines as well. Besides protein stability, therapeutic proteins require suitable pharmacokinetic properties, implying a prolonged serum half-life in most cases (Szlachcic et al. 2011). Despite exhibiting molecular masses above the threshold for renal clearance of 60 kDa (Kontermann 2011), murine homologs of Duokines and scDuokines displayed rather short plasma half-lives. In accordance with the observed strong binding to immune cells, the fusion proteins are immediately captured by circulating immune cells. This assumption is supported by the fact that mscCD40L-mscCD27L, which targets the two constitutively expressed TNFRSF receptors CD40 and CD27, was not detectable in serum at all, while the proteins targeting one constitutively and one inducibly expressed receptor displayed at least very short plasma half-lives. Due to the immune cell-specific capturing, the effective half-live of scDuokines is mainly determined by the receptor expression patterns and the life span of the respective target cells. Strong binding of scDuokines to immune cells might represent a generally favorable characteristic, but in the future it has to be ensured that tumor-selective T cells are primarily activated. Therefore, the frequency of tumor-specific T cells can be increased for example by vaccination strategies, which have been reported to enhance the anti-tumoral effects of combined 4-1BB-costimulation and CTLA-4-blockade (Curran et al. 2011). Additionally, local delivery of non-targeted costimulatory therapeutics might present a suitable option for tumor-selective T cell activation as well. Anti-CD40 antibodies have been delivered to the tumor site through formulation with a slow-release agent resulting in the activation of tumor-specific $CD8^+$ T cells (Fransen et al. 2011). Particle-based strategies might be favorable as well, which is exemplified by the successful encapsulation of anti-CD40 or anti-CTLA-4 antibodies in polymeric microparticles and their sustained release (Rahimian et al. 2015).

Costimulatory activity in terms of enhanced proliferation of anti-CD3 stimulated T cells has been observed for Duokines and scDuokines in a soluble setting and a setting mimicking trans-presentation via immobilized TNFRSF receptors. In order to simplify the explanations,

this and the following sections will always refer to “duokines” (written in lower case), if both Duokines and scDuokines are meant. All experiments were performed with bulk PBMC populations enabling potential crosstalk and interactions between different immune cell subsets, resembling the situation in the body where all cell types are present. The artificial trans-setting proved that binding of the duokine via one TNFSF ligand resembles the membrane-anchorage of the other TNFSF ligand, which induces the secondary TNFRSF clustering necessary for costimulatory activity. Receptor-mediated presentation of cis-acting duokines directly addresses T cells irrespective of which TNFSF ligand is accessible as effector moiety. If a trans-acting duokine is presented via binding to CD27, 4-1BB or OX40 though, CD40L acts as effector moiety. Consequently, the observed enhancement of T cell proliferation is in this case the result of secondary T cell activation by CD40-activated antigen-presenting cells (here represented by B cells). This observation is supported by a report on an agonistic anti-CD40-antibody, which directly activated B cells and strongly enhanced their T cell costimulatory potential, eventually resulting in T cell activation (Carpenter et al. 2009).

In regards to the soluble setting, three different modes of action are anticipated for duokines: (i) trans-activation among APCs and T cells via trans-acting duokines, (ii) trans-activation among two different T cells via cis-acting duokines and (iii) cis-activation on single T cells via cis-acting duokines. In setting (i) and (ii) costimulation is provided upon cell-cell-interaction, which can be explained on the basis of the known mechanisms of TNFRSF receptor activation (Wajant 2015). Duokines bind with one TNFSF ligand to the first cell (APC or T cell) and simultaneously with the other TNFSF ligand to the second cell (T cell), bringing both cells in close proximity. This crosslinking mimics the membrane-presentation of each ligand and induces secondary $ligand_3$-$receptor_3$ clustering, thus resulting in the delivery of simultaneous signaling to both cells (Figure 44 A, B). Furthermore, it is hypothesized for setting (iii) that simultaneous binding of the duokine to its two different receptors shifts the receptors into very close proximity on the cell membrane. Since the receptors of the TNFRSF have highly conserved tertiary structures, possibly two different receptor types induce heterogeneous $ligand_3$-$receptor_3$ clustering that induces active signaling complexes (Figure 44 C). The actual detailed TNFRSF signaling pathways in T cells have not been resolved yet (Croft 2014). Thus it is hypothesized, that in the case of heterogeneous clustering functional

intracellular signal transduction may occur through common TRAFs that are shared by some TNFRSF receptors. Currently it is known that CD27, 4-1BB and OX40 interact with TRAF2 and TRAF3, while CD27 and OX40 additionally bind TRAF5 (Croft 2003a). In other studies, atypical heterogeneous clustering of receptors belonging to different superfamilies accompanied with unique signaling has been described upon stimulation with various GM-CSF interleukin fusion transgenes (GIFTs; Ng & Galipeau 2015, Li et al. 2013).

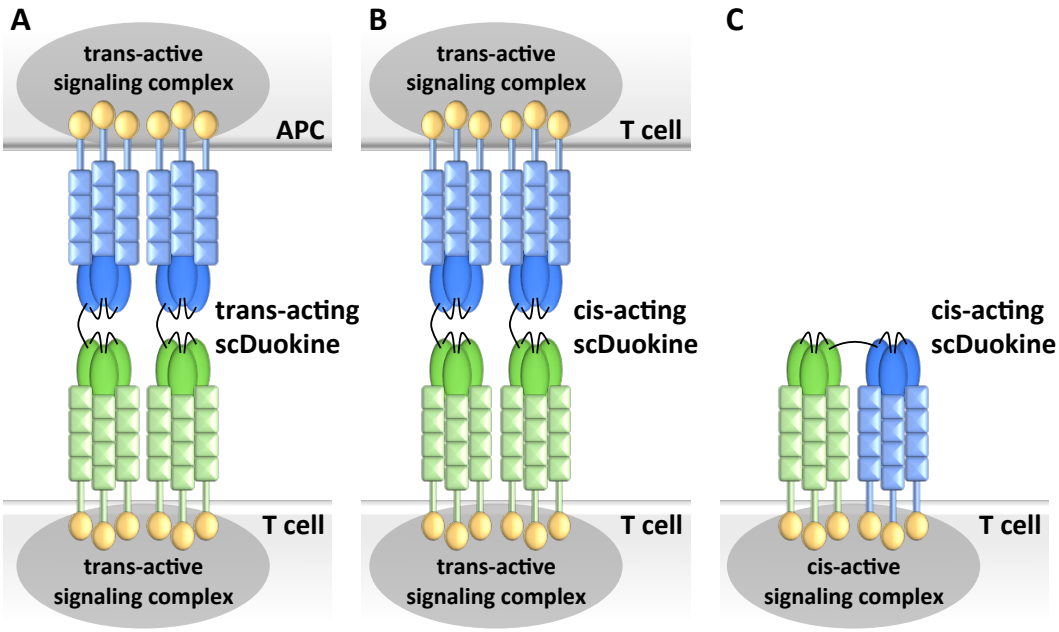

Figure 44: Hypothetical model for receptor activation via duokines. A) Trans-activation among APCs and T cells via trans-acting duokines. **B)** Trans-activation between two different T cells via cis-acting duokines. **C)** Cis-activation on single T cells via cis-acting duokines. Although scDuokines are depicted, the model applies to Duokines as well. Graphical implementation inspired by Wajant 2015.

Compared to Duokines, scDuokines generally exhibited an increased costimulatory activity on CD3-stimulated T cells, which is probably due to their more stable protein format. Therefore, the subsequently discussed results have been obtained solely with scDuokines. Regarding T cell activation, trans-acting as well as cis-acting scDuokines enhanced CD3-mediated proliferation of $CD4^+$ and $CD8^+$ T cells that are both known responders to stimulation via CD27L, 4-1BBL and OX40L (Kurche et al. 2010, Kober et al. 2008, Bansal-Palaka et al. 2004, Cannons et al. 2001). Since enhanced T cell proliferation was only observed after initial CD3-mediated T cell activation, the cis-acting scDuokines (sc4-1BBL-scCD27L and scOX40L-scCD27L) exhibited no direct effects on resting T cells, proving their strictly costimulatory nature. In contrast, the trans-acting scDuokines sc4-1BBL-scCD40L, scCD40L-scCD27L and scOX40L-scCD40L showed some minor, but significant effects on

unstimulated, i.e. resting T cells and strongly activated unstimulated B cells. Stimulation of B cells was mediated directly by the trans-acting scDuokines via engagement of constitutively expressed CD40. Based on this observation, it is assumed that these activated B cells mediate the *de novo* T cell activation that has been induced upon stimulation with trans-acting scDuokines. Besides the previously discussed study by Carpenter and colleagues (2009) describing T cell activation via anti-CD40 antibody-stimulated B cells, numerous other studies report the effect that CD40-stimulated B cells can act as potent APCs generating effective cytotoxic T cell responses without $CD4^+$ T cell help (Khong et al. 2012, Jackaman & Nelson 2012, Ritchie et al. 2004, Lapointe et al. 2003, French et al. 1999). Regarding the setting without primary anti-CD3 stimulation, these studies support the assumption that the effective stimulation of B cells via trans-acting scDuokines most probably renders them as APCs, which are subsequently able to trigger the activation of resting T cells. Translation into the setting with CD3 stimulation indicates that not only direct costimulation of activated T cells via trans-acting scDuokines occurs, but also the indirect effects via activated B cells contribute to overall T cell costimulation. Consequently, this addition of trans-acting scDuokine-induced direct as well as indirect (via activated B cells) effects on T cells explains the observation that trans-activating scDuokines induced slightly stronger proliferation of CD3-stimulated T cells than cis-acting scDuokines. In the literature trans-activation of T cells via APCs is known as bystander effect that has been described for example as response to TLR agonists (Kamath et al. 2005) or vaccination (Di Genova et al. 2010).

In a last step, the antitumoral activity of scDuokines was assessed in a spontaneous B16 lung tumor model in immunocompetent C57BL/6 mice. In combination with a T cell-engaging bispecific antibody both trans-acting msc4-1BBL-mscCD40L and cis-acting msc4-1BBL-mscCD27L significantly reduced the tumor burden in the lungs, which demonstrated that costimulation mediated by scDuokines combining 4-1BBL and a second TNFSF ligand, provides beneficial effects in a combinatorial setting. This observation is supported by several studies with the B16 mouse melanoma model describing sustained antitumor responses for combinations of anti-4-1BB therapy with other immunotherapeutic strategies like anti-OX40 mAb (Gray et al. 2008), B7.1-Db (Hornig et al. 2013), IL-12 (Huang et al. 2010, Xu et al. 2004), GM-CSF (Li et al. 2007) or adoptive T cell therapy (Weigelin et al. 2015). Treatment with the scDuokines as single agents did not result in reduced tumor formation in

this poorly immunogenic model, which is in agreement with the literature reporting for example a vaccine-based approach, where costimulation via an anti-4-1BB mAb alone exhibited no beneficial effects on tumor reduction but proved to be effective combined with anti-CTLA-4 mAb (Curran et al. 2011). Furthermore, the treatment with the bispecific antibody alone had no anti-tumoral effects in the present study, which clearly stands in contrast to the tumor-growth inhibition observed previously with the same bispecific single-chain diabody (Hornig et al. 2013). This indicates that the chosen dosages for all therapeutic fusion proteins might have to be increased in order to receive a more significant outcome. In conclusion, first promising results achieved with scDuokines suggest that the combination of two costimulatory TNFSF ligands in one molecule offers high potential to enhance the therapeutic effect of primary immunotherapeutic approaches like T-cell engaging antibodies or vaccination.

4.4 EHD2-scDuokines as initial approach towards directed oligomerization of bifunctional cytokine fusion proteins

As previously discussed, current models of TNFRSF receptor activation define the requirement for secondary clustering of preformed ligand-receptor complexes in order to effectively induce activating signaling complexes. Other than 4-1BBL and OX40L, which interact as homotrimeric ligands with the equal number of receptors resulting in $ligand_3$-$receptor_3$ clusters (Wajant 2015), the homotrimeric CD40L interacts with two instead of three CD40 receptors (An et al. 2011). Initial 3:2 ligand-receptor stoichiometries are also assumed for the interaction of homotrimeric CD27L with CD27, which is expressed as a disulfide-linked homodimer on the cell membrane (van Lier et al. 1987). Regarding this special conformation, Wajant (2016) proposed a model for CD27 activation induced by $(ligand_3)_2$-$(receptor_2)_3$ clustering, which might also be applicable for CD40 activation. Both models of receptor clustering require either cell surface-presentation or oligomerization of at least two homotrimeric TNFSF ligands for effective signaling, as soluble TNFSF ligands are not capable of sufficient TNFRSF receptor activation. The most-studied approach on ligand-oligomerization is the introduction of an antibody's Fc part that has been successfully applied on various TNFSF ligands like OX40L, CD40L, CD27L, 4-1BBL and GITRL resulting in improved properties (Wyzgol et al. 2009, Sadun et al. 2008, Hu et al. 2008, N Müller et al. 2008, Rowley & Al-Shamkhani 2004). However, the covalent linkage of a trimerizing TNFSF

ligand with a dimerizing Fc fragment results in rather large and complexly assembled proteins that are at high risk for undesired protein conformations, which is confirmed by very heterogeneous protein compositions including dimers, trimers, hexamers and higher-order oligomers that have been reported for Fc-TRAIL (Wang et al. 2014). Consequently, some studies report the introduction of an additional small trimerization domain like TNC or ILZ between the TNFSF ligand and the Fc part (Wyzgol et al. 2009), supporting the intended hexameric assembly of the Fc-TNFSF fusion proteins. MEDI6383, an ILZ-stabilized Fc:OX40L fusion protein (Morris et al. 2007), has demonstrated potent anti-tumor activity in xenograft mouse tumor models and is currently being evaluated in a phase I clinical trial (Hammond et al. 2015, Bauer et al. 2015). More suitable approaches of directed oligomerization include stabilized single-chain TNFSF ligands (e.g. scTRAIL, scTNF) that are engineered with various dimerization modules like a diabody (Siegemund et al. 2012), an Fc part (Gieffers et al. 2013), an MHD2 domain (Seifert et al. 2012) or an EHD2 domain (Seifert et al. 2014) resulting in proteins with defined conformations. In this study, the concept of EHD2-mediated homodimerization was adapted to scDuokines, creating dimeric dodecavalent fusion proteins that combine four homotrimeric single-chain TNFSF ligands (with two specificities) in one molecule. Consequently, EHD2-scDuokines are assumed to effectively induce receptor activation without the need for cross-linking of the targeted cells, which translates into enhanced costimulatory activity that should even exceed those of scDuokines. Initial characterization revealed that only a minor fraction of the EHD2-scDuokines correctly assembled into the intended homodimeric conformation, which implies that they basically resembled scDuokines with according receptor activation and costimulatory properties. However, since the EHD2 domain has been reported as a versatile and robust homodimerization domain, further engineering of EHD2-scDuokines will likely result in promising second generation scDuokines with improved properties.

4.5 Conclusion and Outlook

In the first part of this study, two scFv fragments directed against EpCAM and CLDN4/6 have been evaluated as suitable model targeting moieties for antibody-cytokine fusion proteins in the conventional homotrimeric and the novel monomeric format, although preceeding humanization resulted in varying outcomes. In the process of further developing the properties of the various antibody-cytokine fusion proteins, the improvement of the antigen-binding affinity of the humanized scFv fragments becomes crucial. Besides genetic manipulation of framework residues (Fransson et al. 2010), in particular affinity maturation via phage display technologies represents a suitable option (Richter 2015, Unverdorben et al. 2015, Steinwand et al. 2014). As EpCAM-directed immunotherapeutic antibodies have already been approved for therapy (catumaxomab) or are currently being clinically evaluated in the promising BiTE format (solitomab), it is advisable to devote future attention to EpCAM – especially as immune-activating and anti-tumoral effects have been reported for anti-EpCAM antibody-cytokine fusion proteins (Brunekreeft et al. 2014, Schanzer et al. 2006).

In the second part of this study the introduction of single-chain derivatives of the TNFSF ligands 4-1BBL and OX40L improved the stability of scFv-ligand fusion proteins. The resulting novel scFv-scTNFSF fusion proteins were costimulatory active, but their individual performance appeared to be influenced by the combination of antibody fragment and tumor target cells. In the concept of tumor-targeted costimulation, it is anticipated that the fusion proteins remain inactive before reaching the tumor site in order to prevent toxic side effects. Therefore, ideally an antibody is chosen that has a higher affinity to its antigen than the costimulatory ligand has to its receptor, indicating that the antibody moiety has to be selected carefully in order to prevent off-target effects in future studies. Furthermore, the functional outcome of scFv-scTNFSF fusion proteins has to be evaluated in depth concerning cytotoxic effector functions, the generation of effector and memory phenotypes as well as the effects on regulatory T cells. With increasing interest in combinatorial strategies, engagement of 4-1BB or OX40 in combination with the activation of other costimulatory receptors or immune checkpoint blockade has been reported to result in strongly enhanced or even synergistic antitumoral effects (Chen et al. 2014, Redmond et al. 2014, Morales-Kastresana et al. 2013b, Lee et al. 2004). It has been described that scFv-4-1BBL can be combined successfully with B7.1-Db or other scFv-TNFSF fusion proteins (Hornig et al. 2013)

and consequently the novel scFv-scTNFSF ought to be investigated in similar directions, ideally extending the spectrum of possible combinations by immune checkpoint blockers. Following the approach from Kermer and colleagues (2014), scFv-scTNFSF furthermore represents due to its simpler and more stable configuration a valuable starting point for the development of second-generation trifunctional tumor-targeted cytokine fusion proteins.

The present study is the first to report the generation of bifunctional cytokine fusion proteins combining two homotrimeric TNFSF ligands. Although both evaluated formats were suitable, the monomeric single-chain format (scDuokines) displayed increased stability and better overall performance. Evidence was provided that scDuokines induce sufficient TNFRSF receptor activation that translates into stimulatory activity on T cells and other immune cell subsets. By flexibly combining various members of the TNF superfamily (CD40L, CD27L, 4-1BBL and OX40L) the spatiotemporal expression of key players of T cell costimulation was successfully utilized in this concept. It was confirmed that scDuokines directly exhibit costimulatory effects on T cells (cis-acting scDuokines) and scDuokines promote additional stimulation of T cell responses by activating antigen-presenting cells that interact with T cells (trans-acting scDuokines). Finally, a first *in vivo* study demonstrated enhanced antitumor effects for scDuokines in combination with a bispecific FAPxCD3 antibody. With regards to this finding, it appears promising to evaluate Duokines together with bispecific T cell engagers. Although BiTEs induce strong CTL responses without the need for peptide antigen presentation or costimulation (Baeuerle & Reinhardt 2009) they are likely to profit from specific costimulation that refines the T cell activation. Compared to antibody-based strategies, Duokines offer a promising alternative as they are at lower risk for systemic toxicity compared to agonistic antibodies. Nevertheless, immunostimulatory strategies always bear the risk for excessive immune activation, as it has been observed or the anti-CD28 monoclonal antibody TGN1412, which induced severe cytokine storm during a phase I clinical trial nearly causing fatalities (Suntharalingam et al. 2006). Consequently, further studies concerning the safety and various aspects associated with the therapeutic applicability of Duokines like precise biological activity, tolerability and tumor-selective delivery have to be conducted. Besides antibody-based strategies, vaccination can benefit from costimulation as well. In this context, the combination of an anti-4-1BB antibody with an anti-OX40 antibody but not anti-4-1BB stimulation alone induced highly effective T cell

responses protecting mice against poorly immunogenic B16 melanoma (Gray et al. 2008). Consequently, the concept of scDuokines is currently adapted into an mRNA-based approach, where they are evaluated as selective amplifiers of antigen-specific T cell responses. As scDuokines are expected to bear lower risks than conventional adjuvants, they are intended for vaccination strategies, possibly also in combination with liposomal delivery of the mRNA, which aims at simplified modulation of biodistribution and pharmacokinetics. So far, first encouraging results have been obtained regarding the costimulatory activity of mRNA-encoded scDuokines, which is comparable to the results for the proteins of this study (F. Gieseke, BioNTech AG, unpublished data).

By establishing Duokines and scDuokines as a novel class of immunostimulatory bifunctional cytokine fusion proteins this study adds a valuable contribution to the field of cancer immunotherapy. Duokines elicit strong costimulatory activity, which can be delivered either selectively or simultaneously to T cells and antigen-presenting cells. Their modular composition enables the implementation of various combinations of TNFSF ligands targeting costimulatory receptors during various stages of the immune response and thus rational design of Duokines potentially enables fine-tuning of T cell responses. Costimulation via Duokines safely enhances the anti-tumoral effects induced by other immunotherapeutic approaches, indicating the future therapeutic relevance of these promising molecules and assigning them with manifold opportunities for future development.

5 Bibliography

Abhinandan, K. R., & Martin, A. C. R. (2007). Analyzing the “degree of humanness” of antibody sequences. *Journal of Molecular Biology*, *369*(3), 852–62.

Abuazza, G., Becker, A., Williams, S. S., Chakravarty, S., Truong, H.-T., Lin, F., & Baum, M. (2006). Claudins 6, 9, and 13 are developmentally expressed renal tight junction proteins. *American Journal of Physiology. Renal Physiology*, *291*(6), F1132–41.

Adams, J. L., Smothers, J., Srinivasan, R., & Hoos, A. (2015). Big opportunities for small molecules in immuno-oncology. *Nature Reviews. Drug Discovery*, *14*(9), 603–22.

Al-Batran, S.-E., Schuler, M. H., Zvirbule, Z., Manikhas, G., Lordick, F., Rusyn, A., … Sahin, U. (2016). FAST: An international, multicenter, randomized, phase II trial of epirubicin, oxaliplatin, and capecitabine (EOX) with or without IMAB362, a first-in-class anti-CLDN18.2 antibody, as first-line therapy in patients with advanced CLDN18.2+ gastric and gast. *J Clin Oncol*, *34*(suppl), abstr LBA4001.

Allard, W. J., Matera, J., Miller, M. C., Repollet, M., Connelly, M. C., Rao, C., … Terstappen, L. W. M. M. (2004). Tumor cells circulate in the peripheral blood of all major carcinomas but not in healthy subjects or patients with nonmalignant diseases. *Clinical Cancer Research : An Official Journal of the American Association for Cancer Research*, *10*(20), 6897–904.

An, H.-J., Kim, Y. J., Song, D. H., Park, B. S., Kim, H. M., Lee, J. D., … Lee, H. (2011). Crystallographic and mutational analysis of the CD40-CD154 complex and its implications for receptor activation. *The Journal of Biological Chemistry*, *286*(13), 11226–35.

Andersson, Y., Engebraaten, O., Juell, S., Aamdal, S., Brunsvig, P., Fodstad, Ø., & Dueland, S. (2015). Phase I trial of EpCAM-targeting immunotoxin MOC31PE, alone and in combination with cyclosporin. *British Journal of Cancer*, *113*(11), 1548–55.

Armitage, R. J., Fanslow, W. C., Strockbine, L., Sato, T. A., Clifford, K. N., Macduff, B. M., … Maliszewski, C. R. (1992). Molecular and biological characterization of a murine ligand for CD40. *Nature*, *357*(6373), 80–2.

Arndt, K. M., Müller, K. M., & Plückthun, A. (1998). Factors influencing the dimer to monomer transition of an antibody single-chain Fv fragment. *Biochemistry*, *37*(37), 12918–26.

Ascierto, P. A., Simeone, E., Sznol, M., Fu, Y.-X., & Melero, I. (2010). Clinical experiences with anti-CD137 and anti-PD1 therapeutic antibodies. *Seminars in Oncology*, *37*(5), 508–16.

Atkins, M. B., & Sznol, M. (2015). Cancer Immunotherapy: Past Progress and Future Directions. *Seminars in Oncology*, *42*(4), 518–22.

Baeuerle, P. A., Kufer, P., & Lutterbüse, R. (2003). Bispecific antibodies for polyclonal T-cell engagement. *Current Opinion in Molecular Therapeutics*, *5*(4), 413–9.

Baeuerle, P. A., & Reinhardt, C. (2009). Bispecific T-cell engaging antibodies for cancer therapy. *Cancer Research*, *69*(12), 4941–4944.

Balkwill, F., & Mantovani, A. (2001). Inflammation and cancer: back to Virchow? *Lancet (London, England)*, *357*(9255), 539–45.

Bansal-pakala, P., Halteman, B. S., Huey-yu, M., Cheng, M. H.-Y., & Croft, M. (2004). Costimulation of CD8 T cell responses by OX40. *Journal of Immunology*, *172*(8), 4821–4825.

Bauer, T., Chae, Y., Patel, S., D'Angelo, S., Blumenschein, G., Norton, J., … Curti, B. (2015). A phase I study of MEDI6383, an OX40 agonist, in adult patients with select advanced solid tumors. *J Clin Oncol*, *33*(suppl), abstr TPS3093.

Beatty, G. L., Torigian, D. A., Chiorean, E. G., Saboury, B., Brothers, A., Alavi, A., … O'Dwyer, P. J. (2013). A phase I study of an agonist CD40 monoclonal antibody (CP-870,893) in combination with gemcitabine in patients with advanced pancreatic ductal adenocarcinoma. *Clinical Cancer Research : An Official Journal of the American Association for Cancer Research*, *19*(22), 6286–95.

Benedict, C. A., MacKrell, A. J., & Anderson, W. F. (1997). Determination of the binding affinity of an anti-CD34 single-chain antibody using a novel, flow cytometry based assay. *Journal of Immunological Methods*, *201*(2), 223–31.

Bodmer, J.-L., Schneider, P., & Tschopp, J. (2002). The molecular architecture of the TNF superfamily. *Trends in Biochemical Sciences*, *27*(1), 19–26.

Bonehill, A., Tuyaerts, S., Van Nuffel, A. M. T., Heirman, C., Bos, T. J., Fostier, K., … Thielemans, K. (2008). Enhancing the T-cell stimulatory capacity of human dendritic cells by co-electroporation with CD40L, CD70 and constitutively active TLR4 encoding mRNA. *Molecular Therapy : The Journal of the American Society of Gene Therapy*, *16*(6), 1170–80.

Borst, J., Hendriks, J., & Xiao, Y. (2005). CD27 and CD70 in T cell and B cell activation. *Current Opinion in Immunology*, *17*(3), 275–81.

Bossen, C., Ingold, K., Tardivel, A., Bodmer, J.-L., Gaide, O., Hertig, S., … Schneider, P. (2006). Interactions of tumor necrosis factor (TNF) and TNF receptor family members in the mouse and human. *The Journal of Biological Chemistry*, *281*(20), 13964–71.

Bremer, E. (2013). Targeting of the tumor necrosis factor receptor superfamily for cancer immunotherapy. *ISRN Oncology*, *2013*, 371854.

Bremer, E., Kuijlen, J., Samplonius, D., Walczak, H., De Leij, L., & Helfrich, W. (2004). Target cell-restricted and -enhanced apoptosis induction by a scFv:sTRAIL fusion protein with specificity for the pancarcinoma-associated antigen EGP2. *International Journal of Cancer*, *109*(2), 281–290.

Bremer, E., Samplonius, D. F., van Genne, L., Dijkstra, M. H., Kroesen, B. J., de Leij, L. F. M. H., & Helfrich, W. (2005). Simultaneous Inhibition of Epidermal Growth Factor Receptor (EGFR) Signaling and Enhanced Activation of Tumor Necrosis Factor-related Apoptosis-inducing Ligand (TRAIL) Receptor-mediated Apoptosis Induction by an scFv:sTRAIL Fusion Protein with Specificity. *Journal of Biological Chemistry*, *280*(11), 10025 –10033.

Brunekreeft, K. L., Strohm, C., Gooden, M. J., Rybczynska, A. A., Nijman, H. W., Grigoleit, G. U., … de Bruyn, M. (2014). Targeted delivery of CD40L promotes restricted activation of antigen-presenting cells and induction of cancer cell death. *Molecular Cancer*, *13*(1), 85.

Buchan, S. L., Manzo, T., Flutter, B., Rogel, A., Edwards, N., Zhang, L., … Chakraverty, R. (2015). OX40- and CD27-mediated costimulation synergizes with anti-PD-L1 blockade by forcing exhausted CD8+ T cells to exit quiescence. *Journal of Immunology (Baltimore, Md. : 1950)*, *194*(1), 125–33.

Burckhart, T., Thiel, M., Nishikawa, H., Wüest, T., Müller, D., Zippelius, A., … Renner, C. (2010). Tumor-specific crosslinking of GITR as costimulation for immunotherapy. *Journal of Immunotherapy (Hagerstown, Md. : 1997)*, *33*(9), 925–34.

Caldas, C., Coelho, V., Kalil, J., Moro, A. M., Maranhão, A. Q., & Brígido, M. M. (2003). Humanization of the anti-CD18 antibody 6.7: An unexpected effect of a framework residue in binding to antigen. *Molecular Immunology*, *39*(15), 941–952.

Cannons, J. L., Lau, P., Ghumman, B., DeBenedette, M. a, Yagita, H., Okumura, K., & Watts, T. H. (2001). 4-1BB ligand induces cell division, sustains survival, and enhances effector function of CD4 and CD8 T cells with similar efficacy. *Journal of Immunology (Baltimore, Md. : 1950)*, *167*(3), 1313–24.

Carpenter, E. L., Mick, R., Rüter, J., & Vonderheide, R. H. (2009). Activation of human B cells by the agonist CD40 antibody CP-870,893 and augmentation with simultaneous toll-like receptor 9 stimulation. *Journal of Translational Medicine*, *7*, 93.

Carswell, E. A., Old, L. J., Kassel, R. L., Green, S., Fiore, N., & Williamson, B. (1975). An endotoxin-induced serum factor that causes necrosis of tumors. *Proceedings of the National Academy of Sciences of the United States of America*, *72*(9), 3666–70.

Cella, M., Scheidegger, D., Palmer-Lehmann, K., Lane, P., Lanzavecchia, A., & Alber, G. (1996). Ligation of CD40 on dendritic cells triggers production of high levels of interleukin-12 and enhances T cell stimulatory capacity: T-T help via APC activation. *The Journal of Experimental Medicine*, *184*(2), 747–52.

Chattopadhyay, K., Lazar-Molnar, E., Yan, Q., Rubinstein, R., Zhan, C., Vigdorovich, V., … Almo, S. C. (2009). Sequence, structure, function, immunity: structural genomics of costimulation. *Immunological Reviews*, *229*(1), 356–86.

Chen, L., & Flies, D. B. (2013). Molecular mechanisms of T cell co-stimulation and co-inhibition. *Nature Reviews. Immunology*, *13*(4), 227–42.

Chen, S., Lee, L.-F., Fisher, T. S., Jessen, B., Elliott, M., Evering, W., … Lin, J. C. (2014). Combination of 4-1BB Agonist and PD-1 Antagonist Promotes Antitumor Effector/Memory CD8 T Cells in a Poorly Immunogenic Tumor Model. *Cancer Immunology Research*, *3*(2), 149–160.

Claus, C., Riether, C., Sch??rch, C., Matter, M. S., Hilmenyuk, T., & Ochsenbein, A. F. (2012). CD27 signaling increases the frequency of regulatory T cells and promotes tumor growth. *Cancer Research*, *72*(14), 3664–3676.

Claus, C., Riether, C., Schürch, C., Matter, M. S., Hilmenyuk, T., & Ochsenbein, A. F. (2012). CD27 signaling increases the frequency of regulatory T cells and promotes tumor growth. *Cancer Research*, *72*(14), 3664–76.

Coley, W. B. (1891). II. Contribution to the Knowledge of Sarcoma. *Annals of Surgery*, *14*(3), 199–220.

Compaan, D. M., & Hymowitz, S. G. (2006). The Crystal Structure of the Costimulatory OX40-OX40L Complex. *Structure*, *14*(8), 1321–1330.

Croft, M. (2003). Co-stimulatory members of the TNFR family: keys to effective T-cell immunity? *Nature Reviews. Immunology*, *3*(8), 609–20.

Croft, M. (2010). Control of immunity by the TNFR-related molecule OX40 (CD134). *Annual Review of Immunology*, *28*(1), 57–78.

Croft, M. (2003). Costimulation of T cells by OX40, 4-1BB, and CD27. *Cytokine & Growth Factor Reviews*, *14*(3-4), 265–73.

Croft, M. (2014). The TNF family in T cell differentiation and function--unanswered questions and future directions. *Seminars in Immunology*, *26*(3), 183–90.

Curran, M. A., Kim, M., Montalvo, W., Al-Shamkhani, A., & Allison, J. P. (2011). Combination CTLA-4 blockade and 4-1BB activation enhances tumor rejection by increasing T-cell infiltration, proliferation, and cytokine production. *PloS One*, *6*(4), e19499.

Curti, B. D., Kovacsovics-Bankowski, M., Morris, N., Walker, E., Chisholm, L., Floyd, K., … Weinberg, A. D. (2013). OX40 is a potent immune-stimulating target in late-stage cancer patients. *Cancer Research*, *73*(24), 7189–98.

de Bruyn, M., Bremer, E., & Helfrich, W. (2013). Antibody-based fusion proteins to target death receptors in cancer. *Cancer Letters*, *332*(2), 175–83.

de Jong, R., Loenen, W. a, Brouwer, M., van Emmerik, L., de Vries, E. F., Borst, J., & van Lier, R. a. (1991). Regulation of expression of CD27, a T cell-specific member of a novel family of membrane receptors. *Journal of Immunology (Baltimore, Md. : 1950)*, *146*(8), 2488–94.

Di Genova, G., Savelyeva, N., Suchacki, A., Thirdborough, S. M., & Stevenson, F. K. (2010). Bystander stimulation of activated CD4+ T cells of unrelated specificity following a booster vaccination with tetanus toxoid. *European Journal of Immunology*, *40*(4), 976–85.

Diegmann, J., Junker, K., Loncarevic, I. F., Michel, S., Schimmel, B., & von Eggeling, F. (2006). Immune escape for renal cell carcinoma: CD70 mediates apoptosis in lymphocytes. *Neoplasia (New York, N.Y.)*, *8*(11), 933–8.

Dixon, J. F., Law, J. L., & Favero, J. J. (1989). Activation of human T lymphocytes by crosslinking of anti-CD3 monoclonal antibodies. *Journal of Leukocyte Biology*, *46*(3), 214–20.

Duddy, M., Niino, M., Adatia, F., Hebert, S., Freedman, M., Atkins, H., … Bar-Or, A. (2007). Distinct effector cytokine profiles of memory and naive human B cell subsets and implication in multiple sclerosis. *Journal of Immunology (Baltimore, Md. : 1950)*, *178*(10), 6092–9.

Edwards, D. P., Grzyb, K. T., Dressler, L. G., Mansel, R. E., Zava, D. T., Sledge, G. W., & McGuire, W. L. (1986). Monoclonal antibody identification and characterization of a Mr 43,000 membrane glycoprotein associated with human breast cancer. *Cancer Research*, *46*(3), 1306–17.

Elgueta, R., Benson, M. J., de Vries, V. C., Wasiuk, A., Guo, Y., & Noelle, R. J. (2009). Molecular mechanism and function of CD40/CD40L engagement in the immune system. *Immunological Reviews*, *229*(1), 152–72.

Eliopoulos, A. G., & Young, L. S. (2004). The role of the CD40 pathway in the pathogenesis and treatment of cancer. *Current Opinion in Pharmacology*, *4*(4), 360–367.

Fanale, M., Assouline, S., Kuruvilla, J., Solal-Céligny, P., Heo, D. S., Verhoef, G., … Freedman, A. S. (2014). Phase IA/II, multicentre, open-label study of the CD40 antagonistic monoclonal antibody lucatumumab in adult patients with advanced non-Hodgkin or Hodgkin lymphoma. *British Journal of Haematology*, *164*(2), 258–265.

Fiedler, W. M., Wolf, M., Kebenko, M., Goebeler, M.-E., Ritter, B., Quaas, A., … Kaubitzsch, S. (2012). A phase I study of EpCAM/CD3-bispecific antibody (MT110) in patients with advanced solid tumors. *J Clin Oncol*, *30*(suppl; abstr 2504).

Fransen, M. F., Sluijter, M., Morreau, H., Arens, R., & Melief, C. J. M. (2011). Local activation of CD8 T cells and systemic tumor eradication without toxicity via slow release and local delivery of agonistic CD40 antibody. *Clinical Cancer Research : An Official Journal of the American Association for Cancer Research*, *17*(8), 2270–80.

Fransson, J., Teplyakov, A., Raghunathan, G., Chi, E., Cordier, W., Dinh, T., … Almagro, J. C. (2010). Human framework adaptation of a mouse anti-human IL-13 antibody. *Journal of Molecular Biology*, *398*(2), 214–31.

French, R. R., Chan, H. T., Tutt, a L., & Glennie, M. J. (1999). CD40 antibody evokes a cytotoxic T-cell response that eradicates lymphoma and bypasses T-cell help. *Nature Medicine*, *5*(5), 548–53.

Furuse, M., Fujita, K., Hiragi, T., Fujomoto, K., & Tsukita, S. (1998). Claudin-1 and -2: novel integral membrane proteins localizing at tight junctions with no sequence homology to occludin. *J Cell Biol*, *141*(7), 1539–1550.

Gieffers, C., Kluge, M., Merz, C., Sykora, J., Thiemann, M., Schaal, R., … Hill, O. (2013). APG350 induces superior clustering of TRAIL receptors and shows therapeutic antitumor efficacy independent of cross-linking via Fcγ receptors. *Molecular Cancer Therapeutics*, *12*(12), 2735–47.

Gillies, S. D., Lan, Y., Brunkhorst, B., Wong, W.-K., Li, Y., & Lo, K.-M. (2002). Bi-functional cytokine fusion proteins for gene therapy and antibody-targeted treatment of cancer. *Cancer Immunology, Immunotherapy : CII*, *51*(8), 449–60.

Gong, T., Zhou, H.-L., & Ba, Y. (2013). [CCL21-CD40L fusion gene induce augmented antitumor activity in colon cancer]. *Zhejiang Da Xue Xue Bao. Yi Xue Ban = Journal of Zhejiang University. Medical Sciences*, *42*(5), 498–503.

Gonzales, N. R., De Pascalis, R., Schlom, J., & Kashmiri, S. V. S. (2005). Minimizing the immunogenicity of antibodies for clinical application. *Tumour Biology : The Journal of the International Society for Oncodevelopmental Biology and Medicine*, *26*(1), 31–43.

Goodwin, R. G., Din, W. S., Davis-Smith, T., Anderson, D. M., Gimpel, S. D., Sato, T. a, … Jenkins, N. a. (1993). Molecular cloning of a ligand for the inducible T cell gene 4-1BB: a member of an emerging family of cytokines with homology to tumor necrosis factor. *European Journal of Immunology*, *23*(10), 2631–41.

Goodwin, R. G., Alderson, M. R., Smith, C. A., Armitage, R. J., VandenBos, T., Jerzy, R., … Beckmann, M. P. (1993). Molecular and biological characterization of a ligand for CD27 defines a new family of cytokines with homology to tumor necrosis factor. *Cell*, *73*(3), 447–456.

Gramaglia, I., Weinberg, A. D., Lemon, M., & Croft, M. (1998). Ox-40 ligand: a potent costimulatory molecule for sustaining primary CD4 T cell responses. *Journal of Immunology (Baltimore, Md. : 1950)*, *161*(12), 6510–7.

Gray, J. C., French, R. R., James, S., Al-Shamkhani, A., Johnson, P. W., & Glennie, M. J. (2008). Optimising anti-tumour CD8 T-cell responses using combinations of immunomodulatory antibodies. *European Journal of Immunology*, *38*(9), 2499–511.

Guo, Z., Wang, X., Cheng, D., Xia, Z., Luan, M., & Zhang, S. (2014). PD-1 blockade and OX40 triggering synergistically protects against tumor growth in a murine model of ovarian cancer. *PLoS ONE*, *9*(2).

Gupta, S., Termini, J. M., Raffa, F. N., Williams, C.-A., Kornbluth, R. S., & Stone, G. W. (2014). Vaccination with a fusion protein that introduces HIV-1 gag antigen into a multitrimer CD40L construct results in enhanced CD8+ T cell responses and protection from viral challenge by vaccinia-gag. *Journal of Virology*, *88*(3), 1492–501.

Halin, C., Gafner, V., Villani, M. E., Borsi, L., Berndt, A., Kosmehl, H., … Neri, D. (2003). Synergistic therapeutic effects of a tumor targeting antibody fragment, fused to interleukin 12 and to tumor necrosis factor alpha. *Cancer Research*, *63*(12), 3202–10.

Hamid, O., Thompson, J., Diab, A., Ros, W., Eskens, F., Bermingham, C., … El-Khoueiry, A. (2016). First in human (FIH) study of an OX40 agonist monoclonal antibody (mAb) PF-04518600 (PF-8600) in adult patients (pts) with select advanced solid tumors: Preliminary safety and pharmacokinetic (PK)/pharmacodynamic results. *J Clin Oncol*, *34*(suppl), abstr 3079.

Hammond, S., Morris, C., Auge, C., Du, Q., Mulgrew, K., McGlinchey, K., … Oberst, M. (2015). Human OX40 ligand fusion protein (MEDI6383) as a potent OX40 agonist and immuno-modulator in vitro and in vivo. *J Clin Oncol*, *33*(auppl), abstr 3056.

He, L.-Z., Prostak, N., Thomas, L. J., Vitale, L., Weidlick, J., Crocker, A., … Keler, T. (2013). Agonist anti-human CD27 monoclonal antibody induces T cell activation and tumor immunity in human CD27-transgenic mice. *Journal of Immunology (Baltimore, Md. : 1950)*, *191*(8), 4174–83.

Hemmerle, T., Hess, C., Venetz, D., & Neri, D. (2014). Tumor targeting properties of antibody fusion proteins based on different members of the murine tumor necrosis superfamily. *Journal of Biotechnology*, *172*(1), 73–6.

Herlyn, M., Steplewski, Z., Herlyn, D., & Koprowski, H. (1979). Colorectal carcinoma-specific antigen: detection by means of monoclonal antibodies. *Proceedings of the National Academy of Sciences of the United States of America*, *76*(3), 1438–42.

Hewitt, K. J., Agarwal, R., & Morin, P. J. (2006). The claudin gene family: expression in normal and neoplastic tissues. *BMC Cancer*, *6*, 186.

Hodi, F. S., O'Day, S. J., McDermott, D. F., Weber, R. W., Sosman, J. A., Haanen, J. B., … Urba, W. J. (2010). Improved survival with ipilimumab in patients with metastatic melanoma. *The New England Journal of Medicine*, *363*(8), 711–23.

Hornig, N., Kermer, V., Frey, K., Diebolder, P., Kontermann, R. E., & Müller, D. (2012). Combination of a bispecific antibody and costimulatory antibody-ligand fusion proteins for targeted cancer immunotherapy. *Journal of Immunotherapy (Hagerstown, Md. : 1997)*, *35*(5), 418–29.

Hornig, N., Reinhardt, K., Kermer, V., Kontermann, R. E., & Müller, D. (2013). Evaluating combinations of costimulatory antibody-ligand fusion proteins for targeted cancer immunotherapy. *Cancer Immunology, Immunotherapy : CII*, *62*(8), 1369–80.

Hu, P., Arias, R. S., Sadun, R. E., Nien, Y.-C., Zhang, N., Sabzevari, H., … Epstein, A. L. (2008). Construction and preclinical characterization of Fc-mGITRL for the immunotherapy of cancer. *Clinical Cancer Research : An Official Journal of the American Association for Cancer Research*, *14*(2), 579–88.

Huang, J.-H., Zhang, S.-N., Choi, K.-J., Choi, I.-K., Kim, J.-H., Lee, M.-G., … Yun, C.-O. (2010). Therapeutic and tumor-specific immunity induced by combination of dendritic cells and oncolytic adenovirus expressing IL-12 and 4-1BBL. *Molecular Therapy : The Journal of the American Society of Gene Therapy*, *18*(2), 264–74.

Hwang, W. Y. K., & Foote, J. (2005). Immunogenicity of engineered antibodies. *Methods (San Diego, Calif.)*, *36*(1), 3–10.

Ito, T., Wang, Y.-H., Duramad, O., Hanabuchi, S., Perng, O. a, Gilliet, M., … Liu, Y.-J. (2006). OX40 ligand shuts down IL-10-producing regulatory T cells. *Proceedings of the National Academy of Sciences of the United States of America*, *103*(35), 13138–43.

Jackaman, C., & Nelson, D. J. (2012). Intratumoral interleukin-2/agonist CD40 antibody drives CD4+ -independent resolution of treated-tumors and CD4+ -dependent systemic and memory responses. *Cancer Immunology, Immunotherapy : CII*, *61*(4), 549–60.

Jahn, T., Zuther, M., Friedrichs, B., Heuser, C., Guhlke, S., Abken, H., & Hombach, A. A. (2012). An IL12-IL2-antibody fusion protein targeting Hodgkin's lymphoma cells potentiates activation of NK and T cells for an anti-tumor attack. *PloS One*, *7*(9), e44482.

Kamath, A. T., Sheasby, C. E., & Tough, D. F. (2005). Dendritic cells and NK cells stimulate bystander T cell activation in response to TLR agonists through secretion of IFN-alpha beta and IFN-gamma. *Journal of Immunology (Baltimore, Md. : 1950)*, *174*(2), 767–76.

Karpusas, M., Hsu, Y. M., Wang, J. H., Thompson, J., Lederman, S., Chess, L., & Thomas, D. (1995). 2 A crystal structure of an extracellular fragment of human CD40 ligand. *Structure (London, England : 1993)*, *3*(12), 1426.

Kermer, V., Baum, V., Hornig, N., Kontermann, R. E., & Müller, D. (2012). An antibody fusion protein for cancer immunotherapy mimicking IL-15 trans-presentation at the tumor site. *Molecular Cancer Therapeutics*, *11*(6), 1279–88.

Kermer, V., Hornig, N., Harder, M., Bondarieva, A., Kontermann, R. E., & Müller, D. (2014). Combining antibody-directed presentation of IL-15 and 4-1BBL in a trifunctional fusion protein for cancer immunotherapy. *Mol. Cancer Ther.*, *13*(1), 112–21.

Khong, A., Nelson, D. J., Nowak, A. K., Lake, R. A., & Robinson, B. W. S. (2012). The use of agonistic anti-CD40 therapy in treatments for cancer. *International Reviews of Immunology*, *31*(4), 246–66.

Kjaergaard, J., Tanaka, J., Kim, J. a, Rothchild, K., Weinberg, A., & Shu, S. (2000). Therapeutic efficacy of OX-40 receptor antibody depends on tumor immunogenicity and anatomic site of tumor growth. *Cancer Research*, *60*(19), 5514–21.

Klebanoff, C. A., Rosenberg, S. A., & Restifo, N. P. (2016). Prospects for gene-engineered T cell immunotherapy for solid cancers. *Nat Med*, *22*(1), 26–36.

Kober, J., Leitner, J., Klauser, C., Woitek, R., Majdic, O., Stöckl, J., … Steinberger, P. (2008). The capacity of the TNF family members 4-1BBL, OX40L, CD70, GITRL, CD30L and LIGHT to costimulate human T cells. *European Journal of Immunology*, *38*(10), 2678–88.

Kominsky, S. L., Vali, M., Korz, D., Gabig, T. G., Weitzman, S. a, Argani, P., & Sukumar, S. (2004). Clostridium perfringens enterotoxin elicits rapid and specific cytolysis of breast carcinoma cells mediated through tight junction proteins claudin 3 and 4. *Am. J. Pathol.*, *164*(5), 1627–1633.

König, R., Huang, L. Y., & Germain, R. N. (1992). MHC class II interaction with CD4 mediated by a region analogous to the MHC class I binding site for CD8. *Nature*, *356*(6372), 796–8.

Kontermann, R. E., Martineau, P., Cummings, C. E., Karpas, A., Allen, D., Derbyshire, E., & Winter, G. (1997). Enzyme immunoassays using bispecific diabodies. *Immunotechnology : An International Journal of Immunological Engineering*, *3*(2), 137–44.

Kontermann, R. E. (2005). Recombinant bispecific antibodies for cancer therapy. *Acta Pharmacologica Sinica*, *26*(1), 1–9.

Kontermann, R. E., Mu, S., Neumeyer, J., Mu, D., Branscha, M., Scheurich, P., & Pfizenmaier, K. (2008). A humanized tumor necrosis factor receptor 1 (TNFR1)-specific antagonistic antibody for selective inhibition of tumor necrosis factor (TNF) action. *Journal of Immunotherapy*, *31*(3), 225–34.

Kontermann, R. E. (2012). Antibody-cytokine fusion proteins. *Archives of Biochemistry and Biophysics*, *526*(2), 194–205.

Kontermann, R. E. (2011). Strategies for extended serum half-life of protein therapeutics. *Current Opinion in Biotechnology*, *22*(6), 868–76.

Kranz, L. M., Diken, M., Haas, H., Kreiter, S., Loquai, C., Reuter, K. C., … Sahin, U. (2016). Systemic RNA delivery to dendritic cells exploits antiviral defence for cancer immunotherapy. *Nature*, 1–16.

Krause, G., Winkler, L., Mueller, S. L., Haseloff, R. F., Piontek, J., & Blasig, I. E. (2008). Structure and function of claudins. *Biochimica et Biophysica Acta - Biomembranes*, *1778*(3), 631–645.

Kreiter, S., Vormehr, M., van de Roemer, N., Diken, M., Löwer, M., Diekmann, J., … Sahin, U. (2015). Mutant MHC class II epitopes drive therapeutic immune responses to cancer. *Nature*, *520*(7549), 692–696.

Krippner-Heidenreich, A., Grunwald, I., Zimmermann, G., Kühnle, M., Gerspach, J., Sterns, T., … Scheurich, P. (2008). Single-chain TNF, a TNF derivative with enhanced stability and antitumoral activity. *Journal of Immunology (Baltimore, Md. : 1950)*, *180*(12), 8176–83.

Kulka, J., Szász, A. M., Németh, Z., Madaras, L., Schaff, Z., Molnár, I. A., & Tokés, A.-M. (2009). Expression of tight junction protein claudin-4 in basal-like breast carcinomas. *Pathology Oncology Research : POR*, *15*(1), 59–64.

Kurche, J. S., Burchill, M. A., Sanchez, P. J., Haluszczak, C., & Kedl, R. M. (2010). Comparison of OX40 ligand and CD70 in the promotion of CD4+ T cell responses. *Journal of Immunology (Baltimore, Md. : 1950)*, *185*(4), 2106–15.

Kwon, B. S., & Weissman, S. M. (1989). cDNA sequences of two inducible T-cell genes. *Proceedings of the National Academy of Sciences of the United States of America*, *86*(6), 1963–7.

Ladwein, M., Pape, U. F., Schmidt, D. S., Schn??lzer, M., Fiedler, S., Langbein, L., … Z??ller, M. (2005). The cell-cell adhesion molecule EpCAM interacts directly with the tight junction protein claudin-7. *Experimental Cell Research*, *309*(2), 345–357.

Lal-Nag, M., & Morin, P. (2009). The claudins. *Genome Biology*, *10*(8), 235.

Lang, I., Füllsack, S., Wyzgol, A., Fick, A., Trebing, J., Arana, J. A. C., … Wajant, H. (2016). Binding Studies of TNF Receptor Superfamily (TNFRSF) Receptors on Intact Cells. *The Journal of Biological Chemistry*, *291*(10), 5022–37.

Lapointe, R., Bellemare-Pelletier, A., Housseau, F., Thibodeau, J., & Hwu, P. (2003). CD40-stimulated B lymphocytes pulsed with tumor antigens are effective antigen-presenting cells that can generate specific T cells. *Cancer Research*, *63*(11), 2836–43.

Larkin, J., Chiarion-Sileni, V., Gonzalez, R., Grob, J. J., Cowey, C. L., Lao, C. D., … Wolchok, J. D. (2015). Combined Nivolumab and Ipilimumab or Monotherapy in Untreated Melanoma. *The New England Journal of Medicine*, *373*(1), 23–34.

Lee, H.-W., Park, S.-J., Choi, B. K., Kim, H. H., Nam, K.-O., & Kwon, B. S. (2002). 4-1BB promotes the survival of CD8+ T lymphocytes by increasing expression of Bcl-xL and Bfl-1. *Journal of Immunology (Baltimore, Md. : 1950)*, *169*(9), 4882–8.

Lee, S.-J., Myers, L., Muralimohan, G., Dai, J., Qiao, Y., Li, Z., … Vella, A. T. (2004). 4-1BB and OX40 dual costimulation synergistically stimulate primary specific CD8 T cells for robust effector function. *Journal of Immunology (Baltimore, Md. : 1950)*, *173*(5), 3002–12.

Lee, S.-J., Myers, L., Muralimohan, G., Dai, J., Qiao, Y., Li, Z., … Vella, A. T. (2004). 4-1BB and OX40 dual costimulation synergistically stimulate primary specific CD8 T cells for robust effector function. *Journal of Immunology (Baltimore, Md. : 1950)*, *173*(5), 3002–12.

Lei, Z., Maeda, T., Tamura, A., Nakamura, T., Yamazaki, Y., Shiratori, H., … Hamada, H. (2012). EpCAM contributes to formation of functional tight junction in the intestinal epithelium by recruiting claudin proteins. *Developmental Biology*, *371*(2), 136–45.

Leidner, R., Patel, S., Fury, M., Ferris, R., McDevitt, J., Lanasa, M., & Glisson, B. (2015). A phase I study to evaluate the safety, tolerability, PK, pharmacodynamics, and preliminary clinical activity of MEDI0562 in patients with recurrent or metastatic (R/M) squamous cell carcinoma of the head and neck (SCCHN). *J Clin Oncol*, *33*(suppl), abstr TPS6083.

Li, B., Lin, J., Vanroey, M., Jure-Kunkel, M., & Jooss, K. (2007). Established B16 tumors are rejected following treatment with GM-CSF-secreting tumor cell immunotherapy in combination with anti-4-1BB mAb. *Clinical Immunology (Orlando, Fla.)*, *125*(1), 76–87.

Li, P., Yuan, S., & Galipeau, J. (2013). A fusion cytokine coupling GMCSF to IL9 induces heterologous receptor clustering and STAT1 hyperactivation through JAK2 promiscuity. *PloS One*, *8*(7), e69405.

Li, X., Iida, M., Tada, M., Watari, A., Kawahigashi, Y., Kimura, Y., … Kondoh, M. (2014). Development of an anti-claudin-3 and -4 bispecific monoclonal antibody for cancer diagnosis and therapy. *J Pharmacol Exp Ther*, *351*(1), 206–213.

Liao, M.-Y., Lai, J.-K., Kuo, M. Y.-P., Lu, R.-M., Lin, C.-W., Cheng, P.-C., … Wu, H.-C. (2015). An anti-EpCAM antibody EpAb2-6 for the treatment of colon cancer. *Oncotarget*, *6*(28), 24947–68.

Lichty, B. D., Breitbach, C. J., Stojdl, D. F., & Bell, J. C. (2014). Going viral with cancer immunotherapy. *Nature Reviews. Cancer*, *14*(8), 559–567.

Locksley, R. M., Killeen, N., & Lenardo, M. J. (2001). The TNF and TNF receptor superfamilies: Integrating mammalian biology. *Cell*, *104*(4), 487–501.

Lu, Y. C., & Robbins, P. F. (2015). Cancer immunotherapy targeting neoantigens. *Seminars in Immunology*, *28*(1), 22–27.

Lynch, T. J., Bondarenko, I., Luft, A., Serwatowski, P., Barlesi, F., Chacko, R., … Reck, M. (2012). Ipilimumab in combination with paclitaxel and carboplatin as first-line treatment in stage IIIB/IV non-small-cell lung cancer: Results from a randomized, double-blind, multicenter phase II study. *Journal of Clinical Oncology*, *30*(17), 2046–2054.

Madireddi, S., Schabowsky, R.-H., Srivastava, A. K., Sharma, R. K., Yolcu, E. S., & Shirwan, H. (2012). SA-4-1BBL costimulation inhibits conversion of conventional CD4+ T cells into CD4+ FoxP3+ T regulatory cells by production of IFN-γ. *PloS One*, *7*(8), e42459.

Mahoney, K. M., Rennert, P. D., & Freeman, G. J. (2015). Combination cancer immunotherapy and new immunomodulatory targets. *Nature Reviews Drug Discovery*, *14*(8), 561–584.

Martin, a C., & Thornton, J. M. (1996). Structural families in loops of homologous proteins: automatic classification, modelling and application to antibodies. *Journal of Molecular Biology*, *263*(5), 800–815.

Maude, S. L., Frey, N., Shaw, P. A., Aplenc, R., Barrett, D. M., Bunin, N. J., … Grupp, S. A. (2014). Chimeric antigen receptor T cells for sustained remissions in leukemia. *The New England Journal of Medicine*, *371*(16), 1507–17.

Melero, I., Shuford, W. W., Newby, S. A., Aruffo, A., Ledbetter, J. A., Hellström, K. E., … Chen, L. (1997). Monoclonal antibodies against the 4-1BB T-cell activation molecule eradicate established tumors. *Nature Medicine*, *3*(6), 682–5.

Melero, I., Berman, D. M., Aznar, M. A., Korman, A. J., Gracia, J. L. P., & Haanen, J. (2015). Evolving synergistic combinations of targeted immunotherapies to combat cancer. *Nature Reviews. Cancer*, *15*(8), 457–72.

Melero, I., Gaudernack, G., Gerritsen, W., Huber, C., Parmiani, G., Scholl, S., … Mellstedt, H. (2014). Therapeutic vaccines for cancer: an overview of clinical trials. *Nature Reviews. Clinical Oncology*, *11*(9), 509–24.

Melero, I., Hirschhorn-Cymerman, D., Morales-Kastresana, A., Sanmamed, M. F., & Wolchok, J. D. (2013). Agonist antibodies to TNFR molecules that costimulate T and NK cells. *Clinical Cancer Research : An Official Journal of the American Association for Cancer Research*, *19*(5), 1044–53.

Michl, P., Buchholz, M., Rolke, M., Kunsch, S., Löhr, M., McClane, B., … Gress, T. M. (2001). Claudin-4: a new target for pancreatic cancer treatment using Clostridium perfringens enterotoxin. *Gastroenterology*, *121*(3), 678–684.

Micke, P., Mattsson, J. S. M., Edlund, K., Lohr, M., Jirström, K., Berglund, A., … Türeci, Ö. (2014). Aberrantly activated claudin 6 and 18.2 as potential therapy targets in non-small-cell lung cancer. *International Journal of Cancer*, *135*(9), 2206–2214.

Mineta, K., Yamamoto, Y., Yamazaki, Y., Tanaka, H., Tada, Y., Saito, K., … Tsukita, S. (2011). Predicted expansion of the claudin multigene family. *FEBS Letters*, *585*(4), 606–612.

Morales-Kastresana, A., Labiano, S., Quetglas, J. I., & Melero, I. (2013). Better performance of CARs deprived of the PD-1 brake. *Clinical Cancer Research*, *19*(20), 5546–5548.

Morales-Kastresana, A., Sanmamed, M. F., Rodriguez, I., Palazon, A., Martinez-Forero, I., Labiano, S., … Melero, I. (2013). Combined immunostimulatory monoclonal antibodies extend survival in an aggressive transgenic hepatocellular carcinoma mouse model. *Clinical Cancer Research*, *19*(22), 6151–6162.

Morin, P. J. (2005). Claudin proteins in human cancer: Promising new targets for diagnosis and therapy. *Cancer Research*, *65*(21), 9603–9606.

Morris, A. E., Remmele, R. L., Klinke, R., Macduff, B. M., Fanslow, W. C., & Armitage, R. J. (1999). Incorporation of an isoleucine zipper motif enhances the biological activity of soluble CD40L (CD154). *The Journal of Biological Chemistry*, *274*(1), 418–23.

Morris, N. P., Peters, C., Montler, R., Hu, H.-M., Curti, B. D., Urba, W. J., & Weinberg, A. D. (2007). Development and characterization of recombinant human Fc:OX40L fusion protein linked via a coiled-coil trimerization domain. *Molecular Immunology*, *44*(12), 3112–21.

Müller, D. (2015). Antibody fusions with immunomodulatory proteins for cancer therapy. *Pharmacology & Therapeutics*, *154*, 57–66.

Müller, D. (2014). Antibody-cytokine fusion proteins for cancer immunotherapy: an update on recent developments. *BioDrugs : Clinical Immunotherapeutics, Biopharmaceuticals and Gene Therapy*, *28*(2), 123–31.

Müller, D., Frey, K., & Kontermann, R. E. (2008). A novel antibody-4-1BBL fusion protein for targeted costimulation in cancer immunotherapy. *Journal of Immunotherapy*, *31*(8), 714–22.

Müller, N., Wyzgol, A., Münkel, S., Pfizenmaier, K., & Wajant, H. (2008). Activity of soluble OX40 ligand is enhanced by oligomerization and cell surface immobilization. *FEBS Journal*, *275*(9), 2296–2304.

Neesse, A., Griesmann, H., Gress, T. M., & Michl, P. (2012). Claudin-4 as therapeutic target in cancer. *Archives of Biochemistry and Biophysics*, *524*(1), 64–70.

Newman, M. J., & Benani, D. J. (2015). A review of blinatumomab, a novel immunotherapy. *Journal of Oncology Pharmacy Practice : Official Publication of the International Society of Oncology Pharmacy Practitioners*.

Ng, S., & Galipeau, J. (2015). Concise review: engineering the fusion of cytokines for the modulation of immune cellular responses in cancer and autoimmune disorders. *Stem Cells Translational Medicine*, *4*(1), 66–73.

Nolte, M. A., Van Olffen, R. W., Van Gisbergen, K. P. J. M., & Van Lier, R. A. W. (2009). Timing and tuning of CD27-CD70 interactions: The impact of signal strength in setting the balance between adaptive responses and immunopathology. *Immunological Reviews*, *229*(1), 216–231.

Palazón, A., Teijeira, A., Martínez-Forero, I., Hervás-Stubbs, S., Roncal, C., Peñuelas, I., … Melero, I. (2011). Agonist anti-CD137 mAb act on tumor endothelial cells to enhance recruitment of activated T lymphocytes. *Cancer Research*, *71*(3), 801–11.

Paterson, D. J., Jefferies, W. A., Green, J. R., Brandon, M. R., Corthesy, P., Puklavec, M., & Williams, A. F. (1987). Antigens of activated rat T lymphocytes including a molecule of 50,000 Mr detected only on CD4 positive T blasts. *Molecular Immunology*, *24*(12), 1281–90.

Patriarca, C., Macchi, R. M., Marschner, A. K., & Mellstedt, H. (2012). Epithelial cell adhesion molecule expression (CD326) in cancer: A short review. *Cancer Treatment Reviews*, *38*(1), 68–75.

Paulie, S., Ehlin-Henriksson, B., Mellstedt, H., Koho, H., Ben-Aissa, H., & Perlmann, P. (1985). A p50 surface antigen restricted to human urinary bladder carcinomas and B lymphocytes. *Cancer Immunology Immunotherapy*, *20*(1), 23–28.

Pesonen, S., Diaconu, I., Kangasniemi, L., Ranki, T., Kanerva, A., Pesonen, S. K., … Hemminki, A. (2012). Oncolytic immunotherapy of advanced solid tumors with a CD40L-expressing replicating adenovirus: assessment of safety and immunologic responses in patients. *Cancer Research*, *72*(7), 1621–31.

Postow, M. a., Chesney, J., Pavlick, A. C., Robert, C., Grossmann, K., McDermott, D., … Hodi, F. S. (2015). Nivolumab and Ipilimumab versus Ipilimumab in Untreated Melanoma. *The New England Journal of Medicine*, 150420053025009.

Powderly, J., Gutierrez, M., Wang, D., Chae, Y., Mahadevan, D., Braiteh, F., … Curti, B. (2015). A phase 1b/2, open-label study to evaluate the safety and tolerability of MEDI6469 in combination with immune therapeutic agents or therapeutic mAbs in patients with selected advanced solid tumors or aggressive B-cell lymphomas. *J Clin Oncol*, *33*(suppl), abstr TPS3091.

Rabu, C., Quéméner, A., Jacques, Y., Echasserieau, K., Vusio, P., & Lang, F. (2005). Production of recombinant human trimeric CD137L (4-1BBL). Cross-linking is essential to its T cell co-stimulation activity. *The Journal of Biological Chemistry*, *280*(50), 41472–81.

Rahimian, S., Fransen, M. F., Kleinovink, J. W., Amidi, M., Ossendorp, F., & Hennink, W. E. (2015). Polymeric microparticles for sustained and local delivery of antiCD40 and antiCTLA-4 in immunotherapy of cancer. *Biomaterials*, *61*, 33–40.

Ranz, I. M. (2014). *Generation and characterization of „fibroblast activation protein“ - directed antibody fusion proteins with mouse4-1BBligand-mutants*.

Rapoport, A. P., Stadtmauer, E. a, Binder-Scholl, G. K., Goloubeva, O., Vogl, D. T., Lacey, S. F., … June, C. H. (2015). NY-ESO-1-specific TCR-engineered T cells mediate sustained antigen-specific antitumor effects in myeloma. *Nature Medicine*, *21*(July), 1–20.

Redmond, W. L., Linch, S. N., & Kasiewicz, M. J. (2014). Combined targeting of costimulatory (OX40) and coinhibitory (CTLA-4) pathways elicits potent effector T cells capable of driving robust antitumor immunity. *Cancer Immunology Research*, *2*(2), 142–53.

Resnick, M. B., Gavilanez, M., Newton, E., Konkin, T., Bhattacharya, B., Britt, D. E., … Moss, S. F. (2005). Claudin expression in gastric adenocarcinomas: A tissue microarray study with prognostic correlation. *Human Pathology*, *36*(8), 886–892.

Richter, F. (2015). *Evolution of the Antagonistic Tumor Necrosis Factor Receptor One-Specific Antibody ATROSAB*.

Ridge, J. P., Di Rosa, F., & Matzinger, P. (1998). A conditioned dendritic cell can be a temporal bridge between a CD4+ T-helper and a T-killer cell. *Nature*, *393*(6684), 474–8.

Ritchie, D. S., Yang, J., Hermans, I. F., & Ronchese, F. (2004). B-Lymphocytes activated by CD40 ligand induce an antigen-specific anti-tumour immune response by direct and indirect activation of CD8(+) T-cells. *Scandinavian Journal of Immunology*, *60*(6), 543–51.

Robert, C., Schachter, J., Long, G. V, Arance, A., Grob, J. J., Mortier, L., … Ribas, A. (2015). Pembrolizumab versus Ipilimumab in Advanced Melanoma. *The New England Journal of Medicine*, *372*(26), 2521–32.

Rogers, P. R., Song, J., Gramaglia, I., Killeen, N., & Croft, M. (2001). OX40 promotes Bcl-xL and Bcl-2 expression and is essential for long-term survival of CD4 T cells. *Immunity*, *15*(3), 445–455.

Roovers, R. C., Henderikx, P., Helfrich, W., van der Linden, E., Reurs, A., de Bruïne, a P., … Hoogenboom, H. R. (1998). High-affinity recombinant phage antibodies to the pan-carcinoma marker epithelial glycoprotein-2 for tumour targeting. *British Journal of Cancer*, *78*, 1407–1416.

Rosenblum, M. G., Horn, S. a, & Cheung, L. H. (2000). A novel recombinant fusion toxin targeting HER-2/NEU-over-expressing cells and containing human tumor necrosis factor. *International Journal of Cancer*, *88*(2), 267–73.

Rowley, T. F., & Al-Shamkhani, A. (2004). Stimulation by soluble CD70 promotes strong primary and secondary CD8+ cytotoxic T cell responses in vivo. *Journal of Immunology (Baltimore, Md. : 1950)*, *172*(10), 6039–46.

Rüter, J., Antonia, S. J., Burris, H. A., Huhn, R. D., & Vonderheide, R. H. (2010). Immune modulation with weekly dosing of an agonist CD40 antibody in a phase I study of patients with advanced solid tumors. *Cancer Biology and Therapy*, *10*(10), 983–993.

Sadun, R. E., Hsu, W.-E., Zhang, N., Nien, Y.-C., Bergfeld, S. A., Sabzevari, H., … Epstein, A. L. (2008). Fc-mOX40L fusion protein produces complete remission and enhanced survival in 2 murine tumor models. *Journal of Immunotherapy (Hagerstown, Md. : 1997)*, *31*(3), 235–45.

Sahin, U., Jaeger, D., Marme, F., Mavratzas, A., Krauss, J., De Greve, J., … Tureci, O. (2015). First-in-human phase I/II dose-escalation study of IMAB027 in patients with recurrent advanced ovarian cancer (OVAR): Preliminary data of phase I part. *Journal of Clinical Oncology (Meeting Abstracts*, *33*(15_suppl), 5537.

Samel, D., Muller, D., Gerspach, J., Assohou-Luty, C., Sass, G., Tiegs, G., … Wajant, H. (2003). Generation of a FasL-based proapoptotic fusion protein devoid of systemic toxicity due to cell-surface antigen-restricted Activation. *The Journal of Biological Chemistry*, *278*(34), 32077–82.

Sanmamed, M. F., Pastor, F., Rodriguez, A., Perez-Gracia, J. L., Rodriguez-Ruiz, M. E., Jure-Kunkel, M., & Melero, I. (2015). Agonists of Co-stimulation in Cancer Immunorapy Directed Against CD137, OX40, GITR, CD27, CD28, and ICOS. *Seminars in Oncology*, *42*(4), 640–655.

Schabowsky, R.-H., Elpek, K. G., Madireddi, S., Sharma, R. K., Yolcu, E. S., Bandura-Morgan, L., … Shirwan, H. (2009). A novel form of 4-1BBL has better immunomodulatory activity than an agonistic anti-4-1BB Ab without Ab-associated severe toxicity. *Vaccine*, *28*(2), 512–22.

Schadendorf, D., Hodi, F. S., Robert, C., Weber, J. S., Margolin, K., Hamid, O., … Wolchok, J. D. (2015). Pooled Analysis of Long-Term Survival Data From Phase II and Phase III Trials of Ipilimumab in Unresectable or Metastatic Melanoma. *Journal of Clinical Oncology : Official Journal of the American Society of Clinical Oncology*, *33*(17), 1889–94.

Schanzer, J. M., Fichtner, I., Baeuerle, P. A., & Kufer, P. (2006). Antitumor activity of a dual cytokine/single-chain antibody fusion protein for simultaneous delivery of GM-CSF and IL-2 to Ep-CAM expressing tumor cells. *Journal of Immunotherapy (Hagerstown, Md. : 1997)*, *29*(5), 477–88.

Schlapschy, M., Gruber, H., Gresch, O., Schäfer, C., Renner, C., Pfreundschuh, M., & Skerra, A. (2004). Functional humanization of an anti-CD30 Fab fragment for the immunotherapy of Hodgkin's lymphoma using an in vitro evolution approach. *Protein Engineering, Design & Selection : PEDS*, *17*(12), 847–60.

Schmoll, H.-J., & Arnold, D. (2009). When wishful thinking leads to a misty-eyed appraisal: the story of the adjuvant colon cancer trials with edrecolomab. *Journal of Clinical Oncology : Official Journal of the American Society of Clinical Oncology*, *27*(12), 1926–9.

Schneeberger, E. E., & Lynch, R. D. (2004). The tight junction: a multifunctional complex. *American Journal of Physiology. Cell Physiology*, *286*(6), C1213–C1228.

Schneider, B., Münkel, S., Krippner-Heidenreich, A., Grunwald, I., Wels, W. S., Wajant, H., … Gerspach, J. (2010). Potent antitumoral activity of TRAIL through generation of tumor-targeted single-chain fusion proteins. *Cell Death & Disease*, *1*, e68.

Schnell, U., Cirulli, V., & Giepmans, B. N. G. (2013). EpCAM: Structure and function in health and disease. *BBA - Biomembranes*, *1828*(8), 1989–2001.

Schönbeck, U., & Libby, P. (2001). The CD40/CD154 receptor/ligand dyad. *Cellular and Molecular Life Sciences : CMLS*, *58*(1), 4–43.

Segal, N. H., Gopal, A. K., Bhatia, S., Kohrt, H. E., Levy, R., Pishvaian, M. J., … Davis, C. (2014). A phase 1 study of PF-05082566 (anti-4-1BB) in patients with advanced cancer. *Journal of Clinical Oncology, 2014 ASCO Annual Meeting Abstracts.*, *32*(No15_suppl), 3007.

Seifert, O., Plappert, A., Fellermeier, S., Siegemund, M., Pfizenmaier, K., & Kontermann, R. E. (2014). Tetravalent antibody-scTRAIL fusion proteins with improved properties. *Molecular Cancer Therapeutics*, *13*(1), 101–11.

Seifert, O., Plappert, A., Heidel, N., Fellermeier, S., Messerschmidt, S. K. E., Richter, F., & Kontermann, R. E. (2012). The IgM CH2 domain as covalently linked homodimerization module for the generation of fusion proteins with dual specificity. *Protein Engineering, Design & Selection : PEDS*, *25*(10), 603–12.

Seimetz, D. (2011). Novel monoclonal antibodies for cancer treatment: The trifunctional an-tibody catumaxomab (Removab®). *Journal of Cancer*, *2*(1), 309–316.

Seledtsov, V. I., Goncharov, A. G., & Seledtsova, G. V. (2015). Multiple-purpose immunotherapy for cancer. *Biomedicine & Pharmacotherapy = Biomédecine & Pharmacothérapie*, *76*, 24–9.

Sharma, R. K., Yolcu, E. S., Elpek, K. G., & Shirwan, H. (2010). Tumor cells engineered to codisplay on their surface 4-1BBL and LIGHT costimulatory proteins as a novel vaccine approach for cancer immunotherapy. *Cancer Gene Therapy*, *17*(10), 730–41.

Shuford, W. W., Klussman, K., Tritchler, D. D., Loo, D. T., Chalupny, J., Siadak, A. W., … Mittler, R. S. (1997). 4-1BB costimulatory signals preferentially induce CD8+ T cell proliferation and lead to the amplification in vivo of cytotoxic T cell responses. *The Journal of Experimental Medicine*, *186*(1), 47–55.

Siegemund, M., Pollak, N., Seifert, O., Wahl, K., Hanak, K., Vogel, a, … Pfizenmaier, K. (2012). Superior antitumoral activity of dimerized targeted single-chain TRAIL fusion proteins under retention of tumor selectivity. *Cell Death and Disease*, *3*(4), e295.

Siegemund, M., Seifert, O., Zarani, M., Džinić, T., De Leo, V., Göttsch, D., … Kontermann, R. E. (2016). An optimized antibody-single-chain TRAIL fusion protein for cancer therapy. *mAbs*, *8*(5), 879–91.

Smyth, M. J., Ngiow, S. F., Ribas, A., & Teng, M. W. L. (2016). Combination cancer immunotherapies tailored to the tumour microenvironment. *Nature Reviews. Clinical Oncology*, *13*(3), 143–58.

So, T., & Croft, M. (2007). Cutting Edge: OX40 Inhibits TGF- - and Antigen-Driven Conversion of Naive CD4 T Cells into CD25+Foxp3+ T cells. *The Journal of Immunology*, *179*(3), 1427–1430.

Soroosh, P., Ine, S., Sugamura, K., & Ishii, N. (2007). Differential requirements for OX40 signals on generation of effector and central memory CD4+ T cells. *Journal of Immunology (Baltimore, Md. : 1950)*, *179*(8), 5014–5023.

Srivastava, A. K., Sharma, R. K., Yolcu, E. S., Ulker, V., MacLeod, K., Dinc, G., & Shirwan, H. (2012). Prime-Boost Vaccination with SA-4-1BBL Costimulatory Molecule and Survivin Eradicates Lung Carcinoma in CD8+ T and NK Cell Dependent Manner. *PLoS ONE*, *7*(11), 1–8.

Stadler, C. R., Bähr-Mahmud, H., Plum, L. M., Schmoldt, K., Kölsch, A. C., Türeci, Ö., & Sahin, U. (2016). Characterization of the first-in-class T-cell-engaging bispecific single-chain antibody for targeted immunotherapy of solid tumors expressing the oncofetal protein claudin 6. *Oncoimmunology*, *5*(3), e1091555.

Steinwand, M., Droste, P., Frenzel, A., Hust, M., Dübel, S., & Schirrmann, T. (2013). The influence of antibody fragment format on phage display based affinity maturation of IgG. *mAbs*, *6*(1), 204–18.

Suntharalingam, G., Perry, M. R., Ward, S., Brett, S. J., Castello-Cortes, A., Brunner, M. D., & Panoskaltsis, N. (2006). Cytokine storm in a phase 1 trial of the anti-CD28 monoclonal antibody TGN1412. *The New England Journal of Medicine*, *355*(10), 1018–28.

Suzuki, M., Kato-Nakano, M., Kawamoto, S., Furuya, A., Abe, Y., Misaka, H., … Ando, H. (2009). Therapeutic antitumor efficacy of monoclonal antibody against Claudin-4 for pancreatic and ovarian cancers. *Cancer Science*, *100*(9), 1623–1630.

Szlachcic, A., Zakrzewska, M., & Otlewski, J. (2011). Longer action means better drug: tuning up protein therapeutics. *Biotechnology Advances*, *29*(4), 436–41.

Todryk, S. M., Tutt, A. L., Green, M. H., Smallwood, J. A., Halanek, N., Dalgleish, A. G., & Glennie, M. J. (2001). CD40 ligation for immunotherapy of solid tumours. *Journal of Immunological Methods*, *248*(1-2), 139–47.

Tokés, A.-M., Kulka, J., Paku, S., Szik, A., Páska, C., Novák, P. K., … Schaff, Z. (2005). Claudin-1, -3 and -4 proteins and mRNA expression in benign and malignant breast lesions: a research study. *Breast Cancer Research : BCR*, *7*(2), R296–R305.

Trzpis, M., McLaughlin, P. M. J., de Leij, L. M. F. H., & Harmsen, M. C. (2007). Epithelial Cell Adhesion Molecule. *The American Journal of Pathology*, *171*(2), 386–395.

Tsukita, S., Furuse, M., & Itoh, M. (2001). Multifunctional strands in tight junctions. *Nature Reviews. Molecular Cell Biology*, *2*(4), 285–293.

Ueda, J., Semba, S., Chiba, H., Sawada, N., Seo, Y., Kasuga, M., & Yokozaki, H. (2007). Heterogeneous expression of claudin-4 in human colorectal cancer: Decreased claudin-4 expression at the invasive front correlates cancer invasion and metastasis. *Pathobiology*, *74*(1), 32–41.

Unverdorben, F., Hutt, M., Seifert, O., & Kontermann, R. E. (2015). A Fab-Selective Immunoglobulin-Binding Domain from Streptococcal Protein G with Improved Half-Life Extension Properties. *PloS One*, *10*(10), e0139838.

Ushiku, T., Shinozaki-Ushiku, A., Maeda, D., Morita, S., & Fukayama, M. (2012). Distinct expression pattern of claudin-6, a primitive phenotypic tight junction molecule, in germ cell tumours and visceral carcinomas. *Histopathology*, *61*(6), 1043–1056.

van Kooten, C., & Banchereau, J. (2000). CD40-CD40 ligand. *Journal of Leukocyte Biology*, *67*(1), 2–17.

van Lier, R. A., Borst, J., Vroom, T. M., Klein, H., Van Mourik, P., Zeijlemaker, W. P., & Melief, C. J. (1987). Tissue distribution and biochemical and functional properties of Tp55 (CD27), a novel T cell differentiation antigen. *Journal of Immunology (Baltimore, Md. : 1950)*, *139*(5), 1589–96.

Vonderheide, R. H., Dutcher, J. P., Anderson, J. E., Eckhardt, S. G., Stephans, K. F., Razvillas, B., … Gribben, J. G. (2001). Phase I study of recombinant human CD40 ligand in cancer patients. *Journal of Clinical Oncology : Official Journal of the American Society of Clinical Oncology*, *19*(13), 3280–7.

Vonderheide, R. H., & Glennie, M. J. (2013). Agonistic CD40 antibodies and cancer therapy. *Clinical Cancer Research*, *19*(5), 1035–1043.

Wajant, H. (2015). Principles of antibody-mediated TNF receptor activation. *Cell Death and Differentiation*, *22*(11), 1727–1741.

Wajant, H., Moosmayer, D., Wüest, T., Bartke, T., Gerlach, E., Schönherr, U., … Pfizenmaier, K. (2001). Differential activation of TRAIL-R1 and -2 by soluble and membrane TRAIL allows selective surface antigen-directed activation of TRAIL-R2 by a soluble TRAIL derivative. *Oncogene*, *20*(30), 4101–6.

Wajant, H. (2016). Therapeutic targeting of CD70 and CD27. *Expert Opinion on Therapeutic Targets*, *8222*(May), 1–15.

Wang, H., Davis, J. S., & Wu, X. (2014). Immunoglobulin Fc domain fusion to TRAIL significantly prolongs its plasma half-life and enhances its antitumor activity. *Molecular Cancer Therapeutics*, *13*(3), 643–50.

Watts, T. H. (2005). TNF/TNFR family members in costimulation of T cell responses. *Annual Review of Immunology*, *23*(1), 23–68.

Weigelin, B., Bolaños, E., Teijeira, A., Martinez-Forero, I., Labiano, S., Azpilikueta, A., … Melero, I. (2015). Focusing and sustaining the antitumor CTL effector killer response by agonist anti-CD137 mAb. *Proceedings of the National Academy of Sciences of the United States of America*, *112*(24), 7551–6.

Weinberg, A. D., Morris, N. P., Kovacsovics-Bankowski, M., Urba, W. J., & Curti, B. D. (2011). Science gone translational: The OX40 agonist story. *Immunological Reviews*, *244*(1), 218–231.

Wen, T., Bukczynski, J., & Watts, T. H. (2002). 4-1BB ligand-mediated costimulation of human T cells induces CD4 and CD8 T cell expansion, cytokine production, and the development of cytolytic effector function. *Journal of Immunology (Baltimore, Md. : 1950)*, *168*(10), 4897–906.

Went, P. T., Lugli, A., Meier, S., Bundi, M., Mirlacher, M., Sauter, G., & Dirnhofer, S. (2004). Frequent EpCam protein expression in human carcinomas. *Human Pathology*, *35*(1), 122–8.

Wilgenhof, S., Corthals, J., Van Nuffel, A. M. T., Benteyn, D., Heirman, C., Bonehill, A., … Neyns, B. (2015). Long-term clinical outcome of melanoma patients treated with messenger RNA-electroporated dendritic cell therapy following complete resection of metastases. *Cancer Immunology, Immunotherapy : CII*, *64*(3), 381–8.

Won, E.-Y., Cha, K., Byun, J.-S., Kim, D.-U., Shin, S., Ahn, B., … Cho, H.-S. (2010). The structure of the trimer of human 4-1BB ligand is unique among members of the tumor necrosis factor superfamily. *The Journal of Biological Chemistry*, *285*(12), 9202–10.

Wüest, T., Gerlach, E., Banerjee, D., Gerspach, J., Moosmayer, D., & Pfizenmaier, K. (2002). TNF-Selectokine: a novel prodrug generated for tumor targeting and site-specific activation of tumor necrosis factor. *Oncogene*, *21*(27), 4257–65.

Wurz, G. T., Kao, C.-J., & DeGregorio, M. W. (2015). Novel cancer antigens for personalized immunotherapies: latest evidence and clinical potential. *Therapeutic Advances in Medical Oncology*, *8*(1), 4–31.

Wyzgol, A., Müller, N., Fick, A., Munkel, S., Grigoleit, G. U., Pfizenmaier, K., & Wajant, H. (2009). Trimer stabilization, oligomerization, and antibody-mediated cell surface immobilization improve the activity of soluble trimers of CD27L, CD40L, 41BBL, and glucocorticoid-induced TNF receptor ligand. *Journal of Immunology (Baltimore, Md. : 1950)*, *183*(3), 1851–1861.

Xu, D., Gu, P., Pan, P.-Y., Li, Q., Sato, A. I., & Chen, S.-H. (2004). NK and CD8+ T cell-mediated eradication of poorly immunogenic B16-F10 melanoma by the combined action of IL-12 gene therapy and 4-1BB costimulation. *International Journal of Cancer*, *109*(4), 499–506.

Yang, Z.-Z., Grote, D. M., Xiu, B., Ziesmer, S. C., Price-Troska, T. L., Hodge, L. S., … Ansell, S. M. (2014). TGF-β upregulates CD70 expression and induces exhaustion of effector memory T cells in B-cell non-Hodgkin's lymphoma. *Leukemia*, *28*(9), 1872–84.

Yao, Q., Cao, S., Li, C., Mengesha, A., Low, P., Kong, B., … Wei, M. (2010). Turn a diarrhoea toxin into a receptor-mediated therapy for a plethora of CLDN-4-overexpressing cancers. *Biochemical and Biophysical Research Communications*, *398*(3), 413–419.

Yuan, X., Lin, X., Manorek, G., Kanatani, I., Cheung, L. H., Rosenblum, M. G., & Howell, S. B. (2009). Recombinant CPE fused to tumor necrosis factor targets human ovarian cancer cells expressing the claudin-3 and claudin-4 receptors. *Molecular Cancer Therapeutics*, *8*, 1906–1915.

Zavala-Zendejas, V. E., Torres-Martinez, A. C., Salas-Morales, B., Fortoul, T. I., Montaño, L. F., & Rendon-Huerta, E. P. (2011). Claudin-6, 7, or 9 overexpression in the human gastric adenocarcinoma cell line AGS increases its invasiveness, migration, and proliferation rate. *Cancer Investigation*, *29*(1), 1–11.

Zhou, Y., He, J., Gou, L., Mu, B., Liao, W., Ma, C., … Yang, J. (2012). Expression of CD40 and growth-inhibitory activity of CD40 agonist in ovarian carcinoma cells. *Cancer Immunology, Immunotherapy : CII*, *61*(10), 1735–43.

6 Sequences

6.1 Single-chain fragment variable

pAB1_scFv22A

```
>pelB leader                                                                  AgeI  >VH 22A
|                                                                             |     |
ATG AAA TAC CTA TTG CCT ACG GCA GCC GCT GGA TTG TTA TTA CTC GCG GCC CAG CCG GCC ATG GCC ACC GGT CAA GCC TAC CTG CAG CAG < 90
M   K   Y   L   L   P   T   A   A   A   G   L   L   L   L   A   A   Q   P   A   M   A   T   G   Q   A   Y   L   Q   Q

TCT GGC GCT GAA CTC GTG CGG CCT GGC GCC TCT GTG AAG ATG AGC TGT AAA GCC AGC GGC TAC ACC TTC ACC AGC TAC ATC ATG CAC TGG <180
S   G   A   E   L   V   R   P   G   A   S   V   K   M   S   C   K   A   S   G   Y   T   F   T   S   Y   I   M   H   W

GTC AAG CAG ACC CCC AGA CAG GGC CTG GAA TGG ATC GGC GCC ATC TAC CCC GGC AAC GGC GAC ACC TCC TAC AAC CAG AAG TTC AAG GGC <270
V   K   Q   T   P   R   Q   G   L   E   W   I   G   A   I   Y   P   G   N   G   D   T   S   Y   N   Q   K   F   K   G

AAG GCC ACC CTG ACC GTG GAC AAG AGC AGC AGC ACC GCC TAC ATG CAG CTG AGC AGC CTG ACC AGC GAG GAC AGC GCC GTG TAC TTC TGC <360
K   A   T   L   T   V   D   K   S   S   S   T   A   Y   M   Q   L   S   S   L   T   S   E   D   S   A   V   Y   F   C

                                                                                  XhoI      >Linker
                                                                                  |         |
GCC AGA AGC CCC AGA AGC AGC AGC GGC CTG TAC GCT ATG GAC TAC TGG GGC CAG GGC ACC AGC GTG ACA GTC TCG AGT GGC GGC GGA GGA <450
A   R   S   P   R   S   S   S   G   L   Y   A   M   D   Y   W   G   Q   G   T   S   V   T   V   S   S   G   G   G   G

                                        >VL 22A
                                        |
TCT GGC GGA GGC GGA AGT GGG GGA GGC GGA TCT GAT GTC GTG ATG ACC CAG CCC CCT CTG AGC CTG CCT GTG TCT CTG GGA GAT CAG GCC <540
S   G   G   G   G   S   G   G   G   G   S   D   V   V   M   T   Q   P   P   L   S   L   P   V   S   L   G   D   Q   A

AGC ATC AGC TGC CGG TCT AGC CAG AGC CTG GTG CAC TTC GAC GGC AAC ACA TAC CTG CAC TGG TAT CTG CAG AAG CCC GGC CAG AGC CCC <630
S   I   S   C   R   S   S   Q   S   L   V   H   F   D   G   N   T   Y   L   H   W   Y   L   Q   K   P   G   Q   S   P

AAG CTG CTG ATC TAC AAG GTG TCC AAC AGA TTC AGC GGC GTG CCC GAC AGA TTC TCC GGC AGC GGC TCT GGC ACC GAC TTC ACC CTG AAG <720
K   L   L   I   Y   K   V   S   N   R   F   S   G   V   P   D   R   F   S   G   S   G   S   G   T   D   F   T   L   K

ATC AGC CGG GTG GAA GCC GAG GAC CTG GGC GTG TAC TTT TGT TTT CAA AGC ACC CAC GTG CCC TAC ACC TTT GGA GGC GGC ACC AGA CTG <810
I   S   R   V   E   A   E   D   L   G   V   Y   F   C   F   Q   S   T   H   V   P   Y   T   F   G   G   G   T   R   L

          NotI                                                          >His-tag                          EcoRI
          |                                                             |                                 |
GAA ATC AAA GCG GCC GCA GAA CAA AAA CTC ATC TCA GAA GAG GAT CTG AAT GGG GCC GCA CAT CAC CAT CAT CAC CAT TAA TAA GAA TTC <900
E   I   K   A   A   A   E   Q   K   L   I   S   E   E   D   L   N   G   A   A   H   H   H   H   H   H   *   *
```

pAB1_scFv33B

```
>pelB leader                                                                  AgeI    >VH 33B
|                                                                             |       |
ATG AAA TAC CTA TTG CCT ACG GCA GCC GCT GGA TTG TTA TTA CTC GCG GCC CAG CCG GCC ATG GCC ACC GGT CAA GCC TAC CTG CAG CAG < 90
M   K   Y   L   L   P   T   A   A   A   G   L   L   L   L   A   A   Q   P   A   M   A   T   G   Q   A   Y   L   Q   Q

TCT GGC GCT GAA CTC GTG CGG CCT GGC GCC TCT GTG AAG ATG AGC TGT AAA GCC AGC GGC TAC ACC TTC ACC AGC TAC ATC ATG CAC TGG <180
S   G   A   E   L   V   R   P   G   A   S   V   K   M   S   C   K   A   S   G   Y   T   F   T   S   Y   I   M   H   W

GTC AAG CAG ACC CCC AGA CAG GGC CTG GAA TGG ATC GGC GCC ATC TAC CCC GGC AAC GGC GAC ACC TCC TAC AAC CAG AAG TTC AAG GGC <270
V   K   Q   T   P   R   Q   G   L   E   W   I   G   A   I   Y   P   G   N   G   D   T   S   Y   N   Q   K   F   K   G

AAG GCC ACC CTG ACC GTG GAC AAG AGC AGC AGC ACC GCC TAC ATG CAG CTG AGC AGC CTG ACC AGC GAG GAC AGC GCC GTG TAC TTC TGC <360
K   A   T   L   T   V   D   K   S   S   S   T   A   Y   M   Q   L   S   S   L   T   S   E   D   S   A   V   Y   F   C

                                                                                  XhoI      >Linker
                                                                                  |         |
GCC AGA AGC CCC AGA AGC AGC AGC GGC CTG TAC GCT ATG GAC TAC TGG GGC CAG GGC ACC AGC GTG ACA GTC TCG AGT GGC GGC GGA GGA <450
A   R   S   P   R   S   S   S   G   L   Y   A   M   D   Y   W   G   Q   G   T   S   V   T   V   S   S   G   G   G   G

                                        >VL 33B
                                        |
TCT GGC GGA GGC GGA AGT GGG GGA GGC GGC AGC GAT ATT CAG ATG ACC CAG AGC AGC TCC AGC TTC AGC GTG TCC CTG GGC GAC AGA GTG <540
S   G   G   G   G   S   G   G   G   G   S   D   I   Q   M   T   Q   S   S   S   S   F   S   V   S   L   G   D   R   V

ACC ATC ACA TGC AAG GCC TCC GAG GAC ATC TAC AAC CGG CTG GCC TGG TAT CAG CAG AAG CCT GGC AAC GCC CCC AGG CTG CTG ATT AGC <630
T   I   T   C   K   A   S   E   D   I   Y   N   R   L   A   W   Y   Q   Q   K   P   G   N   A   P   R   L   L   I   S

GGA GCC ACC TCT CTG GAA ACC GGC GTG CCC AGC AGA TTT TCC GGC AGC GGC TCT GGC AAG GAC TGC ACC CTG AGC ATC ACC AGC CTG CAG <720
G   A   T   S   L   E   T   G   V   P   S   R   F   S   G   S   G   S   G   K   D   C   T   L   S   I   T   S   L   Q

                                                                                                      NotI
                                                                                                      |
ACC GAG GAC GTG GCC ACC TAC TAC TGC CAG CAG TAC TGG TCC ACC CCC CTG ACC TTT GGA GCC GGC ACC AAG CTG GAA CTG AAA GCG GCC <810
T   E   D   V   A   T   Y   Y   C   Q   Q   Y   W   S   T   P   L   T   F   G   A   G   T   K   L   E   L   K   A   A
```

```
                                                  >His-Tag                    EcoRI
                                                  |                           |
GCA GAA CAA AAA CTC ATC TCA GAA GAG GAT CTG AAT GGG GCC GCA CAT CAC CAT CAT CAC CAT TAA TAA GAA TTC                  <885
A  E  Q  K  L  I  S  E  E  D  L  N  G  A  A  H  H  H  H  H  H  *  *
```

pAB1_scFv4H6E9

```
>pelB leader                                                                  AgeI    >VH 4H6E9
|                                                                             |       |
ATG AAA TAC CTA TTG CCT ACG GCA GCC GCT GGA TTG TTA TTA CTC GCG GCC CAG CCG GCC ATG GCC ACC GGT GAA GTG CAG CTG CAG CAG < 90
M  K  Y  L  L  P  T  A  A  A  G  L  L  L  L  A  A  Q  P  A  M  A  T  G  E  V  Q  L  Q  Q

TCT GGC CCC GAG CTC GTG AAA CCT GGC GCC TCC GTG AAG ATC AGC TGC AAG ACC AGC GGC TAC ACC TTC ACC GAG TAC ACC ATC CAC TGG <180
S  G  P  E  L  V  K  P  G  A  S  V  K  I  S  C  K  T  S  G  Y  T  F  T  E  Y  T  I  H  W

GTC AAG CAG AGC CAC GGC AAG AGC CTG GAA TGG ATC GGC GGC ATC AAC CCC AAG AAC GGC GGC ACC ACC TAC AAG CAG AAG TTC AAG GGC <270
V  K  Q  S  H  G  K  S  L  E  W  I  G  G  I  N  P  K  N  G  G  T  T  Y  K  Q  K  F  K  G

AAG GCC ACC CTG ACC GTG GAC AAG AGC AGC AGC ACC GCC TAC ATG GAA CTG CGG AGC CTG ACC AGC GAG GAC AGC GCC GTG TAC TAC TGC <360
K  A  T  L  T  V  D  K  S  S  S  T  A  Y  M  E  L  R  S  L  T  S  E  D  S  A  V  Y  Y  C

                                                                  XhoI    >Linker
                                                                  |       |
GCC AGA GAT GGC CGG TCC TAC TAC TAC GCT ATG GAC TAC TGG GGC CAG GGC ACC AGC GTG ACA GTC TCG AGT GGC GGC GGA GGA TCT GGC <450
A  R  D  G  R  S  Y  Y  Y  A  M  D  Y  W  G  Q  G  T  S  V  T  V  S  S  G  G  G  G  S  G

                           >VL 4H6E9
                           |
GGA GGC GGA AGT GGG GGA GGC GGC AGC GAT ATT CAG ATG ACC CAG AGC AGC TCC AGC TTC AGC GTG TCC CTG GGC GAC AGA GTG ACC ATC <540
G  G  G  S  G  G  G  G  S  D  I  Q  M  T  Q  S  S  S  S  F  S  V  S  L  G  D  R  V  T  I

         StuI
         |
ACA TGC AAG GCC TCC GAG GAC ATC TAC AAC CGG CTG GCC TGG TAT CAG CAG AAG CCC GGC AAC GCC CCT CGG CTG CTG ATT TCT GGC GCC <630
T  C  K  A  S  E  D  I  Y  N  R  L  A  W  Y  Q  Q  K  P  G  N  A  P  R  L  L  I  S  G  A

ACC TCT CTG GAA ACC GGC GTG CCC AGC AGA TTT TCC GGC AGC GGC TCC GGC AAG GAC TAC ACC CTG AGC ATC ACC AGC CTG CAG ACC GAG <720
T  S  L  E  T  G  V  P  S  R  F  S  G  S  G  S  G  K  D  Y  T  L  S  I  T  S  L  Q  T  E

                                                                        NotI
                                                                        |
GAC GTG GCC ACC TAC TAC TGC CAG CAG TAC TGG TCC ACC CCC CGG ACA TTT GGC GGA GGG ACC AAG CTG GAA ATC AAA GCG GCC GCA GAA <810
D  V  A  T  Y  Y  C  Q  Q  Y  W  S  T  P  R  T  F  G  G  G  T  K  L  E  I  K  A  A  A  E

                                          >His-tag                    EcoRI
                                          |                           |
CAA AAA CTC ATC TCA GAA GAG GAT CTG AAT GGG GCC GCA CAT CAC CAT CAT CAC CAT TAA TAA GAA TTC                        <879
Q  K  L  I  S  E  E  D  L  N  G  A  A  H  H  H  H  H  H  *  *
```

pAB1_scFvhu4H-2a & pAB1_scFvhu4H-2b

The amino acid substitutions shown in red lead to pAB1_scFvhu4H-2b.

```
>pelB leader                                                                  AgeI    >VH hu4H-2a
|                                                                             |       |
ATG AAA TAC CTA TTG CCT ACG GCA GCC GCT GGA TTG TTA TTA CTC GCG GCC CAG CCG GCC ATG GCC ACC GGT GAA GTG CAG CTG GTG GAA < 90
M  K  Y  L  L  P  T  A  A  A  G  L  L  L  L  A  A  Q  P  A  M  A  T  G  E  V  Q  L  V  E

TCT GGC GGC GGA CTC GTG AAG CCT GGC GGC TCT CTG AGA CTG AGC TGT GCC GCC AGC GGC TTC ACC TTC AGC GAG TAC ACC ATC CAC TGG <180
S  G  G  G  L  V  K  P  G  G  S  L  R  L  S  C  A  A  S  G  F  T  F  S  E  Y  T  I  H  W

GTG CGC CAG GCC CCT GGC AAA GGA CTG GAA TGG GTG TCC GGC ATC AAC CCC AAG AAC GGC GGC ACC ACC TAC AAG CAG AAG TTC AAG GGC <270
V  R  Q  A  P  G  K  G  L  E  W  V  S  G  I  N  P  K  N  G  G  T  T  Y  K  Q  K  F  K  G

                  CGG
                  R
CGG TTC ACC ATC AGC GTG GAC AAC GCC AAG AAC AGC CTG TAC CTG CAG ATG AAC TCC CTG CGG GCC GAG GAC ACC GCC GTG TAC TAC TGT <360
R  F  T  I  S  V  D  N  A  K  N  S  L  Y  L  Q  M  N  S  L  R  A  E  D  T  A  V  Y  Y  C

                                                                  XhoI    >Linker
                                                                  |       |
GCC AGA GAT GGC CGG TCC TAC TAC TAC GCT ATG GAC TAC TGG GGC CAG GGC ACC ACC GTG ACA GTC TCG AGT GGC GGA GGC GGA TCA GGC <450
A  R  D  G  R  S  Y  Y  Y  A  M  D  Y  W  G  Q  G  T  T  V  T  V  S  S  G  G  G  G  S  G

                           >VL hu4H-2a
                           |
GGC GGA GGA TCT GGG GGA GGG GGC AGC GAT ATT CAG ATG ACC CAG AGC CCC AGC AGC CTG AGC GCC TCT GTG GGC GAC AGA GTG ACC ATC <540
G  G  G  S  G  G  G  G  S  D  I  Q  M  T  Q  S  P  S  S  L  S  A  S  V  G  D  R  V  T  I

                                                                        TAC
                                                                        Y
ACA TGC AAG GCC AGC GAG GAC ATC TAC AAC CGG CTG GCC TGG TAT CAG CAG AAG CCC GGC AAG GCC CCC AAG CTG CTG ATT AGC GGA GCC <630
T  C  K  A  S  E  D  I  Y  N  R  L  A  W  Y  Q  Q  K  P  G  K  A  P  K  L  L  I  S  G  A

ACC AGC CTG GAA ACC GGC GTG CCA AGC AGA TTT TCC GGC AGC GGC TCC GGC ACC GAC TTC ACC CTG ACA ATC AGC TCC CTG CAG CCA GAG <720
T  S  L  E  T  G  V  P  S  R  F  S  G  S  G  S  G  T  D  F  T  L  T  I  S  S  L  Q  P  E
```

```
                                                                                                                NotI
                                                                                                                |
GAC TTC GCC ACC TAC TAC TGC CAG CAG TAC TGG TCC ACC CCC CGG ACA TTT GGC CAG GGG ACC AAG CTG GAA ATC AAA GCG GCC GCA GAA <810
D   F   A   T   Y   Y   C   Q   Q   Y   W   S   T   P   R   T   F   G   Q   G   T   K   L   E   I   K   A   A   A   E

                                                  >His-tag                      EcoRI
                                                  |                             |
CAA AAA CTC ATC TCA GAA GAG GAT CTG AAT GGG GCC GCA CAT CAC CAT CAT CAC CAT TAA TAA GAA TTC                          <879
Q   K   L   I   S   E   E   D   L   N   G   A   A   H   H   H   H   H   H   *   *
```

pAB1_scFvhu4H-S1b & pAB1_scFvhu4H-S1a

The amino acid substitutions shown in red lead to pAB1_scFvhu4H-S1a.
pAB1_scFvhu4H-S1b is the basis for the following humanized scFvs (VL exchange via XhoI/NotI).

```
>pelB leader                                                                                  AgeI    >VH hu4H-S1b
|                                                                                             |       |
ATG AAA TAC CTA TTG CCT ACG GCA GCC GCT GGA TTG TTA TTA CTC GCG GCC CAG CCG GCC ATG GCC ACC GGT CAA GTG CAG CTG GTG CAG < 90
M   K   Y   L   L   P   T   A   A   A   G   L   L   L   L   A   A   Q   P   A   M   A   T   G   Q   V   Q   L   V   Q

TCT GGC GCC GAA GTG AAG AAA CCA GGC GCC AGC GTG AAG GTG TCC TGC AAG GCC AGC GGC TAC ACC TTT ACC GAG TAC ACC ATC CAC TGG <180
S   G   A   E   V   K   K   P   G   A   S   V   K   V   S   C   K   A   S   G   Y   T   F   T   E   Y   T   I   H   W

GTG CGC CAG GCC CCT GGC CAG AGA CTG GAA TGG ATG GGC GGC ATC AAC CCC AAG AAC GGC GGC ACC ACC TAC AAG CAG AAA TTC AAG GGC <270
V   R   Q   A   P   G   Q   R   L   E   W   M   G   G   I   N   P   K   N   G   G   T   T   Y   K   Q   K   F   K   G

                    AGA
                    R
AGA GTG ACC ATC ACC GTG GAC ACC AGC GCC AGC ACC GCC TAC ATG GAA CTG AGC AGC CTG CGG AGC GAG GAC ACC GCC GTG TAC TAC TGT <360
R   V   T   I   T   V   D   T   S   A   S   T   A   Y   M   E   L   S   S   L   R   S   E   D   T   A   V   Y   Y   C

                                                                                  XhoI      >Linker
                                                                                  |         |
GCC AGG GAC GGC CGG TCC TAC TAC TAC GCT ATG GAC TAC TGG GGC CAG GGC ACC ACC GTG ACA GTC TCG AGT GGC GGC GGA GGA TCT GGC <450
A   R   D   G   R   S   Y   Y   Y   A   M   D   Y   W   G   Q   G   T   T   V   T   V   S   S   G   G   G   G   S   G

                                    >VL hu4H-S1b
                                    |
GGA GGC GGA AGT GGG GGA GGC GGC AGC GAT ATT CAG ATG ACC CAG AGC CCC AGC AGC CTG AGC GCC TCT GTG GGC GAC AGA GTG ACA ATT <540
G   G   G   S   G   G   G   G   S   D   I   Q   M   T   Q   S   P   S   S   L   S   A   S   V   G   D   R   V   T   I

                                                                                                        TAC
                                                                                                        Y
ACA TGC AAG GCC TCC GAG GAC ATC TAC AAC CGG CTG GCC TGG TAT CAG CAG AAG CCC GGC AAG GCC CCC AAG CTG CTG ATT AGC GGA GCC <630
T   C   K   A   S   E   D   I   Y   N   R   L   A   W   Y   Q   Q   K   P   G   K   A   P   K   L   L   I   S   G   A

ACC AGC CTG GAA ACC GGC GTG CCA AGC AGA TTT TCC GGC AGC GGC TCC GGC ACC GAC TTC ACC TTC ACC ATC AGC TCC CTG CAG CCC GAG <720
T   S   L   E   T   G   V   P   S   R   F   S   G   S   G   S   G   T   D   F   T   F   T   I   S   S   L   Q   P   E

                                                                                                                NotI
                                                                                                                |
GAT ATT GCC ACC TAC TAC TGC CAG CAG TAC TGG TCC ACC CCC CGG ACA TTT GGC GGA GGG ACC AAG GTG GAA ATC AAA GCG GCC GCA GAA <810
D   I   A   T   Y   Y   C   Q   Q   Y   W   S   T   P   R   T   F   G   G   G   T   K   V   E   I   K   A   A   A   E

                                                  >His-tag                      EcoRI
                                                  |                             |
CAA AAA CTC ATC TCA GAA GAG GAT CTG AAT GGG GCC GCA CAT CAC CAT CAT CAC CAT TAA TAA GAA TTC                          <879
Q   K   L   I   S   E   E   D   L   N   G   A   A   H   H   H   H   H   H   *   *
```

VLmohu hu4H-S1b

```
                                                                                  XhoI      >Linker
                                                                                  |         |
                                                                            ... GTC TCG AGT GGC GGC GGA GGA TCT GGC <450
                                                                            ... V   S   S   G   G   G   G   S   G

                                    >VL4H6E9 (FR1-CDRL1-FR2-CDRL2)
                                    |
GGA GGC GGA AGT GGG GGA GGC GGC AGC GAT ATT CAG ATG ACC CAG AGC AGC TCC AGC TTC AGC GTG TCC CTG GGC GAC AGA GTG ACC ATC <540
G   G   G   S   G   G   G   G   S   D   I   Q   M   T   Q   S   S   S   S   F   S   V   S   L   G   D   R   V   T   I

         StuI
         |
ACA TGC AAG GCC TCC GAG GAC ATC TAC AAC CGG CTG GCC TGG TAT CAG CAG AAG CCC GGC AAC GCC CCT CGG CTG CTG ATT TCT GGC GCC <630
T   C   K   A   S   E   D   I   Y   N   R   L   A   W   Y   Q   Q   K   P   G   N   A   P   R   L   L   I   S   G   A

                    >VLhu4H-S1b (FR3-CDRL3-FR4)
                    | KpnI
                    | |
ACC TCT CTG GAA ACC GGG GTA CCC AGC AGA TTT TCC GGC AGC GGC TCC GGC ACC GAC TTC ACC TTC ACC ATC AGC TCC CTG CAG CCC GAG <720
T   S   L   E   T   G   V   P   S   R   F   S   G   S   G   S   G   T   D   F   T   F   T   I   S   S   L   Q   P   E
```

```
                                                                                                                    NotI
                                                                                                                    |
GAT ATT GCC ACC TAC TAC TGC CAG CAG TAC TGG TCC ACC CCC CGG ACA TTT GGC GGA GGG ACC AAG GTG GAA ATC AAA GCG GCC GCA ... <807
D   I   A   T   Y   Y   C   Q   Q   Y   W   S   T   P   R   T   F   G   G   G   T   K   V   E   I   K   A   A   A   ...
```

VLhumo hu4H-S1b

```
                                                                                                  XhoI      >Linker
                                                                                                  |         |
                                                                                          ... GTC TCG AGT GGC GGC GGA GGA TCT GGC <450
                                                                                          ... V   S   S   G   G   G   G   S   G

                                    >VLhu4H-S1b (FR1-CDRL1-FR2-CDRL2)
                                    |
GGA GGC GGA AGT GGG GGA GGC GGC AGC GAT ATT CAG ATG ACC CAG AGC CCC AGC AGC CTG AGC GCC TCT GTG GGC GAC AGA GTG ACA ATT <540
G   G   G   S   G   G   G   G   S   D   I   Q   M   T   Q   S   P   S   S   L   S   A   S   V   G   D   R   V   T   I

         StuI
         |
ACA TGC AAG GCC TCC GAG GAC ATC TAC AAC CGG CTG GCC TGG TAT CAG CAG AAG CCC GGC AAG GCC CCC AAG CTG CTG ATT AGC GGA GCC <630
T   C   K   A   S   E   D   I   Y   N   R   L   A   W   Y   Q   Q   K   P   G   K   A   P   K   L   L   I   S   G   A

                  >VL4H6E9 (FR3-CDRL3-FR4)
                  | KpnI
                  | |
ACC AGC CTG GAA ACC GGG GTA CCC AGC AGA TTT TCC GGC AGC GGC TCC GGC AAG GAC TAC ACC CTG AGC ATC ACC AGC CTG CAG ACC GAG <720
T   S   L   E   T   G   V   P   S   R   F   S   G   S   G   S   G   K   D   Y   T   L   S   I   T   S   L   Q   T   E

                                                                                                                    NotI
                                                                                                                    |
GAC GTG GCC ACC TAC TAC TGC CAG CAG TAC TGG TCC ACC CCC CGG ACA TTT GGC GGA GGG ACC AAG CTG GAA ATC AAA GCG GCC GCA ... <807
D   V   A   T   Y   Y   C   Q   Q   Y   W   S   T   P   R   T   F   G   G   G   T   K   L   E   I   K   A   A   A   ...
```

VLx hu4H-S1b

```
                                                                                                  XhoI      >Linker
                                                                                                  |         |
                                                                                          ... GTC TCG AGT GGC GGC GGA GGA TCT GGC <450
                                                                                          ... V   S   S   G   G   G   G   S   G

                                    > VLx hu4H-S1b
                                    |
GGA GGC GGA AGT GGG GGA GGC GGC AGC GAT ATT CAG ATG ACC CAG AGC AGC AGC AGC TTC AGC GTG TCC CTG GGC GAC AGA GTG ACC ATC <540
G   G   G   S   G   G   G   G   S   D   I   Q   M   T   Q   S   S   S   S   F   S   V   S   L   G   D   R   V   T   I

         StuI
         |
ACA TGC AAG GCC TCC GAG GAC ATC TAC AAC CGG CTG GCC TGG TAT CAG CAG AAG CCC GGC AAG GCC CCC AAG CTG CTG ATT AGC GGA GCC <630
T   C   K   A   S   E   D   I   Y   N   R   L   A   W   Y   Q   Q   K   P   G   K   A   P   K   L   L   I   S   G   A

ACC AGC CTG GAA ACC GGC GTG CCA AGC AGA TTT TCC GGC AGC GGC TCC GGC ACC GAC TTC ACC TTC ACC ATC AGC TCC CTG CAG CCC GAG <720
T   S   L   E   T   G   V   P   S   R   F   S   G   S   G   S   G   T   D   F   T   F   T   I   S   S   L   Q   P   E

                                                                                                                    NotI
                                                                                                                    |
GAT ATT GCC ACC TAC TAC TGC CAG CAG TAC TGG TCC ACC CCC CGG ACA TTT GGC GGA GGG ACC AAG GTG GAA ATC AAA GCG GCC GCA ... <807
D   I   A   T   Y   Y   C   Q   Q   Y   W   S   T   P   R   T   F   G   G   G   T   K   V   E   I   K   A   A   A    ...
```

VLy hu4H-S1b

```
                                                                                                  XhoI      >Linker
                                                                                                  |         |
                                                                                          ... GTC TCG AGT GGC GGC GGA GGA TCT GGC <450
                                                                                          ... V   S   S   G   G   G   G   S   G

                                    > VLy hu4H-S1b
                                    |
GGA GGC GGA AGT GGG GGA GGC GGC AGC GAT ATT CAG ATG ACC CAG AGC CCC AGC AGC CTG AGC GCC TCT GTG GGC GAC AGA GTG ACA ATT <540
G   G   G   S   G   G   G   G   S   D   I   Q   M   T   Q   S   P   S   S   L   S   A   S   V   G   D   R   V   T   I

         StuI
         |
ACA TGC AAG GCC TCC GAG GAC ATC TAC AAC CGG CTG GCC TGG TAT CAG CAG AAG CCC GGC AAG GCC CCC AAG CTG CTG ATT AGC GGA GCC <630
T   C   K   A   S   E   D   I   Y   N   R   L   A   W   Y   Q   Q   K   P   G   K   A   P   K   L   L   I   S   G   A

ACC AGC CTG GAA ACC GGG GTA CCC AGC AGA TTT TCC GGC AGC GGC TCC GGC AAG GAC TAC ACC CTG ACC ATC AGC AGC CTG CAG ACC GAG <720
T   S   L   E   T   G   V   P   S   R   F   S   G   S   G   S   G   K   D   Y   T   L   T   I   S   S   L   Q   T   E

                                                                                                                    NotI
                                                                                                                    |
GAT ATT GCC ACC TAC TAC TGC CAG CAG TAC TGG TCC ACC CCC CGG ACA TTT GGC GGA GGG ACC AAG CTG GAA ATC AAA GCG GCC GCA ... <807
D   I   A   T   Y   Y   C   Q   Q   Y   W   S   T   P   R   T   F   G   G   G   T   K   L   E   I   K   A   A   A   ...
```

VLxy hu4H-S1b

```
                                                                                                XhoI      >Linker
                                                                                                 |         |
                                                                                          ... GTC TCG AGT GGC GGC GGA GGA TCT GGC <450
                                                                                          ... V   S   S   G   G   G   G   S   G
> VLxy hu4H-S1b
                                        |
GGA GGC GGA AGT GGG GGA GGC GGC AGC GAT ATT CAG ATG ACC CAG AGC AGC AGC AGC TTC AGC GTG TCC CTG GGC GAC AGA GTG ACC ATC <540
G   G   G   S   G   G   G   G   S   D   I   Q   M   T   Q   S   S   S   S   F   S   V   S   L   G   D   R   V   T   I

          StuI
           |
ACA TGC AAG GCC TCC GAG GAC ATC TAC AAC CGG CTG GCC TGG TAT CAG CAG AAG CCC GGC AAG GCC CCC AAG CTG CTG ATT AGC GGA GCC <630
T   C   K   A   S   E   D   I   Y   N   R   L   A   W   Y   Q   Q   K   P   G   K   A   P   K   L   L   I   S   G   A

ACC AGC CTG GAA ACC GGG GTA CCC AGC AGA TTT TCC GGC AGC GGC TCC GGC AAG GAC TAC ACC CTG ACC ATC AGC AGC CTG CAG ACC GAG <720
T   S   L   E   T   G   V   P   S   R   F   S   G   S   G   S   G   K   D   Y   T   L   T   I   S   S   L   Q   T   E

                                                                                                                NotI
                                                                                                                 |
GAT ATT GCC ACC TAC TAC TGC CAG CAG TAC TGG TCC ACC CCC CGG ACA TTT GGC GGA GGG ACC AAG CTG GAA ATC AAA GCG GCC GCA ... <807
D   I   A   T   Y   Y   C   Q   Q   Y   W   S   T   P   R   T   F   G   G   G   T   K   L   E   I   K   A   A   A   ...
```

pAB1_scFv323A3

pAB1_scFv323A3 is the basis for pAB1_scFv323A3hu1, hu2, hu3, hu4, hu5 & hu6.

```
>pelB leader                                                                                    AgeI    >VH323A3
|                                                                                               |       |
ATG AAA TAC CTA TTG CCT ACG GCA GCC GCT GGA TTG TTA TTA CTC GCG GCC CAG CCG GCC ATG GCC ACC GGT CAA ATT CAG CTG GTG CAG < 90
M   K   Y   L   L   P   T   A   A   A   G   L   L   L   L   A   A   Q   P   A   M   A   T   G   Q   I   Q   L   V   Q

AGC GGC CCT GAG CTG AAG AAA CCC GGC GAG ACA GTG AAG ATC AGC TGC AAG GCC AGC GGC TAC ACC TTC ACC AAC TAC GGC ATG AAC TGG <180
S   G   P   E   L   K   K   P   G   E   T   V   K   I   S   C   K   A   S   G   Y   T   F   T   N   Y   G   M   N   W

GTG CGC CAG GCC TCT GGC GAG GGC CTG AAA TGG ATG GGC TGG ATC AAC ACC TAC ACC GGC GAG CCC ACC TAC GGC GAG GAC TTC AAG GGC <270
V   R   Q   A   S   G   E   G   L   K   W   M   G   W   I   N   T   Y   T   G   E   P   T   Y   G   E   D   F   K   G

AGA TTC GCC TTC AGC CTG GAA ACC AGC GCC AGC ACC GCC TAC CTG CAG ATC AAC AAC CTG AAG AAC GAG GAC ACC GCC ACC TAC TTT TGC <360
R   F   A   F   S   L   E   T   S   A   S   T   A   Y   L   Q   I   N   N   L   K   N   E   D   T   A   T   Y   F   C

                                                                XhoI      >Linker
                                                                 |         |
GCC AGA TTC GGC AAC TAC GTG GAC TAC TGG GGC CAG GGC ACC ACC CTG ACA GTC TCG AGT GGC GGG GGA GGA TCT GGG GGA GGG GGA AGC <450
A   R   F   G   N   Y   V   D   Y   W   G   Q   G   T   T   L   T   V   S   S   G   G   G   G   S   G   G   G   G   S

                  >VL323A3
                   |
GGA GGC GGG GGA TCT GAT ATT GTG ATG ACC CAG GCC GCC TTC TCC AAC CCC GTG ACA CTG GGC ACA AGC GCC TCC ATC AGC TGC CGG TCC <540
G   G   G   G   S   D   I   V   M   T   Q   A   A   F   S   N   P   V   T   L   G   T   S   A   S   I   S   C   R   S

AGC AAG AAC CTG CTG CAC AGC AAC GGC ATC ACC TAC CTG TAC TGG TAT CTG CAG AAG CCC GGC CAG AGC CCC CAT CTG CTG ATC TAC CAG <630
S   K   N   L   L   H   S   N   G   I   T   Y   L   Y   W   Y   L   Q   K   P   G   Q   S   P   H   L   L   I   Y   Q

ATG AGC AAC CTG GCC TCC GGC GTG CCC GAC AGA TTT TCT AGC AGC GGC AGC GGC ACC GAC TTC ACC CTG AGA ATC AGC CGG GTG GAA GCC <720
M   S   N   L   A   S   G   V   P   D   R   F   S   S   S   G   S   G   T   D   F   T   L   R   I   S   R   V   E   A

                                                                                                                NotI
                                                                                                                 |
GAG GAC GTG GGC GTG TAC TAC TGC GCC CAG AAC CTG GAA ATC CCC CGG ACC TTT GGA GGC GGC ACC AAG CTG GAA ATC AAG AGA GCG GCC <810
E   D   V   G   V   Y   Y   C   A   Q   N   L   E   I   P   R   T   F   G   G   G   T   K   L   E   I   K   R   A   A

                                                        >His-tag                    EcoRI
                                                        |                           |
GCA GAA CAA AAA CTC ATC TCA GAA GAG GAT CTG AAT GGG GCC GCA CAT CAC CAT CAT CAC CAT TAA TAA GAA TTC                   <885
A   E   Q   K   L   I   S   E   E   D   L   N   G   A   A   H   H   H   H   H   H   *   *
```

huVH1 323A3

VH exchange via AgeI/XhoI leads to pAB1_scFv323A3hu1 & pAB1_scFv323A3hu2.

```
                                                                                                AgeI    >huVH1 323A3
                                                                                                 |       |
                                                                                          ... ACC GGT CAA GTG CAG CTG GTG CAG < 90
                                                                                          ... T   G   Q   V   Q   L   V   Q

AGC GGC AGC GAG CTG AAA AAG CCT GGC GCC TCC GTG AAG GTG TCC TGC AAG GCC AGC GGC TAC ACC TTT ACC AAC TAC GGC ATG AAC TGG <180
S   G   S   E   L   K   K   P   G   A   S   V   K   V   S   C   K   A   S   G   Y   T   F   T   N   Y   G   M   N   W

GTG CGC CAG GCC CCT GGA CAG GGC CTG GAA TGG ATG GGC TGG ATC AAC ACC TAC ACC GGC GAG CCC ACC TAC GGC GAG GAC TTC AAG GGC <270
V   R   Q   A   P   G   Q   G   L   E   W   M   G   W   I   N   T   Y   T   G   E   P   T   Y   G   E   D   F   K   G
```

```
AGA TTC GTG TTC AGC CTG GAC ACC AGC GTG TCC ACC GCC TAC CTG CAG ATC AGC AGC CTG AAG GCC GAG GAC ACC GCC GTG TAC TAC TGC <360
R   F   V   F   S   L   D   T   S   V   S   T   A   Y   L   Q   I   S   S   L   K   A   E   D   T   A   V   Y   Y   C

                                                        XhoI
                                                        |
GCC AGA TTC GGC AAC TAC GTG GAC TAC TGG GGC CAG GGC ACC CTC GTG ACA GTC TCG AGT ...                                 <420
A   R   F   G   N   Y   V   D   Y   W   G   Q   G   T   L   V   T   V   S   S   ...
```

huVH2 323A3

VH exchange via AgeI/XhoI leads to pAB1_scFv323A3hu3 & pAB1_scFv323A3hu5.

```
                                                                    AgeI    >huVH2 323A3
                                                                    |       |
                                                                ... ACC GGT CAA GTG CAG CTG GTG CAG < 90
                                                                ... T   G   Q   V   Q   L   V   Q

TCT GGC GCC GAA GTG AAG AAA CCA GGC GCC AGC GTG AAG GTG TCC TGC AAG GCC AGC GGC TAC ACC TTT ACC AAC TAC GGC ATG AAC TGG <180
S   G   A   E   V   K   K   P   G   A   S   V   K   V   S   C   K   A   S   G   Y   T   F   T   N   Y   G   M   N   W

GTG CGC CAG GCC CCT GGC CAG AGA CTG GAA TGG ATG GGC TGG ATC AAC ACC TAC ACC GGC GAG CCC ACC TAC GGC GAG GAC TTC AAG GGC <270
V   R   Q   A   P   G   Q   R   L   E   W   M   G   W   I   N   T   Y   T   G   E   P   T   Y   G   E   D   F   K   G

AGA GTG ACC ATC ACC CTG GAC ACC AGC GCC AGC ACC GCC TAC ATG GAA CTG AGC AGC CTG CGG AGC GAG GAC ACC GCC GTG TAC TAC TGC <360
R   V   T   I   T   L   D   T   S   A   S   T   A   Y   M   E   L   S   S   L   R   S   E   D   T   A   V   Y   Y   C

                                                        XhoI
                                                        |
GCC AGA TTC GGC AAC TAC GTG GAC TAC TGG GGC CAG GGC ACC CTC GTG ACA GTC TCG AGT ...                                 <420
A   R   F   G   N   Y   V   D   Y   W   G   Q   G   T   L   V   T   V   S   S ...
```

huVH3 323A3

VH exchange via AgeI/XhoI leads to pAB1_scFv323A3hu4 & pAB1_scFv323A3hu6.

```
                                                                    AgeI    >huVH3 323A3
                                                                    |       |
                                                                ... ACC GGT CAA GTG CAG CTG GTG GAA < 90
                                                                ... T   G   Q   V   Q   L   V   E

TCT GGC GGC GGA GTG GTG CAG CCT GGC AGA AGC CTG AGA CTG AGC TGT GCC GCC AGC GGC TTC ACC TTC AGC AAC TAC GGC ATG AAC TGG <180
S   G   G   G   V   V   Q   P   G   R   S   L   R   L   S   C   A   A   S   G   F   T   F   S   N   Y   G   M   N   W

GTG CGC CAG GCC CCT GGC AAA GGC CTG GAA TGG GTG GCC TGG ATC AAC ACC TAC ACC GGC GAG CCT ACC TAC GGC GAG GAC TTC AAG GGC <270
V   R   Q   A   P   G   K   G   L   E   W   V   A   W   I   N   T   Y   T   G   E   P   T   Y   G   E   D   F   K   G

CGG TTC ACC ATC AGC CTG GAC AAC AGC AAG AAC ACC CTG TAC CTG CAG ATG AAC AGC CTG CGG GCC GAG GAC ACC GCC GTG TAC TAC TGT <360
R   F   T   I   S   L   D   N   S   K   N   T   L   Y   L   Q   M   N   S   L   R   A   E   D   T   A   V   Y   Y   C

                                                        XhoI
                                                        |
GCC AGA TTC GGC AAC TAC GTG GAC TAC TGG GGC CAG GGC ACC CTC GTG ACA GTC TCG AGT ...                                 <420
A   R   F   G   N   Y   V   D   Y   W   G   Q   G   T   L   V   T   V   S   S   ...
```

huVL1 323A3

VL exchange via XhoI/NotI leads to pAB1_scFv323A3hu1, pAB1_scFv323A3hu5 & pAB1_scFv323A3hu6.

```
                                                        XhoI    >Linker
                                                        |       |
                                                    ... GTC TCG AGT GGC GGC GGA GGA TCT GGC GGA GGC GGA AGT <450
                                                    ... V   S   S   G   G   G   G   S   G   G   G   G   S

                    >huVL1 323A3
                    |
GGG GGA GGC GGC AGC GAT ATT GTG ATG ACC CAG AGC CCC CTG AGC CTG CCT GTG ACA CCT GGC GAA CCT GCC AGC ATC AGC TGC AGA AGC <540
G   G   G   G   S   D   I   V   M   T   Q   S   P   L   S   L   P   V   T   P   G   E   P   A   S   I   S   C   R   S

AGC AAG AAC CTG CTG CAC AGC AAC GGC ATC ACC TAC CTG TAC TGG TAT CTG CAG AAA CCC GGC CAG TCC CCC CAG CTG CTG ATC TAC CAG <630
S   K   N   L   L   H   S   N   G   I   T   Y   L   Y   W   Y   L   Q   K   P   G   Q   S   P   Q   L   L   I   Y   Q

ATG AGC AAC CTG GCC AGC GGC GTG CCC GAT AGA TTT TCT GGC AGC GGC TCC GGC ACC GAC TTC ACC CTG AAG ATC AGC CGG GTG GAA GCC <720
M   S   N   L   A   S   G   V   P   D   R   F   S   G   S   G   S   G   T   D   F   T   L   K   I   S   R   V   E   A

                                                                                                        NotI
                                                                                                        |
GAG GAC GTG GGC GTG TAC TAC TGC GCC CAG AAC CTG GAA ATC CCC CGG ACC TTT GGC CAG GGC ACC AAG CTG GAA ATC AAG AGA GCG GCC GCA
E   D   V   G   V   Y   Y   C   A   Q   N   L   E   I   P   R   T   F   G   Q   G   T   K   L   E   I   K   R   A   A   A
```

huVL2 323A3

VL exchange via XhoI/NotI leads to pAB1_scFv323A3hu2, pAB1_scFv323A3hu3 & pAB1_scFv323A3hu4.

```
                                                        XhoI      >Linker
                                                         |         |
                                                  ... GTC TCG AGT GGC GGC GGA GGA TCT GGC GGA GGC GGA AGT <450
                                                  ... V   S   S   G   G   G   G   S   G   G   G   G   S

                    >huVL2 323A3
                     |
GGG GGA GGC GGA TCT GAG ATC GTG CTG ACA CAG AGC CCT GGC ACC CTG AGC CTG TCT CCA GGC GAA AGA GCC ACC CTG TCC TGC AGA AGC <540
  G   G   G   G   S   E   I   V   L   T   Q   S   P   G   T   L   S   L   S   P   G   E   R   A   T   L   S   C   R   S

AGC AAG AAC CTG CTG CAC AGC AAC GGC ATC ACC TAC CTG TAC TGG TAT CAG CAG AAG CCC GGC CAG GCC CCC AGA CTG CTG ATC TAC CAG <630
S   K   N   L   L   H   S   N   G   I   T   Y   L   Y   W   Y   Q   Q   K   P   G   Q   A   P   R   L   L   I   Y   Q

ATG AGC AAC CTG GCC AGC GGC ATC CCC GAC AGA TTT TCT GGC AGC GGC TCC GGC ACC GAC TTC ACC CTG ACA ATC AGC AGA CTG GAA CCC <720
M   S   N   L   A   S   G   I   P   D   R   F   S   G   S   G   S   G   T   D   F   T   L   T   I   S   R   L   E   P

                                                                                                        NotI
                                                                                                         |
GAG GAC TTC GCC GTG TAC TAC TGC GCC CAG AAC CTG GAA ATC CCC CGG ACC TTT GGC CAG GGC ACC AAG CTG GAA ATC AAG AGA GCG GCC GCA
E   D   F   A   V   Y   Y   C   A   Q   N   L   E   I   P   R   T   F   G   Q   G   T   K   L   E   I   K   R   A   A   A
```

6.2 TNFSF ligands

pIRESpuro3_CD40L

```
>Leader VH                                                                                  >Flag-tag                    NheI
|                                                                                           |                            |
ATG GAC TGG ACC TGG CGG GTG TTC TGC CTG CTG GCT GTG GCT CCT GGC GCT CAC TCT GGC GGC GAC TAC AAG GAC GAC GAC GAC AAG GCT < 90
M   D   W   T   W   R   V   F   C   L   L   A   V   A   P   G   A   H   S   G   G   D   Y   K   D   D   D   D   K   A

    >hCD40L (aa 116-261)
    |
AGC GGC GAC CAG AAC CCC CAG ATT GCC GCC CAC GTG ATC AGC GAG GCC AGC AGC AAG ACC ACC TCC GTG CTG CAG TGG GCC GAG AAG GGC <180
S   G   D   Q   N   P   Q   I   A   A   H   V   I   S   E   A   S   S   K   T   T   S   V   L   Q   W   A   E   K   G

TAC TAC ACC ATG AGC AAC AAC CTC GTG ACC CTG GAA AAC GGC AAG CAG CTG ACC GTG AAG CGG CAG GGC CTG TAC TAC ATC TAC GCC CAA <270
Y   Y   T   M   S   N   N   L   V   T   L   E   N   G   K   Q   L   T   V   K   R   Q   G   L   Y   Y   I   Y   A   Q

GTG ACC TTC TGC AGC AAC AGA GAG GCC AGC TCC CAG GCC CCC TTT ATC GCC AGC CTG TGC CTG AAG TCC CCC GGC AGA TTC GAG AGA ATC <360
V   T   F   C   S   N   R   E   A   S   S   Q   A   P   F   I   A   S   L   C   L   K   S   P   G   R   F   E   R   I

CTG CTG AGA GCC GCC AAC ACC CAC AGC AGC GCC AAG CCT TGT GGC CAG CAG TCT ATC CAC CTG GGC GGC GTG TTC GAA CTG CAG CCT GGC <450
L   L   R   A   A   N   T   H   S   S   A   K   P   C   G   Q   Q   S   I   H   L   G   G   V   F   E   L   Q   P   G

                                                                                                                    NotI
                                                                                                                     |
GCC TCC GTG TTC GTG AAC GTG ACC GAT CCT AGC CAG GTG TCC CAC GGC ACC GGC TTC ACC AGC TTC GGA CTG CTG AAG CTG TGA TGA GCG <540
A   S   V   F   V   N   V   T   D   P   S   Q   V   S   H   G   T   G   F   T   S   F   G   L   L   K   L   *   *   A

GCC GCA TAG                                                                                                             <549
A   A   *
```

pIRESpuro3_CD27L

```
>Leader VH                                                                                  >Flag-tag                    NheI
|                                                                                           |                            |
ATG GAC TGG ACC TGG CGG GTG TTC TGC CTG CTG GCT GTG GCT CCT GGC GCT CAC TCT GGC GGC GAC TAC AAG GAC GAC GAC GAC AAG GCT  < 90
M   D   W   T   W   R   V   F   C   L   L   A   V   A   P   G   A   H   S   G   G   D   Y   K   D   D   D   D   K   A

    >hCD27L (aa 52-193)
    |
AGC AGC CTG GGC TGG GAT GTG GCC GAA CTG CAG CTG AAT CAC ACC GGC CCT CAG CAG GAC CCC AGA CTG TAT TGG CAG GGC GGA CCT GCC  <180
  S   S   L   G   W   D   V   A   E   L   Q   L   N   H   T   G   P   Q   Q   D   P   R   L   Y   W   Q   G   G   P   A

CTG GGC AGA TCC TTT CTG CAC GGC CCC GAG CTG GAT AAG GGC CAG CTG AGA ATC CAC CGG GAC GGC ATC TAC ATG GTG CAC ATC CAA GTG  <270
L   G   R   S   F   L   H   G   P   E   L   D   K   G   Q   L   R   I   H   R   D   G   I   Y   M   V   H   I   Q   V

ACC CTG GCC ATC TGC AGC AGC ACC ACC GCC AGC AGA CAC CAT CCT ACC ACA CTG GCC GTG GGC ATC TGT AGC CCT GCC AGC AGA TCC ATC  <360
T   L   A   I   C   S   S   T   T   A   S   R   H   H   P   T   T   L   A   V   G   I   C   S   P   A   S   R   S   I

AGC CTG CTG CGG CTG AGC TTC CAC CAG GGC TGT ACA ATC GCC AGC CAG AGA CTG ACC CCA CTG GCC AGA GGC GAT ACC CTG TGC ACC AAT  <450
S   L   L   R   L   S   F   H   Q   G   C   T   I   A   S   Q   R   L   T   P   L   A   R   G   D   T   L   C   T   N

                                                                                                        NotI
                                                                                                         |
CTG ACC GGC ACC CTG CTG CCC AGC CGG AAC ACC GAC GAG ACA TTC TTC GGC GTG CAG TGG GTG CGC CCC TGA TGA GCG GCC GCA TAG      <537
L   T   G   T   L   L   P   S   R   N   T   D   E   T   F   F   G   V   Q   W   V   R   P   *   *   A   A   A   *
```

pIRESpuro3_4-1BBL

```
>Leader VH                                                                  >Flag-tag                  NheI
|                                                                           |                          |
ATG GAC TGG ACC TGG CGG GTG TTC TGC CTG CTG GCT GTG GCT CCT GGC GCT CAC TCT GGC GGC GAC TAC AAG GAC GAC GAC GAC AAG GCT < 90
M   D   W   T   W   R   V   F   C   L   L   A   V   A   P   G   A   H   S   G   G   D   Y   K   D   D   D   D   K   A

        >h4-1BBL (aa 71-254)
        |
AGC TCT AGA GAG GGA CCC GAG CTG AGC CCC GAT GAT CCT GCT GGA CTG CTG GAC CTG CGG CAG GGC ATG TTT GCT CAG CTG GTG GCC CAG <180
S   S   R   E   G   P   E   L   S   P   D   D   P   A   G   L   L   D   L   R   Q   G   M   F   A   Q   L   V   A   Q

AAC GTG CTG CTG ATC GAT GGC CCC CTG AGC TGG TAC AGC GAT CCT GGA CTG GCT GGC GTG TCA CTG ACA GGC GGC CTG AGC TAC AAA GAG <270
N   V   L   L   I   D   G   P   L   S   W   Y   S   D   P   G   L   A   G   V   S   L   T   G   G   L   S   Y   K   E

GAC ACC AAA GAA CTG GTG GTG GCC AAG GCC GGC GTG TAC TAC GTG TTC TTT CAG CTG GAA CTG CGG AGA GTG GTG GCC GGC GAA GGA TCT <360
D   T   K   E   L   V   V   A   K   A   G   V   Y   Y   V   F   F   Q   L   E   L   R   R   V   V   A   G   E   G   S

GGC TCT GTG TCT CTG GCC CTG CAT CTG CAG CCT CTG AGA AGC GCT GCT GGC GCT GCA GCT CTG GCA CTG ACA GTG GAT CTG CCT CCT GCC <450
G   S   V   S   L   A   L   H   L   Q   P   L   R   S   A   A   G   A   A   A   L   A   L   T   V   D   L   P   P   A

AGC TCC GAG GCC AGA AAC AGC GCA TTC GGG TTT CAA GGC AGG CTG CTG CAC CTG TCT GCC GGC CAG AGG CTG GGA GTG CAT CTG CAC ACA <540
S   S   E   A   R   N   S   A   F   G   F   Q   G   R   L   L   H   L   S   A   G   Q   R   L   G   V   H   L   H   T

GAG GCC AGG GCT AGA CAC GCC TGG CAG CTG ACA CAG GGC GCT ACA GTG CTG GGC CTG TTC AGA GTG ACC CCC GAG ATT CCA GCC GGC CTG <630
E   A   R   A   R   H   A   W   Q   L   T   Q   G   A   T   V   L   G   L   F   R   V   T   P   E   I   P   A   G   L

                            NotI
                            |
CCT TCT CCA AGA AGC GAA TGA TGA GCG GCC GCA TAG                                                                    <666
P   S   P   R   S   E   *   *   A   A   A   *
```

pIRESpuro3_OX40L

```
>Leader VH                                                                  >Flag-tag                  NheI
|                                                                           |                          |
ATG GAC TGG ACC TGG CGG GTG TTC TGC CTG CTG GCT GTG GCT CCT GGC GCT CAC TCT GGC GGC GAC TAC AAG GAC GAC GAC GAC AAG GCT < 90
M   D   W   T   W   R   V   F   C   L   L   A   V   A   P   G   A   H   S   G   G   D   Y   K   D   D   D   D   K   A

    >hOX40L (aa 51-183)
    |
AGC CAG GTA TCA CAT CGG TAT CCT CGA ATT CAA AGT ATC AAA GTA CAA TTT ACC GAA TAT AAG AAG GAG AAA GGT TTC ATC CTC ACT TCC <180
S   Q   V   S   H   R   Y   P   R   I   Q   S   I   K   V   Q   F   T   E   Y   K   K   E   K   G   F   I   L   T   S

CAA AAG GAG GAT GAA ATC ATG AAG GTG CAG AAC AAC TCA GTC ATC ATC AAC TGT GAT GGG TTT TAT CTC ATC TCC CTG AAG GGC TAC TTC <270
Q   K   E   D   E   I   M   K   V   Q   N   N   S   V   I   I   N   C   D   G   F   Y   L   I   S   L   K   G   Y   F

TCC CAG GAA GTC AAC ATT AGC CTT CAT TAC CAG AAG GAT GAG GAG CCC CTC TTC CAA CTG AAG AAG GTC AGG TCT GTC AAC TCC TTG ATG <360
S   Q   E   V   N   I   S   L   H   Y   Q   K   D   E   E   P   L   F   Q   L   K   K   V   R   S   V   N   S   L   M

GTG GCC TCT CTG ACT TAC AAA GAC AAA GTC TAC TTG AAT GTG ACC ACT GAC AAT ACC TCC CTG GAT GAC TTC CAT GTG AAT GGC GGA GAA <450
V   A   S   L   T   Y   K   D   K   V   Y   L   N   V   T   T   D   N   T   S   L   D   D   F   H   V   N   G   G   E

                                                    NotI
                                                    |
CTG ATT CTT ATC CAT CAA AAT CCT GGT GAA TTC TGT GTC CTT TGA TGA GCG GCC GCA TAG                                    <510
L   I   L   I   H   Q   N   P   G   E   F   C   V   L   *   *   A   A   A   *
```

6.3 Single-chain TNFSF ligands

pIRESpuro3_scCD40L

```
>Leader VH                                                                  >Flag-tag                  NheI
|                                                                           |                          |
ATG GAC TGG ACC TGG CGG GTG TTC TGC CTG CTG GCT GTG GCT CCT GGC GCT CAC TCT GGC GGC GAC TAC AAG GAC GAC GAC GAC AAG GCT < 90
M   D   W   T   W   R   V   F   C   L   L   A   V   A   P   G   A   H   S   G   G   D   Y   K   D   D   D   D   K   A

    >hCD40L (aa 116-261)
    |
AGC GGC GAC CAG AAC CCT CAG ATT GCC GCC CAC GTG ATC AGC GAG GCC AGC AGC AAG ACC ACC AGC GTG CTG CAG TGG GCC GAG AAG GGC <180
S   G   D   Q   N   P   Q   I   A   A   H   V   I   S   E   A   S   S   K   T   T   S   V   L   Q   W   A   E   K   G

TAC TAC ACC ATG AGC AAC AAC CTC GTG ACC CTG GAA AAC GGC AAG CAG CTG ACC GTG AAG CGG CAG GGC CTG TAC TAC ATC TAC GCC CAA <270
Y   Y   T   M   S   N   N   L   V   T   L   E   N   G   K   Q   L   T   V   K   R   Q   G   L   Y   Y   I   Y   A   Q

GTG ACC TTC TGC AGC AAC AGA GAG GCC AGC TCC CAG GCC CCC TTT ATC GCC AGC CTG TGC CTG AAG TCC CCC GGC AGA TTC GAG AGA ATC <360
V   T   F   C   S   N   R   E   A   S   S   Q   A   P   F   I   A   S   L   C   L   K   S   P   G   R   F   E   R   I

CTG CTG AGA GCC GCC AAC ACC CAC AGC AGC GCC AAG CCT TGT GGC CAG CAG TCT ATC CAC CTG GGC GGC GTG TTC GAA CTG CAG CCT GGC <450
L   L   R   A   A   N   T   H   S   S   A   K   P   C   G   Q   Q   S   I   H   L   G   G   V   F   E   L   Q   P   G
```

```
                                                                                                                >Linker BamHI
                                                                                                                |      |
GCC TCC GTG TTC GTG AAC GTG ACC GAT CCT AGC CAG GTG TCC CAC GGC ACC GGC TTC ACA AGC TTC GGC CTG CTG AAA CTG GGC GGA GGA <540
A  S  V  F  V  N  V  T  D  P  S  Q  V  S  H  G  T  G  F  T  S  F  G  L  L  K  L  G  G  G

                  >hCD40L (aa 116-261)
                  |
TCC GGC GGA GGC GGC GAT CAG AAT CCA CAG ATC GCT GCT CAT GTG ATC TCC GAG GCC TCT AGC AAG ACA ACA TCT GTG CTG CAG TGG GCT <630
S  G  G  G  G  D  Q  N  P  Q  I  A  A  H  V  I  S  E  A  S  S  K  T  T  S  V  L  Q  W  A

GAA AAA GGG TAC TAT ACA ATG TCC AAC AAT CTC GTG ACA CTG GAA AAT GGG AAA CAG CTG ACA GTG AAG AGA CAG GGG CTG TAT TAT ATC <720
E  K  G  Y  Y  T  M  S  N  N  L  V  T  L  E  N  G  K  Q  L  T  V  K  R  Q  G  L  Y  Y  I

TAT GCT CAA GTG ACA TTT TGC TCC AAC CGC GAG GCC TCC AGC CAG GCC CCT TTC ATT GCT TCC CTG TGT CTG AAA AGC CCT GGG CGC TTC <810
Y  A  Q  V  T  F  C  S  N  R  E  A  S  S  Q  A  P  F  I  A  S  L  C  L  K  S  P  G  R  F

GAG CGG ATT CTG CTG AGG GCT GCC AAT ACT CAC TCC TCC GCC AAG CCC TGC GGA CAG CAG AGC ATT CAT CTG GGA GGG GTG TTC GAG CTG <900
E  R  I  L  L  R  A  A  N  T  H  S  S  A  K  P  C  G  Q  Q  S  I  H  L  G  G  V  F  E  L

CAG CCA GGG GCT AGT GTG TTT GTG AAT GTG ACA GAC CCC TCT CAG GTG TCA CAT GGC ACA GGG TTT ACC TCA TTT GGA CTG CTG AAG CTG <990
Q  P  G  A  S  V  F  V  N  V  T  D  P  S  Q  V  S  H  G  T  G  F  T  S  F  G  L  L  K  L

>Linker     BspEI              >hCD40L (aa 116-261)
|           |                  |
GGA GGC GGC TCC GGA GGC GGA GGG GAC CAG AAT CCT CAG ATC GCA GCA CAC GTG ATC TCT GAA GCC AGC TCC AAG ACC ACT TCC GTG CTG <1080
G  G  G  S  G  G  G  G  D  Q  N  P  Q  I  A  A  H  V  I  S  E  A  S  S  K  T  T  S  V  L

CAG TGG GCA GAA AAG GGA TAT TAC ACT ATG TCT AAC AAC CTC GTG ACT CTG GAA AAT GGG AAG CAG CTG ACC GTG AAA CGC CAG GGA CTG <1170
Q  W  A  E  K  G  Y  Y  T  M  S  N  N  L  V  T  L  E  N  G  K  Q  L  T  V  K  R  Q  G  L

TAT TAT ATC TAC GCA CAA GTG ACT TTC TGT TCC AAC CGG GAA GCC AGT TCT CAG GCT CCA TTC ATT GCA AGT CTG TGT CTG AAG AGT CCC <1260
Y  Y  I  Y  A  Q  V  T  F  C  S  N  R  E  A  S  S  Q  A  P  F  I  A  S  L  C  L  K  S  P

GGA CGC TTT GAA CGC ATC CTG CTG CGC GCT GCT AAC ACA CAC TCC AGC GCC AAA CCA TGC GGA CAG CAG TCA ATT CAC CTG GGG GGA GTG <1350
G  R  F  E  R  I  L  L  R  A  A  N  T  H  S  S  A  K  P  C  G  Q  Q  S  I  H  L  G  G  V

TTT GAG CTG CAG CCT GGC GCA AGC GTG TTC GTG AAT GTG ACT GAT CCA TCC CAG GTG TCC CAT GGA ACA GGA TTC ACA TCT TTC GGG CTG <1440
F  E  L  Q  P  G  A  S  V  F  V  N  V  T  D  P  S  Q  V  S  H  G  T  G  F  T  S  F  G  L

                  NotI
                  |
CTG AAG CTG TGA TGA GCG GCC GCA TAG                                                                              <1467
L  K  L  *  *  A  A  A  *
```

pIRESpuro3_scCD27L

```
>Leader VH                                                                                  >Flag-tag                    NheI
|                                                                                           |                            |
ATG GAC TGG ACC TGG CGG GTG TTC TGC CTG CTG GCT GTG GCT CCT GGC GCT CAC TCT GGC GGC GAC TAC AAG GAC GAC GAC GAC AAG GCT < 90
M  D  W  T  W  R  V  F  C  L  L  A  V  A  P  G  A  H  S  G  G  D  Y  K  D  D  D  D  K  A

    >hCD27L (aa 52-193)
    |
AGC TCT CTG GGA TGG GAT GTG GCC GAA CTG CAG CTG AAC CAC ACC GGC CCT CAG CAG GAC CCC AGA CTG TAT TGG CAG GGC GGA CCT GCC <180
S  S  L  G  W  D  V  A  E  L  Q  L  N  H  T  G  P  Q  Q  D  P  R  L  Y  W  Q  G  G  P  A

CTG GGC AGA TCC TTT CTG CAC GGC CCC GAG CTG GAT AAG GGC CAG CTG AGA ATC CAC CGG GAC GGC ATC TAC ATG GTG CAC ATC CAA GTG <270
L  G  R  S  F  L  H  G  P  E  L  D  K  G  Q  L  R  I  H  R  D  G  I  Y  M  V  H  I  Q  V

ACC CTG GCC ATC TGC AGC AGC ACC ACC GCC AGC AGA CAC CAT CCT ACC ACA CTG GCC GTG GGC ATC TGT AGC CCT GCC AGC AGA TCC ATC <360
T  L  A  I  C  S  S  T  T  A  S  R  H  H  P  T  T  L  A  V  G  I  C  S  P  A  S  R  S  I

AGC CTG CTG CGG CTG AGC TTC CAC CAG GGC TGT ACA ATC GCC AGC CAG AGA CTG ACC CCA CTG GCC AGA GGC GAT ACC CTG TGC ACC AAT <450
S  L  L  R  L  S  F  H  Q  G  C  T  I  A  S  Q  R  L  T  P  L  A  R  G  D  T  L  C  T  N

                                                                                                    Linker  BamHI
                                                                                                    |       |
CTG ACC GGC ACC CTG CTG CCC AGC CGG AAC ACC GAC GAG ACA TTC TTC GGC GTG CAG TGG GTG CGC CCT GGC GGA GGA TCC GGG GGA GGA <540
L  T  G  T  L  L  P  S  R  N  T  D  E  T  F  F  G  V  Q  W  V  R  P  G  G  G  S  G  G  G

hCD27L (aa 52-193)
|
TCA CTG GGC TGG GAC GTG GCA GAA CTG CAG CTG AAT CAT ACA GGA CCA CAG CAG GAC CCT CGG CTG TAC TGG CAG GGG GGA CCA GCT CTG <630
S  L  G  W  D  V  A  E  L  Q  L  N  H  T  G  P  Q  Q  D  P  R  L  Y  W  Q  G  G  P  A  L

GGA CGG TCT TTC CTG CAC GGA CCT GAA CTG GAC AAA GGA CAG CTG CGC ATC CAC AGA GAT GGG ATC TAT ATG GTG CAT ATT CAA GTG ACA <720
G  R  S  F  L  H  G  P  E  L  D  K  G  Q  L  R  I  H  R  D  G  I  Y  M  V  H  I  Q  V  T

CTG GCT ATT TGC TCC TCC ACC ACA GCC AGC CGG CAC CAC CCA ACA ACC CTG GCA GTG GGA ATC TGC TCC CCC GCC TCC AGA TCT ATC TCC <810
L  A  I  C  S  S  T  T  A  S  R  H  H  P  T  T  L  A  V  G  I  C  S  P  A  S  R  S  I  S

CTG CTG AGA CTG TCA TTT CAC CAG GGA TGC ACC ATT GCC TCC CAG CGG CTG ACA CCT CTG GCT AGG GGC GAC ACA CTG TGT ACA AAC CTG <900
L  L  R  L  S  F  H  Q  G  C  T  I  A  S  Q  R  L  T  P  L  A  R  G  D  T  L  C  T  N  L

                                                                                        Linker      BspEI          >hCD27L
                                                                                        |           |              |
ACA GGG ACA CTG CTG CCC TCC AGA AAT ACC GAC GAA ACC TTT TTT GGA GTG CAG TGG GTG CGG CCA GGG GGA GGC TCC GGA GGC GGA AGT <990
T  G  T  L  L  P  S  R  N  T  D  E  T  F  F  G  V  Q  W  V  R  P  G  G  G  S  G  G  G  S
```

```
CTG GGC TGG GAT GTG GCT GAA CTG CAG CTG AAT CAC ACT GGC CCC CAG CAG GAC CCA AGG CTG TAT TGG CAG GGG GGA CCC GCC CTG GGG <1080
L  G  W  D  V  A  E  L  Q  L  N  H  T  G  P  Q  Q  D  P  R  L  Y  W  Q  G  G  P  A  L  G

CGC AGT TTT CTG CAT GGG CCA GAA CTG GAC AAG GGG CAG CTG AGG ATT CAT AGG GAT GGC ATC TAT ATG GTG CAC ATC CAA GTG ACA CTG <1170
R  S  F  L  H  G  P  E  L  D  K  G  Q  L  R  I  H  R  D  G  I  Y  M  V  H  I  Q  V  T  L

GCA ATT TGT TCT AGC ACC ACC GCT TCC AGA CAC CAC CCC ACT ACA CTG GCA GTG GGG ATT TGT TCT CCC GCC AGC CGG TCC ATC TCT CTG <1260
A  I  C  S  S  T  T  A  S  R  H  H  P  T  T  L  A  V  G  I  C  S  P  A  S  R  S  I  S  L

CTG AGG CTG AGT TTT CAT CAG GGG TGC ACT ATC GCT AGT CAG CGC CTG ACT CCC CTG GCA CGG GGA GAT ACT CTG TGC ACT AAC CTG ACT <1350
L  R  L  S  F  H  Q  G  C  T  I  A  S  Q  R  L  T  P  L  A  R  G  D  T  L  C  T  N  L  T

                                                                                  NotI
                                                                                  |
GGA ACT CTG CTG CCT TCT CGG AAT ACC GAT GAG ACT TTC TTT GGG GTG CAG TGG GTG CGC CCA TGA TGA GCG GCC GCA TAG            <1431
G  T  L  L  P  S  R  N  T  D  E  T  F  F  G  V  Q  W  V  R  P  *  *  A  A  A  *
```

pIRESpuro3_sc4-1BBL

```
>Leader VH                                                                                  >Flag-tag                    NheI
|                                                                                           |                            |
ATG GAC TGG ACC TGG CGG GTG TTC TGC CTG CTG GCT GTG GCT CCT GGC GCT CAC TCT GGC GGC GAC TAC AAG GAC GAC GAC GAC AAG GCT < 90
M   D   W   T   W   R   V   F   C   L   L   A   V   A   P   G   A   H   S   G   G   D   Y   K   D   D   D   D   K   A

        >h4-1BBL (aa 71-254)
        |
AGC TCT AGA GAG GGA CCC GAG CTG AGC CCC GAT GAT CCT GCT GGA CTG CTG GAC CTG CGG CAG GGC ATG TTT GCT CAG CTG GTG GCC CAG <180
S  S  R  E  G  P  E  L  S  P  D  D  P  A  G  L  L  D  L  R  Q  G  M  F  A  Q  L  V  A  Q

AAC GTG CTG CTG ATC GAT GGC CCC CTG AGC TGG TAC AGC GAT CCT GGA CTG GCT GGC GTG TCA CTG ACA GGC GGC CTG AGC TAC AAA GAG <270
N  V  L  L  I  D  G  P  L  S  W  Y  S  D  P  G  L  A  G  V  S  L  T  G  G  L  S  Y  K  E

GAC ACC AAA GAA CTG GTG GTG GCC AAG GCC GGC GTG TAC TAC GTG TTC TTT CAG CTG GAA CTG CGG AGA GTG GTG GCC GGC GAA GGA TCT <360
D  T  K  E  L  V  V  A  K  A  G  V  Y  Y  V  F  F  Q  L  E  L  R  R  V  V  A  G  E  G  S

GGC TCT GTG TCT CTG GCC CTG CAT CTG CAG CCT CTG AGA AGC GCT GCT GGC GCT GCA GCT CTG GCA CTG ACA GTG GAT CTG CCT CCT GCC <450
G  S  V  S  L  A  L  H  L  Q  P  L  R  S  A  A  G  A  A  A  L  A  L  T  V  D  L  P  P  A

AGC TCC GAG GCC AGA AAC AGC GCA TTC GGG TTT CAA GGC AGG CTG CTG CAC CTG TCT GCC GGC CAG AGG CTG GGA GTG CAT CTG CAC ACA <540
S  S  E  A  R  N  S  A  F  G  F  Q  G  R  L  L  H  L  S  A  G  Q  R  L  G  V  H  L  H  T

GAG GCC AGG GCT AGA CAC GCC TGG CAG CTG ACA CAG GGC GCT ACA GTG CTG GGC CTG TTC AGA GTG ACC CCC GAG ATT CCA GCC GGC CTG <630
E  A  R  A  R  H  A  W  Q  L  T  Q  G  A  T  V  L  G  L  F  R  V  T  P  E  I  P  A  G  L

                    >Linker                    BamHI                                                  >h4-1BBL (aa 71-254)
                    |                          |                                                      |
CCT TCT CCA AGA AGC GAA GGC GGC GGA GGA AGC GGA GGC GGA GGA TCC GGC GGA GGG GGA TCT GGG GGA GGC GGA TCA AGA GAA GGC CCA <720
P  S  P  R  S  E  G  G  G  G  S  G  G  G  G  S  G  G  G  G  S  G  G  G  G  S  R  E  G  P

GAG CTG TCC CCT GAC GAT CCA GCC GGG CTG CTG GAT CTG AGA CAG GGA ATG TTC GCC CAG CTG GTG GCT CAG AAT GTG CTG CTG ATT GAC <810
E  L  S  P  D  D  P  A  G  L  L  D  L  R  Q  G  M  F  A  Q  L  V  A  Q  N  V  L  L  I  D

GGA CCT CTG TCC TGG TAC TCC GAC CCA GGG CTG GCA GGG GTG TCC CTG ACT GGG GGA CTG TCC TAC AAA GAA GAT ACA AAA GAA CTG GTG <900
G  P  L  S  W  Y  S  D  P  G  L  A  G  V  S  L  T  G  G  L  S  Y  K  E  D  T  K  E  L  V

GTG GCT AAA GCT GGG GTG TAC TAT GTG TTT TTT CAG CTG GAA CTG AGG CGG GTG GTG GCT GGG GAG GGC TCA GGA TCT GTG TCC CTG GCT <990
V  A  K  A  G  V  Y  Y  V  F  F  Q  L  E  L  R  R  V  V  A  G  E  G  S  G  S  V  S  L  A

CTG CAT CTG CAG CCA CTG CGC TCT GCT GCT GGC GCA GCT GCA CTG GCT CTG ACT GTG GAC CTG CCA CCA GCC TCT AGC GAG GCT CGG AAC <1080
L  H  L  Q  P  L  R  S  A  A  G  A  A  A  L  A  L  T  V  D  L  P  P  A  S  S  E  A  R  N

TCC GCA TTT GGG TTC CAA GGA CGC CTG CTG CAT CTG AGC GCC GGA CAG CGC CTG GGA GTG CAT CTG CAT ACT GAA GCC AGA GCC CGG CAT <1170
S  A  F  G  F  Q  G  R  L  L  H  L  S  A  G  Q  R  L  G  V  H  L  H  T  E  A  R  A  R  H

GCT TGG CAG CTG ACC CAG GGG GCA ACT GTG CTG GGA CTG TTT CGC GTG ACA CCT GAG ATC CCT GCC GGA CTG CCA AGC CCT AGA TCA GAA <1260
A  W  Q  L  T  Q  G  A  T  V  L  G  L  F  R  V  T  P  E  I  P  A  G  L  P  S  P  R  S  E

>Linker                          BspEI                                  >h4-1BBL (aa 71-254)
|                                |                                      |
GGG GGG GGA GGC TCT GGC GGA GGC GGC TCC GGA GGG GGC GGA TCT GGC GGG GGA GGC AGT AGA GAA GGA CCT GAA CTG TCT CCC GAT GAC <1350
G  G  G  G  S  G  G  G  G  S  G  G  G  G  S  G  G  G  G  S  R  E  G  P  E  L  S  P  D  D

CCC GCA GGA CTG CTG GAC CTG AGA CAG GGC ATG TTC GCA CAG CTG GTG GCC CAG AAT GTG CTG CTG ATC GAC GGG CCA CTG AGT TGG TAT <1440
P  A  G  L  L  D  L  R  Q  G  M  F  A  Q  L  V  A  Q  N  V  L  L  I  D  G  P  L  S  W  Y

TCC GAT CCC GGC CTG GCC GGC GTG TCC CTG ACC GGC GGA CTG AGT TAC AAA GAG GAT ACA AAA GAA CTG GTG GTG GCA AAG GCA GGG GTG <1530
S  D  P  G  L  A  G  V  S  L  T  G  G  L  S  Y  K  E  D  T  K  E  L  V  V  A  K  A  G  V

TAC TAT GTG TTC TTT CAG CTG GAA CTG AGA AGG GTG GTG GCC GGC GAG GGA AGC GGA TCA GTG TCA CTG GCA CTG CAT CTG CAG CCC CTG <1620
Y  Y  V  F  F  Q  L  E  L  R  R  V  V  A  G  E  G  S  G  S  V  S  L  A  L  H  L  Q  P  L

AGA TCA GCT GCA GGG GCC GCT GCC CTG GCC CTG ACC GTG GAT CTG CCC CCA GCT TCT TCT GAG GCC CGG AAT AGT GCA TTC GGG TTT CAA <1710
R  S  A  A  G  A  A  A  L  A  L  T  V  D  L  P  P  A  S  S  E  A  R  N  S  A  F  G  F  Q

GGA CGC CTG CTG CAC CTG TCC GCT GGA CAG AGA CTG GGA GTG CAT CTG CAT ACC GAG GCT CGC GCC AGA CAT GCA TGG CAG CTG ACA CAG <1800
G  R  L  L  H  L  S  A  G  Q  R  L  G  V  H  L  H  T  E  A  R  A  R  H  A  W  Q  L  T  Q
```

```
                                                                                                                    EcoRI   NotI
                                                                                                                    |       |
GGC GCA ACC GTG CTG GGA CTG TTT AGA GTG ACT CCA GAA ATC CCC GCT GGC CTG CCT AGC CCT CGG AGC GAA TGA GAA TTC GCG GCC GCA <1890
G   A   T   V   L   G   L   F   R   V   T   P   E   I   P   A   G   L   P   S   P   R   S   E   *   E   F   A   A   A
```

pIRESpuro3_scOX40L

```
>Leader VH                                                                                          >Flag-tag                   NheI
|                                                                                                   |                           |
ATG GAC TGG ACC TGG CGG GTG TTC TGC CTG CTG GCT GTG GCT CCT GGC GCT CAC TCT GGC GGC GAC TAC AAG GAC GAC GAC GAC AAG GCT < 90
M   D   W   T   W   R   V   F   C   L   L   A   V   A   P   G   A   H   S   G   G   D   Y   K   D   D   D   D   K   A

    >hOX40L (aa 51-183)
    |
AGC CAG GTG TCC CAC AGA TAC CCC AGA ATC CAG AGC ATC AAG GTG CAG TTC ACC GAG TAC AAG AAA GAG AAG GGC TTC ATC CTG ACC AGC <180
S   Q   V   S   H   R   Y   P   R   I   Q   S   I   K   V   Q   F   T   E   Y   K   K   E   K   G   F   I   L   T   S

CAG AAA GAG GAC GAG ATC ATG AAG GTG CAG AAC AAC AGC GTG ATC ATC AAC TGC GAC GGC TTC TAC CTG ATC AGC CTG AAG GGC TAC TTC <270
Q   K   E   D   E   I   M   K   V   Q   N   N   S   V   I   I   N   C   D   G   F   Y   L   I   S   L   K   G   Y   F

AGC CAG GAA GTG AAC ATC AGC CTG CAC TAC CAG AAG GAC GAG GAA CCC CTG TTC CAG CTG AAG AAA GTG CGG AGC GTG AAC AGC CTG ATG <360
S   Q   E   V   N   I   S   L   H   Y   Q   K   D   E   E   P   L   F   Q   L   K   K   V   R   S   V   N   S   L   M

GTG GCC AGC CTG ACC TAC AAG GAC AAG GTG TAC CTG AAC GTG ACC ACC GAC AAC ACC AGC CTG GAC GAC TTC CAC GTG AAC GGC GGC GAG <450
V   A   S   L   T   Y   K   D   K   V   Y   L   N   V   T   T   D   N   T   S   L   D   D   F   H   V   N   G   G   E

                                                        >Linker BamHI               >hOX40L (aa 51-183)
                                                        |       |                   |
CTG ATC CTG ATT CAC CAG AAC CCC GGC GAG TTC TGC GTG CTG GGC GGA GGA TCC GGC GGA GGA CAG GTG TCA CAT CGG TAT CCT AGA ATC <540
L   I   L   I   H   Q   N   P   G   E   F   C   V   L   G   G   G   S   G   G   G   Q   V   S   H   R   Y   P   R   I

CAG TCT ATT AAG GTG CAG TTT ACA GAG TAT AAG AAA GAA AAA GGC TTT ATT CTG ACT TCC CAG AAA GAA GAT GAG ATT ATG AAG GTG CAG <630
Q   S   I   K   V   Q   F   T   E   Y   K   K   E   K   G   F   I   L   T   S   Q   K   E   D   E   I   M   K   V   Q

AAC AAT TCC GTG ATT ATC AAT TGT GAT GGG TTT TAT CTG ATC TCC CTG AAA GGA TAC TTT AGT CAG GAA GTG AAT ATT TCT CTG CAC TAT <720
N   N   S   V   I   I   N   C   D   G   F   Y   L   I   S   L   K   G   Y   F   S   Q   E   V   N   I   S   L   H   Y

CAG AAA GAT GAA GAA CCT CTG TTC CAG CTG AAA AAA GTG CGC TCC GTG AAC TCT CTG ATG GTG GCT TCC CTG ACA TAC AAA GAC AAA GTG <810
Q   K   D   E   E   P   L   F   Q   L   K   K   V   R   S   V   N   S   L   M   V   A   S   L   T   Y   K   D   K   V

TAT CTG AAT GTG ACA ACA GAT AAT ACC TCC CTG GAT GAT TTC CAT GTG AAT GGG GGG GAA CTG ATT CTG ATC CAT CAG AAT CCT GGG GAA <900
Y   L   N   V   T   T   D   N   T   S   L   D   D   F   H   V   N   G   G   E   L   I   L   I   H   Q   N   P   G   E

                >Linker     BspEI           >hOX40L (aa51-183)
                |           |               |
TTT TGT GTG CTG GGA GGC GGC TCC GGA GGC GGC CAG GTG TCC CAT AGG TAT CCC CGC ATT CAG TCC ATC AAA GTG CAG TTT ACT GAG TAC <990
F   C   V   L   G   G   G   S   G   G   G   Q   V   S   H   R   Y   P   R   I   Q   S   I   K   V   Q   F   T   E   Y

AAA AAA GAG AAA GGA TTC ATT CTG ACC TCT CAG AAA GAG GAC GAA ATT ATG AAG GTG CAG AAC AAC TCT GTG ATC ATT AAC TGT GAT GGA <1080
K   K   E   K   G   F   I   L   T   S   Q   K   E   D   E   I   M   K   V   Q   N   N   S   V   I   I   N   C   D   G

TTC TAT CTG ATT AGT CTG AAA GGA TAT TTC AGC CAG GAA GTG AAC ATT TCC CTG CAT TAC CAG AAG GAT GAA GAA CCA CTG TTC CAG CTG <1170
F   Y   L   I   S   L   K   G   Y   F   S   Q   E   V   N   I   S   L   H   Y   Q   K   D   E   E   P   L   F   Q   L

AAG AAA GTG CGC TCT GTG AAT AGT CTG ATG GTG GCC TCT CTG ACT TAT AAG GAT AAG GTG TAC CTG AAT GTG ACA ACT GAC AAT ACT TCT <1260
K   K   V   R   S   V   N   S   L   M   V   A   S   L   T   Y   K   D   K   V   Y   L   N   V   T   T   D   N   T   S

                                                                                                                    NotI
                                                                                                                    |
CTG GAC GAC TTT CAT GTG AAC GGG GGA GAG CTG ATT CTG ATC CAC CAG AAT CCA GGC GAG TTC TGT GTG CTG TGA TGA GCG GCC GCA TAG <1350
L   D   D   F   H   V   N   G   G   E   L   I   L   I   H   Q   N   P   G   E   F   C   V   L   *   *   A   A   A   *
```

6.4 scFv-ligand fusion proteins

Sequences of scFvs (chapter 6.1), TNFSF ligands (only the ECD) or scTNFSF ligands (three ECDs connected by linkers as shown in chapter 6.2) are inserted at the indicated sites.

pIRESpuro3_scFv-TNFSF

```
>Leader VH                                                                                          >Flag-Tag
|                                                                                                   |
ATG GAC TGG ACC TGG CGG GTG TTC TGC CTG CTG GCT GTG GCT CCT GGC GCT CAC TCT GGC GGC GAC TAC AAG GAC GAC GAC GAC AAG GGC < 90
M   D   W   T   W   R   V   F   C   L   L   A   V   A   P   G   A   H   S   G   G   D   Y   K   D   D   D   D   K   G

              >scFv
    AgeI      |   >Linker                                                 NheI      >TNFSF      NotI
    |         |   |                                                       |         |           |
GGA ACC GGT ... ... GGT GGA GGC GGA AGT GGC GGT GGG GGA TCT GGA GGT GGC GCT AGC ... ... TGA TGA GCG GCC GCA TAG
G   T   G   ... ... G   G   G   G   S   G   G   G   G   S   G   G   G   A   S   ... ... *   *   A   A   A   *
```

pIRESpuro3_scFv-scTNFSF

```
>Leader VH                                                                  >Flag-Tag
|                                                                           |
ATG GAC TGG ACC TGG CGG GTG TTC TGC CTG CTG GCT GTG GCT CCT GGC GCT CAC TCT GGC GGC GAC TAC AAG GAC GAC GAC GAC AAG GGC < 90
M   D   W   T   W   R   V   F   C   L   L   A   V   A   P   G   A   H   S   G   G   D   Y   K   D   D   D   D   K   G

              >scFv
    AgeI      |    >Linker                                          NheI       >scTNFSF     NotI
    |         |    |                                                |          |            |
GGA ACC GGT ... ... GGT GGA GGC GGA AGT GGC GGT GGG GGA TCT GGA GGT GGC GCT AGC ... ... TGA TGA GCG GCC GCA TAG
G   T   G   ... ... G   G   G   G   S   G   G   G   G   S   G   G   G   A   S   ... ... *   *   A   A   A   *
```

6.5 Dual-acting Cytokines

Sequences of TNFSF ligands (only the ECD) or scTNFSF ligands (three ECDs connected by linkers as shown in chapter 6.2) are inserted at the indicated sites.

pIRESpuro3_Duokine

Linker configuration in the case of combinations of CD40L, CD27L, OX40L.

```
>Leader VH                                                                  >Flag-tag                    NheI
|                                                                           |                            |
ATG GAC TGG ACC TGG CGG GTG TTC TGC CTG CTG GCT GTG GCT CCT GGC GCT CAC TCT GGC GGC GAC TAC AAG GAC GAC GAC GAC AAG GCT < 90
M   D   W   T   W   R   V   F   C   L   L   A   V   A   P   G   A   H   S   G   G   D   Y   K   D   D   D   D   K   A

       >TNFSF1
       |    >Linker                        BamHI                        >TNFSF2      NotI
       |    |                              |                            |            |
AGC ... ... GGC GGC GGA GGA AGC GGC GGC GGA GGA TCC GGC GGC GGA GGA AGC ... ... TGA TGA GCG GCC GCA TAG
S   ... ... G   G   G   G   S   G   G   G   G   S   G   G   G   G   S   ... ... *   *   A   A   A   *
```

pIRESpuro3_Duokine

Linker configuration in the case of combinations of 4-1BBL with CD40L, CD27L, OX40L.

```
>Leader VH                                                                  >Flag-tag                    NheI
|                                                                           |                            |
ATG GAC TGG ACC TGG CGG GTG TTC TGC CTG CTG GCT GTG GCT CCT GGC GCT CAC TCT GGC GGC GAC TAC AAG GAC GAC GAC GAC AAG GCT < 90
M   D   W   T   W   R   V   F   C   L   L   A   V   A   P   G   A   H   S   G   G   D   Y   K   D   D   D   D   K   A

       >TNFSF1
       |    >Linker                        BamHI                                                >TNFSF2      NotI
       |    |                              |                                                    |            |
AGC ... ... GGC GGC GGA GGA AGC GGC GGC GGA GGA TCC GGC GGC GGA GGA AGC GGC GGA GGG GGA AGT ... ... TGA TGA GCG GCC GCA TAG
S   ... ... G   G   G   G   S   G   G   G   G   S   G   G   G   G   S   G   G   G   G   S   ... ... *   *   A   A   A   *
```

pIRESpuro3_scDuokine

```
>Leader VH                                                                  >Flag-tag                    NheI
|                                                                           |                            |
ATG GAC TGG ACC TGG CGG GTG TTC TGC CTG CTG GCT GTG GCT CCT GGC GCT CAC TCT GGC GGC GAC TAC AAG GAC GAC GAC GAC AAG GCT < 90
M   D   W   T   W   R   V   F   C   L   L   A   V   A   P   G   A   H   S   G   G   D   Y   K   D   D   D   D   K   A

       >scTNFSF1
       |    >Linker                              AgeI                    >scTNFSF2    NotI
       |    |                                    |                       |            |
AGC ... ... GGC GGC GGA GGA TCT GGC GGA GGC GGA ACC GGT GGA GGC GGC AGC ... ... TGA TGA GCG GCC GCA TAG
S   ... ... G   G   G   G   S   G   G   G   G   T   G   G   G   G   S   ... ... *   *   A   A   A   *
```

pSecTagA_EHD2-scDuokine

```
>Igk leader                                                 AgeI    >FLAG-tag                    >Linker
|                                                           |       |                            |
ATG GAG ACA GAC ACA CTC CTG CTA TGG GTA CTG CTG CTC TGG GTT CCA GGT TCC ACC GGT GAC TAC AAA GAC GAT GAC GAT AAA GGC GGT < 90
M   E   T   D   T   L   L   L   W   V   L   L   L   W   V   P   G   S   T   G   D   Y   K   D   D   D   D   K   G   G
```

```
                >scTNFSF1
            XbaI    |    EcoRI    >Linker             >EHD2
            |       |    |        |                   |
GGC GGA TCA TCT ... ... GAA TTC GGG GGA AGC GGC GGT GAT TTC ACC CCC CCC ACA GTG AAG ATC CTC CAG AGC AGC TGT GAC GGC GGA
G   G   S   S   ... ... E   F   G   G   S   G   G   D   F   T   P   P   T   V   K   I   L   Q   S   S   C   D   G   G

GGC CAC TTC CCA CCT ACC ATC CAG CTG CTG TGT CTG GTG TCC GGC TAC ACC CCC GGC ACC ATC AAC ATC ACC TGG CTG GAA GAT GGA CAA
G   H   F   P   P   T   I   Q   L   L   C   L   V   S   G   Y   T   P   G   T   I   N   I   T   W   L   E   D   G   Q

GTG ATG GAC GTG GAC CTG AGC ACC GCC AGC ACC ACA CAG GAA GGC GAG CTG GCC TCT ACC CAG AGC GAG CTG ACA CTG AGC CAG AAG CAC
V   M   D   V   D   L   S   T   A   S   T   T   Q   E   G   E   L   A   S   T   Q   S   E   L   T   L   S   Q   K   H

                                                                                                                >Linker
                                                                                                                |
TGG CTG AGC GAC CGG ACC TAC ACC TGT CAA GTG ACC TAC CAG GGC CAC ACC TTC GAG GAC AGC ACC AAG AAG TGC GCC GAC AGC AAC GGG
W   L   S   D   R   T   Y   T   C   Q   V   T   Y   Q   G   H   T   F   E   D   S   T   K   K   C   A   D   S   N   G

                HindIII     >scTNFSF2
                |           |
GGA AGC GGC GGT AAG CTT ... ... TGA TGA GCG GCC GCC
G   S   G   G   K   L   ... ... *   *   A   A   A
```

6.6 Murine dual-acting Cytokines

pIRESpuro3_m4-1BBL-mCD40L

```
>Leader VH                                                                                  >Flag-tag                       NheI
|                                                                                           |                               |
ATG GAC TGG ACC TGG CGG GTG TTC TGC CTG CTG GCT GTG GCT CCT GGC GCT CAC TCT GGC GGC GAC TAC AAG GAC GAC GAC GAC AAG GCT < 90
M   D   W   T   W   R   V   F   C   L   L   A   V   A   P   G   A   H   S   G   G   D   Y   K   D   D   D   D   K   A

    >m4-1BBL (aa 104-309)
    |
AGC AGA ACC GAG CCC AGA CCC GCC CTG ACC ATC ACC ACC AGC CCC AAC CTG GGC ACC AGA GAG AAC AAC GCC GAC CAG GTG ACA CCC GTG <180
S   R   T   E   P   R   P   A   L   T   I   T   T   S   P   N   L   G   T   R   E   N   N   A   D   Q   V   T   P   V

TCC CAC ATC GGC TGC CCC AAC ACC ACC CAG CAG GGC AGC CCC GTG TTC GCC AAG CTG CTG GCC AAG AAC CAG GCC AGC CTG TGC AAT ACC <270
S   H   I   G   C   P   N   T   T   Q   Q   G   S   P   V   F   A   K   L   L   A   K   N   Q   A   S   L   C   N   T

ACC CTG AAC TGG CAC AGC CAG GAC GGC GCT GGC AGC AGC TAC CTG AGC CAG GGC CTG AGA TAC GAA GAG GAC AAG AAA GAA CTG GTG GTG <360
T   L   N   W   H   S   Q   D   G   A   G   S   S   Y   L   S   Q   G   L   R   Y   E   E   D   K   K   E   L   V   V

GAC AGC CCT GGC CTG TAC TAC GTG TTC CTG GAA CTG AAG CTG AGC CCC ACC TTC ACC AAC ACC GGC CAC AAG GTG CAG GGC TGG GTG TCA <450
D   S   P   G   L   Y   Y   V   F   L   E   L   K   L   S   P   T   F   T   N   T   G   H   K   V   Q   G   W   V   S

CTG GTG CTG CAG GCC AAG CCC CAG GTG GAC GAC TTC GAC AAC CTG GCC CTG ACC GTG GAA CTG TTC CCC TGC AGC ATG GAA AAC AAG CTG <540
L   V   L   Q   A   K   P   Q   V   D   D   F   D   N   L   A   L   T   V   E   L   F   P   C   S   M   E   N   K   L

GTG GAC AGA AGC TGG TCC CAG CTG CTG CTG CTG AAG GCC GGC CAC AGA CTG AGC GTG GGC CTG AGA GCC TAC CTG CAT GGC GCC CAG GAC <630
V   D   R   S   W   S   Q   L   L   L   L   K   A   G   H   R   L   S   V   G   L   R   A   Y   L   H   G   A   Q   D

                                                                                                                >Linker
                                                                                                                |
GCC TAC CGG GAC TGG GAG CTG AGC TAC CCC AAC ACA ACC AGC TTC GGC CTG TTC CTG GTG AAA CCC GAC AAC CCC TGG GAG GGC GGC GGA <720
A   Y   R   D   W   E   L   S   Y   P   N   T   T   S   F   G   L   F   L   V   K   P   D   N   P   W   E   G   G   G

                                    BamHI                   >mCD40L (aa 115-260)
                                    |                       |
GGA AGC GGC GGA GGG GGA TCT GGC GGC GGA GGA TCC GGC GGC GGA GGA AGC GGC GAT GAA GAT CCG CAG ATT GCG GCG CAT GTG GTG AGC <810
G   S   G   G   G   G   S   G   G   G   G   S   G   G   G   G   S   G   D   E   D   P   Q   I   A   A   H   V   V   S

GAA GCG AAC AGC AAC GCG GCG AGC GTG CTG CAG TGG GCG AAA AAA GGC TAT TAT ACC ATG AAG TCC AAC CTC GTG ATG CTG GAA AAC GGC <900
E   A   N   S   N   A   A   S   V   L   Q   W   A   K   K   G   Y   Y   T   M   K   S   N   L   V   M   L   E   N   G

AAG CAG CTG ACC GTG AAG CGC GAG GGC CTG TAC TAT GTG TAC ACC CAA GTG ACA TTC TGC AGC AAC AGA GAG CCC AGC AGC CAG CGG CCT <990
K   Q   L   T   V   K   R   E   G   L   Y   Y   V   Y   T   Q   V   T   F   C   S   N   R   E   P   S   S   Q   R   P

TTC ATC GTG GGA CTG TGG CTG AAG CCT AGC AGC GGC AGC GAG AGA ATC CTG CTG AAG GCC GCC AAC ACC CAC AGC AGC TCT CAG CTG TGC <1080
F   I   V   G   L   W   L   K   P   S   S   G   S   E   R   I   L   L   K   A   A   N   T   H   S   S   S   Q   L   C

GAG CAG CAG TCT GTG CAC CTG GGC GGA GTG TTC GAG CTG CAA GCT GGC GCC TCC GTG TTC GTG AAT GTG ACC GAG GCC AGC CAA GTG ATC <1170
E   Q   Q   S   V   H   L   G   G   V   F   E   L   Q   A   G   A   S   V   F   V   N   V   T   E   A   S   Q   V   I

                                                    NotI
                                                    |
CAC AGA GTG GGC TTC AGC AGC TTC GGC CTG CTG AAA CTG TGA TGA GCG GCC GCA                                                 <1224
H   R   V   G   F   S   S   F   G   L   L   K   L   *   *   A   A   A
```

msc4-1BBL

```
    >m4-1BBL (aa 104-309)
    |
    AGG ACC GAG CCA CGG CCC GCC CTC ACC ATC ACC ACC AGC CCT AAC CTG GGC ACC AGA GAG AAC AAC GCC GAC CAA GTG ACC CCC GTG <180
    R   T   E   P   R   P   A   L   T   I   T   T   S   P   N   L   G   T   R   E   N   N   A   D   Q   V   T   P   V
```

```
TCC CAC ATC GGC TGC CCT AAC ACA ACA CAG CAG GGC AGC CCC GTG TTC GCC AAG CTG CTG GCT AAG AAC CAG GCC AGC CTG TGC AAC ACC <270
S   H   I   G   C   P   N   T   T   Q   Q   G   S   P   V   F   A   K   L   L   A   K   N   Q   A   S   L   C   N   T

ACC CTG AAC TGG CAC AGC CAG GAC GGC GCT GGC AGC AGC TAT CTG AGC CAG GGC CTG AGA TAC GAG GAA GAT AAG AAA GAA CTG GTG GTG <360
T   L   N   W   H   S   Q   D   G   A   G   S   S   Y   L   S   Q   G   L   R   Y   E   E   D   K   K   E   L   V   V

GAC AGC CCT GGC CTG TAC TAC GTG TTC CTG GAA CTG AAG CTG AGC CCC ACC TTC ACC AAC ACC GGC CAC AAG GTG CAG GGC TGG GTG TCA <450
D   S   P   G   L   Y   Y   V   F   L   E   L   K   L   S   P   T   F   T   N   T   G   H   K   V   Q   G   W   V   S

CTG GTG CTG CAG GCT AAG CCT CAG GTG GAC GAC TTC GAC AAC CTG GCC CTG ACA GTG GAA CTG TTC CCC TGC AGC ATG GAA AAC AAG CTG <540
L   V   L   Q   A   K   P   Q   V   D   D   F   D   N   L   A   L   T   V   E   L   F   P   C   S   M   E   N   K   L

GTG GAT AGA AGC TGG TCC CAG CTC CTG CTG CTG AAG GCT GGC CAC AGA CTG AGC GTG GGC CTG AGG GCT TAT CTG CAC GGC GCC CAG GAC <630
V   D   R   S   W   S   Q   L   L   L   L   K   A   G   H   R   L   S   V   G   L   R   A   Y   L   H   G   A   Q   D

                                                                                                                >Linker
                                                                                                                |
GCC TAC AGA GAC TGG GAG CTG AGC TAC CCC AAC ACA ACC AGC TTC GGC CTG TTC CTC GTG AAA CCT GAT AAT CCC TGG GAG GGC GGC GGA <720
A   Y   R   D   W   E   L   S   Y   P   N   T   T   S   F   G   L   F   L   V   K   P   D   N   P   W   E   G   G   G

                                                                    >m4-1BBL (aa 104-309)
                                                                    |
GGA AGC GGA GGC GGA GGG TCC GGC GGA GGG GGA TCT GGG GGA GGC GGA TCA AGA ACA GAA CCT AGA CCT GCT CTG ACC ATC ACC ACC AGC <810
G   S   G   G   G   G   S   G   G   G   G   S   G   G   G   G   S   R   T   E   P   R   P   A   L   T   I   T   T   S

CCT AAC CTG GGC ACC AGA GAG AAC AAC GCC GAC CAA GTG ACC CCC GTG TCC CAC ATC GGC TGC CCT AAC ACA ACA CAG CAG GGC AGC CCC <900
P   N   L   G   T   R   E   N   N   A   D   Q   V   T   P   V   S   H   I   G   C   P   N   T   T   Q   Q   G   S   P

GTG TTC GCC AAG CTG CTG GCT AAG AAC CAG GCC AGC CTG TGC AAC ACC ACC CTG AAC TGG CAC AGC CAG GAC GGC GCT GGC AGC AGC TAT <990
V   F   A   K   L   L   A   K   N   Q   A   S   L   C   N   T   T   L   N   W   H   S   Q   D   G   A   G   S   S   Y

CTG AGC CAG GGC CTG AGA TAC GAG GAA GAT AAG AAA GAA CTG GTG GTG GAC AGC CCT GGC CTG TAC TAC GTG TTC CTG GAA CTG AAG CTG <1080
L   S   Q   G   L   R   Y   E   E   D   K   K   E   L   V   V   D   S   P   G   L   Y   Y   V   F   L   E   L   K   L

AGC CCC ACC TTC ACC AAC ACC GGC CAC AAG GTG CAG GGC TGG GTG TCA CTG GTG CTG CAG GCT AAG CCT CAG GTG GAC GAC TTC GAC AAC <1170
S   P   T   F   T   N   T   G   H   K   V   Q   G   W   V   S   L   V   L   Q   A   K   P   Q   V   D   D   F   D   N

CTG GCC CTG ACA GTG GAA CTG TTC CCC TGC AGC ATG GAA AAC AAG CTG GTG GAT AGA AGC TGG TCC CAG CTC CTG CTG CTG AAG GCT GGC <1260
L   A   L   T   V   E   L   F   P   C   S   M   E   N   K   L   V   D   R   S   W   S   Q   L   L   L   L   K   A   G

CAC AGA CTG AGC GTG GGC CTG AGG GCT TAT CTG CAC GGC GCC CAG GAC GCC TAC AGA GAC TGG GAG CTG AGC TAC CCC AAC ACA ACC AGC <1350
H   R   L   S   V   G   L   R   A   Y   L   H   G   A   Q   D   A   Y   R   D   W   E   L   S   Y   P   N   T   T   S

                                                >Linker
                                                |
TTC GGC CTG TTC CTC GTG AAA CCT GAT AAT CCC TGG GAG GGG GGG GGA GGC TCT GGC GGA GGC GGC TCC GGA GGG GGC GGA TCT GGC GGG <1440
F   G   L   F   L   V   K   P   D   N   P   W   E   G   G   G   G   S   G   G   G   G   S   G   G   G   G   S   G   G

        >m4-1BBL (aa 104-309)
        |
GGA GGC AGT AGA ACA GAA CCT AGA CCT GCT CTG ACC ATC ACC ACC AGC CCT AAC CTG GGC ACC AGA GAG AAC AAC GCC GAC CAA GTG ACC <1530
G   G   S   R   T   E   P   R   P   A   L   T   I   T   T   S   P   N   L   G   T   R   E   N   N   A   D   Q   V   T

CCC GTG TCC CAC ATC GGC TGC CCT AAC ACA ACA CAG CAG GGC AGC CCC GTG TTC GCC AAG CTG CTG GCT AAG AAC CAG GCC AGC CTG TGC <1620
P   V   S   H   I   G   C   P   N   T   T   Q   Q   G   S   P   V   F   A   K   L   L   A   K   N   Q   A   S   L   C

AAC ACC ACC CTG AAC TGG CAC AGC CAG GAC GGC GCT GGC AGC AGC TAT CTG AGC CAG GGC CTG AGA TAC GAG GAA GAT AAG AAA GAA CTG <1710
N   T   T   L   N   W   H   S   Q   D   G   A   G   S   S   Y   L   S   Q   G   L   R   Y   E   E   D   K   K   E   L

GTG GTG GAC AGC CCT GGC CTG TAC TAC GTG TTC CTG GAA CTG AAG CTG AGC CCC ACC TTC ACC AAC ACC GGC CAC AAG GTG CAG GGC TGG <1800
V   V   D   S   P   G   L   Y   Y   V   F   L   E   L   K   L   S   P   T   F   T   N   T   G   H   K   V   Q   G   W

GTG TCA CTG GTG CTG CAG GCT AAG CCT CAG GTG GAC GAC TTC GAC AAC CTG GCC CTG ACA GTG GAA CTG TTC CCC TGC AGC ATG GAA AAC <1890
V   S   L   V   L   Q   A   K   P   Q   V   D   D   F   D   N   L   A   L   T   V   E   L   F   P   C   S   M   E   N

AAG CTG GTG GAT AGA AGC TGG TCC CAG CTC CTG CTG CTG AAG GCT GGC CAC AGA CTG AGC GTG GGC CTG AGG GCT TAT CTG CAC GGC GCC <1980
K   L   V   D   R   S   W   S   Q   L   L   L   L   K   A   G   H   R   L   S   V   G   L   R   A   Y   L   H   G   A

CAG GAC GCC TAC AGA GAC TGG GAG CTG AGC TAC CCC AAC ACA ACC AGC TTC GGC CTG TTC CTC GTC AAG CCC GAC AAC CCT TGG GAG
Q   D   A   Y   R   D   W   E   L   S   Y   P   N   T   T   S   F   G   L   F   L   V   K   P   D   N   P   W   E
```

mscCD27L

```
                                                >mCD27L (aa 54-195)
                                                |
                                                CAC CCC GAG CCC CAC ACC GCC GAA CTG CAG CTG AAC CTG ACC GTG CCC
                                                H   P   E   P   H   T   A   E   L   Q   L   N   L   T   V   P

AGA AAG GAC CCC ACC CTG AGA TGG GGA GCT GGC CCT GCT CTG GGC AGA TCC TTT ACA CAC GGC CCC GAG CTG GAA GAA GGC CAC CTG AGA
R   K   D   P   T   L   R   W   G   A   G   P   A   L   G   R   S   F   T   H   G   P   E   L   E   E   G   H   L   R

ATC CAC CAG GAC GGC CTG TAC AGA CTG CAC ATC CAA GTG ACC CTG GCC AAC TGC AGC AGC CCT GGC TCT ACC CTG CAG CAC AGA GCC ACA
I   H   Q   D   G   L   Y   R   L   H   I   Q   V   T   L   A   N   C   S   S   P   G   S   T   L   Q   H   R   A   T

CTG GCC GTG GGC ATC TGT AGC CCT GCT GCT CAC GGA ATC AGC CTG CTG AGA GGC AGA TTC GGC CAG GAC TGT ACC GTG GCC CTG CAG AGG
L   A   V   G   I   C   S   P   A   A   H   G   I   S   L   L   R   G   R   F   G   Q   D   C   T   V   A   L   Q   R

CTG ACC TAT CTG GTG CAT GGC GAC GTG CTG TGC ACC AAC CTG ACA CTG CCT CTG CTG CCC AGC AGA AAC GCC GAC GAA ACA TTC TTT GGA
L   T   Y   L   V   H   G   D   V   L   C   T   N   L   T   L   P   L   L   P   S   R   N   A   D   E   T   F   F   G
```

```
                     >Linker                   >mCD27L (aa 54-195)
                     |                         |
GTG CAG TGG ATT TGT CCT GGC GGA GGG TCC GGG GGA GGA CAC CCA GAA CCT CAT ACA GCT GAA CTG CAG CTG AAC CTG ACC GTG CCC AGA
V  Q  W  I  C  P  G  G  G  S  G  G  G  H  P  E  P  H  T  A  E  L  Q  L  N  L  T  V  P  R

AAG GAC CCC ACC CTG AGA TGG GGA GCT GGC CCT GCT CTG GGC AGA TCC TTT ACA CAC GGC CCC GAG CTG GAA GAA GGC CAC CTG AGA ATC
K  D  P  T  L  R  W  G  A  G  P  A  L  G  R  S  F  T  H  G  P  E  L  E  E  G  H  L  R  I

CAC CAG GAC GGC CTG TAC AGA CTG CAC ATC CAA GTG ACC CTG GCC AAC TGC AGC AGC CCT GGC TCT ACC CTG CAG CAC AGA GCC ACA CTG
H  Q  D  G  L  Y  R  L  H  I  Q  V  T  L  A  N  C  S  S  P  G  S  T  L  Q  H  R  A  T  L

GCC GTG GGC ATC TGT AGC CCT GCT GCT CAC GGA ATC AGC CTG CTG AGA GGC AGA TTC GGC CAG GAC TGT ACC GTG GCC CTG CAG AGG CTG
A  V  G  I  C  S  P  A  A  H  G  I  S  L  L  R  G  R  F  G  Q  D  C  T  V  A  L  Q  R  L

ACC TAT CTG GTG CAT GGC GAC GTG CTG TGC ACC AAC CTG ACA CTG CCT CTG CTG CCC AGC AGA AAC GCC GAC GAA ACA TTC TTT GGA GTG
T  Y  L  V  H  G  D  V  L  C  T  N  L  T  L  P  L  L  P  S  R  N  A  D  E  T  F  F  G  V

                  >Linker                   >mCD27L (aa 54-195)
                  |                         |
CAG TGG ATT TGT CCT GGG GGA GGC TCC GGA GGC GGA CAC CCT GAA CCT CAT ACA GCT GAA CTG CAG CTG AAC CTG ACC GTG CCC AGA AAG
Q  W  I  C  P  G  G  G  S  G  G  G  H  P  E  P  H  T  A  E  L  Q  L  N  L  T  V  P  R  K

GAC CCC ACC CTG AGA TGG GGA GCT GGC CCT GCT CTG GGC AGA TCC TTT ACA CAC GGC CCC GAG CTG GAA GAA GGC CAC CTG AGA ATC CAC
D  P  T  L  R  W  G  A  G  P  A  L  G  R  S  F  T  H  G  P  E  L  E  E  G  H  L  R  I  H

CAG GAC GGC CTG TAC AGA CTG CAC ATC CAA GTG ACC CTG GCC AAC TGC AGC AGC CCT GGC TCT ACC CTG CAG CAC AGA GCC ACA CTG GCC
Q  D  G  L  Y  R  L  H  I  Q  V  T  L  A  N  C  S  S  P  G  S  T  L  Q  H  R  A  T  L  A

GTG GGC ATC TGT AGC CCT GCT GCT CAC GGA ATC AGC CTG CTG AGA GGC AGA TTC GGC CAG GAC TGT ACC GTG GCC CTG CAG AGG CTG ACC
V  G  I  C  S  P  A  A  H  G  I  S  L  L  R  G  R  F  G  Q  D  C  T  V  A  L  Q  R  L  T

TAT CTG GTG CAT GGC GAC GTG CTG TGC ACC AAC CTG ACA CTG CCT CTG CTG CCC AGC AGA AAC GCC GAC GAG ACC TTC TTC GGC GTC CAG
Y  L  V  H  G  D  V  L  C  T  N  L  T  L  P  L  L  P  S  R  N  A  D  E  T  F  F  G  V  Q

TGG ATC TGC CCC
W  I  C  P
```

mscCD40L

```
    >mCD40L (aa 115-260)
    |
    GGC GAC GAG GAC CCC CAG ATC GCC GCC CAC GTG GTG TCT GAG GCC AAC AGC AAC GCC GCC TCT GTG CTG CAG TGG GCC AAG AAA GGC
    G  D  E  D  P  Q  I  A  A  H  V  V  S  E  A  N  S  N  A  A  S  V  L  Q  W  A  K  K  G

TAC TAC ACC ATG AAG TCC AAC CTC GTG ATG CTG GAA AAC GGC AAG CAG CTG ACC GTG AAG CGC GAG GGC CTG TAC TAT GTG TAC ACC CAA
Y  Y  T  M  K  S  N  L  V  M  L  E  N  G  K  Q  L  T  V  K  R  E  G  L  Y  Y  V  Y  T  Q

GTG ACA TTC TGC AGC AAC CGC GAG CCC AGC AGC CAG AGG CCT TTT ATC GTG GGC CTG TGG CTG AAG CCT AGC AGC GGC AGC GAG AGA ATC
V  T  F  C  S  N  R  E  P  S  S  Q  R  P  F  I  V  G  L  W  L  K  P  S  S  G  S  E  R  I

CTG CTG AAG GCC GCC AAC ACC CAC AGC AGC TCT CAG CTG TGC GAG CAG CAG TCT GTG CAC CTG GGA GGC GTG TTC GAG CTG CAA GCT GGC
L  L  K  A  A  N  T  H  S  S  S  Q  L  C  E  Q  Q  S  V  H  L  G  G  V  F  E  L  Q  A  G

                                                                                                                >Linker
                                                                                                                |
GCT TCC GTG TTC GTG AAC GTG ACC GAG GCC AGC CAA GTG ATC CAC AGA GTG GGC TTC AGC AGC TTT GGA CTG CTC AAA CTG GGC GGA GGG
A  S  V  F  V  N  V  T  E  A  S  Q  V  I  H  R  V  G  F  S  S  F  G  L  L  K  L  G  G  G

                  >mCD40L (aa 115-260)
                  |
TCC GGC GGA GGC GGA GAT GAA GAT CCT CAG ATT GCT GCC CAC GTG GTG TCT GAG GCC AAC AGC AAC GCC GCC TCT GTG CTG CAG TGG GCC
S  G  G  G  G  D  E  D  P  Q  I  A  A  H  V  V  S  E  A  N  S  N  A  A  S  V  L  Q  W  A

AAG AAA GGC TAC TAC ACC ATG AAG TCC AAC CTC GTG ATG CTG GAA AAC GGC AAG CAG CTG ACC GTG AAG CGC GAG GGC CTG TAC TAT GTG
K  K  G  Y  Y  T  M  K  S  N  L  V  M  L  E  N  G  K  Q  L  T  V  K  R  E  G  L  Y  Y  V

TAC ACC CAA GTG ACA TTC TGC AGC AAC CGC GAG CCC AGC AGC CAG AGG CCT TTT ATC GTG GGC CTG TGG CTG AAG CCT AGC AGC GGC AGC
Y  T  Q  V  T  F  C  S  N  R  E  P  S  S  Q  R  P  F  I  V  G  L  W  L  K  P  S  S  G  S

GAG AGA ATC CTG CTG AAG GCC GCC AAC ACC CAC AGC AGC TCT CAG CTG TGC GAG CAG CAG TCT GTG CAC CTG GGA GGC GTG TTC GAG CTG
E  R  I  L  L  K  A  A  N  T  H  S  S  S  Q  L  C  E  Q  Q  S  V  H  L  G  G  V  F  E  L

CAA GCT GGC GCT TCC GTG TTC GTG AAC GTG ACC GAG GCC AGC CAA GTG ATC CAC AGA GTG GGC TTC AGC AGC TTT GGA CTG CTC AAA CTG
Q  A  G  A  S  V  F  V  N  V  T  E  A  S  Q  V  I  H  R  V  G  F  S  S  F  G  L  L  K  L

>Linker                   >mCD40L (aa 115-260)
|                         |
GGA GGC GGC TCC GGA GGC GGA GGA GAT GAA GAT CCT CAG ATT GCT GCC CAC GTG GTG TCT GAG GCC AAC AGC AAC GCC GCC TCT GTG CTG
G  G  G  S  G  G  G  G  D  E  D  P  Q  I  A  A  H  V  V  S  E  A  N  S  N  A  A  S  V  L

CAG TGG GCC AAG AAA GGC TAC TAC ACC ATG AAG TCC AAC CTC GTG ATG CTG GAA AAC GGC AAG CAG CTG ACC GTG AAG CGC GAG GGC CTG
Q  W  A  K  K  G  Y  Y  T  M  K  S  N  L  V  M  L  E  N  G  K  Q  L  T  V  K  R  E  G  L

TAC TAT GTG TAC ACC CAA GTG ACA TTC TGC AGC AAC CGC GAG CCC AGC AGC CAG AGG CCT TTT ATC GTG GGC CTG TGG CTG AAG CCT AGC
Y  Y  V  Y  T  Q  V  T  F  C  S  N  R  E  P  S  S  Q  R  P  F  I  V  G  L  W  L  K  P  S

AGC GGC AGC GAG AGA ATC CTG CTG AAG GCC GCC AAC ACC CAC AGC AGC TCT CAG CTG TGC GAG CAG CAG TCT GTG CAC CTG GGA GGC GTG
S  G  S  E  R  I  L  L  K  A  A  N  T  H  S  S  S  Q  L  C  E  Q  Q  S  V  H  L  G  G  V
```

```
TTC GAG CTG CAA GCT GGC GCT TCC GTG TTC GTG AAC GTG ACC GAG GCC AGC CAA GTG ATC CAC AGA GTG GGC TTC TCC TCC TTC GGC CTC
F   E   L   Q   A   G   A   S   V   F   V   N   V   T   E   A   S   Q   V   I   H   R   V   G   F   S   S   F   G   L

CTG AAG CTG
L   K   L
```

pIRESpuro3_mscDuokine

Sequences of murine scTNFSF ligands (shown above) are inserted at the indicated sites leading to pIRESpuro3_msc4-1BBL-mscCD40L, pIRESpuro3_msc4-1BBL-mscCD27L & pIRESpuro3_mscCD40L-mscCD27L.

```
>Leader VH                                                                    >Flag-tag                    NheI
|                                                                             |                            |
ATG GAC TGG ACC TGG CGG GTG TTC TGC CTG CTG GCT GTG GCT CCT GGC GCT CAC TCT GGC GGC GAC TAC AAG GAC GAC GAC GAC AAG GCT < 90
M   D   W   T   W   R   V   F   C   L   L   A   V   A   P   G   A   H   S   G   G   D   Y   K   D   D   D   D   K   A

       >mscTNFSF1
       |    >Linker                                                  >mscTNFSF2   NotI
       |    |                                                        |            |
AGC ... ... GGA GGC GGT GGT AGT GGA GGT GGC GGG TCC GGT GGA GGT GGA AGC ... ... TGA TGA GCG GCC GCA
S   ... ... G   G   G   G   S   G   G   G   G   S   G   G   G   G   S   ... ... *   *   A   A   A
```

6.7 TNFRSF receptor-Fc fusion proteins

pSecTagA_hCD40-Fc

pSecTagA_hCD40-Fc is the basis for pSecTagA_hCD27-Fc, h4-1BB-Fc & hOX40-Fc (exchange via AgeI/NotI).

```
>Igk Leader                                                                  AgeI    >hCD40 (aa 21-193)
|                                                                            |       |
ATG GAG ACA GAC ACA CTC CTG CTA TGG GTA CTG CTG CTC TGG GTT CCA GGT TCC ACC GGT GAA CCT CCC ACC GCC TGC AGA GAG AAG CAG < 90
M   E   T   D   T   L   L   L   W   V   L   L   L   W   V   P   G   S   T   G   E   P   P   T   A   C   R   E   K   Q

TAC CTG ATC AAC AGC CAG TGC TGC AGC CTG TGC CAG CCC GGC CAG AAA CTG GTG TCC GAC TGC ACC GAG TTC ACC GAG ACA GAG TGC CTG <180
Y   L   I   N   S   Q   C   C   S   L   C   Q   P   G   Q   K   L   V   S   D   C   T   E   F   T   E   T   E   C   L

CCT TGC GGC GAG AGC GAG TTC CTG GAC ACC TGG AAC AGA GAG ACA CAC TGC CAC CAG CAC AAG TAC TGC GAC CCC AAC CTG GGC CTG CGG <270
P   C   G   E   S   E   F   L   D   T   W   N   R   E   T   H   C   H   Q   H   K   Y   C   D   P   N   L   G   L   R

GTG CAG CAG AAG GGC ACC AGC GAG ACA GAC ACC ATC TGC ACC TGT GAA GAG GGA TGG CAC TGC ACC TCC GAG GCC TGC GAG AGC TGT GTG <360
V   Q   Q   K   G   T   S   E   T   D   T   I   C   T   C   E   E   G   W   H   C   T   S   E   A   C   E   S   C   V

CTG CAC AGA AGC TGC AGC CCC GGC TTC GGC GTG AAG CAG ATT GCT ACC GGC GTG TCC GAT ACC ATC TGC GAG CCT TGC CCC GTG GGC TTC <450
L   H   R   S   C   S   P   G   F   G   V   K   Q   I   A   T   G   V   S   D   T   I   C   E   P   C   P   V   G   F

TTC AGC AAT GTG TCC AGC GCC TTC GAG AAG TGC CAC CCC TGG ACC AGC TGC GAG ACA AAG GAC CTG GTG GTG CAG CAG GCC GGC ACC AAC <540
F   S   N   V   S   S   A   F   E   K   C   H   P   W   T   S   C   E   T   K   D   L   V   V   Q   Q   A   G   T   N

                                            NotI        >IgG1 hinge region                    >IgG1 CH2
                                            |           |                                     |
AAG ACC GAT GTC GTG TGC GGA CCT CAG GAT CGG CTG AGA GCG GCC GCA GAC AAA ACT CAC ACA TGC CCA CCG TGC CCA GCA CCT GAA CTC <630
K   T   D   V   V   C   G   P   Q   D   R   L   R   A   A   A   D   K   T   H   T   C   P   P   C   P   A   P   E   L

CTG GGG GGA CCG TCA GTC TTC CTC TTC CCC CCA AAA CCC AAG GAC ACC CTC ATG ATC TCC CGG ACC CCT GAG GTC ACA TGC GTG GTG GTG <720
L   G   G   P   S   V   F   L   F   P   P   K   P   K   D   T   L   M   I   S   R   T   P   E   V   T   C   V   V   V

GAC GTG AGC CAC GAA GAC CCT GAG GTC AAG TTC AAC TGG TAC GTG GAC GGC GTG GAG GTG CAT AAT GCC AAG ACA AAG CCG CGG GAG GAG <810
D   V   S   H   E   D   P   E   V   K   F   N   W   Y   V   D   G   V   E   V   H   N   A   K   T   K   P   R   E   E

CAG TAC AAC AGC ACG TAC CGG GTG GTC AGC GTC CTC ACC GTC CTG CAC CAG GAC TGG CTG AAT GGC AAG GAG TAC AAG TGC AAG GTC TCC <900
Q   Y   N   S   T   Y   R   V   V   S   V   L   T   V   L   H   Q   D   W   L   N   G   K   E   Y   K   C   K   V   S

                                                        >IgG1 CH3
                                                        |
AAC AAA GCC CTC CCA GCC CCC ATC GAG AAA ACC ATC TCC AAA GCC AAA GGG CAG CCC CGA GAA CCA CAG GTG TAC ACC CTG CCC CCA TCC <990
N   K   A   L   P   A   P   I   E   K   T   I   S   K   A   K   G   Q   P   R   E   P   Q   V   Y   T   L   P   P   S

CGG GAT GAG CTG ACC AAG AAC CAG GTC AGC CTG ACC TGC CTG GTC AAA GGC TTC TAT CCC AGC GAC ATC GCC GTG GAG TGG GAG AGC AAT <1080
R   D   E   L   T   K   N   Q   V   S   L   T   C   L   V   K   G   F   Y   P   S   D   I   A   V   E   W   E   S   N

GGG CAG CCG GAG AAC AAC TAC AAG ACC ACG CCT CCC GTG CTG GAC TCC GAC GGC TCC TTC TTC CTC TAC AGC AAG CTC ACC GTG GAC AAG <1170
G   Q   P   E   N   N   Y   K   T   T   P   P   V   L   D   S   D   G   S   F   F   L   Y   S   K   L   T   V   D   K

AGC AGG TGG CAG CAG GGG AAC GTC TTC TCA TGC TCC GTG ATG CAT GAG GCT CTG CAC AAC CAC TAC ACG CAG AAG AGC CTC TCC CTG TCT <1260
S   R   W   Q   Q   G   N   V   F   S   C   S   V   M   H   E   A   L   H   N   H   Y   T   Q   K   S   L   S   L   S

                XbaI
                |
CCG GGT AAA TGA TCT AGA                                                                                          <1278
P   G   K   *
```

hCD27

```
                                                                AgeI    >hCD27 (aa 20-183)
                                                                 |       |
                                                            ... ACC GGT GCC ACA CCA GCC CCT AAG AGC TGC CCC GAG < 90
                                                            ... T   G   A   T   P   A   P   K   S   C   P   E

AGA CAC TAT TGG GCT CAG GGC AAG CTG TGC TGC CAG ATG TGC GAG CCT GGC ACC TTC CTC GTG AAG GAC TGC GAC CAG CAC AGA AAG GCC <180
R   H   Y   W   A   Q   G   K   L   C   C   Q   M   C   E   P   G   T   F   L   V   K   D   C   D   Q   H   R   K   A

GCC CAG TGC GAC CCT TGT ATC CCC GGC GTG TCC TTC AGC CCC GAC CAC CAC ACA AGA CCC CAC TGC GAG AGC TGC CGG CAC TGC AAT TCT <270
A   Q   C   D   P   C   I   P   G   V   S   F   S   P   D   H   H   T   R   P   H   C   E   S   C   R   H   C   N   S

GGA CTG CTC GTG CGG AAC TGC ACC ATC ACC GCC AAT GCC GAG TGC GCC TGC AGA AAC GGC TGG CAG TGC AGA GAC AAA GAA TGC ACC GAG <360
G   L   L   V   R   N   C   T   I   T   A   N   A   E   C   A   C   R   N   G   W   Q   C   R   D   K   E   C   T   E

TGT GAC CCC CTG CCC AAC CCT AGC CTG ACA GCC AGA TCT AGC CAG GCC CTG TCC CCT CAC CCT CAG CCT ACC CAT CTG CCC TAC GTG TCC <450
C   D   P   L   P   N   P   S   L   T   A   R   S   S   Q   A   L   S   P   H   P   Q   P   T   H   L   P   Y   V   S

GAG ATG CTG GAA GCC AGA ACA GCC GGC CAC ATG CAG ACC CTG GCC GAC TTC AGA CAG CTG CCC GCC AGA ACC CTG AGC ACC CAT TGG CCC <540
E   M   L   E   A   R   T   A   G   H   M   Q   T   L   A   D   F   R   Q   L   P   A   R   T   L   S   T   H   W   P

                NotI
                  |
CCT CAG AGA TCT GCG GCC GCA ...                                                                                   <561
P   Q   R   S   A   A   A   ...
```

h4-1BB

```
                                                                AgeI    >h4-1BB (aa 24-186)
                                                                 |       |
                                                            ... ACC GGT CTG CAG GAC CCC TGC AGC AAT TGT CCT GCC < 90
                                                            ... T   G   L   Q   D   P   C   S   N   C   P   A

GGC ACC TTC TGC GAC AAC AAC CGG AAC CAG ATC TGC AGC CCC TGC CCC CCC AAT AGC TTT AGC TCT GCC GGC GGA CAG CGG ACC TGC GAC <180
G   T   F   C   D   N   N   R   N   Q   I   C   S   P   C   P   P   N   S   F   S   S   A   G   G   Q   R   T   C   D

ATC TGC AGA CAG TGC AAG GGC GTG TTC CGG ACC CGG AAA GAG TGC AGC AGC ACC TCC AAC GCC GAG TGC GAT TGC ACC CCT GGC TTC CAC <270
I   C   R   Q   C   K   G   V   F   R   T   R   K   E   C   S   S   T   S   N   A   E   C   D   C   T   P   G   F   H

TGT CTG GGA GCC GGC TGT AGC ATG TGC GAG CAG GAT TGC AAG CAG GGC CAG GAA CTG ACC AAG AAG GGC TGC AAG GAC TGC TGC TTC GGC <360
C   L   G   A   G   C   S   M   C   E   Q   D   C   K   Q   G   Q   E   L   T   K   K   G   C   K   D   C   C   F   G

ACC TTT AAC GAC CAG AAG AGA GGC ATC TGC CGG CCC TGG ACC AAC TGC AGC CTG GAT GGC AAG AGC GTG CTC GTG AAC GGC ACC AAA GAA <450
T   F   N   D   Q   K   R   G   I   C   R   P   W   T   N   C   S   L   D   G   K   S   V   L   V   N   G   T   K   E

CGG GAC GTC GTG TGC GGA CCT AGC CCT GCC GAT CTG TCT CCT GGC GCC TCT AGC GTG ACA CCT CCT GCC CCT GCT AGA GAG CCT GGA CAT <540
R   D   V   V   C   G   P   S   P   A   D   L   S   P   G   A   S   S   V   T   P   P   A   P   A   R   E   P   G   H

            NotI
             |
TCT CCT CAG GCG GCC GCA ...                                                                                       <558
S   P   Q   A   A   A   ...
```

hOX40

```
                                                                AgeI    >hOX40 (aa 29-214)
                                                                 |       |
                                                            ... ACC GGT CTC CAC TGT GTG GGC GAC ACC TAC CCC AGC < 90
                                                            ... T   G   L   H   C   V   G   D   T   Y   P   S

AAC GAC AGA TGC TGC CAC GAG TGC AGA CCC GGC AAC GGC ATG GTG TCC AGA TGC AGC AGA TCC CAG AAC ACC GTG TGC AGG CCT TGC GGC <180
N   D   R   C   C   H   E   C   R   P   G   N   G   M   V   S   R   C   S   R   S   Q   N   T   V   C   R   P   C   G

CCT GGC TTC TAC AAC GAC GTG GTG TCC TCC AAG CCC TGC AAG CCT TGC ACC TGG TGT AAC CTG AGA AGC GGC AGC GAG CGG AAG CAG CTG <270
P   G   F   Y   N   D   V   V   S   S   K   P   C   K   P   C   T   W   C   N   L   R   S   G   S   E   R   K   Q   L

TGT ACC GCC ACC CAG GAT ACC GTG TGC CGG TGT AGA GCC GGA ACC CAG CCC CTG GAC AGC TAC AAA CCT GGC GTG GAC TGC GCC CCT TGT <360
C   T   A   T   Q   D   T   V   C   R   C   R   A   G   T   Q   P   L   D   S   Y   K   P   G   V   D   C   A   P   C

CCC CCT GGG CAC TTT AGC CCT GGC GAC AAC CAG GCC TGC AAA CCC TGG ACC AAT TGC ACC CTG GCC GGC AAG CAC ACA CTG CAG CCT GCC <450
P   P   G   H   F   S   P   G   D   N   Q   A   C   K   P   W   T   N   C   T   L   A   G   K   H   T   L   Q   P   A

AGC AAT AGC AGC GAC GCC ATC TGC GAG GAC AGA GAT CCT CCT GCC ACC CAG CCT CAG GAA ACC CAG GGA CCT CCA GCC AGA CCC ATC ACC <540
S   N   S   S   D   A   I   C   E   D   R   D   P   P   A   T   Q   P   Q   E   T   Q   G   P   P   A   R   P   I   T

                                                                                                        NotI
                                                                                                         |
GTG CAG CCT ACA GAG GCC TGG CCT AGA ACC AGC CAG GGA CCC AGC ACC AGA CCC GTG GAA GTG CCT GGC GGC AGA GCA GCG GCC GCA ... <627
V   Q   P   T   E   A   W   P   R   T   S   Q   G   P   S   T   R   P   V   E   V   P   G   G   R   A   A   A   A   ...
```

List of Figures

Figure 1: The evolution of combinatorial cancer immunotherapy. 17
Figure 2: Costimulatory and co-inhibitory signaling at the immune synapse. 19
Figure 3: Antitumoral immune activation through TNFSF members. 25
Figure 4: T cell activation via tumor-targeted costimulatory antibody-cytokine fusion proteins. 27
Figure 5: Production and binding analysis of anti-CLDN4/6 scFv antibodies from hybridoma. 62
Figure 6: Alignment of scFv4H6E9 with germline genes and humanized sequences. 63
Figure 7: Humanized variants of scFv4H6E9. 64
Figure 8: Chimeric versions of scFvhu4H-S1a and scFvhu4H-S1b. 65
Figure 9: Variants of scFvhu4H-S1b with chimeric VL domains. 65
Figure 10: Comparison of scFv4H6E9 with final humanized variants. 66
Figure 11: Alignment of scFv323A3 with germline genes and humanized sequences. 68
Figure 12: Production of humanized scFv323A3 antibody fragments. 68
Figure 13: Target cell binding and biochemical properties of scFv323A3 variants. 69
Figure 14: Design and biochemical characterization of scFv-ligand fusion proteins. 71
Figure 15: Antigen binding of scFv-ligand fusion proteins. 73
Figure 16: Cytokine receptor binding of scFv-ligand fusion proteins. 74
Figure 17: TNFRSF receptor activation measured via IL-8 release upon NFκB activation. 74
Figure 18: *In vitro* stability of scFv-ligand fusion proteins. 76
Figure 19: *In vivo* pharmacokinetics of scFv-ligand fusion proteins. 77
Figure 20: Costimulatory effects of scFv-ligand fusion proteins in a targeted setting. 78
Figure 21: Target- and cytokine-dependence of costimulatory scFv-ligand fusion proteins. 79
Figure 22: Concept of dual-acting immunostimulatory cytokine fusion proteins. 81
Figure 23: Summary of all Duokines and single-chain Duokines. 81
Figure 24: SDS-PAGE analysis of Duokines and scDuokines. 82
Figure 25: Size exclusion chromatography of Duokines and scDuokines. 83
Figure 26: TNFRSF receptor binding of Duokines and scDuokines. 85
Figure 27: Simultaneous binding of two TNFRSF receptors by Duokines and scDuokines. 87
Figure 28: Receptor activation measured via IL-8 release upon TNFRSF-dependent NFκB activation. 88
Figure 29: Plasma stability of Duokines and scDuokines. 91
Figure 30: Costimulatory activity of soluble Duokines and scDuokines analyzed by proliferation. 92
Figure 31: Costimulatory activity of surface-presented Duokines and scDuokines analyzed by proliferation. 93
Figure 32: Identification of different immune cell subpopulations. 95

Figure 33: TNFRSF receptor expression on and binding of scDuokines to immune cell subpopulations.96
Figure 34: B cell stimulatory activity of selected scDuokines. 97
Figure 35: T cell stimulatory activity of selected scDuokines. 98
Figure 36: Pharmacokinetics of selected Duokines and scDuokines. 99
Figure 37: Characterization of proteins used for the *in vivo* lung tumor model. 101
Figure 38: Anti-tumor activity of scDuokines in a combinatorial setting *in vivo*. 102
Figure 39: Design and biochemical characterization of EHD2-scDuokines. 104
Figure 40: Binding of TNFRSF receptors by EHD2-scDuokines. 105
Figure 41: Receptor activation measured via IL-8 release upon NFκB activation. 106
Figure 42: Plasma stability of EHD2-scDuokines. 107
Figure 43: Costimulatory activity of EHD2-scDuokines in solution analyzed by proliferation. 108
Figure 44: Hypothetical model for receptor activation via duokines. 121

List of Tables

Table 1: Immunomodulatory antibodies for cancer treatment approved or in ongoing clinical trials. 16
Table 2: Antibodies used in this study. 33
Table 3: Cell lines used in this study. 35
Table 4: Primer for sequencing. 39
Table 5: Primer for cloning. 39
Table 6: Combinations of scFv323A3. 45
Table 7: Chimera of scFv4H6E9 and scFvhu4H-S1a / scFvhu4H-S1b. 45
Table 8: Cloning of VL chimera of scFvhu4H-S1b. 46
Table 9: Versions of scFvhu4H-S1b with mutated VL. 46
Table 10: Cloning of Duokines. 47
Table 11: Cloning of single-chain Duokines. 48
Table 12: Composition of polyacrylamide gels (two each). 54
Table 13: Identification of leukocyte subpopulations. 56
Table 14: Parameters of human germline genes used for humanization of scFv4H6E9. 63
Table 15: Parameters of human germline genes used for humanization of scFv323A3. 67
Table 16: Biochemical characteristics of scFv-ligand fusion proteins. 72
Table 17: EC_{50} values [nM] for antigen binding and TNFRSF receptor binding and activation. 75
Table 18: Pharmacokinetic properties of scFv-ligand fusion proteins. 77
Table 19: Biochemical characteristics of Duokines & scDuokines. 84
Table 20: EC_{50} values [nM] for TNFRSF receptor binding by Duokines & scDuokines. 86
Table 21: EC_{50} values [nM] for TNFRSF receptor activation by Duokines & scDuokines. 90
Table 22: Pharmacokinetic properties of murine Duokines and scDuokines. 100
Table 23: Biochemical characteristics of EHD2-scDuokines. 105
Table 24: EC_{50} values [nM] for TNFRSF receptor binding and activation by EHD2-scDuokines. 107

Declaration

I hereby declare that this submission is my own work that I prepared without any illegitimate help. All sources used have been quoted adequately.

Erklärung

Hiermit erkläre ich, dass die vorgelegte Dissertation von mir persönlich ohne unrechtmäßige Hilfe angefertigt wurde. Alle genutzten Quellen sind entsprechend zitiert.

Mainz, December 9, 2016

Danksagung

Mein erster Dank gebührt Prof. Dr. Roland Kontermann für die allzeit hervorragende Betreuung während meiner Doktorarbeit, die hilfreichen Diskussionen und Anregungen. Danke für die Ermöglichung vieler Projekte sowie die ungezwungene Atmosphäre im Labor und außerhalb - „Heimat verbindet“ gilt in unserem Fall wohl zusätzlich ganz besonders.

Herzlichst danke ich apl. Prof. Dr. Wolfgang Hauber für die Erstellung des Zweitgutachtens. Vielen Dank an Prof. Dr. Klaus Pfizenmaier für die wertvolle Projektmitarbeit und an Dr. Dafne Müller, die mit ihrem umfangreichen Wissen im Bereich der Krebsimmuntherapie eine unverzichtbare Hilfe war.

Unseren Projektpartnern von der BioNTech AG in Mainz, namentlich vor allem Dr. Friederike Gieseke, Dr. Sebastian Kreiter und Prof. Dr. Ugur Sahin, danke ich für die inspirierende Kooperation und ich freue mich sehr, jetzt bei euch ins Berufsleben starten zu können. Das Projekt zur vorliegenden Arbeit wurde während der ersten 3 Jahre durch die BioNTech AG finanziert und weiterführend im Rahmen des Immunotransporter-Projektes durch das Bundesministerium für Bildung und Forschung (BMBF) gefördert.

Besonderer Dank gilt meinem Diplomstudenten Jan-Erik Meyer für seine hervorragenden Arbeiten zum Teilprojekt der scFv-Fusionsproteine. Es war eine Freude mit dir zu arbeiten!

4 Jahre Promotion – 4 Jahre mit den besten Kollegen: Meike Hutt, Dr. Felix Unverdorben, Dr. Oliver Seifert und Dr. Fabian Richter. Ohne euch wäre diese Zeit nur halb so schön und außerdem so manches gar nicht möglich gewesen. Felix, das Schicksal hat entschieden, dass wir uns am ersten Tag meines Studiums begegneten – unsere Freundschaft wird über das Ende unserer Doktorarbeiten hinaus sicher noch sehr lange anhalten. Liebe Meike, von der besten Kollegin zu einer meiner wichtigsten Freundinnen. Mehr Worte braucht es nicht.

Vielen Dank auch an alle anderen „Kontermänner“ – wir waren im und außerhalb des Labors ein super Team. Zudem möchte ich den TAs Sabine Münkel und Elke Gerlach, sowie den Tierpflegerinnen Alexandra Kraske und Beatrice Reiser für ihre Unterstützung danken.

Den wichtigsten Personen danke ich zuletzt: Jonathan für seine Unterstützung, seine Liebe und seinen Glauben an uns in allen Zeiten und Lebenslagen. Dann, Danke meinen Eltern. Euch ist diese Arbeit gewidmet, da ihr mich immer bedingungslos unterstützt und seit jeher an meinen Erfolg geglaubt habt. Hier haltet ihr das Resultat in den Händen.

Short Curriculum Vitae

Professional experience

since 08/2016 **BioNTech RNA Pharmaceuticals GmbH, Mainz** | Scientist

09/2011 – 10/2011 **micro-biolytics GmbH, Esslingen am Neckar** | Internship

Education

03/2012 – 06/2016 **PhD Thesis at the University of Stuttgart**

11/2005 – 02/2012 **Diploma in Technical Biology, University of Stuttgart**

08/2010 – 08/2011 **Diploma Thesis at the University of Stuttgart**

10/2009 – 04/2010 **Research Project at the University of New South Wales, Sydney**

09/1996 – 06/2005 **Abitur at Max-Planck-Gymnasium Schorndorf**

Conference contributions, trainings and workshops

05/2015 *11th PEGS Boston* | 30 & 10 min oral presentation, poster presentation

05/2015 *14th CIMT Annual Meeting* | poster presentation

08/2013 *15th International Congress of Immunology* | poster presentation

Patents

Sahin U, Gieseke F, Backer R, Kreiter S, Kontermann R, Pfizenmaier K, Fellermeier S, Müller D. Cytokine fusion proteins. 2015. PCT/EP2015/050682

Publications

Fellermeier S, Müller D, Pfizenmaier K, Kontermann RE. Duokines and single-chain Duokines – novel immunomodulatory fusion proteins. In preparation.

Fellermeier S, Beha N, Meyer JE, Ring S, Bader S, Kontermann RE, Müller D. Advancing targeted costimulation with antibody-fusion proteins by introducing TNF superfamily members in a single-chain format. Oncoimmunology Vol. 5, Iss. 11, 2016.

Seifert O, Plappert A, Fellermeier S, Siegemund M, Pfizenmaier K, Kontermann RE. Tetravalent antibody-scTRAIL fusion proteins with improved properties. Mol Cancer Ther. 2014 Jan; 13(1):101-11.

Seifert O, Plappert A, Heidel N, Fellermeier S, Messerschmidt SK, Richter F, Kontermann RE. The IgM CH2 domain as covalently linked homodimerization module for generation of fusion proteins with dual specificity. Protein Eng Des Sel. 2012 Oct; 25(10):603-12.

Mack K, Rüger R, Fellermeier S, Seifert O, Kontermann RE. Dual Targeting of Tumor Cells with Bispecific Single-Chain Fv-Immunoliposomes. Antibodies 2012, 1(2), 199-214.

Ayer A, Fellermeier S, Fife C, Li SS, Smits G, Meyer AJ, Dawes IW, Perone GG. A genome-wide screen in yeast identifies specific oxidative stress genes required for the maintenance of sub-cellular redox homeostasis. PLoS ONE 2012, 7(9):e44278